EE543 Winter 2018
Robot Manipulators

Blake Hannaford

December 20, 2017

Contents

Chapter 1

Introduction

This text has evolved from lecture notes for EE543 at the University of Washington. It will be evident to the reader that it is still very much a work in progress. It owes a great deal to the book "Introduction to Robotics, Mechanics and Control," by John Craig.

As you read this book, please report typos or suggestions (by page and line number) to
`https://catalyst.uw.edu/gopost/board/blake/20007/`

1.1 Background and Motivational Examples

1.2 Definitions

A robot manipulator is a chain of *links* connected by *joints*.

1.2.1 Degree of Freedom

A degree of freedom (DOF) is a motion which can be completely described by a scalar and its time derivatives.

1.2.2 Joints

Joints constrain the relative position of two links in all but one degree of freedom.

Rotary joints permit revolute motion about a line in space refered to as the motion axis.

Prismatic joints permit translational motion along a line in space refered to as the motion axis.

Three key components of joints are actuators, sensors, and bearings.

Actuators do work on the joint through the application of force or torque. Most robot manipulators use electric motors as actuators but hydraulic, pneumatic, and other more exotic actuators can also be used.

Sensors measure the motion of the degree of freedom of the joint and send this information to a control system.

Bearings are devices which restrict motion in all but one degree of freedom. They act as rigid structural elements in the constrained directions and minimize friction in the degree of freedom.

1.2.3 End Effector

The end effector of a robot is a device attached to a link in the chain (typically at the end of a serial chain) designed to accomplish a task. Typical end effectors include grippers, spray guns, and tools.

1.2.4 Joint Space

1.2.5 Task Space

1.2.6 Workspace

1.3 Fundamental Problems in Manipulator Control

This book will use a large set of mathematical tools to model and analyze robot manipulators. In learning all of these tools, it will be useful to keep in mind that all of them are used to answer fundamental and straightforward questions which must be answered in order to use robot manpipulators.

- Description of a positioning task

  Q: How do we specify the position and orientation of robot arms and objects?

  A: Frames, Homogeneous Transformations, and joint-space teaching.

- Forward kinematics

  Q: What is the position and orientation (configuration) of a robot end effector if joint positions are known?

  A: A linear transformation (4x4 matrix) which is a function of the joint positions (angles, displacements) and specifies end effector configuration in the base frame. This matrix can also map a point in the end effector frame to its representation in the base frame.

- Inverse kinematics

  Q: What joint positions θ, do I need to achieve a given end effector configuration?

  A: Form an equation by setting the 4x4 matrix of the foward kinematics problem equal to one specifiing the *desired* position and orientation. Then solve this equation for the joint positions. Be sure to watch out for existence of solutions and multiple solutions.

- Velocity transformation

  Q: What joint velocities, $\dot{\theta}$, do I need to achieve a given velocity of the end effector (both linear and angular velocity) in all three dimensions of a convenient reference frame?

  A: Compute the "Jacobian Matrix", the matrix derivative, of the forward kinematic equations and invert it. Watch out for singular matrix in which case the inverse does not exist.

$$\dot{\theta} = J^{-1}\dot{x}$$

- Force transformation

  Q: What joint torques, τ, correspond to a given set of end effector forces and torques, F?

  A: $\tau = J^T F$

- Inverse dynamics

  Q: For a given motion, $\ddot{\theta}, \dot{\theta}, \theta(t)$, what are the required joint torques?

  A: We can derive a dynamic equation

$$\tau(t) = M(\theta)\ddot{\theta} + C(\theta, \dot{\theta}) + g(\theta)$$

  by using the Recursive Newton-Euler or Lagrangian methods.

- Position Control

  Q: How can we command joint torques to achieve a desired end effector trajectory?

  A: PID control, Feed-forward dynamic control (the method of computed torques).

- Force Control

  Q: How can we command joint torques to achieve a set of forces and torques at the end effector?

  A: Open loop we can use $\tau = J^T F$. However because of friction and other losses in many typical manipulators we must use force sensing at the end effector and closed loop force control.

- Trajectory Generation

  Q: If we know a trajectory we want to follow, how do we generate a time-function which is a quick but smooth and attainable trajectory between two configurations "A" and "B"?

  A: Methods include polynomial splines and trapezoidal velocity profiles.

- Motion Planning

  Q: How do we decide the path to take between two configurations "A" and "B"?

  A: Without considering obstacles, the most common approach is straight line interpolation. When obstacles and joint limits must be considered this becomes the AI motion planning problem.

- Sensor Based Control

  Q: How can I make use of non-joint sensor information (e.g. vision, proximity, etc.) to control robot motion (for example, to follow 1cm above an unknown surface).

  A: Robot vision, vision servoing, sensor data fusion, world modeling, operational space control.

- Telemanipulation

  Q: How can a human operator control a remote manipulator in a "natural" and productive way to achieve a task goal?

  A: Generalized bi-lateral teleoperation.

1.4 Summary of Notation

This explains the notation of chapter 1.

Chapter 2

Coordinate Transformations and Rigid Body Motions

To properly control the manipulation of objects with robots, we must have precise and useful ways to describe their position and orientation. In this chapter we start out with some definitions, and then develop the mathematical tools for this surprisingly non-straightforward task. Finally we will combine position and orientation into a clever 4x4 matrix which represents both in one object.

2.1 Problem Statement and Learning Objectives

Problem Statement The problem this chapter addresses is to represent the position and orientation of rigid bodies and frames of reference in useful ways.

Learning Objectives Upon completing this Chapter, the reader should be able to

- Work with vectors and vector products.
- Derive several mathematical represenations of 3D rigid body rotation
- Represent any displacement and rotation of a rigid body by a 4x4 matrix (the homogeneous transformation).
- Solve for unknown spatial relationships in terms of known spatial relationships using homogeneous transformations and transform graphs.

2.2 Description of Position and Orientation

2.2.1 Vectors and Translation

We use vectors to represent the location of objects and also to represent translation movements from one point to another.

Vector Cross Product

We will sometimes need the vector cross product which is briefly defined here.

The cross product of two vectors, represented

$$c = a \times b$$

is a vector who's magnitude is

$$|c| = |a||b| \sin(\theta)$$

where θ is the angle between the two vectors. and whos direction is orthogonal to both a and b. There are two orthogonal directions to a and b and the cross product sign is set by the right hand rule (sweeping

the fingers from a to b and observing direction of thumb). We will frequently consider the cross product of vectors separated by 90° (for example the X and Y axes) and in this case

$$|c| = |a||b|$$

Another, equivalent, definition of the vector cross product can be expressed in matrix notation as

$$a \times b = \begin{bmatrix} 0 & -a_3 & a_2 \\ a_3 & 0 & -a_1 \\ -a_2 & a_1 & 0 \end{bmatrix} b$$

Example 2.1
1) Find the magnitude of the cross product $a \times b$ where

$$a = [3 \quad 4 \quad 7]^T \qquad b = [2 \quad 4 \quad -3]^T$$

$$c = a \times b$$

$$|c| = |a||b| = 8.6 \times 5.39 = 46.3$$

2) Find the elements of the cross product.

To get the components, it is easiest to use the matrix definition:

$$c = \begin{bmatrix} 0 & -7 & 4 \\ 7 & 0 & -3 \\ -4 & 3 & 0 \end{bmatrix} \begin{bmatrix} 2 \\ 4 \\ -3 \end{bmatrix} = \begin{bmatrix} -40 \\ 23 \\ 4 \end{bmatrix}$$

You can verify that the magnitude of this vector is also 46.3.

2.2.2 Coordinate Systems and Frames

Of course when we use them numerically, our vectors must be defined with respect to axes in space. Such a coordinate system contains three axes oriented to measure displacement in each of the three spatial dimensions. We denote these axes x, y, z and we will require that this system is *right handed* so that

$$x \times y = z$$

where $\times$ represents the vector cross product. We can have as many coordinate systems as we like and they can differ from one another in two ways. The location of their origin can be different, in which case we say they are *offset* or *displaced* from one another, and their orientation can be different, in which case we say they are *rotated* from one another.

Another term for coordinate system is *reference frame* or simply *frame*.

2.2.3 Points

The numerical value or location of a point in space is only defined with respect to a selected coordinate system. Thus if we have a point, P, and a coordinate system, A, it will have a specific numerical location with respect to A. For example:

$${}^A P = \begin{bmatrix} 1.7 \\ 0.25 \\ -3.1 \end{bmatrix}$$

While P designates the point in the abstract, we add the leading subscript, ${}^A P$ to indicate P's representation in coordinate system A.

The origin of a frame is also a point. The displacement between two frames can thus be represented by a point, the origin of one frame, expressed in a second frame. For example, imagine that M and N, are two

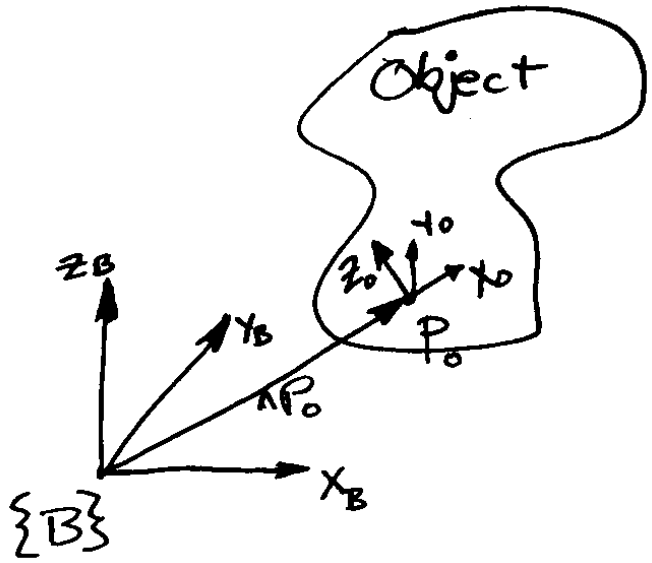

Figure 2.1: Representation of a rigid object in terms of an origin, P_0, and a frame attached to the object (frame 0).

coordinate systems not rotated with respect to each other, but their origins, O_M and O_N, are separated by 5 cm in the x direction. Then

$$^MO_N = [0.05 \quad 0.0 \quad 0.0]^T$$

and

$$^NO_M = [-.05 \quad 0.0 \quad 0.0]^T$$

2.2.4 Rigid Objects

We will view rigid objects as a collection of points with a fixed relationship to one another. How can we describe a rigid object's configuration in space with respect to some base frame, frame B?

First choose a point on the object, P_0 (Figure 2.1). Then create a frame, O, whos origin is P_0. The origin of P_0 does not have to be on or inside the object as long as all points in the object have a *fixed* representation in frame O. The orientation of frame O does not matter either as long as the previous condition is satisfied. We can represent the location of the object in frame B by simply the position of its origin, $^BP_0$.

Representation of the orientation of the object is somewhat more involved. We can imagine that if we only know the location, P_0, the object is still free to rotate about P_0 in multiple ways. Now, if we specify a second point on the object, P_1, the object is more constrained, but can still freely spin around the line connecting P_0 and P_1 without violating our assumption. If we specify a third point on the object, we fully describe the object in both position and orientation.

We will be a little bit redundant and specify the object's configuration with four points: the origin, P_0, and the tips of the three unit vectors of frame O: x_o, y_o, z_o. However we will remove the translation portion from these three points by subtracting P_0 to create

$$\hat{x_0} = x_0 - P_0, \qquad \hat{y_0} = y_0 - P_0, \qquad \hat{z_0} = z_0 - P_0$$

To capture the object's orientation, we represent these vectors in the base frame, frame B.

$$^B\hat{x_0} = {}^Bx_0 - {}^BP_0 \quad \text{etc.}$$

Our representation of the object's configuration at this point is the tuple:

$$^BObj = \left\{ \begin{bmatrix} ^BP_x \\ ^BP_y \\ ^BP_z \end{bmatrix}, \begin{bmatrix} ^B\hat{x}_{Ox} & ^B\hat{y}_{Ox} & ^B\hat{z}_{Ox} \\ ^B\hat{x}_{Oy} & ^B\hat{y}_{Oy} & ^B\hat{z}_{Oy} \\ ^B\hat{x}_{Oz} & ^B\hat{y}_{Oz} & ^B\hat{z}_{Oz} \end{bmatrix} \right\}$$

we refer to the collection of $\hat{x_O}, \hat{y_O}, \hat{z_O}$ vectors into a matrix as a *rotation matrix.*.

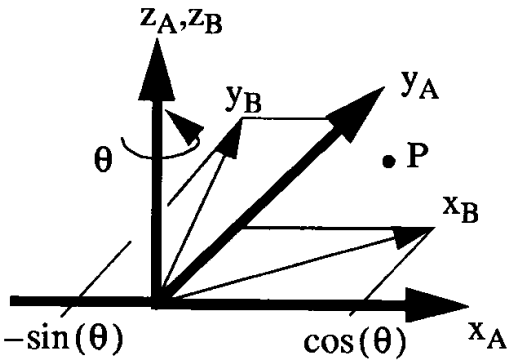

Figure 2.2: Two frames which are rotated relative to each other by the angle θ about the axis z.

2.3 Rotation Matrix

We will study the rotation matrix from the point of view of four definintions. Although these four definitions seem different at first, they are all simultaneously true. In this section we will consider only frames which differ in orientation. We will add translation later.

The rotation matrix ${}^A_B R$ is:

1. A matrix which specifies frame B in terms of frame A. The columns of ${}^A_B R$ are the unit vectors of frame B specified in frame A.
2. A matrix which maps a point expressed in frame B, ${}^B P$ to its representation in frame A, ${}^A P$, by matrix pre-multiplication:
$$ {}^A P = {}^A_B R \, {}^B P $$
3. A description of an *operation* such as physically turning from frame A to frame B.
4. A 3×3 matrix with mathematical constraints: If $R = [a \quad b \quad c]$ where a, b, c are 3-vectors, then
$$ |a| = |b| = |c| = 1 $$
and
$$ a \times b = c, \quad b \times c = a, \quad c \times a = b $$
where $\times$ is the vector cross product.

2.4 Descriptions of Rotations

There are many subtle aspects to rotation of objects and representing them mathematically. In this section we will consider ways to describe rotations and combinations of rotations using the rotation matrix.

2.4.1 Rotation in the Plane

Consider rotation in the x, y plane about the axis z. When we say "about," we mean that any point along the line indicated by z is unchanged by the rotation. Also, the z coordinate of any point is unchanged by rotation about the z axis. In Figure 2.2 we have two frames, A, in bold, and B. B is rotated about the z axis with respect to A. Consider the tip of the unit vector x_A. After its rotation to x_B, it has components

which we can project back on to x_A and y_A. It still has no component in z. If we have rotated around z by angle θ, then these projections are

$$ {}^A x_B = \begin{bmatrix} cos(\theta) \\ sin(\theta) \\ 0 \end{bmatrix} $$

Similarly,

$$ {}^A y_B = \begin{bmatrix} -sin(\theta) \\ cos(\theta) \\ 0 \end{bmatrix} $$

These are two columns of the rotation matrix ${}^A_B R$:

$$ {}^A_B R = \begin{bmatrix} cos(\theta) & -sin(\theta) & ? \\ sin(\theta) & cos(\theta) & ? \\ 0 & 0 & ? \end{bmatrix} $$

We can get column 3 of ${}^A_B R$ two ways. First, as we have just done, we can note that

$$ {}^A z_B = {}^A z_A = \begin{bmatrix} 0 \\ 0 \\ 1 \end{bmatrix} $$

Therefore our complete matrix must be

$$ {}^A_B R = \begin{bmatrix} cos(\theta) & -sin(\theta) & 0 \\ sin(\theta) & cos(\theta) & 0 \\ 0 & 0 & 1 \end{bmatrix} $$

A second way to complete the rotation matrix is to use definition 4, which specifies that the magnitude of each row or column must be one (Sec 2.3). Thus

$$ |r_{31}|^2 = 1 - \cos(\theta)^2 - \sin(\theta)^2 = 0 $$

etc.

Our favorite point, P, has the representation $\{P_{XA}, P_{YA}\}$ in the x, y plane. P_{ZA} can have any value for this discussion since our rotation is about z. Just as it did with the unit vectors, ${}^A_B R$ maps P's representation in B to its representation in A:

$$ {}^A P = {}^A_B R \, {}^B P $$

One way we can see this is by an argument of superposition since matrix multiplication is a linear transformation and ${}^B P$ can be expressed as a linear combination of the unit vectors of B.

Rotational Operators

By similar arguments we can derive rotation matrices for rotation around the other axes, x, and y. Let's denote the unit vectors,

$$ \hat{x} \equiv [1 \quad 0 \quad 0]^T \quad \hat{y} \equiv [0 \quad 1 \quad 0]^T \quad \hat{z} \equiv [0 \quad 0 \quad 1]^T $$

These are not vectors in any particular coordinate system, just the numerical values shown above. We will define the matrices

$$ \mathrm{Rot}(\hat{x}, \theta) = \begin{bmatrix} 1 & 0 & 0 \\ 0 & \cos(\theta) & -\sin(\theta) \\ 0 & \sin(\theta) & \cos(\theta) \end{bmatrix} $$

$$ \mathrm{Rot}(\hat{y}, \theta) = \begin{bmatrix} \cos(\theta) & 0 & \sin(\theta) \\ 0 & 1 & 0 \\ -\sin(\theta) & 0 & \cos(\theta) \end{bmatrix} $$

$$ \mathrm{Rot}(\hat{z}, \theta) = \begin{bmatrix} \cos(\theta) & -\sin(\theta) & 0 \\ \sin(\theta) & \cos(\theta) & 0 \\ 0 & 0 & 1 \end{bmatrix} $$

to designate rotations about the three main axes of a frame. At this point let's introduce a shorter notation:

$$c\theta \equiv cos(\theta), \quad s\theta \equiv sin(\theta)$$

and

$$c_1 = \cos(\theta_1), \quad s_1 = sin(\theta_1)$$

for example,

$$\text{Rot}(\hat{x}, \theta_3) = \begin{bmatrix} 1 & 0 & 0 \\ 0 & c_3 & -s_3 \\ 0 & s_3 & c_3 \end{bmatrix}$$

Example 2.2
A point in frame B is

$${}^{B}P = \begin{bmatrix} -2 \\ 2 \\ 0.707 \end{bmatrix}$$

and there exists a frame A, whose rotation relative to B is given by

$${}^{A}_{B}R = \text{Rot}(\hat{x}, \pi/4)$$

1) What are the elements of ${}^{A}_{B}R$?
Answer:

$${}^{A}_{B}R = \begin{bmatrix} 1 & 0 & 0 \\ 0 & 0.707 & -0.707 \\ 0 & 0.707 & 0.707 \end{bmatrix}$$

2) What is ${}^{A}P$?
Answer:

$${}^{A}P = {}^{A}_{B}R\, {}^{B}P = \begin{bmatrix} -2.0 \\ 0.914 \\ 1.914 \end{bmatrix}$$

3) What is the change in magnitude of P when it is rotated?
Answer:

$$\frac{|{}^{A}P|}{|{}^{B}P|} = \frac{2.915}{2.915} = 1$$

A rotation matrix should never change the magnitude of a point.

We can verify the fourth definition of the rotation matrix with the rotation operators. For example, using $\text{Rot}(\hat{x}, \theta)$ we can easily verify that its columns have magnitude 1. We can verify the cross product constraints as well. Using $\text{Rot}(\hat{x}, \theta)$, then let a and b equal the first two columns

$$a = [1 \quad 0 \quad 0]^T, \quad b = [0 \quad c\theta \quad s\theta]^T$$

We want to show that $a \times b = c$. Recall that one definition of the vector cross product is

$$a \times b = \begin{bmatrix} 0 & -a_3 & a_2 \\ a_3 & 0 & -a_1 \\ -a_2 & a_1 & 0 \end{bmatrix} b$$

so returning to our example,

$$c = a \times b = \begin{bmatrix} 0 & 0 & 0 \\ 0 & 0 & -1 \\ 0 & 1 & 0 \end{bmatrix} \begin{bmatrix} 0 \\ c\theta \\ s\theta \end{bmatrix} = \begin{bmatrix} 0 \\ -s\theta \\ c\theta \end{bmatrix}$$

which is the answer we expect (i.e the third column of $\text{Rot}(\hat{x}, \theta)$) and verifies that the third column is orthogonal to the first two.

2.4.2 Inverse of a Rotation Matrix

The properties given in our fourth definition describe an *orthonormal* matrix. Any orthonormal matrix has an inverse which is equal to its transpose. Thus for rotation matrices

$$R^{-1} = R^T$$

Clearly the inverse of a rotation matrix always exists because the transpose always exists. When we apply this to the coordinate transform application of rotation matrices:

$$({}^A_B R)^{-1} = ({}^A_B R)^T = {}^B_A R$$

2.4.3 Composition of Rotations

Suppose there are two rotations which create a more complex relationship between two frames. If we can transform a point from a rotated frame back to the base frame by premultiplying by the rotation matrix, then we should be able to do this twice to represent two rotations.

Example 2.3

Two frames, A, and B, start out coincident (${}^A_B R = I$). Then frame B is rotated about z_A by θ and then frame B is rotated about y_B by ϕ. Note that the second axis, y_B, is known in the most recent frame:

$${}^B y_B = [0 \quad 1 \quad 0]^T = \hat{y}$$

.
1) What is ${}^A_B R(\theta, \phi)$? In other words, what matrix represents the combination of both rotations?
Answer: Consider an intermediate frame, A', to represent the frame after the first rotation:

$${}^A_{A'} R = \text{Rot}(\hat{z}, \theta)$$

by definition 3

$${}^{A'}_B R = \text{Rot}(\hat{y}, \phi)$$

So now consider mapping a point in frame B, ${}^B P$, back to A using definition 2 twice:

$${}^A P = {}^A_{A'} R {}^{A'}_B R {}^B P$$

Thus,

$${}^A_B R = \text{Rot}(\hat{z}, \theta)\text{Rot}(\hat{y}, \phi)$$

We may combine successive rotations by *post*multiplication if each rotation is about a vector represented in the *current* rotated frame. In Example 2.3, the first rotation, $\text{Rot}(\hat{z}, \theta)$, is postmultiplied by the second rotation, $\text{Rot}(\hat{y}, \phi)$ to get the compound rotation ${}^A_B R$. This gives

$${}^A_B R(\theta, \phi) = \begin{bmatrix} c\theta & -s\theta & 0 \\ s\theta & c\theta & 0 \\ 0 & 0 & 1 \end{bmatrix} \begin{bmatrix} c\phi & 0 & s\phi \\ 0 & 1 & 0 \\ -s\phi & 0 & c\phi \end{bmatrix} = \begin{bmatrix} c\theta c\phi & -s\theta & c\theta s\phi \\ s\theta c\phi & c\theta & s\theta s\phi \\ -s\phi & 0 & c\phi \end{bmatrix}$$

When successive rotations are described with respect to a single, fixed frame (in contrast to the compound example above), we may combine these by *pre*multiplication. To illustrate this, we'll take the previous example of compound rotations and change just one thing: the second rotation will take place around y_A instead of y_B.

Example 2.4

Two frames, A, and B, start out coincident (${}^A_B R = I$). Then frame B is rotated about z_A by θ and then frame B is rotated about y_A by ϕ. Unlike the previous example, the second axis is known only in the original frame, frame A. So we know:

$$ {}^B y_A \neq [0 \quad 1 \quad 0]^T $$

1) What is ${}^A_B R(\theta, \phi)$ this time?

Answer: As before, consider the intermediate frame, A', to represent the frame after the first rotation:

$$ {}^A_{A'} R = \text{Rot}(\hat{z}, \theta) $$

by definition 3 (Section 2.3). For the second rotation let's use the point mapping interpretation, definition 2. The second rotation must be represented by a matrix which maps a point from B to A'. This rotation is *not* one of our three cannonical rotation matrices because $y_A \neq \hat{y}$ in our current frame. We can derive the proper transformation by breaking it down into three steps:

1. Rotate (as in physical move) A' to A using ${}^{A'}_{A} R$.
2. $\text{Rot}(\hat{y}, \phi)$
3. Rotate back to A' using ${}^A_{A'} R$.

Thus,

$$ {}^{A'}_B R = \text{Step 1} \times \text{Step 2} \times \text{Step 3} $$

$$ {}^{A'}_B R = {}^{A'}_A R \, \text{Rot}(\hat{y}, \phi) \, {}^A_{A'} R $$

Now the complete mapping from B to A is

$$ {}^A_B R = {}^A_{A'} R \, {}^{A'}_B R = {}^A_{A'} R \, {}^{A'}_A R \, \text{Rot}(\hat{y}, \phi) \, {}^A_{A'} R $$

Because ${}^A_{A'} R = {}^{A'}_A R^{-1}$, the first two rotation matrices cancel giving

$$ {}^A_B R = \text{Rot}(\hat{y}, \phi) {}^A_{A'} R = \text{Rot}(\hat{y}, \phi) \text{Rot}(\hat{z}, \theta) $$

expanding this:

$$ {}^A_B R = \begin{bmatrix} c\phi & 0 & s\phi \\ 0 & 1 & 0 \\ -s\phi & 0 & c\phi \end{bmatrix} \begin{bmatrix} c\theta & -s\theta & 0 \\ s\theta & c\theta & 0 \\ 0 & 0 & 1 \end{bmatrix} = \begin{bmatrix} c\phi c\theta & -c\phi s\theta & s\phi \\ s\theta & c\theta & 0 \\ -s\phi c\theta & s\phi c\theta & c\phi \end{bmatrix} $$

Note that after the cancelation, it is as though the second rotation *pre*multiplies the first one.

Example 2.5
Two frames A and B start out superimposed. Then

B is rotated about x_A by θ_1.
B is rotated about y_B by θ_2.
B is rotated about y_A by θ_3.

What is ${}^A_B R$?

Answer:
Set up intermediate frames as above: A', A''. Then

$$ {}^A_B R = {}^A_{A'} R \, {}^{A'}_{A''} R \, {}^{A''}_{B} R $$

Considering the first rotation, since in the initial frame, $x_A = \hat{x}$ we can write

$$ {}^A_{A'} R = \mathrm{Rot}(\hat{x}, \theta_1) $$

In the second rotation, the axis is also known in the current frame: ${}^{A'} y_B = \hat{y}$, we can similarly write:

$$ {}^{A'}_{A''} R = \mathrm{Rot}(\hat{y}, \theta_2) $$

However for the third rotation we have to go all the way back to the initial frame:

$$ {}^{A''}_{B} R = \underbrace{{}^{A''}_{A'} R \, {}^{A'}_{A} R \, \mathrm{Rot}(\hat{y}, \theta_3) \, {}^{A}_{A'} R \, {}^{A'}_{A''} R}_{} $$

Combining

$$ {}^A_B R = \underbrace{{}^A_{A'} R \, {}^{A'}_{A''} R \, {}^{A''}_{A'} R \, {}^{A'}_{A} R}_{=I} \mathrm{Rot}(\hat{y}, \theta_3) \, {}^A_{A'} R \, {}^{A'}_{A''} R = \mathrm{Rot}(\hat{y}, \theta_3) \, {}^A_{A'} R \, {}^{A'}_{A''} R $$

$$ {}^A_B R = \mathrm{Rot}(\hat{y}, \theta_3) \mathrm{Rot}(\hat{x}, \theta_1) \mathrm{Rot}(\hat{y}, \theta_2) $$

Example 2.6

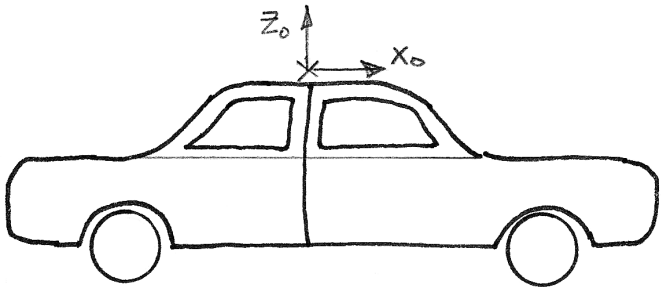

($\rightarrow$ front of car)

A robotic car drives straight for 10 meters then turns right by 90°. Then it drives up a 45° incline and comes to a stop.
A frame mounted to the top of the vehicle is called F_0. The onboard computer can store the current value of F_0 at any time from navigation instruments as a 3x3 matrix. Before driving the computer stores

$$F_1 = F_0$$

Then after the drive above, it stores the new orientation,

$$F_2 = F_0$$

What is the rotation matrix ${}^1_2R$ which describes the change in orientation?
Answer:
We have rotation matrices describing the three stages of the trip:
1) Drive straight for 10 meters: $\begin{bmatrix}1 & 0 & 0\\ 0 & 1 & 0\\ 0 & 0 & 1\end{bmatrix}$
2) Turn right by 90°: Rot($\hat{z}$, $-90°$): $\begin{bmatrix}0 & 1 & 0\\ -1 & 0 & 0\\ 0 & 0 & 1\end{bmatrix}$
3) Go up 45° incline: Rot($\hat{y}, -45°$): $\begin{bmatrix}0.707 & 0 & -0.707\\ 0 & 1 & 0\\ 0.707 & 0 & 0.707\end{bmatrix}$
(about the *local* frame).
Then we can combine them by postmultiplication:

$${}^1_2R = \begin{bmatrix}1 & 0 & 0\\ 0 & 1 & 0\\ 0 & 0 & 1\end{bmatrix}\begin{bmatrix}0 & 1 & 0\\ -1 & 0 & 0\\ 0 & 0 & 1\end{bmatrix}\begin{bmatrix}0.707 & 0 & -0.707\\ 0 & 1 & 0\\ 0.707 & 0 & 0.707\end{bmatrix}$$

$${}^1_2R = \begin{bmatrix}0 & 1 & 0\\ -0.707 & 0 & 0.707\\ 0.707 & 0 & 0.707\end{bmatrix}$$

It can be confusing to remember the order of multiplication for multiple rotations. One way to think about it is we always post-multiply successive rotations. If the rotation is about the first, fixed frame, then we must use the similarity transformation as shown in Examples 4 and 5 of this chapter. The effect of this similarity transformation is to make this appear like pre-multiplication.

To summarize, if we are careful, we can use the following rules of thumb to determine the order of matrix multiplication:

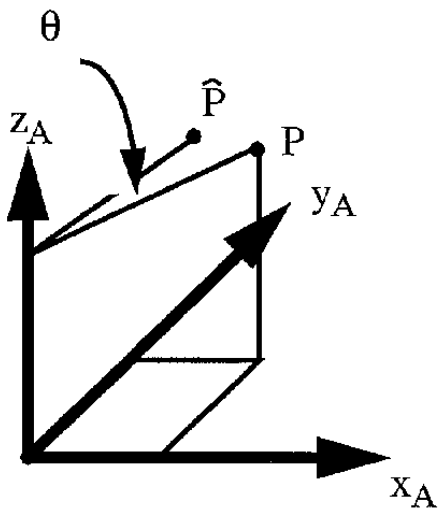

Figure 2.3: Rotation of a point around the z axis by angle θ. Here we consider the point to actually move in a single frame, A.

1. If the rotation is about an axis in the *original fixed* frame, pre-multiply
2. If the rotation is about an axis in the *current* frame, post-multiply

2.4.4 Rotation of a Point

The rotation matrix also describes the physical act of turning something (Figure 2.3). So how can we describe the rotation of a point about an axis in a certain frame but still representing the point in the same frame?

We consider the point's rotation to be positive if the angle from the orginal point, P, to the rotated point, $\hat{P}$, is positive in the right hand sense around the axis. Consider for example, rotation of the point around the $\hat{z}$ axis. By our third definition (Section 2.3),

$$^{A}\hat{P} = \text{Rot}(\hat{z}, \theta)^{A}P$$

2.4.5 Rotations about axes other than x, y, z

Suppose we have an arbitrarily rotated frame, F:

$$F = {}^{O}_{F}R$$

Geometrically, this might look like Figure 2.4. Now we will use frame F to study more general rotations. Suppose ${}^{O}_{F}R$ is known and we want to do a rotation about z_F? How do we represent a rotation about z_F in frame O by θ? Put another way, if the point ${}^{O}P$ is rotated about z_F by θ to get ${}^{O}\hat{P}$, what is ${}^{O}\hat{P}$?

We solve this similarly to the last example by transforming back to frame F and doing the canonical rotation about $\hat{z}$:

$$^{O}\hat{P} = {}^{O}_{F}R\text{Rot}\left(\begin{bmatrix}0\\0\\1\end{bmatrix}, \theta\right){}^{F}_{O}R$$

$$= \mathcal{R}\text{Rot}(\hat{z}, \theta)\mathcal{R}^{T}\,{}^{O}P$$

where $\mathcal{R} \equiv {}^{O}_{F}R$. Another way to look at this is to define

$$\text{Rot}(z_F, \theta) = \mathcal{R}\text{Rot}(\hat{z}, \theta)\mathcal{R}^{T}$$

Mathematically, this is a "similarity transform" which can be used to rotate about an arbitrarily rotated vector, in this case, z_F.

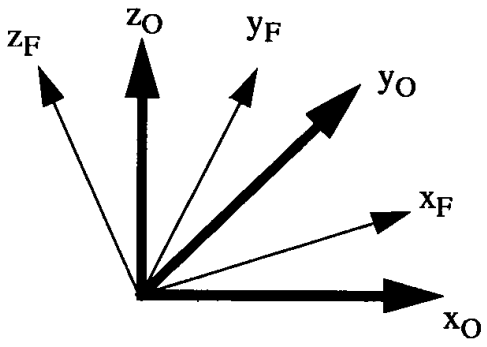

Figure 2.4: Frame F has an arbitrary orientation relative to frame O

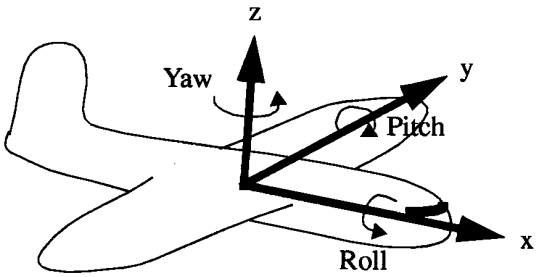

Figure 2.5: Roll-Pitch-Yaw angles (commonly used in avaition) describe rotations in a fixed order about x, y, z axes of a fixed coordinate system.

2.5 Three Parameter Representations of Rotation

Although nine numbers are required to make a rotation matrix, only 3 of them are independent (this is because there are six constraints on the matrix in definition 4 of Section 2.3). This implies that there should be representations of rotation needing only 3 parameters.

2.5.1 Roll-Pitch-Yaw Angles (XYZ Fixed Angles)

In aviation, aeronautics and sailing, the terms "roll, pitch, and yaw" are commonly used. These terms describe rotations about the x, y, z axes of a fixed coordinate system in that order (Figure 2.5). When we say that the coordinate system is "fixed," we mean *not* that it is fixed to the object (i.e. the aircraft of Figure 2.5), but that its orientation is fixed in space. Following the argument of Section 2.4.3, since these rotations are about a fixed frame, they should be combined by *pre-multiplication*:

$$R_{RPY} = \mathrm{Rot}(\hat{z}, Yaw)\mathrm{Rot}(\hat{y}, Pitch)\mathrm{Rot}(\hat{x}, Roll) \tag{2.1}$$

If we define the amounts of Roll, Pitch, and Yaw, (positive in the right hand sense) about x, y, z to be C, B, A respectively, then

$$R_{RPY} = \mathrm{Rot}(\hat{z}, A)\mathrm{Rot}(\hat{y}, B)\mathrm{Rot}(\hat{x}, C)$$

$$= \begin{bmatrix} cA & -sA & 0 \\ sA & cA & 0 \\ 0 & 0 & 1 \end{bmatrix} \begin{bmatrix} cB & 0 & sB \\ 0 & 1 & 0 \\ -sB & 0 & cB \end{bmatrix} \begin{bmatrix} 1 & 0 & 0 \\ 0 & cC & -sC \\ 0 & sC & cC \end{bmatrix} = \begin{bmatrix} cAcB & cAsBsC - sAcC & cAsBcC + sAsC \\ sAcB & sAsBsC + cAcC & sAsBcC - cAsC \\ -sB & cBsC & cBcC \end{bmatrix}$$

2.5.2 ZYX Euler Angles

Another 3-parameter representation which is commonly used is Euler Angles. In this case the rotations are taken about the axes of a *rotating* frame. Start with $F_1 = \{x_1, y_1, z_1\}$ superimposed on F_0. Then rotate through the three steps labeled A-C in Figure 2.6.

1. Rotate about z_0 by A to create F_1.
2. Rotate about y_1 by B to create F_2.
3. Rotate about x_2 by C to create F_3.

By definition (3), step one defines ${}^0_1R$, step two defines ${}^1_2R$, etc. By definition (2)

$$ {}^0_1R = \text{Rot}(\hat{z}, A) = \text{Rot}\,(\hat{z}, A) $$

maps a point in frame 1 to frame 0.

$$ {}^1_2R = \text{Rot}(\hat{y}, B) = \text{Rot}\,(\hat{y}, B) $$

maps a point in frame 2 to frame 1. And

$$ {}^2_3R = \text{Rot}(\hat{x}, C) = \text{Rot}\,(\hat{x}, C) $$

maps a point in frame 3 to frame 2.

Using the point mapping interpretation, the complete mapping is

$$ {}^0_3R = {}^0_1\,R\,{}^1_2R\,{}^2_3R = \text{Rot}(\hat{z}, A)\text{Rot}(\hat{y}, B)\text{Rot}(\hat{x}, C) \tag{2.2} $$

Note that (2.1) is the same as (2.2). But, the Roll Pitch and Yaw angles are *not* equivalent to ZYX Euler angles, because the rotations A, B, and C were applied in opposite orders in the two cases. Specifically, for roll-pitch-yaw angles, we used C for roll, but roll is applied *first* in the RPY method.

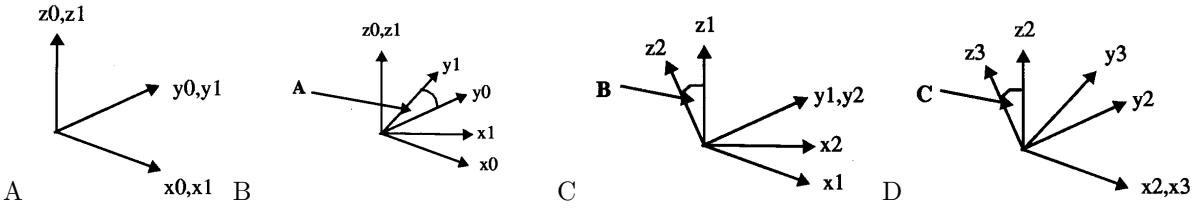

Figure 2.6: Initial Frames and rotations which make up the ZYX Euler Angles.

2.6 Equivalent Angle-Axis

Euler proved that any state of 3D rotation can be expressed by a single axis (i.e. a unit vector) and an amount of rotation. Let the axis of rotation be

$$ K = [K_X \quad K_Y \quad K_Z]^T $$

and the amount of rotation (in the right hand sense around K) be θ, then

$$ R_{K\theta} = \begin{bmatrix} K_X^2 v\theta + c\theta & K_X K_Y v\theta - K_Z s\theta & K_X K_Z v\theta + K_Y s\theta \\ K_X K_Y v\theta + K_Z s\theta & K_Y^2 v\theta + c\theta & K_Y K_Z v\theta - K_X s\theta \\ K_X K_Z v\theta - K_Y s\theta & K_Y K_Z v\theta + K_X s\theta & K_Z^2 v\theta + c\theta \end{bmatrix} $$

where

$$ v\theta = 1 - \cos(\theta) \qquad c\theta = \cos(\theta) \qquad s\theta = \sin(\theta) $$

Example 2.7
Work out $R_{K\theta}$ for the special case of the Z axis and compare the result to $rot(\hat{z}, \theta)$.
Let

$$K = [0 \quad 0 \quad 1]^T$$

Then setting K_X and K_Y to zero,

$$R_{K\theta} = \begin{bmatrix} c\theta & -K_Z s\theta & 0 \\ K_Z s\theta & c\theta & 0 \\ 0 & 0 & K_Z^2(1-c\theta)+c\theta \end{bmatrix}$$

Since $K_Z = 1$, this is equivalent to $rot(\hat{z}, \theta)$.

2.7 Quaternions

Another way to represent rotations of rigid bodies uses quaternions, a system like complex numbers which uses three "imaginary" variables instead of just i.

To understand how a quaternion represents rotations, first consider basic complex numbers of the form $M = a + bi$. The real and imaginary components of M form a point in the complex plane. For the purposes of rotation, we can assume that the magnitude of M is 1 ($|M| = 1$). In polar form,

$$|M| = \sqrt{a^2 + b^2} \qquad \angle M = \text{atan2}(a, b)$$

Remembering the rule "Angles add, magnitudes multiply," or

$$\angle(MN) = \angle(M) + \angle(N)$$

Since $|M| = 1$, we can think of multiplying a complex number by M as an operator which rotates the point to a new angle. Electrical engineers will be familiar with this concept used to describe phase relationships between AC signals of the same frequency (phasors).

Quaternions can be thought of as a generalization of complex numbers using the symbols i, j, and k, where

$$i^2 = j^2 = k^2 = ijk = -1$$

and where the multiplication of these elements is NOT commutitive (i.e. $ij \neq ji$). The "quaternion" has three imaginary components and one real component:

$$q = a + bi + cj + dk$$

The quaternion q can also be thought of as the sum of a scalar (a) and a vector ($bi + cj + dk$).

Just as a complex number $M = a+bi$ has a complex conjugate, $M^* = a-bi$, quaternions have a quaternion conjugate

$$q^* = a - (bi + cj + dk) \tag{2.3}$$

Just as a normal complex number can represent a rotation in the plane, quaternions can represent rotations in three dimensions. The rotation is described by an axis of rotation, K, and a degree of rotation θ. As we saw above in Section 2.6, any rotation can be expressed this way as long as $\theta \neq 0$.

The well-known Euler's forumula for complex numbers is

$$e^{i\theta} = \cos(\theta) + i\sin(\theta)$$

The corresponding formula for quaternions is

$$e^{\alpha(a_x i + a_y j + a_z k)} = \cos(\alpha) + (a_x i + a_y j + a_z k)\sin(\alpha)$$

To use this to represent rotations we set $\alpha = \theta/2$. Thus for an axis of rotation $K = (K_x, K_y, K_z)$ the quaternion representation of a rotation by θ around the axis K is

$$q = e^{\frac{\theta}{2}(K_x i + K_y j + K_z k)} = \cos(\theta/2) + (K_x i + K_y j + K_z k)\sin(\theta/2)$$

The magnitude of K is not used for rotation and often we require $|K| = 1$. The resulting quaternion is a unit quaternion.

To represent this quaternion without using i, j, k (for example in some software), we just write down the four components

$$q = \cos(\theta/2) + K_x i \sin(\theta/2) + K_y j \sin(\theta/2) + K_z k \sin(\theta/2) = [w, x, y, z] \tag{2.4}$$

$$w = \cos(\theta/2) \qquad x = K_x \sin(\theta/2) \qquad y = K_y \sin(\theta/2) \qquad z = K_z \sin(\theta/2)$$

$$q = [w, x, y, z] \tag{2.5}$$

Multiplication of quaternions is best left to the computer! If two quaternions are given by

$$q_1 = a_1 + b_1 i + c_1 j + d_1 k \qquad q_2 = a_2 + b_2 i + c_2 j + d_2 k$$

Their product is

$$q_{12} = a_1a_2 - b_1b_2 - c_1c_2 - d_1d_2 + (a_1b_2 + b_1a_2 + c_1d_2 - d_1c_2)i + (a_1c_2 - b_1d_2 + c_1a_2 + d_1b_2)j + (a_1d_2 + b_1c_2 - c_1b_2 + d_1a_2)k \tag{2.6}$$

or equivalently

$$q_{12} = \begin{matrix}[a_1a_2 - b_1b_2 - c_1c_2 - d_1d_2, & (a_1b_2 + b_1a_2 + c_1d_2 - d_1c_2), & (a_1c_2 - b_1d_2 + c_1a_2 + d_1b_2), \\ (a_1d_2 + b_1c_2 - c_1b_2 + d_1a_2)]\end{matrix}$$

whenever we write the product of two quaternions (i.e. $q_1 q_2$) we refer to this computation (which, like matrix multiplication, is not commutative).

The quaternion can be expressed as a rotation matrix as follows

$$R(q) = \begin{bmatrix} c\theta + K_x^2(1-c\theta) & K_xK_y(1-c\theta) - K_z s\theta & K_xK_z(1-c\theta) + K_y s\theta \\ K_yK_x(1-c\theta) + K_z s\theta & c\theta + K_y^2(1-c\theta) & K_yK_z(1-c\theta) - K_x s\theta \\ K_zK_x(1-c\theta) - K_y s\theta & K_zK_y(1-c\theta) + K_x s\theta & c\theta + K_z^2(1-c\theta) \end{bmatrix}$$

where $s\theta = \sin(\theta)$ and $c\theta = \cos(\theta)$. Equivalently, for $q = [w, x, y, z]$,

$$R(q) = \begin{bmatrix} 1 - 2y^2 - 2z^2 & 2(xy - wz) & 2(wy + xz) \\ 2(wz + yx) & 1 - 2x^2 - 2z^2 & 2(yz - xw) \\ 2(xz - wy) & 2(yz + xw) & 1 - 2y^2 - 2x^2 \end{bmatrix}$$

Since each quaternion corresponds to a rotation matrix, combining successive rotations represented by quaternions should be done in the same order as combining rotation matrices. I.e. if the next rotation is expressed as a quaternion in the local coordinate system, post-multply and if it is expressed in a fixed original coordinate system, pre-multiply.

Example 2.8

Two frames A and B, are initially aligned. Frame B is first rotated by 30° about the vector $[0.371, 0.557, 0.743]$. Then Frame B is further rotated by 45° about the vector $[0.684, 0.570, 0.456]$ (in the current frame). Find the quaternion representing the complete rotation.

$$q_1 = [\cos(15°), \quad 0.371\sin(15°), \quad 0.557\sin(15°), \quad 0.743\sin(15°)]$$
$$q_2 = [\cos(22.5°), \quad 0.684\sin(22.5°), \quad 0.570\sin(22.5°), \quad 0.456\sin(22.5°)]$$
$$q_{12} = q_1 q_2$$

Using the computer:

$$q_1 = [0.966, 0.096, 0.144, 0.193] \qquad q_2 = [0.924, 0.262, 0.218, 0.174]$$

$$q_{12} = q_1 q_2 = [0.802 \quad 0.325, \quad 0.377 \quad 0.330]$$

Example 2.9

A rotation is to be performed about the vector $Rv = (0, 1, 0)$ by 45°. Compute the quaternion to represent this rotation, and express it as a Rotation matrix.

First, $\theta = 45°$, and the axis of rotation, $K = [0, 1, 0]$, so using equation 2.5,

$$q = [\cos(\theta/2), \quad 0\sin(\theta/2), \quad 1\sin(\theta/2), \quad 0\sin(\theta/2)]$$
$$q = [.924, \quad 0, \quad .383, \quad 0]$$

Using either matrix form above,

$$R(q) = \begin{bmatrix} 0.707 & 0 & 0.707 \\ 0 & 1 & 0 \\ -0.707 & 0 & 0.707 \end{bmatrix}$$

Which is the expected result since q represents a rotation of 45° about the y axis.

Example 2.10
Using the quaternions q_1 and q_2 from Example 2.8, Compute their two rotation matrices, multiply them together, and compare the result with the matrix version of q_{12} from Example 2.8.

First, convert q_1, q_2 to rotation matrices:

```
-->Ra = quat2rot1(qtimes(q1,q2))
 Ra  =

    0.4988392  - 0.2837947    0.8199695
    0.7742173    0.5728992  - 0.2723774
  - 0.3917614    0.7701054    0.5051711

-->Rb = quat2rot1(q1) * quat2rot1(q2)
 Rb  =

    0.4987583  - 0.2839447    0.8202152
    0.7744610    0.5728083  - 0.2725517
  - 0.3919257    0.7703584    0.5050751
```

Comparing the results we see that the two matrices are nearly identical. More precisely, we can subtract the two matrices and find the maximum absolute error:

```
-->max(abs(Rb-Ra))
 ans  =

    0.0002530
```

Since the columns and rows of rotation matrices must have magnitude 1, we can see that this error is very small.

The inverse of a rotatation is the conjugate of the corresponding quaternion. If q is defined as in equation (2.4), then

$$q^* = \cos(\theta/2) - K_x i \sin(\theta/2) - K_y j \sin(\theta/2) - K_z k \sin(\theta/2) = [w, -x, -y, -z]$$

To use a quaternion for rotation of a point, if we define a point $P_1 = (P_x, P_y, P_z)$. To rotate it around axis K by θ, let

$$q_1 = \cos(\theta/2) + (K_x i + K_y j + K_z k) \sin(\theta/2)$$

and then

$$P_2 = q_1 \hat{P} q_1^* \tag{2.7}$$

where

$$\hat{P} = [0,\ P_X,\ P_Y,\ P_Z]$$

and the products are formed by quaternion-style multiplication.

Example 2.11
A rotation defined by a 63° rotation about the axis $[-0.349, 0.814, 0.465]$ is applied to the point, $P2 = [52.3, 67.0, -48.72]$. Find the new point using quaternions and compare it with the equivalent angle-axis method.

Using equation 2.2.7,

```
-->q4=quaternion([-.349,.814, .465], 63)
 q4  =

    0.8526402
  - 0.1822953
    0.4251816
    0.2428863

-->P2=[52.3,67,-48.72]
 P2  =

    52.3    67.  - 48.72

--> P2a = qtimes(q4, qtimes([0,P2],qcomp(q4)))
 P2a  =
    0.
  - 41.927377
    42.98847
  - 77.408106

// check by matrix rotation of point P2

-->R=quat2rot1(q4)
 R  =

    0.5204537  - 0.5692065    0.6364998
    0.2591720    0.8155493    0.5174062
  - 0.8136079  - 0.1043230    0.5719780

-->R*P2'
 ans  =
  - 41.927377
    42.98847
  - 77.408106
```

2.8 Side Topic: Rotations in higher dimensions

We have seen that at least three parameters are sufficient and necessary to specify rotation in three dimensions. Is it a coincidence that 3 dimensional space has 3 rotation parameters? Any hope for this simple rule is dashed by considering that only 1 orientation parameter is needed in 2 dimensions. How many parameters are required to specify rotations of a 4 dimensional object?

We will use definition 4 to rephrase and generalize the question: How many parameters does it take to specify an $n \times n$ orthonormal matrix?

The total number of matrix elements is n^2. Then there are two sets of constraints:

1. $C_i \cdot C_j = 0$
2. $|C_i| = 1$

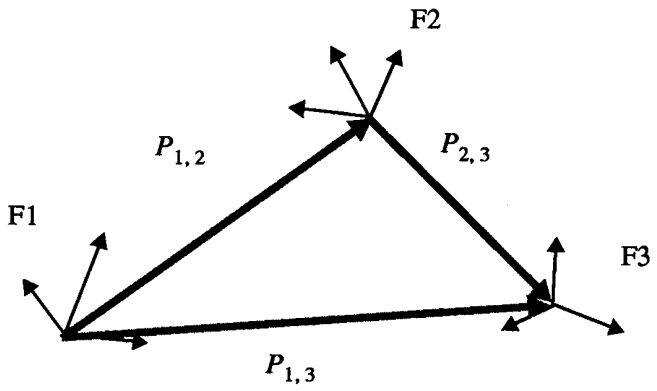

Figure 2.7: Three frames which are offset from each other in position and orientation. Vectors show displacements between the origins of the frames.

where C_i is the ith column of the matrix.

The number of constraints due to the first condition is

$$\binom{n}{2} = \frac{n!}{2(n-2)!}$$

and the number of constraints of the second type is n. So the total number of parameters is the number of matrix elements minus the number of constraints:

$$N = n^2 - \frac{n!}{2(n-2)!}$$

which can be simplified to

$$N = \frac{1}{2}(n^2 - n)$$

So for a four dimensional object we need 6 parameters and for a 10 dimensional one we need 45 parameters(!).

2.9 Homogeneous Transformation

Considering several nice properties of the Rotation Matrix, in this Section, we will find a way to add translation to our matrix description of the configuration of a rigid object. Earlier we used the x, y, z coordinates of the origin of a frame attached to an object, with the rotation matrix of that frame, to have its configuration completely specified relative to some "base frame," B i.e.

$$\text{configuration} = \{{}^B x, {}^B y, {}^B z, {}^B_0 R\}$$

More generally, this gives us a way to relate frames to each other. Suppose we have a series of frames with different positions and orientations, and some relations between them as in Figure 2.7.

We can pose the following questions about these three frames:

If we know $P_{1,2}, P_{2,3}, {}^1_2R, {}^2_3R$, what is $P_{1,3}, {}^1_3R$?

Consider a point expressed in frame 3, ${}^3P$. It can be expressed in frame 2 by the affine transformation

$${}^2P = P_{2,3} + {}^2_3R\, {}^3P$$

and in frame 1 by

$${}^1P = P_{1,2} + {}^1_2R(P_{2,3} + {}^2_3R\, {}^3P)$$

Equivalently,

$${}^1P = \underbrace{P_{1,2} + {}^1_2RP_{2,3}} + \underbrace{{}^1_2R\, {}^2_3R}\, {}^3P$$

from which we can conclude

$$P_{1,3} = P_{1,2} + {}^1_2RP_{2,3} \qquad {}^1_3R = {}^1_2R\, {}^2_3R$$

Although the preceding can be used as a general way to represent the spatial relationships between objects and robots, it is messy because we must add as well as multiply. This is a problem because we often have to represent a series of these transforms which yields ever more complicated expressions.

An alternative is presented by "homogeneous coordinates" which cleverly use an additional dimension to reduce the affine transformation to pure matrix multiplication. We define the homogeneous transform

$$^1P = {}^1_2T\,{}^2P$$

where

$${}^1_2T = \begin{bmatrix} \begin{bmatrix} & {}^1_2R & \end{bmatrix} & \begin{bmatrix} {}^1P_{1,2} \\ \end{bmatrix} \\ \begin{bmatrix} 0 & 0 & 0 \end{bmatrix} & 1 \end{bmatrix}$$

This 4×4 matrix compactly describes both the rotation and the position offset. When we work with homogeneous transforms, we augment our position vectors by adding a 1 in the fourth position. i.e.

$$^1P = \begin{bmatrix} {}^1P_x \\ {}^1P_y \\ {}^1P_z \\ 1 \end{bmatrix}$$

in the example above,

$$^1P = {}^1_2\,T\,{}^2P = \begin{bmatrix} \begin{bmatrix} & {}^1_2R & \end{bmatrix} & \begin{bmatrix} {}^1P_{1,2} \\ \end{bmatrix} \\ \begin{bmatrix} 0 & 0 & 0 \end{bmatrix} & 1 \end{bmatrix} \begin{bmatrix} {}^2P_x \\ {}^2P_y \\ {}^2P_z \\ 1 \end{bmatrix}$$

$$= \begin{bmatrix} {}^1_2R_{[1]} \cdot {}^2P + {}^1P_{1,2_{[1]}} \\ {}^1_2R_{[2]} \cdot {}^2P + {}^1P_{1,2_{[2]}} \\ {}^1_2R_{[3]} \cdot {}^2P + {}^1P_{1,2_{[3]}} \\ 1 \end{bmatrix} = \begin{bmatrix} {}^1P_{1,2} + {}^1_2R\,{}^2P \\ 1 \end{bmatrix}$$

where ${}^1_2R_{[i]}$ represents row i of ${}^1_2R$, and ${}^2P + {}^1P_{1,2_{[i]}}$ represents the ith element of ${}^1P_{1,2}$. Notice that the final expression is completely equivalent to multiplying by a rotation matrix and then adding a translation.

With homogeneous transformations at our disposal, a series of spatial replationships can be expressed by a series of matrix multiplications as with pure rotation. For example, solving the problem posed above for the three frames, $F1, F2, F3$,

$${}^1_3T = {}^1_2T\,{}^2_3T$$

which is more compact indeed.

Homogeneous Transformation Definitions The homogeneous transformation has definitions analogous to those we made for rotation:

The homogeneous transformation ${}^A_BT$ is

1. A matrix which specifies frame B in terms of frame A.
2. A matrix which maps a point represented in frame B, ${}^BP$, to its representation in frame A, ${}^AP$.
3. A description of an operator, perhaps corresponding to a physical move, *from* frame A, *to* frame B.
4. A 4×4 matrix with the structure given above.

Example 2.12

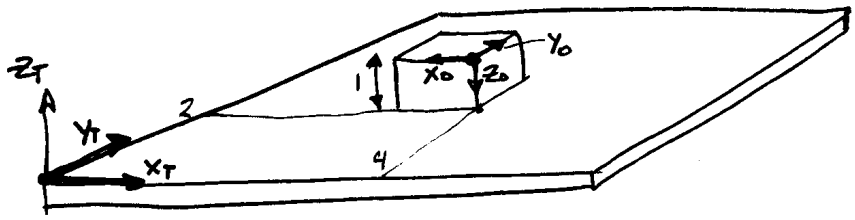

Find the 4×4 homogeneous transformation which represents the configuration of the box on the table. Frame 0 is placed on a corner of the box and frame T is at a corner of the table such that X_T and Y_T are in the plane of the table top.
Question: What is ${}^{T}_{0}T$?
Answer: First, find the translation offset between the origin of the box frame (O) and the table frame (T):

$$ {}^{T}P_O = \begin{bmatrix} 4 \\ 2 \\ 1 \end{bmatrix} $$

Then, identify the rotation matrix. First, align the frames by redrawing frame O without the offset superimposed on T. Then write each column of ${}^{T}_{O}R$. Each column is the vector $\{x_O, y_O, z_O\}$ written in frame T:

$$ {}^{T}_{O}R = \begin{bmatrix} -1 & 0 & 0 \\ 0 & 1 & 0 \\ 0 & 0 & -1 \end{bmatrix} $$

The homogeneous transform is thus:

$$ \begin{bmatrix} -1 & 0 & 0 & 4 \\ 0 & 1 & 0 & 2 \\ 0 & 0 & -1 & 1 \\ 0 & 0 & 0 & 1 \end{bmatrix} $$

Example 2.13

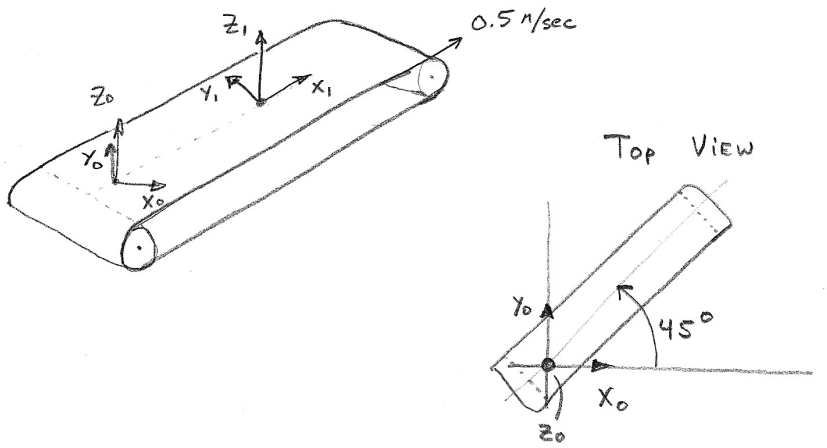

Two frames are on a conveyor belt. We have the following facts about the system

- The belt runs at 0.5 meters/sec.
- The belt is in the $\{X_0, Y_0\}$ plane.
- The belt is oriented 45° from the X_0 axis as shown in the "Top View".
- The origin of Frame F_1 is aligned with the origin of F_0 at $t = 0$.
- Frame F_1 moves with the belt but Frame F_0 does not.
- X_1 is pointing along the belt (same direction as belt velocity.)

Find the 4x4 homogenous transform (which is a function of time) of F_1
Answer:
O: The origin of F_1 is a function of time moving along the belt.

$$O = \begin{bmatrix} 0.5t\cos(45^\circ) \\ 0.5t\sin(45^\circ) \\ 0 \end{bmatrix} = [0.35t, \quad 0.35t, \quad 0]^T$$

Rotation = $rot(\hat{z}, 45^\circ)$

$$\begin{bmatrix} 0.707 & -0.707 & 0 \\ 0.707 & 0.707 & 0 \\ 0 & 0 & 1 \end{bmatrix}$$

$$^0_1T = \begin{bmatrix} 0.707 & -0.707 & 0 & 0.35t \\ 0.707 & 0.707 & 0 & 0.35t \\ 0 & 0 & 1 & 0 \\ 0 & 0 & 0 & 1 \end{bmatrix}$$

2.9.1 Inverse of Homogeneous Transforms

We will frequently need the inverse of the 4x4 homogeneous transform matrix. It seems intuitive that this inverse always exists because physical rotations and translations can always be "undone." It is straightfoward to derive the inverse of the 4x4 homogeneous transform,

Consider mapping a point in frame B to its value in frame A with both translation and rotation:

$$^{A}P = {}^{A}_{B}T\,{}^{B}P = {}^{A}O + {}^{A}_{B}R\,{}^{B}P$$

Where ^{A}O is the origin of frame B expressed in A. To invert this we seek a 4x4 matrix, $({}^{A}_{B}T)^{-1}$ such that

$$^{B}P = ({}^{A}_{B}T)^{-1}\,{}^{A}P$$

Solving

$$\begin{aligned} {}^{B}P &= ({}^{A}_{B}R)^{-1}({}^{A}P - {}^{A}O) \\ &= {}^{B}_{A}R\,{}^{A}P - {}^{B}_{A}R\,{}^{A}O \end{aligned}$$

$${}^{A}_{B}T^{-1} = \begin{bmatrix} \begin{bmatrix} & {}^{A}_{B}R^{T} & \end{bmatrix} & \begin{bmatrix} -{}^{A}_{B}R^{T}\,{}^{A}O \end{bmatrix} \\ \begin{bmatrix} 0 & 0 & 0 \end{bmatrix} & \begin{bmatrix} 1 \end{bmatrix} \end{bmatrix}$$

You can verify this by showing that $TT^{-1} = I_{4\times4}$.

2.10 Transform Equations

It is useful to develop a slightly more formal description of the relationships between frames. Spatial relationships can be expressed as transforms, products of transforms, or transform graphs. Transform graphs are directed graphs. Links specify transform matrices between frames. We represent a transform between two frames A, and B, by

$$A \rightarrow B$$

The arrow above is a graphical representation of ${}^{A}_{B}T$ and also of ${}^{B}_{A}T^{-1}$. A series of links (a path) in the transform graph corresponds to *post* multiplication of the transforms in the direction of the path.

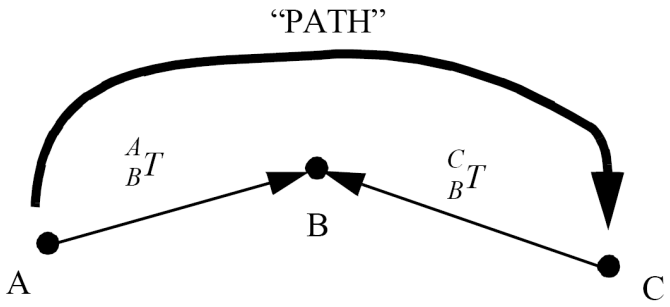

Figure 2.8: A path is a directed arrow along a chain of transformations.

The transform which shows the PATH in Figure 2.8 is therefore:

$${}^{A}_{C}T = \quad {}^{A}_{B}T({}^{C}_{B}T)^{-1} = \quad {}^{A}_{B}T\,{}^{B}_{C}T$$

In the first right hand side, ${}^{C}_{B}T$ is inverted because it represents an arrow which goes opposite to the path. A closed path in such a graph can be cut at two nodes to form a tranform equation.

In Figure 2.9, the loop is cut at nodes U and C, and the two paths, P1, and P2 represent the same displacement. Each path corresponds to an equation

$$\text{P1}: \quad {}^{U}_{C}T = {}^{U}_{A}T\;{}^{B}_{A}T^{-1}\;{}^{B}_{C}T$$

$$\text{P2}: \quad {}^{U}_{C}T = {}^{U}_{D}T\;{}^{D}_{C}T$$

And, we can equate the two right hand sides:

$${}^{U}_{A}T\;{}^{B}_{A}T^{-1}\;{}^{B}_{C}T = {}^{U}_{D}T\;{}^{D}_{C}T$$

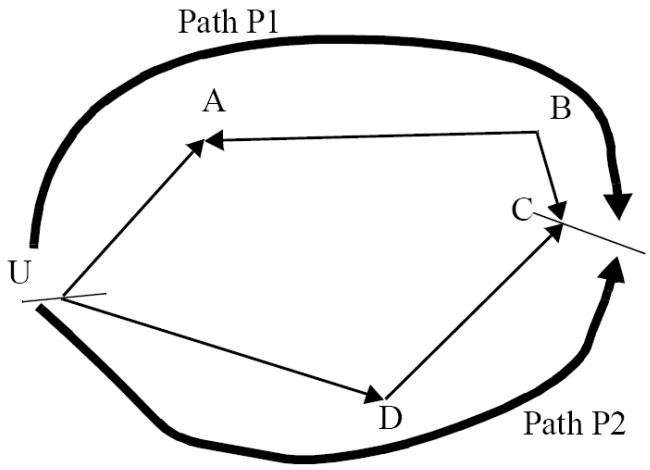

Figure 2.9: Two paths which start and end at the same point define an equation.

Furthermore, we can write the equation for a big path going completely around the loop in, for example, the clockwise direction:

$$P1(P2)^{-1} = {}^{U}_{C}T\ {}^{U}_{C}T^{-1} = I_{4\times 4}$$

This is expected since by going completely around the loop we wind up in our original configuration or frame. Note that when we interpret it as a homogeneous transform, $I_{4\times 4}$ corresponds to

$$\text{Rot}(x,0), \text{Trans}\left(\begin{bmatrix} 0 \\ 0 \\ 0 \end{bmatrix}\right)$$

Example 2.14

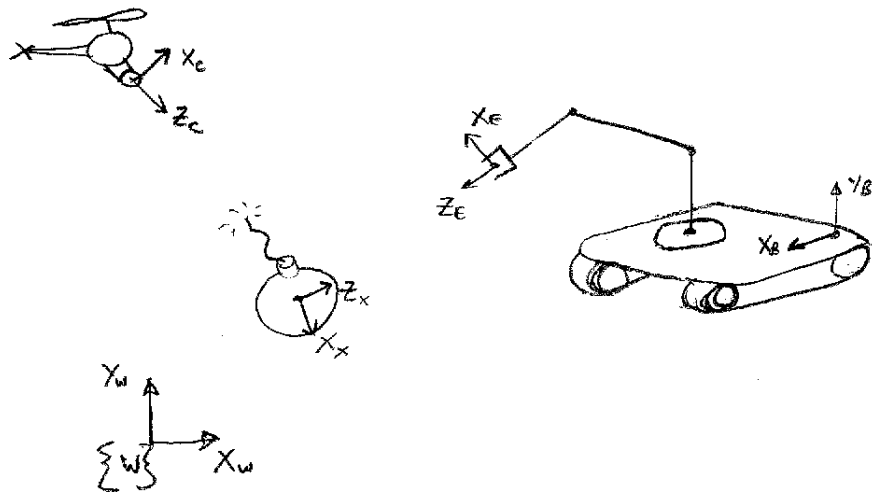

A helicopter mounted camera identifies the location and orientation of a bomb. A bomb disposal robot must understand how to move its arm to pick up the bomb. The following transforms are known: ${}^{C}_{W}T, {}^{C}_{X}T, {}^{B}_{C}T, {}^{B}_{E}T$
A) Draw the transform graph
B) Solve for ${}^{X}_{B}T$
C) Solve for ${}^{W}_{E}T$
Answer:
A)

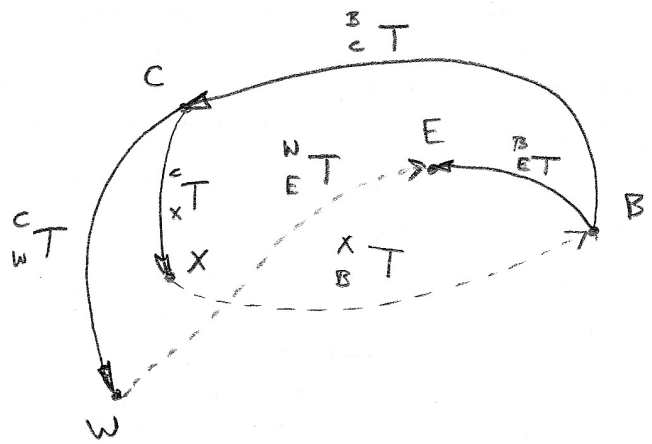

B)

$$ {}^{X}_{B}T = ({}^{C}_{X}T)^{-1}({}^{B}_{C}T)^{-1} $$

C)

$$ {}^{W}_{E}T = ({}^{C}_{W}T)^{-1}({}^{B}_{C}T)^{-1}{}^{B}_{E}T $$

Example 2.15

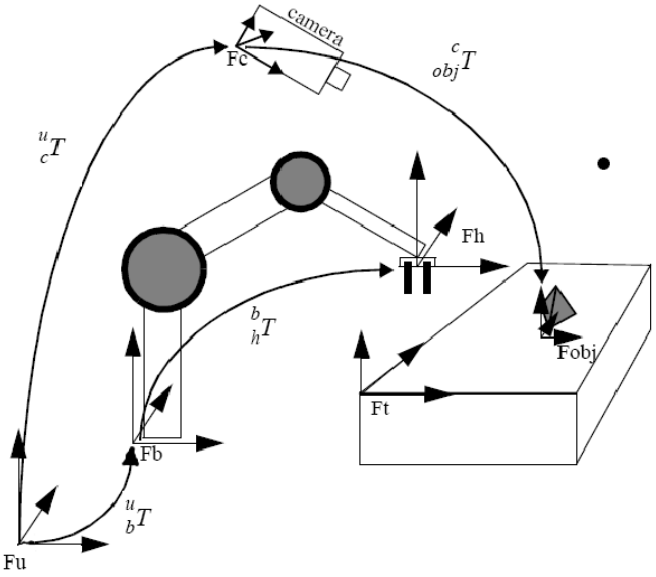

Lets consider a factory workstation with a robot arm, worktable, vision camera, and an object on the table. The known spatial relationships are shown by links in the diagram. Suppose we need to specify the position and orientation of the object so that the robot can pick it up. The robot controller must have the configuration in Fb, the base frame of the robot.

Q1: What is the configuration of the object in Fb?

A1: The object can be "reached" by a path in the transform graph from Fb through Fu, and Fc, to Fobj. Note that the first link has a direction opposite to the path we take to the object. The equation of this path is:

$$^{b}_{obj}T = ^{u}_{b}T^{-1}\ ^{u}_{c}T\ ^{c}_{obj}T$$

Q2: Suppose we want to find the unknown transforms $^{h}_{t}T, ^{t}_{obj}T$?

A2: If we add these two transforms to the graph (draw them in yourself), we now have a loop. We can cut this loop at any two points to make an equation. Suppose we make these cuts at the hand and at the object. Now we have

$$^{b}_{h}T^{-1}\ ^{u}_{b}T^{-1}\ ^{u}_{c}T\ ^{c}_{obj}T = ^{h}_{t}T\ ^{t}_{obj}T$$

Since the two transforms on the right hand side are unknown, we cannot solve this without another equation. Now suppose we go out to the factory floor and measure the location and orientation of the table. This gives us $^{u}_{t}T$. Drawing this link into the transform graph, we see that another loop is formed tangent to the original loop so that we have another equation. One such equation is

$$^{u}_{b}T\ ^{b}_{h}T\ ^{h}_{t}T = ^{u}_{t}T$$

We can solve this for one of our unknowns giving:

$$^{h}_{t}T = ^{b}_{h}T^{-1}\ ^{u}_{b}T^{-1}\ ^{u}_{t}T$$

Then we substitute to get

$$^{b}_{h}T^{-1}\ ^{u}_{b}T^{-1}\ ^{u}_{c}T\ ^{c}_{obj}T = ^{b}_{h}T^{-1}\ ^{u}_{b}T^{-1}\ ^{u}_{t}T\ ^{t}_{obj}T$$

$$^{c}_{obj}T = ^{u}_{c}T^{-1}\ ^{u}_{t}T\ ^{t}_{obj}T$$

Example 2.16
A revitalized GM plant has installed massive assembly robots. Such a robot arm must install the engine into a car body. Frames have been applied to the body and engine as shown below.

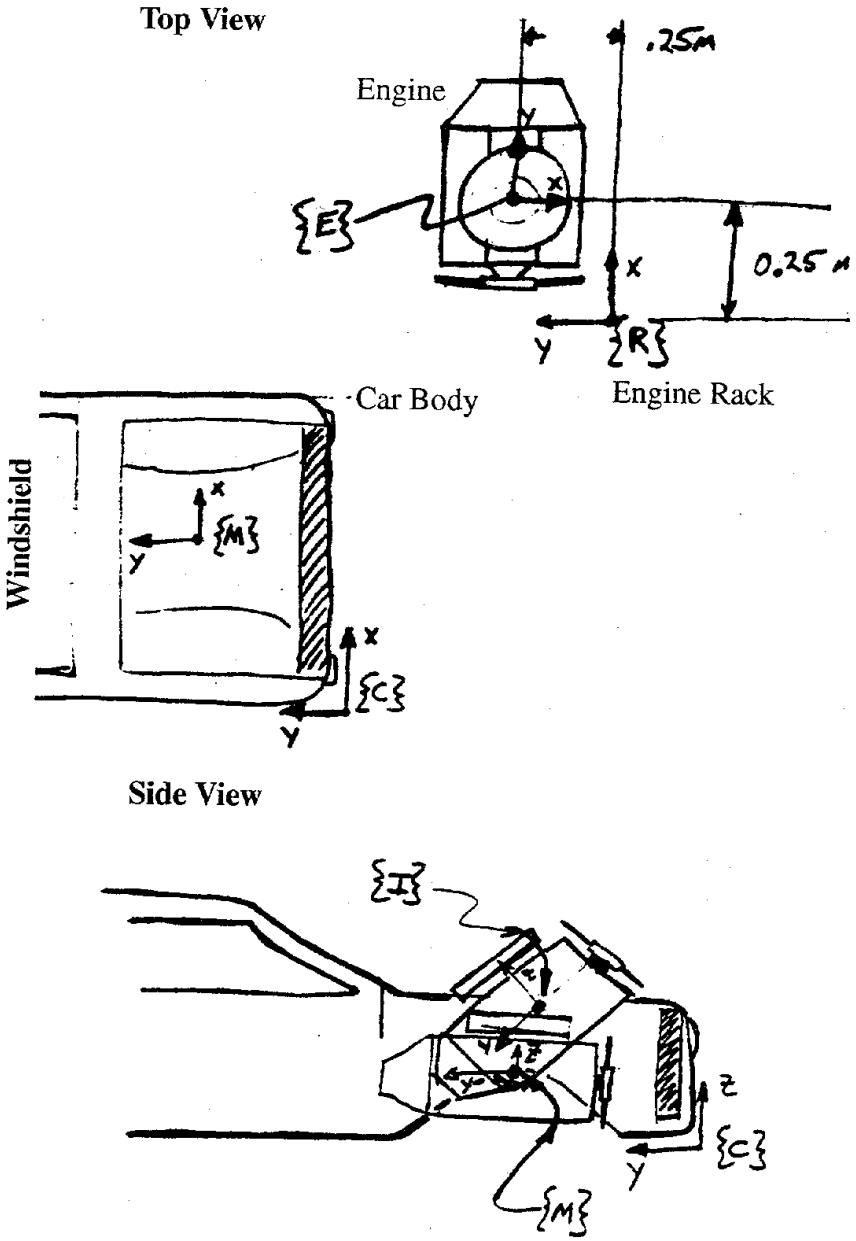

The following facts are known:

1. The engine must be lowered through an intermediate position in order for the transmission to clear the body. This position is ${}^{M}_{I}T$. Then the engine will be moved into its final position, ${}^{M}_{C}T$.
2. The car and engine rack are located at known tranforms ${}^{U}_{C}T$, and ${}^{U}_{R}T$ respectively.
3. GM has finally switched over to the metric system!

Questions:
Q1) Give the transform (in numerical form) which specfies the engine position in the rack, ${}^{R}_{E}T$. Assume that the z position coordinate is zero.

Example 2.16 cont.

Solution

Obtain the rotation matrix by writing the unit vectors of E expressed in R, *or* evaluating $\text{Rot}(\hat{z}, -90°)$.

$$ {}^{R}_{E}T = \begin{bmatrix} 0 & 1 & 0 & 0.25 \\ -1 & 0 & 0 & 0.25 \\ 0 & 0 & 1 & 0 \\ 0 & 0 & 0 & 1 \end{bmatrix} $$

Q2) You need to program the robot to take the engine from the rack and put it in the intermediate position. Solve for the transform which represents the intermediate engine position and orientation relative the engine rack, ${}^{R}_{I}T$ in terms of the known transforms above.

Solution

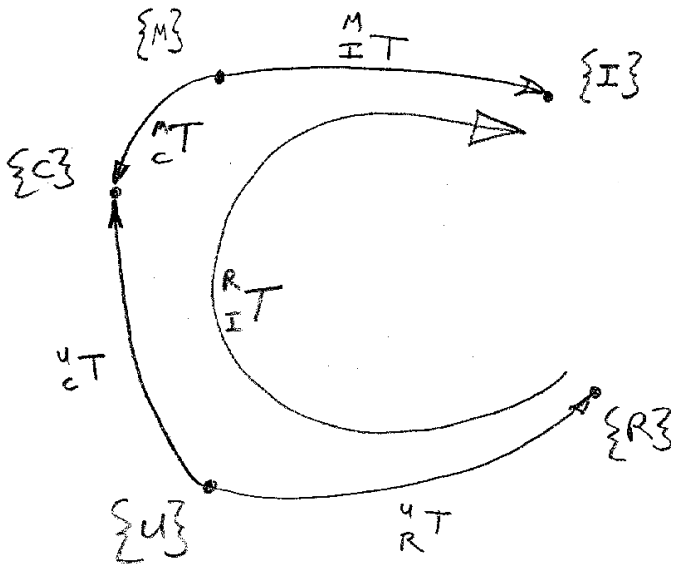

going around the transform graph in the direction shown, we have:

$$ {}^{R}_{I}T \quad = \quad {}^{U}_{R}T^{-1} \quad {}^{U}_{C}T \quad {}^{M}_{C}T^{-1} \quad {}^{M}_{I}T $$

Example 2.17

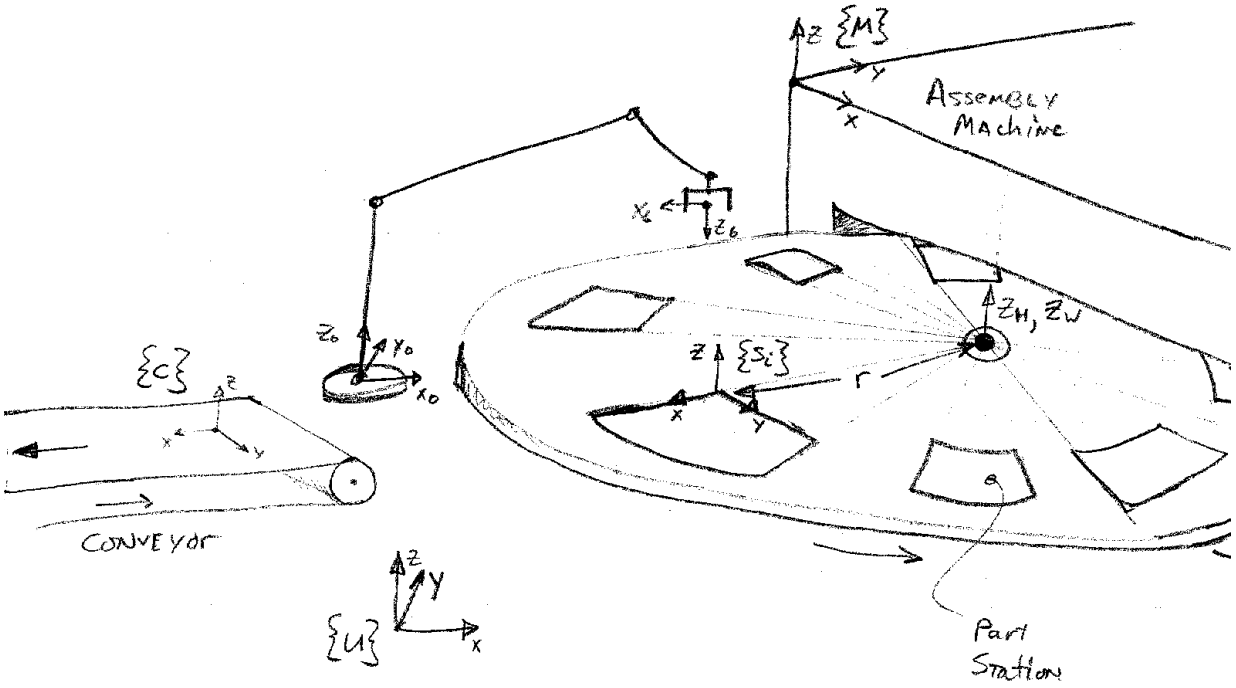

Pizza Problem

Completed assemblies (pizzas?) come out of a machine on a large rotary table. You must program a robot arm to pick up the pizzas and transfer them to a conveyer.
Use the following facts:

- The part stations are spaced every 36° on the wheel.
- The robot base frame is {0} and the end effector frame is {6}.
- The origin of frame H is located at the wheel hub:

$$ {}^{U}_{H}T = \begin{bmatrix} 1 & 0 & 0 & 10 \\ 0 & 1 & 0 & 10 \\ 0 & 0 & 1 & 2 \\ 0 & 0 & 0 & 1 \end{bmatrix} $$

- The i^{th} part station has frame $\{S_i\}$ located at its corner. The distance from the origin of $\{H\}$ to the origin of $\{S_i\}$ is $r = 5$.
- Another frame $\{W\}$ has the same origin as $\{H\}$, but X_W always points to the origin of $\{S_1\}$.
- The front panel of the machine is at

$$ {}^{U}_{M}T = \begin{bmatrix} 0 & 1 & 0 & 10 \\ -1 & 0 & 0 & 16 \\ 0 & 0 & 1 & 4 \\ 0 & 0 & 0 & 1 \end{bmatrix} $$

- $\Theta_W(t)$ describes the rotation of the wheel. Θ_W is the angle from X_H to X_W.

Example 2.17 cont.
Q1: If t is in seconds, $\Theta_W(t) = \frac{\pi}{15}t$ rad or $\Theta_W(t) = 12t$ degrees, what is ${}^U_S T(i,t)$, i.e. what is the transform from frame U to frame S_i (multiply out your answer).

Solution:

$$ {}^U_{Si}T \quad = \quad {}^U_H T \quad {}^H_W T \quad {}^W_{Si} T $$

From the facts,

$$ {}^H_W T = \text{Rot}(\hat{z}, 12t^\circ) $$

$$ {}^W_{Si} T = \text{Rot}(\hat{z}, (36(i-1))^\circ) $$

$$ {}^U_H T \quad = \quad \begin{bmatrix} 1 & 0 & 0 & 10 \\ 0 & 1 & 0 & 10 \\ 0 & 0 & 1 & 2 \\ 0 & 0 & 0 & 1 \end{bmatrix} $$

Since the last two are both about the $\hat{z}$ axis, we can add their displacements to simplify. Let

$$ \alpha = (12t + 36(i-1))^\circ $$

Then

$$ {}^U_{Si}T \quad = \quad \begin{bmatrix} 1 & 0 & 0 & 10 \\ 0 & 1 & 0 & 10 \\ 0 & 0 & 1 & 2 \\ 0 & 0 & 0 & 1 \end{bmatrix} \text{Rot}(\hat{z}, \alpha) $$

$$ {}^U_{Si}T \quad = \quad \begin{bmatrix} 1 & 0 & 0 & 10 \\ 0 & 1 & 0 & 10 \\ 0 & 0 & 1 & 2 \\ 0 & 0 & 0 & 1 \end{bmatrix} \begin{bmatrix} c\alpha & -s\alpha & 0 & 0 \\ s\alpha & c\alpha & 0 & 0 \\ 0 & 0 & 1 & 0 \\ 0 & 0 & 0 & 1 \end{bmatrix} $$

$$ {}^U_{Si}T \quad = \quad \begin{bmatrix} c\alpha & -s\alpha & 0 & 10 \\ s\alpha & c\alpha & 0 & 10 \\ 0 & 0 & 1 & 2 \\ 0 & 0 & 0 & 1 \end{bmatrix} $$

Q2: If ${}^U_0 T, \quad {}^0_6 T, \quad {}^U_S T(i,t)$ are known, draw a transform graph, and solve for ${}^6_S T(i,t)$.

Solution:

Transform Graph:

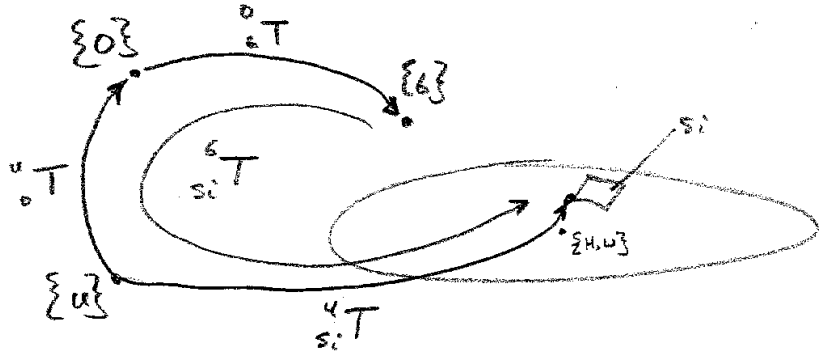

$$ {}^6_{Si}T \quad = \quad {}^0_6 T^{-1} \quad {}^U_0 T^{-1} \quad {}^U_{Si} T $$

2.11 Exponential Coordinates

The following elegant notation and derivation is based closely on **Murray, Li, and Sastry, "A Mathematical Introduction to Robotic Manipulation", CRC Press, 1994.**

2.11.1 Rotation

Consider the velocity of a point q which is rotating about an axiz ω. We assume that $|\omega| = 1$ and its direction is the axis of rotation. We can write the velocity of the point as

$$\dot{q}(t) = \omega \times q(t)$$

Recall that the vector cross product ($\times$) can be represented as the product of a special skew-symmetric matrix,

$$\hat{\omega} = \begin{bmatrix} 0 & -\omega_3 & \omega_2 \\ \omega_3 & 0 & -\omega_1 \\ -\omega_2 & \omega_1 & 0 \end{bmatrix}$$

with the vector, i.e.

$$\omega \times q = \hat{\omega} q$$

So we have

$$\dot{q}(t) = \hat{\omega} q(t)$$

This is a first order differential equation with the solution

$$q(t) = e^{\hat{\omega} t} q(0)$$

Now we need to understand what it means to take the exponential of a matrix! Using the Taylor series expansion, we have:

$$\exp(A) = I + A + \frac{A^2}{2!} + \frac{A^3}{3!} + ...$$

We are interested in the special case of

$$A = \hat{\omega} t$$

where $\hat{\omega}$ is the matrix defined as above and t is a scalar (time). One interpretation is that we can parameterize any rotation by the amount of time it takes at unit velocity ($|\omega| = 1$). Thus we can also write

$$R(\omega, \Theta) = e^{\hat{\omega}\Theta}$$

where

$$\Theta = |\omega| t$$

To evaluate the matrix exponential, we sort the series out into odd and even terms (and perform a few other tricks) to get:

$$e^{\hat{\omega}\Theta} = I + \left(\Theta - \frac{\Theta^3}{3!} + \frac{\Theta^5}{5!} + \dots\right)\hat{\omega} + \left(\frac{\Theta^2}{2!} + \frac{\Theta^4}{4!} + \frac{\Theta^6}{6!} + \dots\right)\hat{\omega}^2$$

Which simplifies to

$$e^{\hat{\omega}\Theta} = I + \hat{\omega}\sin\Theta + \hat{\omega}^2(1 - \cos\Theta)$$

So $e^{\hat{\omega}\theta}$ is the rotation matrix which expresses rotation by θ about axis ω.

This can also be inverted (See Murray, Li, Sastry, equations (2.17) and (2.18), or Craig, equations (2.81) and (2.82)):

$$\theta = cos^{-1}\left(\frac{r_{11} + r_{22} + r_{33} - 1}{2}\right) \tag{2.8}$$

$$\omega = \frac{1}{2sin\theta}\begin{bmatrix} r_{32} - r_{23} \\ r_{13} - r_{31} \\ r_{21} - r_{12} \end{bmatrix} \tag{2.9}$$

2.11.2 Translation and Rotation

Consider a point, $p(t)$ whos position is a function of time. Assume that the point is displaced due to rotation about an axis, ω, separate from the point. We assume that $|\omega| = 1$ and that q is a point **off** the axis. The velocity of the point is then

$$\dot{p}(t) = \omega \times (p(t) - q)$$

or

$$\dot{p}(t) = \omega \times p(t) - \omega \times q$$

Using $\hat{\omega}$ as defined above, if we define

$$\hat{\xi} = \begin{bmatrix} \hat{\omega} & -\omega \times q \\ 0 & 0 \end{bmatrix}$$

and we express $p(t)$ and its derivative in homogeneous coordinates,

$$\dot{p} = \begin{bmatrix} \hat{\omega} & -\omega \times q \\ 0 & 0 \end{bmatrix} \begin{bmatrix} p \\ 1 \end{bmatrix}$$

In this special case (of rotation about an axis remote from ω) the velocity of the point p is $-\omega \times q$. More generally, we can write

$$\dot{p} = \begin{bmatrix} \hat{\omega} & v \\ 0 & 0 \end{bmatrix} \begin{bmatrix} p \\ 1 \end{bmatrix}$$

More compactly:

$$\dot{p} = \hat{\xi} p$$

the matrix $\hat{\xi}$ is refered to as a *twist*.

This is a first order differential equation which has the solution:

$$p(t) = e^{\hat{\xi} t} p(0).$$

Recall that $\hat{\xi}$ doesn't have as simple a form as $\hat{\omega}$ and so it is not as easy to get an expression for $e^{\hat{\xi} t}$. It can be shown that (see Murray, Li, and Sastry, Proposition 2.8) that for a displacement which consists of rotation $\hat{\omega}\Theta$ and displacement $v\theta$

$$e^{\hat{\xi}\theta} = \begin{bmatrix} e^{\hat{\omega}\theta} & (I - e^{\hat{\omega}\theta})(\omega \times v) + \omega\omega^T v\theta \\ 0 & 1 \end{bmatrix} \tag{2.10}$$

As used here, θ is a general motion parameter and need not be an angle. The interpretation of $e^{\hat{\xi}\theta}$ is a description of a physical manipulation i.e.

$${}^A p(\theta) = e^{\hat{\xi}\theta} {}^A p(0)$$

Note that both ${}^A p(\theta)$ and ${}^A p(0)$ are represented in the same frame, A, which should also be the same as that used for ω and v.

To represent a known physical displacement as a twist, we first must know the 4x4 homogeneous transform defining the displacement, ${}^A_B T$ which the authors call g_{ab}. Given g_{ab}, we solve for the "twist coordinates", ω, θ, v equating (2.10) with the known g:

$$g = \begin{bmatrix} R & P \\ 0 & 1 \end{bmatrix} = \begin{bmatrix} e^{\hat{\omega}\theta} & (I - e^{\hat{\omega}\theta})(\omega \times v) + \omega\omega^T v\theta \\ 0 & 1 \end{bmatrix}$$

for

$$R = e^{\hat{\omega}\theta}$$

we had equation (2.8 and (2.9) to find θ and ω. To get v, we have

$$P = (I - e^{\hat{\omega}\theta})(\omega \times v) + \omega\omega^T v\theta$$

which we can solve by hand calculation or Mathematica for v. There are some useful special cases. For example for a simple axis such as

$$\omega = \begin{bmatrix} 0 \\ 0 \\ 1 \end{bmatrix}$$

the equation to solve is

$$\begin{bmatrix} s\theta & c\theta - 1 & 0 \\ 1 - c\theta & s\theta & 0 \\ 0 & 0 & \theta \end{bmatrix} v = P$$

In the special case of revolute motion about the axis ω, v is only due to the rotation and so it is known:

$$v = -\omega \times q$$

2.11.3 Groups

Murray, Li, and Sastry take some pains to relate these kinematic ideas to group theory. The basic properties of a group are

- It consists of a set of objects, G and a binary operation, $\times$.
- It is "closed" in the sense that if any two objects in the group are applied to the binary operation, the result is another member of the group.
- There exists an "identity element", i, which is a member of the group such that $g \times i = g$.
- For every element of the group, g, there is a unique inverse, also a an element of the group, g^{-1} such that $g \times g^{-1} = i$.
- The operation is associative: $(g_1 \times g_2) \times g_3 = g_1 \times (g_2 \times g_3)$.

For example, you can verify that these five properties hold for the set of orthonormal 3x3 rotation matrices together with the operation of matrix multiplication, and so they must form a group.

Murray, Li, and Sastry named four groups which are relevant to robotic manipulation:

$se(3)$ the group of 4x4 skew symmetric matrices (twists)

$so(3)$ the group of 3x3 skew symmetric matrices ($\hat{\omega}$).

$SE(3)$ the group of 4x4 homogeneous transforms

$SO(3)$ the group of 3x3 orthonormal rotation matrices

2.12 Summary of Notation

Chapter 3

Forward Kinematics

3.1 Problem Statement and Learning Objectives

Problem Statement This chapter addresses the problem of computing the position and orientation of an end effector, knowing the geometry of the manipulator and the position values of each joint. Joints may be rotary in which case the joint value is an angle, or prismatic, in which case the joint value is a displacement. We seek a general way to represent any serial manipulator.

Learning Objectives After completing this chapter, the student will be able to derive the forward kinematic model of a serial manipulator. Specifically to

- Identify the link and joint geometry from a picture or engineering drawing of a serial mechanism containing rotary and prismatic joints.
- Be able to assign a coordinate system to each link in a standardized manner.
- Be able to derive Denavit-Hartenberg parameters for each link
- Be able to form the 4x4 homogeneous transform for each link based on the DH parameters and be able to multiply these link matrices together to get a symbolic expression for the forward kinematic equations in the form of a 4x4 homogenous transform matrix.

The result is a computation of the position and orientation of the end effector knowing the geometric dimensions of each link and the position of each joint in the mechanism.

3.2 Serial Mechanisms

3.2.1 Links and Joints

Links

In this chapter we study the spatial relationships (transforms) between the links of a robot arm. First we define an *axis of motion* as

> A line in 3-space which contains points which are not moved by a particular rotation (a *rotary* axis), or which contains a direction describing linear motion (a *translation* axis).

We will define a *link* as

> A spatial relation, enforced by a rigid object, between two axes of motion.

In a typical robot arm, the links are rigid structural elements (most often of metal) which hold at each end the bearings for a joint. Their rigidity enforces a constant spatial relationship between axes of motion at the *proximal* (closer to the base) and *distal* (closer to the end effector) ends.

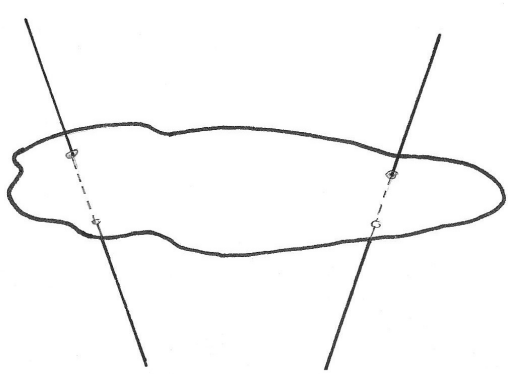

Figure 3.1: "Link", a rigid body which enforces a fixed spatial relationship between two axes of motion.

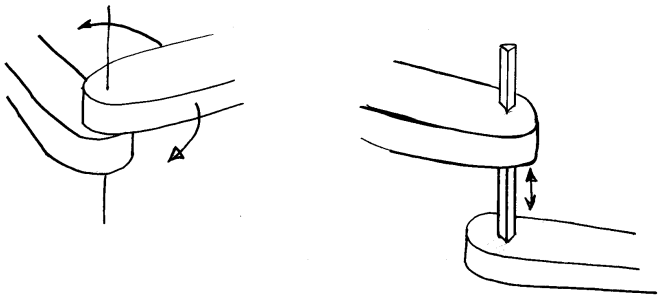

Figure 3.2: Two types of joints, rotational and translational/prismatic.

Joints

Joints connect the links in a serial kinematic chain. We define a joint as

> A structural element which allows relative motion between two bodies in only one degree of freedom. Such motion is constrained to translational motion along a line or rotation around a line.

We have two classes of joints, *rotational* and *translational*, also known as *prismatic*[1]. Combining the definitions of link and joint, we see that each axis of motion is fixed in the two links adjoining the joint. The degree of translation or rotation (the single motion freedom of the joint) is called the joint variable. Since the joint constrains relative motion of the two links to a single degree of freedom, the joint variable is sufficient to describe the spatial relationship between them.

A series of such links bridging adjacent axes is an open kinematic chain (also known as a robot arm!). The *forward kinematics* problem is to find the position and orientation of the last link in the chain (i.e. the robot hand) knowing only the robot's geometry and the angles or displacements of the joints. To make our method general, we will assume that there can be any amount of twiset, displacement, and offset between the ends of each link. This make the problem difficult unless we employ a systematic approach. We will use the approach invented by Denavit and Hartenberg in which we will construct a virtual kinematic chain which is equivalent to the original robot but is easier to analyze. The virtual kinematic chain in the "DH" method consists of the joint axes and their *common normals*. The common normal between two lines or axes is a unique[2] line which is perpendicular to both axes.

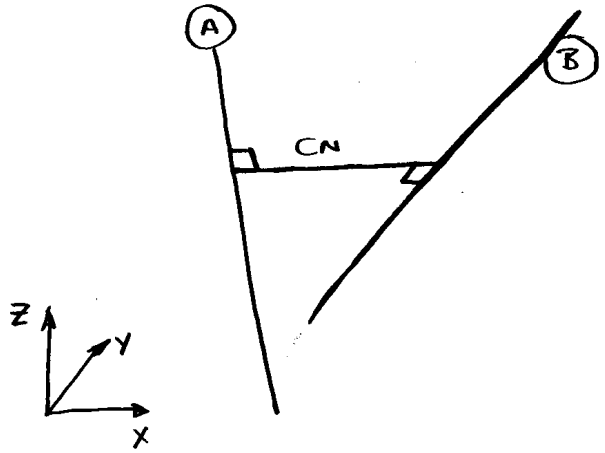

Figure 3.3: The Common Normal (CN) is the shortest line which intersects two given lines. It intersects lines **A** and **B** at a right angle.

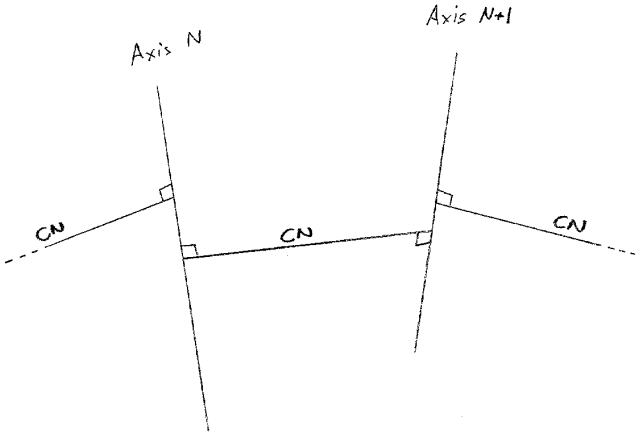

Figure 3.4: Virtual Links between axes are formed by the Common Normals.

3.2.2 Modeling Links and Joints

Assignment of Frames to Links

We will define a series of frames along the virtual kinematic chain and identify the key rotations and translations which define their relationships.

Common Normal The CN will be our virtual link between two axes in space. It is worth noting that the CN might be completely outside the physical structure of the robot. However our virtual manipulator constructed using CNs will be an exact representation of the kinematics of the real one. It turns out that we can identify the CN of each link rather informally. We do not need to write the equation for each CN line segment but it will be more important to identify the two end points.

There will be a CN for each pair of joint axes (Figure 3.4). If the two joint axes are parallel, there are an infinite number of CNs so we just choose one arbitrarily. If the two axes intersect, then the CN has zero length but it still has a direction which is the cross product

$$CN = \text{Axis}_N \otimes \text{Axis}_{N+1} \tag{3.1}$$

Example 3.1
Find the Common Normal between the following lines:

$$x = 0, y = 0$$

and

$$z = 1, x = 1$$

The common normal is also the shortest line segment which intersects both lines. The first line is a vertical along the z axis. The second goes in the y direction through the point $[1 \quad 0 \quad 1]^T$. The shortest line segment connecting these two lines is the line segement between $[0 \quad 0 \quad 1]^T$ and $[1 \quad 0 \quad 1]^T$ which is the line

$$z = 1, y = 0$$

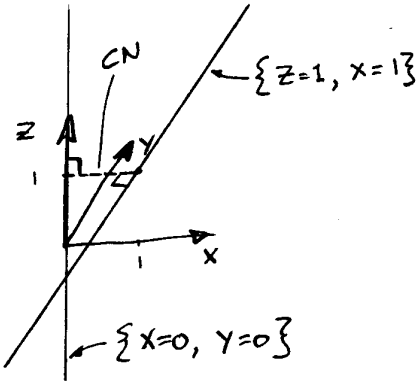

3.2.3 Fixing Frames to Links

Once we identify common normals between the manipulator axes, we are ready to locate a frame, rigidly attached to each link. Although conceptually these could be anywhere, our convention will locate them on the joint axes. We will first choose the location of the origin, and then the directions for two axes. The third axis follows by the right hand rule.

The origin of the link frame will be at the point where Axis N intersects the CN to Axis $N+1$. Let's call this point A_N. The X_N axis will point along the CN toward its intersection with the following axis. Let's call the other end of the CN B_N. Z_N will point along the joint axis. There are two ways that Z_N can point

[1] Think of a prism sliding inside a hole shaped to match its profile. It can slide in and out, but not rotate.
[2] Not always unique but see below.

along Z_N. For rotary joints, we will require that we choose the direction of Z_N so that positive rotation of the joint is consistent with the right-hand-rule about Z_N. The points A_N and B_N are shown in Figure 3.7.

Now that X_N and Z_N are fixed, we choose Y_N simply by

$$Y_N = Z_N \otimes X_N$$

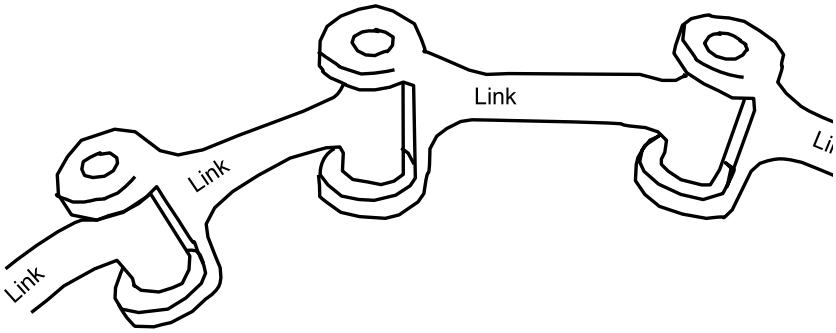

A)

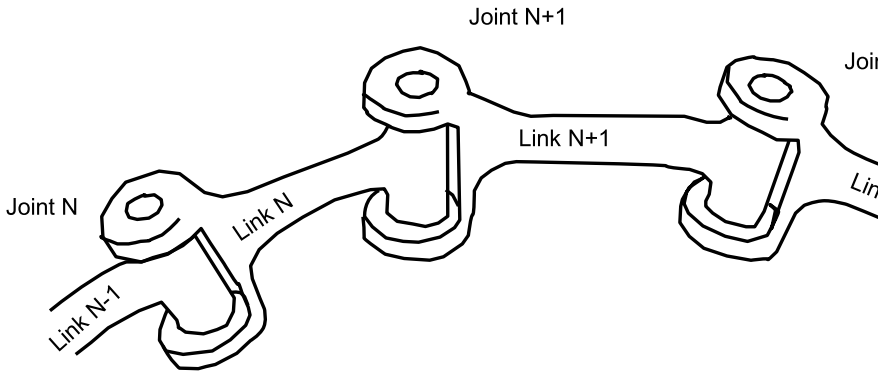

B)

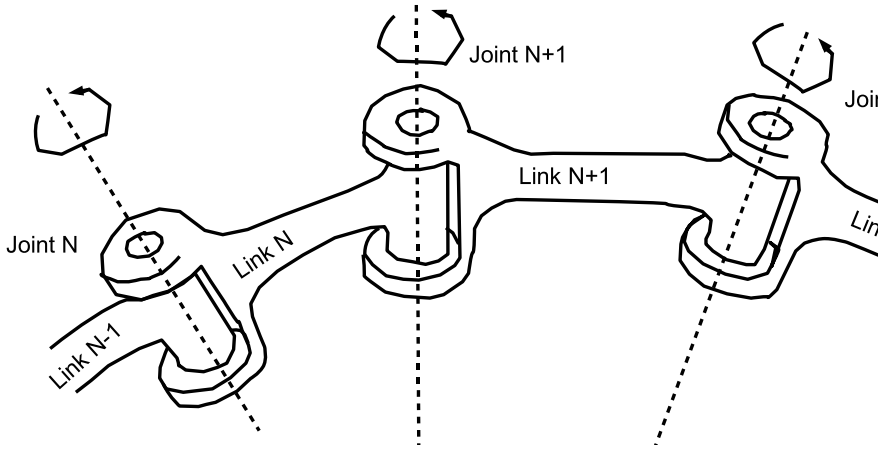

C)

Figure 3.5: Summary of steps for analyzing the DH parameters of a serial chain.

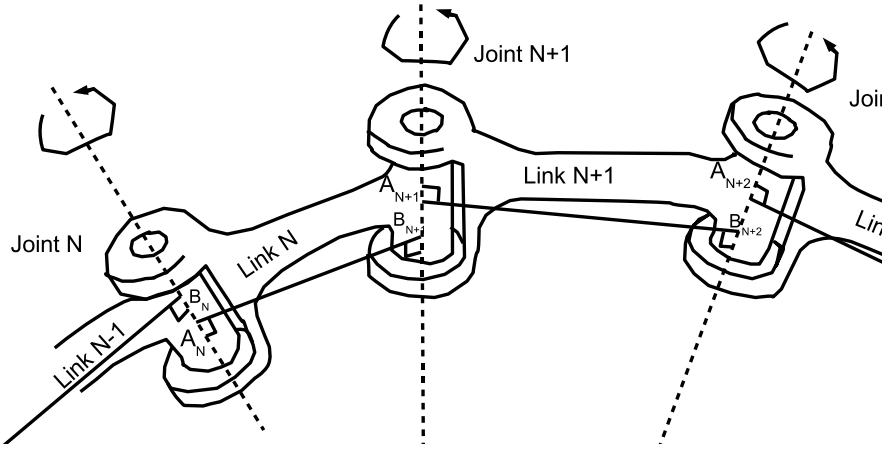

D)

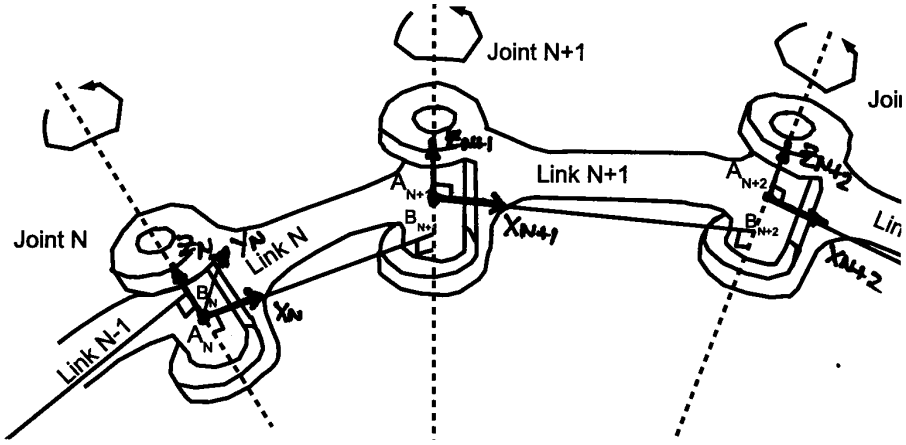

E)

Figure 3.6: Figure 3.5 cont.

3.3 Summary of Link Frame Assignment Methodology

We will use the following procedure identify and assign link frames:

1. Understand the geometry and dimensions of the mechanism. Figure 3.5A shows two links (plus parts of two others) of a mechanism we will analyze.
2. Number the links and joints. The Base of the mechanism is, by convention link 0, and the first joint from the base is numbered joint 1. In Figure 3.5B we have applied numbers to the links (somewhere in the middle of the chain).
3. Identify the axes of motion and the directions which you will call positive motion (Figure 3.5C).
4. Draw common normals (CNs) and find their intersections with joint axes. Define two points on each link:

   A_N the intersection of Axis N with the CN to Axis $N+1$.

   B_N the intersection of Axis N with the CN to Axis $N-1$.

   (Figure 3.5D)
5. Assign a frame to each link as follows:

   The origin of Frame N is A_N.

   Z_N points along Axis N.

   X_N points along the CN to B_{N+1}

   Y_N completes a right handed coordinate system.

   (Figure 3.5E)

Q: What if it appears that there is no common normal because the axes intersect?
A: Create a common normal vector with direction but zero length (draw it like a unit vector). Choose X_N to be normal to Z_N and Z_{N+1}.
Q: What if Z_N and Z_{N+1} are parallel and there is no *unique* CN?
A: Just choose one of the set of CNs arbitrarily. Typically you can simplify subsequent analysis by choosing a CN which intersects B_N.
Q: What if Z_N and Z_{N+1} are co-linear?
A: Then choose any zero-length vector perpendicular to both of the axes.

Example 3.2
Assign link frames to the arm shown below. This arm has two degrees of freedom, but we will define a third frame at the end effector as though the end effector had a degree of freedom attached. The thickness (width) of the arm links is 20cm.
First, we identify the links and joints and number them, starting with link zero and with joint 1 between link zero and link one (blue).

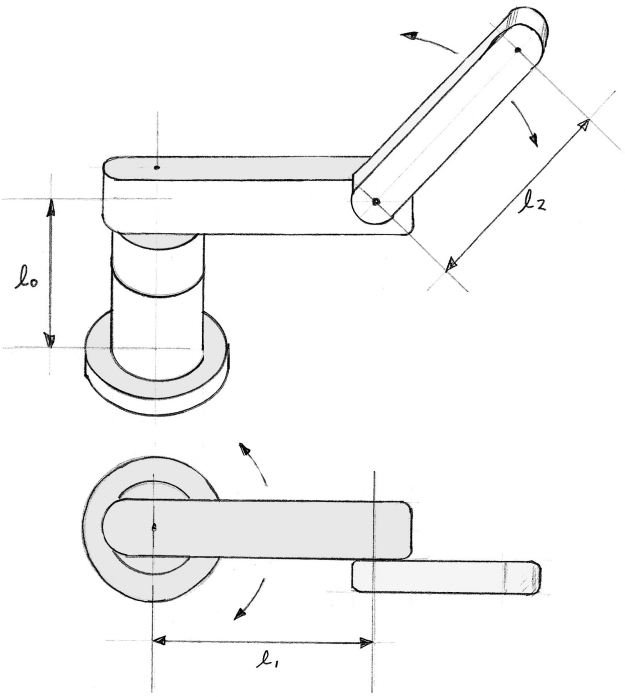

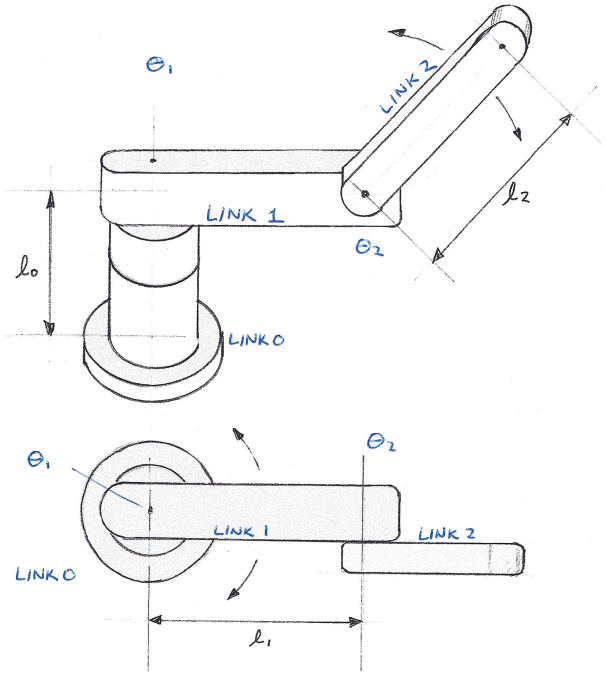

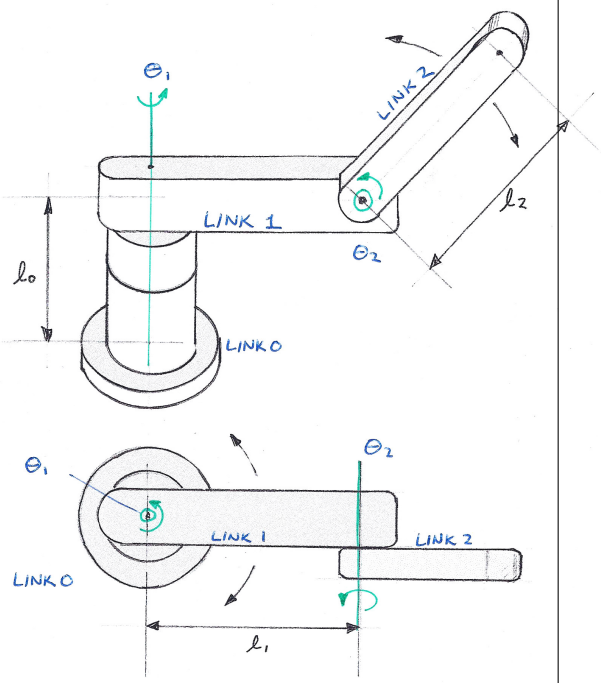

Example 3.2 cont.

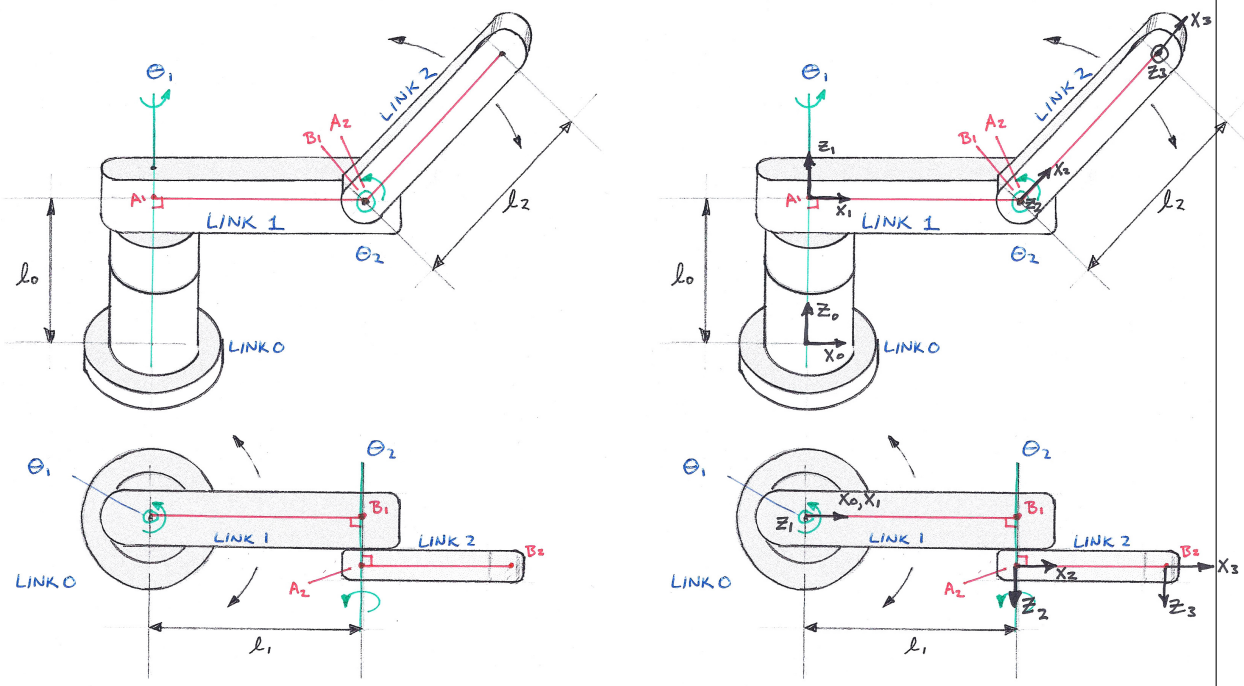

Second we identify the joint axis lines and choose directions of rotation around them (for rotary joints) which we denote to be positive (green).
Third, we draw in the common normals between the identified joint axes (red).
Finally, we identify the origins of each link frame, draw in z_i pointing so that positive rotation follows the RHR, and draw x_i along the common normal to the next axis (black).
A simplified stick figure (below) can sometimes help in visualizing the frame assignments:

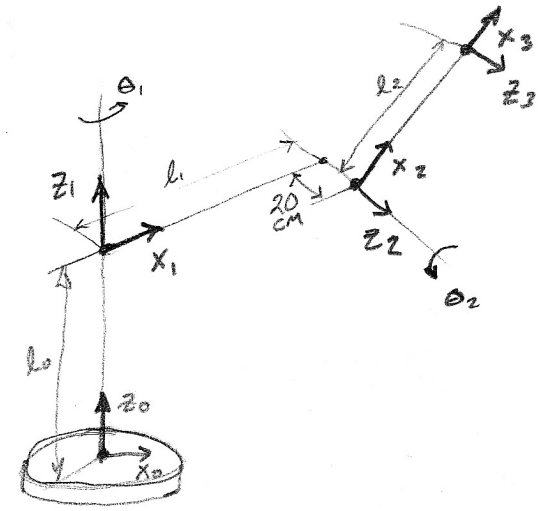

Example 3.3

This example considers the 6 DOF arm designed by Bernard Roth, the "Stanford Arm". The series of four drawings shows the steps in analyzing and applying frames to the arm. Following the steps above in Section 3.3.
1) Understand the geometry and dimensions of the mechanism. The first drawing indicates only the shape and motions of the arm.
2) In step two we number the links and joints. It turns out that numbering the Joints is most important and we skip explicitly numbering the joints here. We add some dimensions for the shoulder height, L_1 and the shoulder offset S.
3) In green in the second drawing, we highlight the directions we will consider positive motion,
4) This arm features all intersecting axes (to simplify the equations). In drawing 3, we show in red CN vectors obtained by crossing sequential axes.
5) In drawing 4 we assign a link frame to each axis according to Step 5 of Section 3.3.

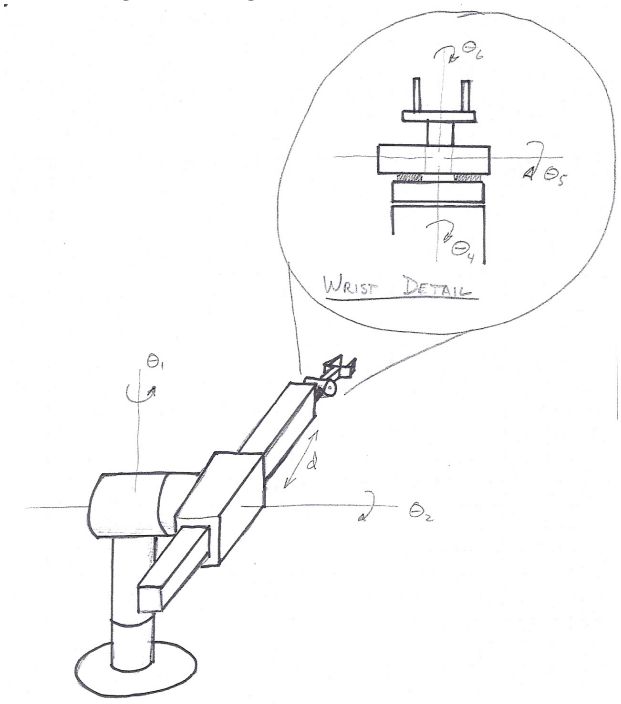

1)

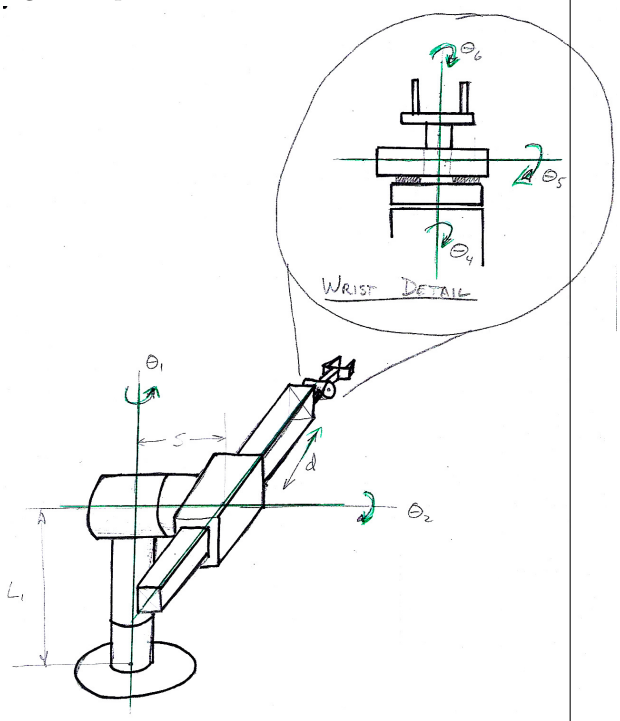

2)

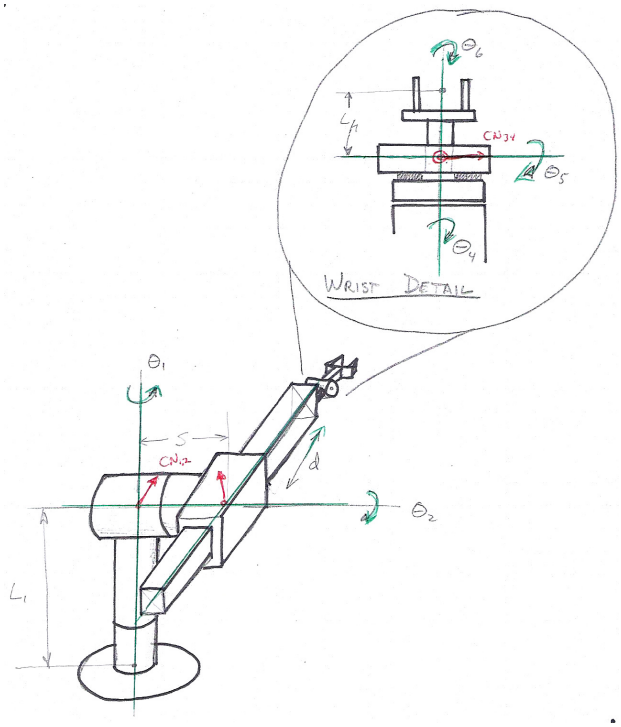

3)

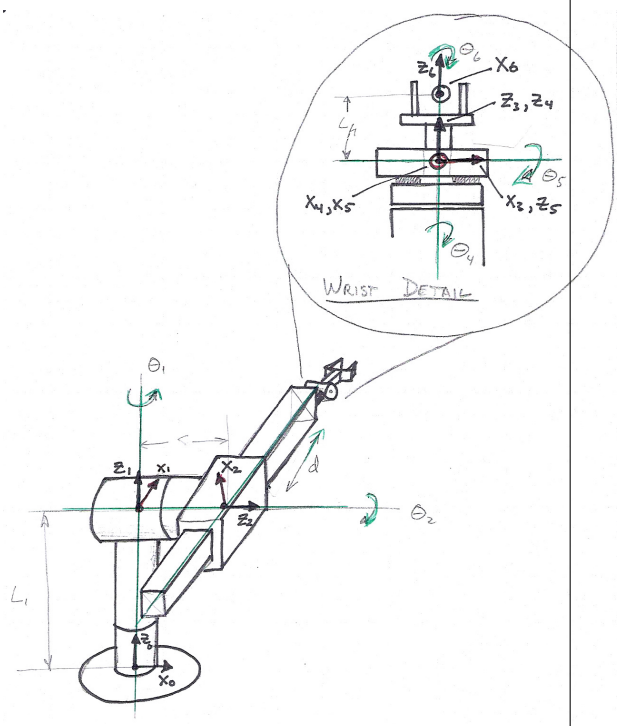

4)

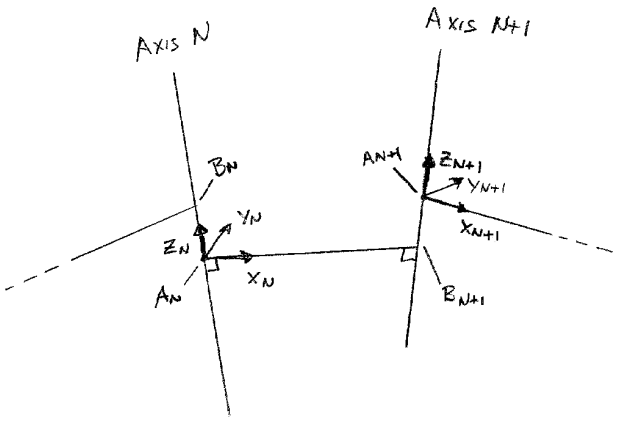

Figure 3.7: Virtual links with link frames fixed in both position and orientation.

3.4 Denavit Hartenberg Parameters

In 1955 Denavit and Hartenburg created a standardized way to derive transforms from one link to another in a serial chain. Once frames have been assigned to each link as described above, for each link, we will be able to identify two specific rotations and two translations which uniquely define the relationship between the links. Of the four Denavit-Hartenberg (DH) parameters, three are fixed constants due to the rigid body nature of the link. A fourth is a variable which specifies the relative motion between the link and the next link. For rotary joints that variable is θ_N and for prismatic joints, that variable is d_N. The definition of the four DH parameters are now given. A very nice video illustration of the DH parameters is available at the wikipedia page for "Denavit-Hartenberg Parameters".

Composition of parameters

We use the DH parameters to describe the spatial relationship between frame $N-1$ and frame N. Notice that a series of axes and CNs forms a continuous path from one link frame origin to the next. We will follow this path through its twists and turns and describe each translation and rotation with a single DH parameter. Each DH parameter represents a rotation or a translation about a single known axis. Since the origin of Frame $N-1$ is A_{N-1} we start there and work our way to the origin of the next frame. Refering to Figure 3.7, we rotate by the **link twist**: $\text{Rot}(\hat{x}, \alpha_{N-1})$, then translate by the **link length**: $\text{Trans}(\hat{x}, a_{N-1})$, then rotate by the **joint angle**: $\text{Rot}(\hat{z}, \theta_N)$, and finally translate by the **joint offset**: $\text{Trans}(\hat{z}, d_N)$. Note that the relationship between link $N-1$ and link N is described by parameters with a mix of subscripts. The Denavit Hartenberg parameters can be visualized in Figure 3.10.

For the common case of rotary joints, $a_{N-1}, \alpha_{N-1}, d_N$ will be fixed constants, dependent on the geometric design of the arm, and θ_N will be a variable joint angle. Some arms include prismatic joints in which θ_N is a constant and d_N is a variable. In evaluating the link transform we typically replace all constant parameters with their measured or design values and keep the single variable parameter in DH form. In rare cases, a joint includes two degrees of freedom such as a cylindrical shaft which can rotate as well as translate[3]. In this case it is best to abstract that joint into two separate joints, one for rotation and one for translation.

Our strategy will be to multiply together 4x4 homogeneous transforms for each of the elemental displacement and rotations above which make up the virutal link. To keep the notation under control we will use the following shorthand:

$$c\theta_j \equiv c_j \equiv cos(\theta_j)$$

[3]See for example, the last two degrees of freedom of the SCARA arm.

$$s\theta_j \equiv s_j \equiv sin(\theta_j)$$

The complete transform is then

$$^{N-1}_{N}T = \text{Rot}(\hat{x}, \alpha_{N-1})\text{Trans}(\hat{x}, a_{N-1})\text{Rot}(\hat{z}, \theta_N)\text{Trans}(\hat{z}, d_N)$$

or equivalently

$$^{N-1}_{N}T = \text{Rot}(\hat{x}, \alpha_{N-1})\text{Trans}(\hat{x}, a_{N-1})\text{Rot}(\hat{z}, \theta_N)\text{Trans}(\hat{z}, d_N)$$

$$= \begin{bmatrix} 1 & 0 & 0 & 0 \\ 0 & c\alpha_{N-1} & -s\alpha_{N-1} & 0 \\ 0 & s\alpha_{N-1} & c\alpha_{N-1} & 0 \\ 0 & 0 & 0 & 1 \end{bmatrix} \begin{bmatrix} 1 & 0 & 0 & a_{N-1} \\ 0 & 1 & 0 & 0 \\ 0 & 0 & 1 & 0 \\ 0 & 0 & 0 & 1 \end{bmatrix} \begin{bmatrix} c\theta_N & -s\theta_N & 0 & 0 \\ s\theta_N & c\theta_N & 0 & 0 \\ 0 & 0 & 1 & 0 \\ 0 & 0 & 0 & 1 \end{bmatrix} \begin{bmatrix} 1 & 0 & 0 & 0 \\ 0 & 1 & 0 & 0 \\ 0 & 0 & 1 & d_N \\ 0 & 0 & 0 & 1 \end{bmatrix}$$

or equivalently

$$^{N}_{N+1}T = \text{Rot}(\hat{x}, \alpha_{N})\text{Trans}(\hat{x}, a_{N})\text{Rot}(\hat{z}, \theta_{N+1})\text{Trans}(\hat{z}, d_{N+1})$$

$$= \begin{bmatrix} 1 & 0 & 0 & 0 \\ 0 & c\alpha_{N} & -s\alpha_{N} & 0 \\ 0 & s\alpha_{N} & c\alpha_{N} & 0 \\ 0 & 0 & 0 & 1 \end{bmatrix} \begin{bmatrix} 1 & 0 & 0 & a_{N} \\ 0 & 1 & 0 & 0 \\ 0 & 0 & 1 & 0 \\ 0 & 0 & 0 & 1 \end{bmatrix} \begin{bmatrix} c\theta_{N+1} & -s\theta_{N+1} & 0 & 0 \\ s\theta_{N+1} & c\theta_{N+1} & 0 & 0 \\ 0 & 0 & 1 & 0 \\ 0 & 0 & 0 & 1 \end{bmatrix} \begin{bmatrix} 1 & 0 & 0 & 0 \\ 0 & 1 & 0 & 0 \\ 0 & 0 & 1 & d_{N+1} \\ 0 & 0 & 0 & 1 \end{bmatrix}$$

Each of these four matrices is a function of one of the four DH parameters. We can then multiply them together to get a single matrix which represents the link.

Generalized Link Transformation

By multiplying all four matrices together we get the following transform for any link which has DH parameters:

$$^{N-1}_{N}T = \begin{bmatrix} c\theta_N & -s\theta_N & 0 & a_{N-1} \\ s\theta_N c\alpha_{N-1} & c\theta_N c\alpha_{N-1} & -s\alpha_{N-1} & -s\alpha_{N-1}d_N \\ s\theta_N s\alpha_{N-1} & c\theta_N s\alpha_{N-1} & c\alpha_{N-1} & c\alpha_{N-1}d_N \\ 0 & 0 & 0 & 1 \end{bmatrix} \tag{3.2}$$

The reader can derive the corresponding matrix for $^{N}_{N+1}T$.

3.4.1 Combining links into a chain

Once we have $^{N-1}_{N}T$ for all of the links, we multiply them together to get the full forward kinematics model. For example in a three link robot we would have

$$^{0}_{3}T = {}^{0}_{1}T\,{}^{1}_{2}T\,{}^{2}_{3}T$$

Usually it is possible and desirable to multiply them together in symbolic form. We will bring this process together in the next section.

3.4.2 Summary of Forward Kinematics Analysis Part 2

1. Derive the Denavit Hartenberg parameters, $a_N, \alpha_N, d_N, \theta_N$, from your assigned link frames as follows:

   a_N is the distance from A_N to B_{N+1}. This is the distance along the CN from Z_N to Z_{N+1}. a_N is refered to as the "link length" (see Figure 3.4 and Figure 3.6 D and E).

   α_N is the angle between Axis N and Axis $N+1$ about the common normal. This is the angle between Z_N and Z_{N+1} about X_N in the RHR sense. α_N is called the "link twist".

   d_N is the distance from B_N to A_N. This is the distance from X_{N-1} to X_N along Z_N. d_N is referred to as the "joint offset".

   θ_N is the angle between CN_{N-1} and CN_N around Axis N. This is the angle between X_{N-1} and X_N around Z_N. θ_N is refered to as the "joint angle".

2. Use equation 3.2 to compute the link transform for each link

3. Multiply all the link transforms together.

Example 3.4
Find the 4x4 matrix representing the forward kinematic equations of the manipulator of Example 3.2.

Step 1. Referring to the procedure of Section 3.4.2

N	α_{N-1}	a_{N-1}	d_N	θ_N
1	0	0	l_0	θ_1
2	90°	l_1	20cm	θ_2
3	0	l_2	0	0

Step 2
Referring to Equation 3.2

link 1)

$$ {}^{0}_{1}T = \begin{bmatrix} c\theta_1 & -s\theta_1 & 0 & 0 \\ s\theta_1 & c\theta_1 & 0 & 0 \\ 0 & 0 & 1 & l_0 \\ 0 & 0 & 0 & 1 \end{bmatrix} $$

$$ C\alpha_{N-1} = C\alpha_0 = 1 $$
$$ S\alpha_{N-1} = S\alpha_0 = 0 $$

link 2)

$$ C\alpha_{N-1} = C\alpha_1 = 0 $$
$$ S\alpha_1 = 1 $$

$$ {}^{1}_{2}T = \begin{bmatrix} c\theta_2 & -s\theta_2 & 0 & l_1 \\ 0 & 0 & -1 & -20cm \\ s\theta_2 & c\theta_2 & 0 & 0 \\ 0 & 0 & 0 & 1 \end{bmatrix} $$

link 3)

$$ {}^{2}_{3}T = \begin{bmatrix} 1 & 0 & 0 & l_2 \\ 0 & 1 & 0 & 0 \\ 0 & 0 & 1 & 0 \\ 0 & 0 & 0 & 1 \end{bmatrix} $$

$$ \alpha_2 = 0 \quad C\alpha_2 = 1 $$

Example 3.4 cont.
Step 3
Now multiplying the three matrices together we get:

$$
{}^{0}_{2}T = \begin{bmatrix} c\theta_1 & -s\theta_1 & 0 & 0 \\ s\theta_1 & c\theta_1 & 0 & 0 \\ 0 & 0 & 1 & l_0 \\ 0 & 0 & 0 & 1 \end{bmatrix} \begin{bmatrix} c\theta_2 & -s\theta_2 & 0 & l_1 \\ 0 & 0 & -1 & -20cm \\ s\theta_2 & c\theta_2 & 0 & 0 \\ 0 & 0 & 0 & 1 \end{bmatrix}
$$

$$
\begin{bmatrix} c_1c_2 & -c_1s_2 & s_1 & l_1c_1 + 20cm\, s_1 \\ s_1c_2 & -s_1s_2 & -c_1 & l_1s_1 - 20cm\, c_1 \\ s_2 & c_2 & 0 & l_0 \\ 0 & 0 & 0 & 1 \end{bmatrix}
$$

$$
{}^{0}_{3}T = \begin{bmatrix} c_1c_2 & -c_1s_2 & s_1 & l_1c_1 + 20cm\, s_1 \\ s_1c_2 & -s_1s_2 & -c_1 & l_1s_1 - 20cm\, c_1 \\ s_2 & c_2 & 0 & l_0 \\ 0 & 0 & 0 & 1 \end{bmatrix} \begin{bmatrix} 1 & 0 & 0 & l_2 \\ 0 & 1 & 0 & 0 \\ 0 & 0 & 1 & 0 \\ 0 & 0 & 0 & 1 \end{bmatrix}
$$

$$
= \begin{bmatrix} c_1c_2 & -c_1s_2 & s_1 & l_1c_1 + 20cm\, s_1 + l_2c_1c_2 \\ s_1c_2 & -s_1s_2 & -c_1 & l_1s_1 - 20cm\, c_1 + l_2s_1c_2 \\ s_2 & c_2 & 0 & l_0 + l_2s_2 \\ 0 & 0 & 0 & 1 \end{bmatrix}
$$

Example 3.5
Find link frame assignments and Denavit Hartenberg parameters for the Rosheim Prehensile Wrist[a]. The following interesting wrist mechanism has an extraordinary range of pitch orientations.

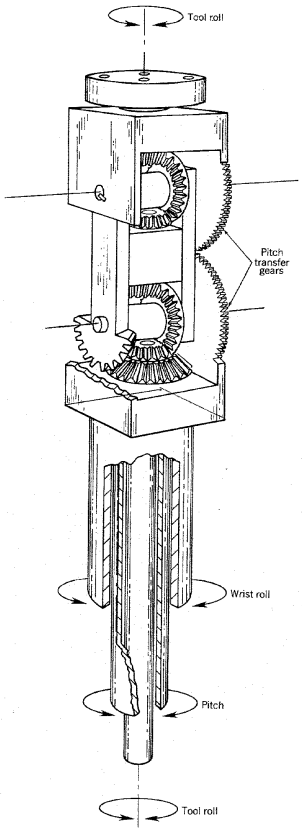

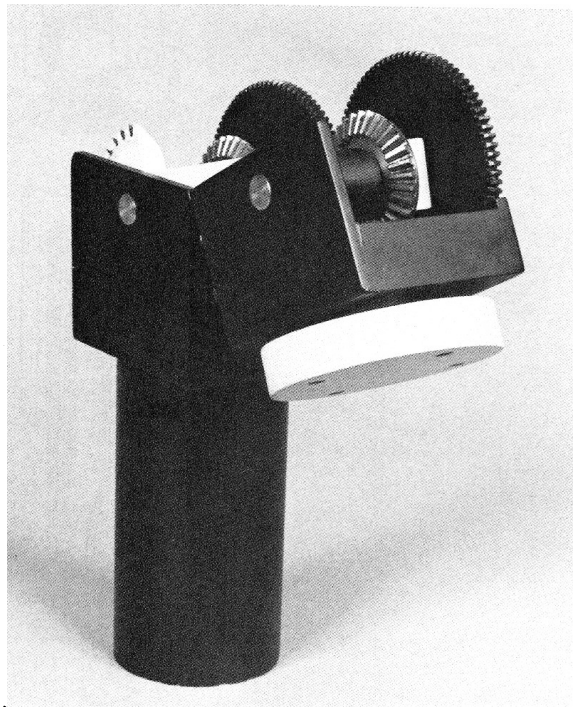

[a]Mark Rosheim, "Robotic Wrist Actuators," John Wiley & Sons, 1989.

Example 3.5 cont.
Following the steps outlined above:
1) Understand the geometry and dimensions. First, we arbitrarily identify the bottom of the rectanglar solid below the first bevel gears as a reference plane (i.e. we will locate Frame 0 there in the next step). We draw diagonals in that plane to locate its center. We also extend the joint axis lines through the joints and give names to the dimentions between them:
2) Number the Links and Joints. Furthermore, the Wrist roll axis intersects the first horizontal axis (which we will call joint 2 in the next step) so that link 1 has zero length:

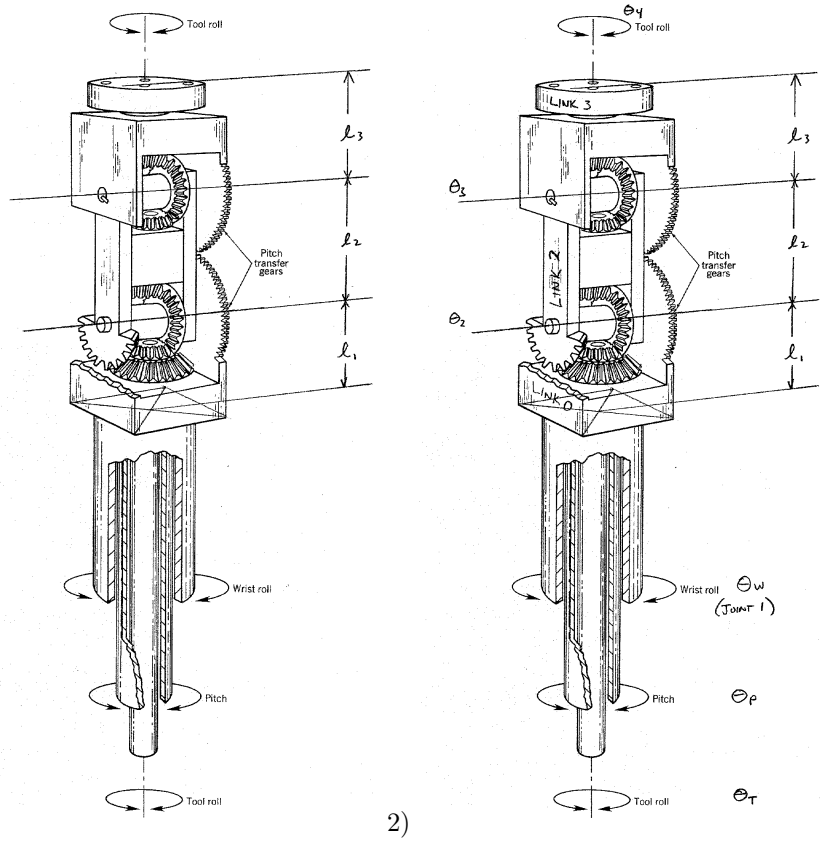

Example 3.5 cont.
3) Identify axes of motion. This is a bit tricky since the "Pitch Transfer Gears" demand that some of the joints do not move independently. However for now we will ignore the pitch transfer gears and consider the two axes to be independent joints. We will ignore the sign convention which places the Z axis along the direction of positive motion and simply point them to the left and up.
4) Draw common normals. The common normal between Z_0 and Z_1 is zero length. The CN between Z_1 and Z_2 is also zero length. The CN from Z_2 to Z_3 is the line up the center of the drawing of length l_2. The CN between axis Z_3 and Z_4 is zero length.
5) Assign a frame to each link. Note that F_0 could go anywhere on the "Wrist roll" body, but we place it along the center axis for convenience. Note that when we move around the Wrist roll axis, F_0 stays where it is and F_1 moves relative to it.

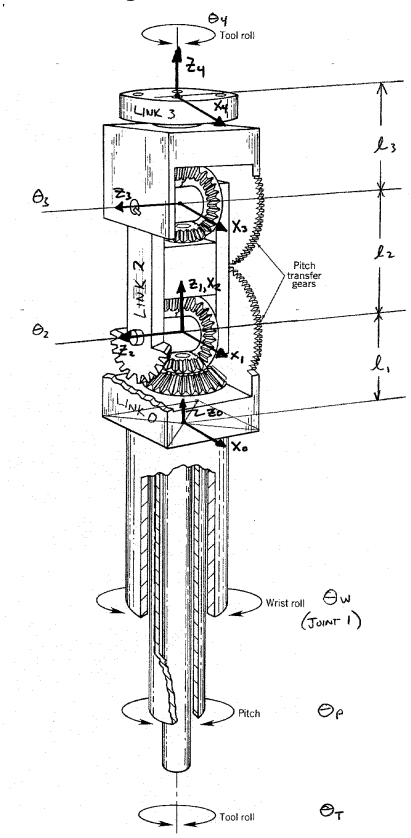

6) Following the procedures of Section 3.4.2, we obtain

N	α_{N-1}	a_{N-1}	d_N	θ_N
1	0	0	l_1	θ_W
2	$\pi/2$	0	0	$\pi/2+\theta_p$
3	0	l_2	0	$-\pi/2+\theta_p$
4	$-\pi/2$	0	l_3	θ_4

Note that joints 2 and 3 form a single degree of freedom driven by θ_p because they are coupled together by the pitch transfer gears.

3.5 Spaces

We have seen that the forward kinematics analysis generates a 4x4 matrix which is a function of N variables where N is the number of joints. As the joints move to different values, the 4x4 matrix specifies different positions and orientations in the task space corresponding to a frame on the last link usually known as the end effector.

Although this matrix maps points in the end effector coordinate system to the base coordinate system, it is sometimes useful to think of this matrix as a description of a mapping from a set of joint values to an end effector configuration. For a manipulator with N joints, the joint values form a point in a N dimensional space we call the *Joint Space*.

The 4x4 matrix ${}^0_N T$ gives us a rotation matrix and X,Y,Z coordinates of the end effector. This is termed a "configuration" of the manipulator end effector. We commonly derive three orientation parameters such as roll, pitch, yaw, angles from the upper 3x3 part of ${}^0_N T$ to give six numbers which characterize the end effector configuration:

$$\begin{bmatrix} X \\ Y \\ Z \\ \text{roll} \\ \text{pitch} \\ \text{yaw} \end{bmatrix} \tag{3.3}$$

The above six numbers define a point in *End Effector Space*. End Effector Space is sometimes called "Task Space" since it is a natural space in which to represent tasks or "Configuration Space" although this term has a slightly different meaning in the context of motion planning.

As a manipulator moves around, a point moves around in joint space representing the values of its joints, and another point moves around in end effector space representing the configuration of the end effector. As we shall see in the next chapter, there may be more than one joint space point which corresponds to the same end effector point, but there is always exactly one point in end effector space for each point in joint space.

Another relevant space is *Actuator Space*. In most serial robots the actuators are located directly on each joint and actuator motion is a linear function of or is equal to the joint motion. However in certain designs, such as the Yakusawa Motoman L-3, actuators may drive the joints through linkages and therefore move somewhat differently than the joints of the serial chain. For good discussion of this consult Chapter 3 of Craig.

$$ {}^{i-1}_{i}T = \begin{bmatrix} c\theta_i & -s\theta_i & 0 & a_{i-1} \\ s\theta_i c\alpha_{i-1} & c\theta_i c\alpha_{i-1} & -s\alpha_{i-1} & -s\alpha_{i-1} d_i \\ s\theta_i s\alpha_{i-1} & c\theta_i s\alpha_{i-1} & c\alpha_{i-1} & c\alpha_{i-1} d_i \\ 0 & 0 & 0 & 1 \end{bmatrix} $$

$$ {}^{i-1}_{i}T = \begin{bmatrix} c\theta_i & -s\theta_i & 0 & a_{i-1} \\ s\theta_i c\alpha_{i-1} & c\theta_i c\alpha_{i-1} & -s\alpha_{i-1} & -s\alpha_{i-1} d_i \\ s\theta_i s\alpha_{i-1} & c\theta_i s\alpha_{i-1} & c\alpha_{i-1} & c\alpha_{i-1} d_i \\ 0 & 0 & 0 & 1 \end{bmatrix} $$

Figure 3.8: Different term types in the DH Link Transform. Matrix elements have dependencies on link *relationship* (θ_i, d_i) or link *structure* (α_{i-1}, a_{i-1}).

3.6 A further look at the DH notation

(The following section may be skipped without loss in future chapters)

3.6.1 Structure of the Link Transform

We can obtain some insight into the computation of link transformations by grouping the terms as shown in Figure 3.8. The clusters in Figure 3.8 represent blocks of terms which depend on a specific DH parameters. Often, with industrial manipulators,

$$\alpha_{i-1} = \{0, \pm\frac{\pi}{2}, \pi\}$$

because they are easier to design and manufacture that way. For these cases, we can see that the final expression for the link transform is simplified by $\cos(\alpha_{i-1}) = \{0, \pm 1\}$.

Finally, we can classify the DH parameters into ones describing the *structure* of the link (θ_i, d_i) versus the *relationship* with the next link (α_{i-1}, a_{i-1}). Each of these two classes has one rotational and one translational parameter:

	Translation	Rotation
Structure	a_{i-1}	α_{i-1}
Relationship	d_i	θ_i

3.6.2 Craig's vs. Paul's Transforms

The first textbook on robot manpiulation was "Robot Manipulators, Mathematics, Mechanics, and Control," by Richard Paul of the University of Pennsylvania (MIT Pres, 1981). This book was very influential in starting research and courses around the world on robotic manipulation. However, Paul used a slightly different variation on the Denavit Hartenberg method which results in different description of links. In looking at the robotic manipulation literature, a researcher will still encounter work done in Paul's notation.

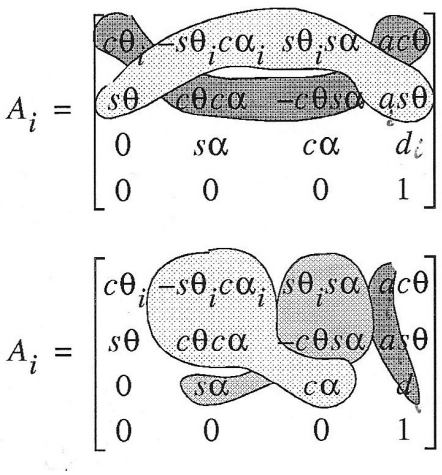

Figure 3.9: Different term types in the DH Link Transform. Matrix elements have dependencies on link *relationship* (θ_i, d_i) or link *structure* (α_{i-1}, a_{i-1}).

Both Craig and Paul's systems use the same DH parameters. The key difference is that Paul's system puts the origin of frame N at the end of the link (point B_{N+1} as defined in this chapter). Thus, different DH parameters are used in Paul's link description (Figure 3.9).

Paul's transform selects different DH parameters to represent the structure and relationships of the links:

Paul's Link Parameters

	Translation	Rotation
Structure	a_i	α_i
Relationship	d_i	θ_i

The obvious advantage of Paul's method is that subscripts are more consistent within the transform for each link. However it has the non-intutive notion that the origin of Frame N lies on axis $N+1$. Craig's method has the more intuitive notion that link frame N is at the beginning of the link, located on axis N, but requires mixing of indeces in the link transform. The two link frame assignment methods are summarized in Figure 3.10.

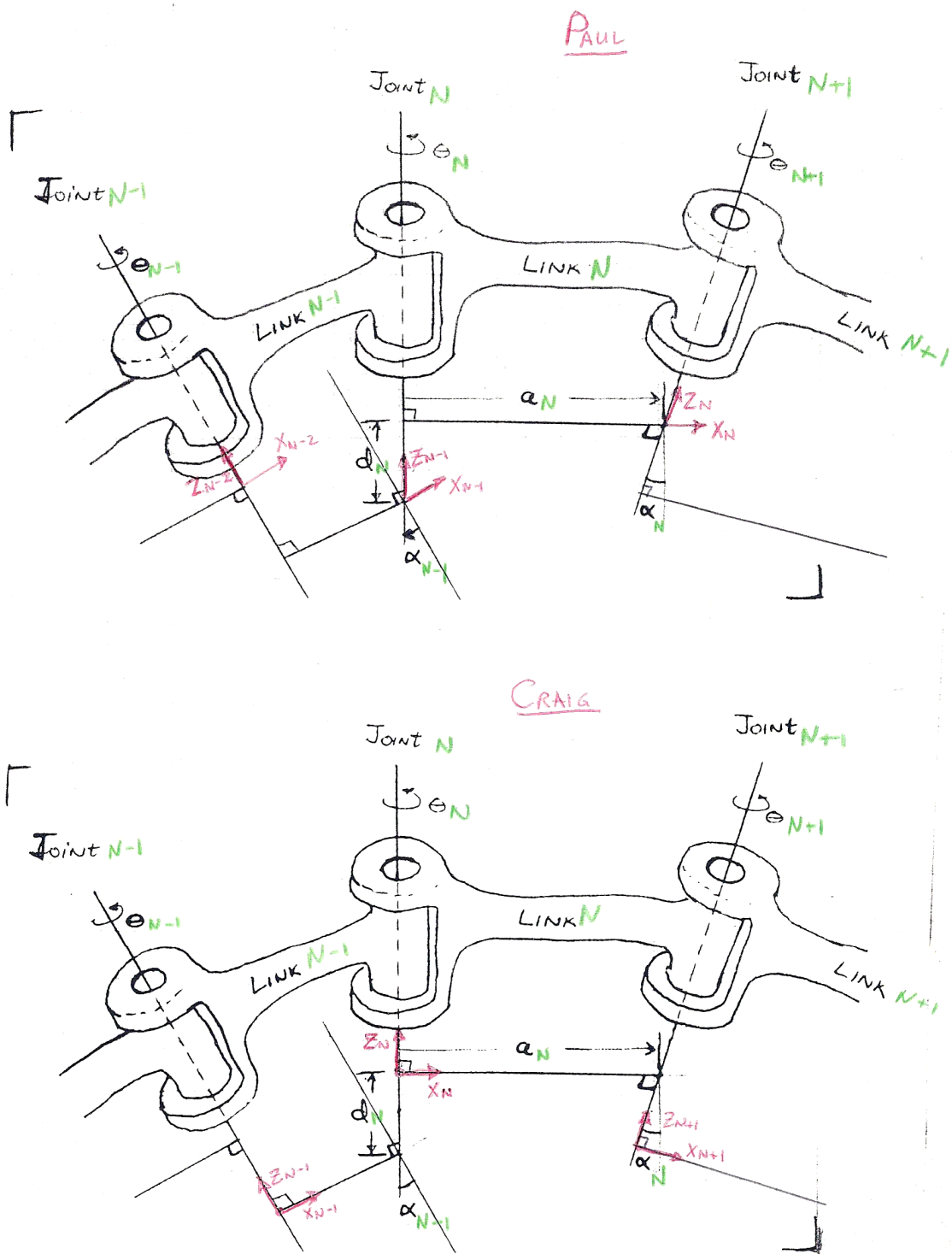

Figure 3.10: Different link frame assignments (within the same DH parameters) for Craig (bottom) and Paul's (top) methods.

Chapter 4

Inverse Kinematics

4.1 Problem Statement and Learning Objectives

Problem Statement The inverse kinematics problem is to find the joint values for a given end effector configuration. The solution to this problem is needed for most practical applications of serial robot arms.

Learning Objectives Upon completing this Chapter, the reader should

- Be able to plot the workspace of a serial manipulator with or without joint limits.
- Be able to solve for the joint angles of a planar robot given the end effector x, y position and orientation.
- Be able to solve for the joint angles of a spatial 3 DOF robot given the x, y, z position of the end effector.
- Be ready to tackle full scale inverse kinematics problems if sufficient time is available.

4.2 Overview

We can express the forward kinematic problem as

$$f(\theta) = {}^0_6T$$

Then, to find the joint angles which correspond to a desired end effector configuration, we need to solve the inverse of this problem, the *Inverse Kinematic Problem*

$$\theta = f^{-1}({}^0_6T_d)$$

where the d subscript indicates the "desired" end effector configuration. Being able to solve the inverse kinematic problem is thus very important for automatic applications of robot manipulators since the control system must know the joint angles, θ, in order to move the end effector to ${}^0_6T_d$.

For serial kinematic chains, this problem is harder than the forward kinematic problem. Among the significant issues are:

- Existence of solutions
- Multiple solutions
- How to find the solution(s)

4.2.1 Workspace

A robot arm, just like the human arm, can only reach a certain number of points. Wrapped up in our inverse kinematics calculation is the question of whether or not the desired end effector configuration is actually reachable. Our mathematics should tell us this automatically when we try to compute the joint angles or displacements. Fortunately, it works out that for a solution to the inverse kinematics problem to exist, ${}^0_6T_d$ must be in the *workspace* of the manipulator. We will use two definitions of workspace:

1. **Dexterous Workspace**. The subset of space in which the robot end effector (EE) can reach all orientations.
2. **Reachable Workspace** The subset of space in which the robot end effector (EE) can reach at least one orientation.

Note that the dexterous workspace is a subset of the reachable workspace.

Example 4.1
Consider a two link planar robot with no joint limits:

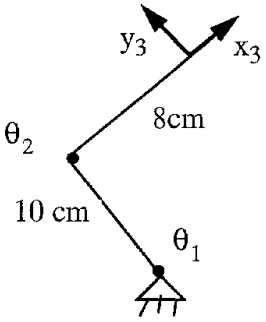

Then the reachable workspace is:

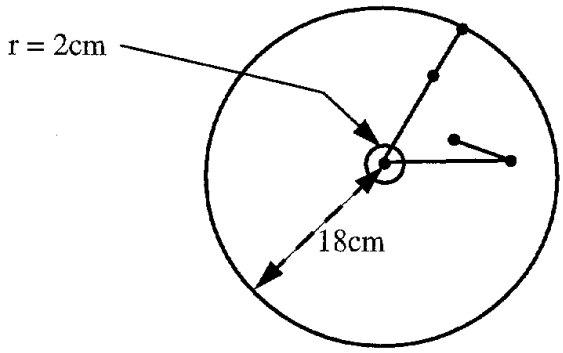

and the dexterous workspace is the empty set.
Now, if $l_1 = l_2 = 9$, the outer radius is the same, and

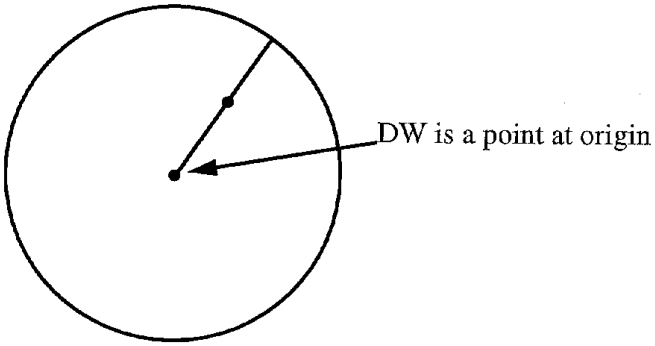

Now the RW is the same but the DW exists at a point at the origin where any orientation can be obtained.

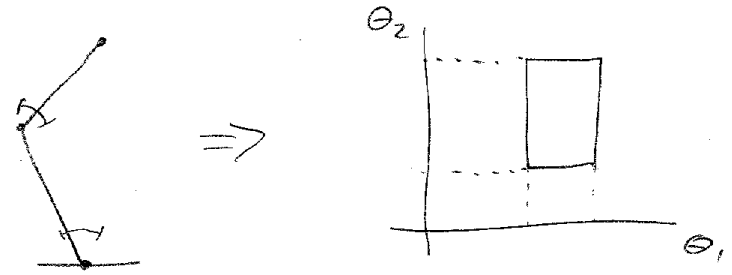

Figure 4.1: Visualization of joint limits for a 2-link manipulator.

Example 4.1 cont.

Now let's add a joint at the wrist

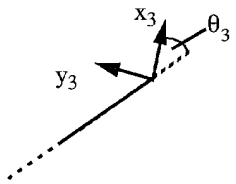

and set link lengths to $l_1 = 8, = l_2 = 10$.

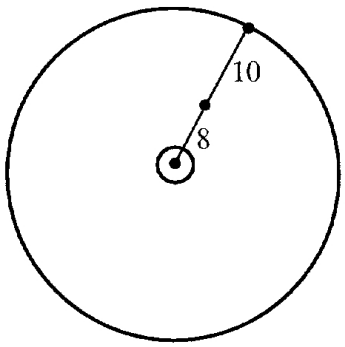

Now the reachable and dexterous workspaces are the same.

Joint Limits The joints in real mechanisms often cannot achieve rotations of $0 - 2\pi$ (or for that matter infinite displacements on prismatic joints!). Thus joint limits

$$\theta_{imin} \leq \theta_i \leq \theta_{imax} \qquad d_{imin} \leq d_i \leq d_{imax}$$

contribute additional limits to the workspace.

Rotary Joints

Without joint limits, the 2-link planar robot makes a donut shaped reachable workspace in the task space (Example 4.1). In joint space, any point can be attained. When joint limits are introduced, a rectangular solid is created defined by θ_{imin} and θ_{imax} for each dimension. To convert this rectangular solid back to task space, we note that each edge of the solid corresponds to varying just one joint at a time. The edges in the joint space thus become arcs in the task space. For the 2 joint manipulator, these limits allow joint configurations inside the rectangle shown in Figure 4.1, right.

Plotting the workspace can be tricky with joint limits. One approach:

1. Identify the corners (vertices) of the joint space rectangular solid.

2. Plot a point in the task space for each vertex.
3. Connect the points with arcs (use a compass to draw) around the joint axis to connect the vertices.
4. Remember that some workspace boundaries may not occur at joint limits such as when the arm is fully stretched out.

Example 4.2
Consider a 2DOF planar manipulator with link lengths $l_1 = 4, l_2 = 1.5$. Assume the joints are limited to

$$0 \leq \theta_1 \leq 180^\circ \qquad -90^\circ \leq \theta_2 \leq 180^\circ$$

Plot the reachable workspace.

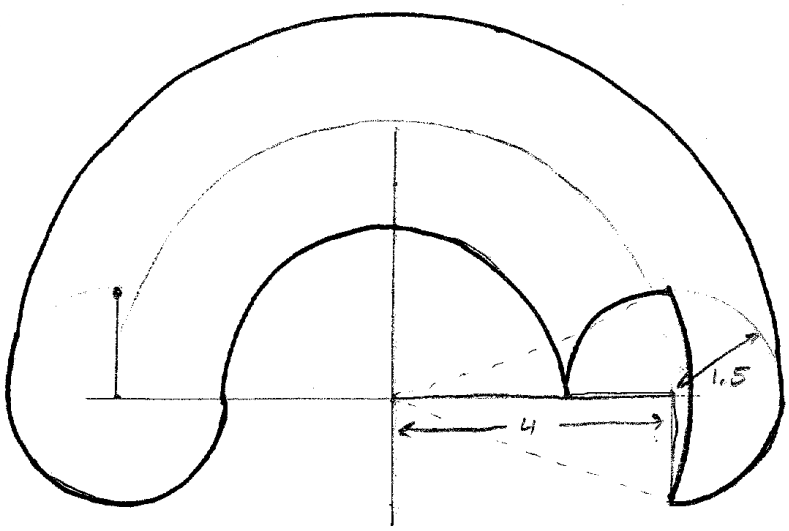

Example 4.3
Same problem as previous example: $l_1 = 3, l_2 = 1.5$. Assume the joints are limited to

$$45^\circ \leq \theta_1 \leq 135^\circ \qquad -45^\circ \leq \theta_2 \leq 90^\circ$$

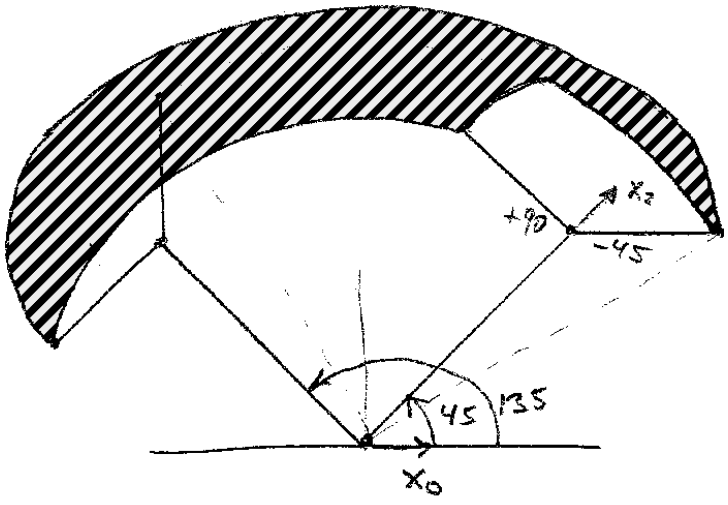

Example 4.4
Generate top view and perspective view of the 3D workspace of the manipulator shown:

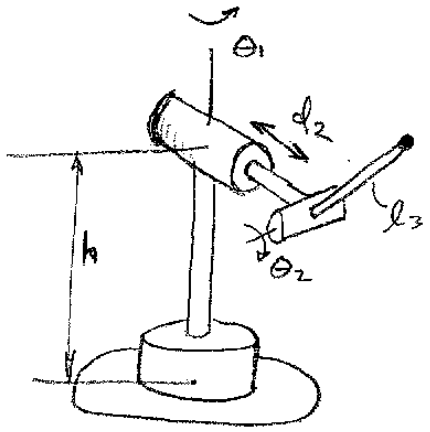

Where the joint limits are

$$0 \leq \theta_1 \leq 90^\circ \qquad 2 < d_2 < 4 \qquad -45^\circ < \theta_3 < 45^\circ$$

First, we look at the plane containing the "d_2" and the "l_3" links (i.e. the vertical plane normal to Z_2.).

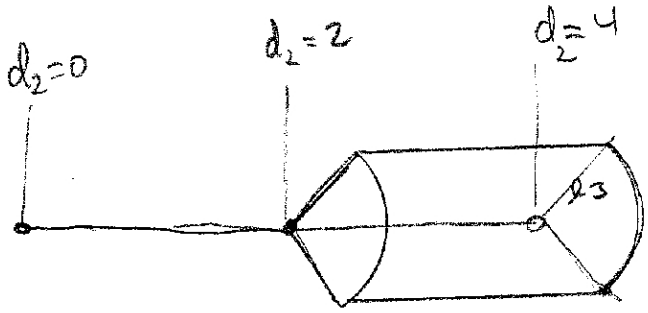

Then by sweeping this planar workspace about Z_1, we generate the top view and perspective view.

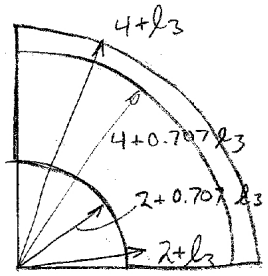

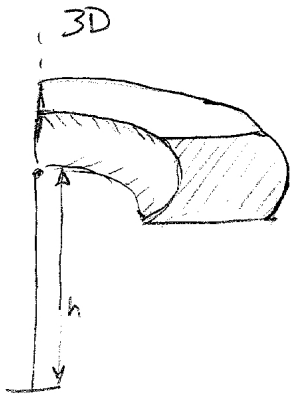

Example 4.5
Draw the 2-D workspace of the planar manipulator drawn below:

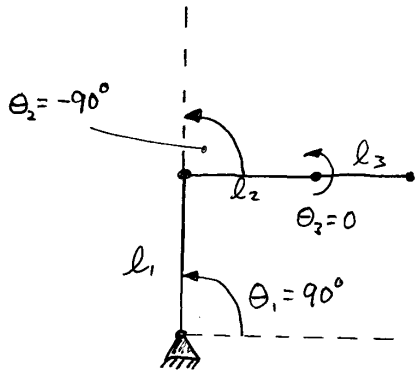

Facts:

- $45° < \theta_1 < 90°$
- $-90° < \theta_2 < 0°$
- $20° < \theta_3 < 120°$
- $l_1 = 5, \quad l_2 = 4, \quad l_3 = 3$

Solution:

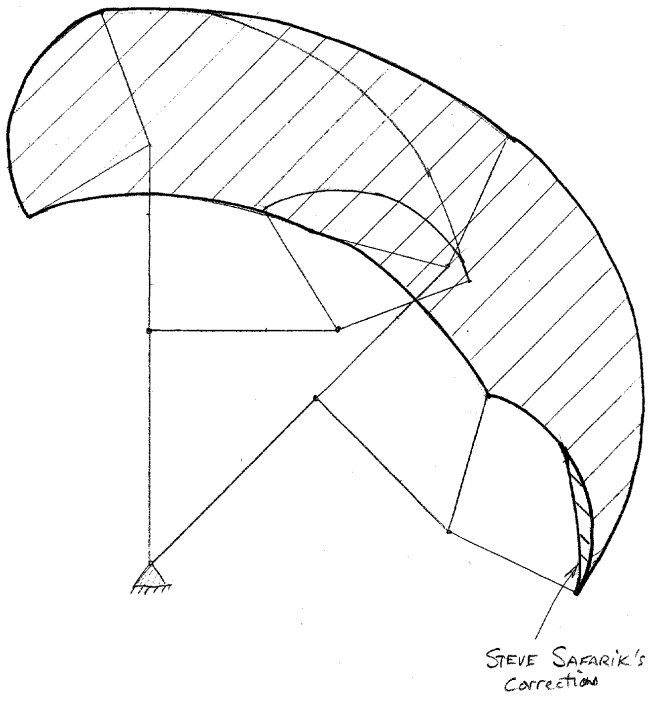

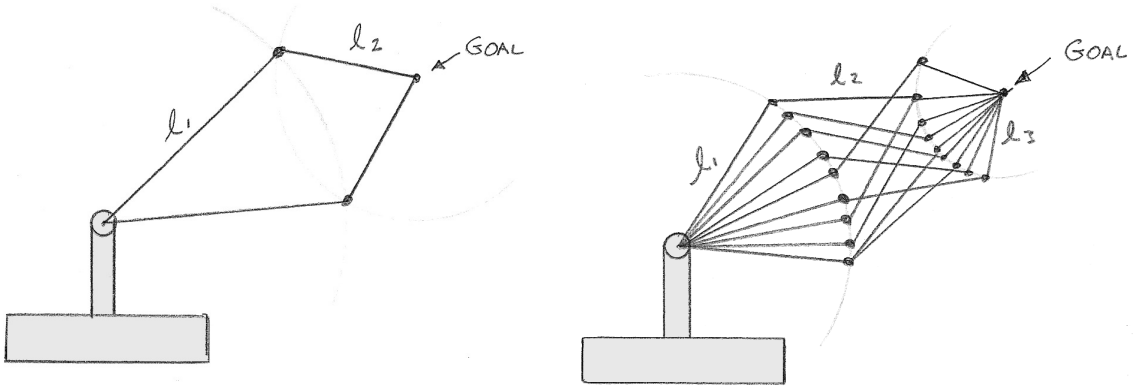

Figure 4.2: Planar manipulators with 2 links (left) and 3 links (right) pointing at the same goal point.

4.2.2 Multiple Solutions

We will consider two important cases: first, when the number of degrees of freedom of the robot are equal to the number in the task, and second when the number of degrees of freedom in the robot are greater than in the task.

1) Consider a 2 link planar arm (Figure 4.2, left).

This arm has two joints and two links. We consider its task to be completely specified by the position of its end effector in the plane. Thus the number of degrees of freedom and the dimensionality of the task are both 2. In this case there are a finite number of solutions (2) which are illustrated above. The planar two-joint arm can reach the goal in two configurations referred to as "elbow-up" and "elbow-down." Each of these configurations is a separate solution to the inverse kinematics problem.

2) Consider a 3-link planar arm with the same goal(Figure 4.2, right).

In this case there are an infinite number of solutions (10 are shown). The robot has three joints and therefore three degrees of freedom, but the task is still only two DOF. This robot is thus underspecified — a situation we call kinematic redundancy. A robot with kinematic redundancy can even move itself around (among the infinite number of solutions) without moving the end effector from the goal. This is called self-motion.

4.2.3 Methods of Solution

There are three principal ways to obtain the inverse kinematics solutions:

1. "Closed Form": An analytic expression for θ as a function of ${}^0_6T_d$ which includes all solutions.
2. Numerical methods.
3. Hybrid approach in which some degrees of freedom are solved in closed form and others numerically.

We will concentrate here on the closed form solution.

There are two standard approaches to obtaining the closed form solution, the algebraic approach, primarily involving manipulation of the forward kinematic equations, and the geometric approach, in which the inverse kinematics problem is reduced to one or more plane geometry problems. However, unlike the forward kinematics problem, there is no straightforward procedure which can be followed to get analytical solutions.

4.3 Inverse Kinematics Tools

4.3.1 Inverse of a Homogeneous Transform

Let's define two frames which are related by a translation $P_{1,2}$ and a rotation ${}^1_2R$ (Figure 4.3).

If we represent this spatial relationship by a homogeneous transform, T, then it is reasonable to assume that an inverse, T^{-1} must always exist

Q: Why?

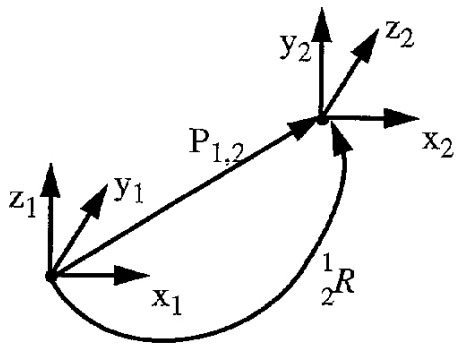

Figure 4.3: Two frames with a position offset, $P_{1,2}$ and a rotation offset ${}^1_2R$

A: One reason: a physical move can always be "undone." Another reason[1], eigenvalues of $T = 1, e^{j\theta}, e^{-j\theta}$, so their product, (the determinant) is always non-zero.

If the homogeneous transform is

$${}^1_2T = \begin{bmatrix} \begin{bmatrix} & {}^1_2R & \end{bmatrix} & \begin{bmatrix} {}^1P_{1,2} \end{bmatrix} \\ \begin{bmatrix} 0 & 0 & 0 \end{bmatrix} & \begin{bmatrix} 1 \end{bmatrix} \end{bmatrix}$$

then it is easy to show that its inverse is

$${}^1_2T^{-1} = {}^2_1T = \begin{bmatrix} \begin{bmatrix} & {}^2_1R & \end{bmatrix} & \begin{bmatrix} -{}^2P_{1,2} \end{bmatrix} \\ \begin{bmatrix} 0 & 0 & 0 \end{bmatrix} & \begin{bmatrix} 1 \end{bmatrix} \end{bmatrix}$$

where ${}^2_1R = {}^1_2R^T$ and $-{}^2P_{1,2} = {}^2_1R\left(-{}^1P_{1,2}\right)$

4.3.2 Inverse of a Quaternion

The inverse of a quaternion (Section 2.7), $q*$,is simply its conjugate, equation (2.3).

$$q^* = \cos(\theta/2) - K_x i \sin(\theta/2) - K_y j \sin(\theta/2) - K_z k \sin(\theta/2) = (w, -x, -y, -z)$$

4.3.3 Inverse Sin and Cos

The basic inverse trigonometric functions are often useful. Remember that they each have two solutions:

$$\sin^{-1}(x) = \{\theta,\ \pi - \theta\} \qquad \cos^{-1}(x) = \pm\theta$$

and that they are only valid for

$$-1 \le x \le 1$$

4.3.4 Atan2(y,x)

We need a slightly more sophisticated form of the arctan() function to find angles. Consider a trivial robot arm with a single link of unit length with a rotary joint at the origin. If we pick a point on the unit circle, then the inverse kinematics problem is simply solved by the arctangent. However, the arctan function domain is limited to the first and fourth quadrants:

$$-\frac{\pi}{2} \le \arctan(\frac{y}{x}) \le \frac{\pi}{2}$$

In real-world problems, we need to solve the inverse kinematics problem for any quadrant (Figure 4.4).

The **atan2(y,x)** function, also known as the four quadrant arctangent, returns an angle between 0 and 2π allowing the solution to occupy any of the four quadrants.

[1] J.M. McCarthy, "Introduction to Theoretical Kinematics," MIT Press, 1990.

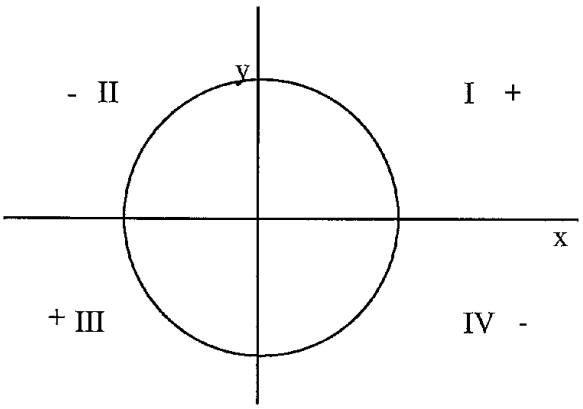

Figure 4.4: Unlike the arctangent function, the `atan2(y,x)` function returns a result in any quadrant, I-IV.

4.3.5 Key Trigonometric Identities

Some trig identities (which may have faded from your mind) will be very useful in solving inverse kinematics problems.

Sum of Angles

If $c_{12} = \cos(\theta_1 + \theta_2)$ and $s_{12} = \sin(\theta_1 + \theta_2)$, then

$$c_{12} = c_1 c_2 - s_1 s_2$$

and

$$s_{12} = c_1 s_2 + s_1 c_2$$

This offers a way to solve the following problem which frequently comes up in inverse kinematics:

"Given k_1, k_2, and x, solve $x = k_1 \cos(\theta_1) + k_2 \sin(\theta_1)$ for θ_1."

Here is one way:

Let $r = \sqrt{k_1^2 + k_2^2}$ and let $\theta_2 = \text{atan2}(k_1, k_2)$. In other words

$$k_1 = r s_2, \quad k_2 = r c_2$$

Rewriting the problem with this change of variables and applying sum-of-angles:

$$x = r s_2 c_1 + r c_2 s_1 = r s_{12}$$

$$\frac{x}{r} = \sin(\theta_1 + \theta_2) = s_{12}$$

We can solve this with the inverse sine function, $\sin^{-1}()$, but there is a preference in the robotics literature to transform it further into an atan2() solution by:

$$c_{12} = \pm\sqrt{1 - s_{12}^2} = \pm\sqrt{1 - \left(\frac{x}{r}\right)^2}$$

$$\theta_1 + \theta_2 = \text{atan2}(s_{12}, c_{12})$$

$$\theta_1 = \text{atan2}\left(\frac{x}{r}, \pm\sqrt{1 - \left(\frac{x}{r}\right)^2}\right) - \text{atan2}(k_1, k_2)$$

Note that there are two solutions to this equation corresponding to the $\pm$ choice of the square root.

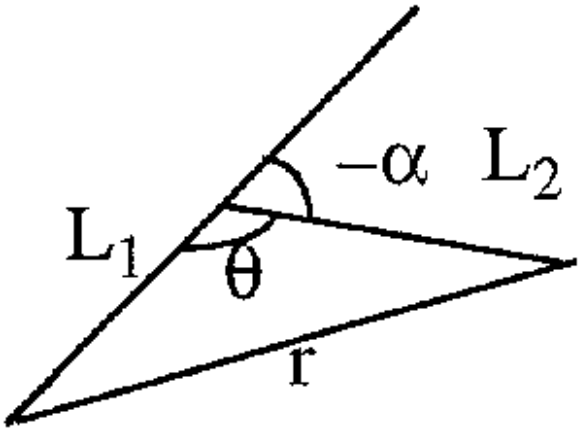

Figure 4.5: Triangle and notation for the Law of Cosines.

A joint angle can only be a real number for a reachable pose. For the real solution to exist, the argument of the square root must be real giving

$$\frac{x^2}{r^2} \leq 1, \quad x^2 \leq r^2, \quad |x| \leq |r|, \quad |x| \leq +\sqrt{k_1^2 + k_2^2}$$

So, if $|x| > \sqrt{k_1^2 + k_2^2}$, no solution exists. This is a mathematical test we can apply during computation to check whether or not the manipulator is capable of reaching the desired point. However this is not the only condition which must be met in practice because we are still considering the idealized case where the joints can take on any value. In real manipulators, joint limits prohibit some points from being reached even if the inverse kinematics solution exists.

4.3.6 Law of Cosines

This old workhorse is a way to solve a frequently arising problem in inverse kinematics when an arm has two parallel axes. Considering a triangle as in Figure 4.5, the law of cosines states:

$$r^2 = L_1^2 + L_2^2 - 2L_1L_2\cos(\theta)$$

for an alternate form, we can use the fact that $\theta = \pi + \alpha$ to get

$$r^2 = L_1^2 + L_2^2 + 2L_1L_2\cos(\pm\alpha)$$

This has two solutions since $\cos(\alpha) = \cos(-\alpha)$.

4.3.7 Manipulator Sub-Space

When the robot has fewer than six DOF, but the task has six DOF, then there are no solutions to the general problem, but only special cases. However, it is often useful to specify a subspace of the full 6 DOF configuration space which has a dimensionality which matches the robot arm. For example, if we restrict our desired EE positions to the plane, then a planar arm is capable of reaching them. This plane, embedded in the six DOF space of possible rigid body configurations, in an example of a manipulator sub-space.

Alternatively, we can think of a planar world in which the configuration of any object consists of the x

and y positions, and α, the orientation of the object.

Example 4.6
Consider the following arm in a planar world which can reach various x, y positions, but has a fixed wrist so that frame 3 has a particular orientation depending on the angles θ_1 and θ_2. Because of this dependence, the arm can only reach two specific orientations corresponding to the "elbow-up" and "elbow-down" solutions.

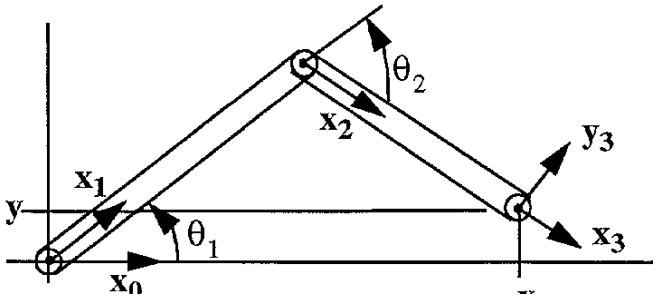

Suppose our task is described by

$$ {}^0_3T = \begin{bmatrix} \begin{bmatrix} & {}^0_3R & \end{bmatrix} & \begin{bmatrix} x \\ y \\ z \end{bmatrix} \\ \begin{bmatrix} 0 & 0 & 0 \end{bmatrix} & 1 \end{bmatrix} $$

Since there is no joint at the wrist of this robot, ${}^0_3R = {}^0_3R(x, y)$ is a multivalued function of x, y. We call

$$ {}^0_3T_D(x, y) = \begin{bmatrix} \begin{bmatrix} & {}^0_3R(x, y) & \end{bmatrix} & \begin{bmatrix} x \\ y \\ 0 \end{bmatrix} \\ \begin{bmatrix} 0 & 0 & 0 \end{bmatrix} & 1 \end{bmatrix} $$

the "Manipulator subspace." In more detail, we can only reach orientations in the x, y plane so ${}^0_3R$ has the form

$$ {}^0_3R(x, y) = \begin{bmatrix} c\alpha & -s\alpha & 0 \\ s\alpha & c\alpha & 0 \\ 0 & 0 & 1 \end{bmatrix} $$

where α is a two-valued function of x, y. If we use the algebraic approach, we would set up the problem:

$$ {}^0_3T_D(x, y) = {}^0_1T(\theta_1) {}^1_2T(\theta_2) {}^2_3T $$

The manipulator sub-space is not always easy to find. In the case of Example 4.6, the inverse kinematics problem is more easily solved with a geometric approach and does not require a manipulator subspace anyway. Sometimes 6 DOF robots are easier to solve than 5DOF robots because they do not require a manipulator subspace to be derived.

4.3.8 Simultaneous Equations

One problem which comes up frequently in inverse kinematics is simulataneous equations in the joint variables[2]. For example,

$$ x = l_1 c_1 + l_2 c_{12} $$
$$ y = l_1 s_1 + l_2 s_{12} $$

where $c_{12} = \cos(\theta_1 + \theta_2)$ (terms involving sums of two joint angles are common when two axes are parallel in a manipulator design). The problem is to find θ_1 when θ_2 is known.

Use the sum-of-angles formulae to rewrite equations as

$$ x = l_1 c_1 + l_2 (c_1 c_2 - s_1 s_2) $$
$$ y = l_1 s_1 + l_2 (c_2 s_1 + s_2 c_1) $$

Now isolate the unknowns:

[2]Thanks to Dr. Pamela Bhatti.

$$x = (l_1 + l_2c_2)c_1 - (l_2s_2)s_1$$
$$y = (l_1 + l_2c_2)s_1 + (l_2s_2)c_1$$

let $k_1 = (l_1 + l_2c_2)$ and $k_2 = l_2s_2$ and place these equations into matrix form:

$$\begin{bmatrix} x \\ y \end{bmatrix} = \begin{bmatrix} k_1 & -k_2 \\ k_2 & k_1 \end{bmatrix} \begin{bmatrix} c_1 \\ s_1 \end{bmatrix}$$

Using standard 2×2 matrix methods to solve for x, y,

$$\text{determinant} = k_1^2 + k_2^2$$
$$c_1 = \frac{xk_1 + yk_2}{k_1^2 + k_2^2}$$
$$s_1 = \frac{yk_1 - xk_2}{k_1^2 + k_2^2}$$

$$\theta_1 = \text{atan2}(yk_1 - xk_2, \quad xk_1 + yk_2)$$

(Since the demoninators are always positive, we can drop them from the atan2. Also, note that we need another equation to get θ_2.)

4.4 Algebraic Solution

4.4.1 Strategy

The forward kinematics analysis of an all rotary 6DOF arm yields an equation

$${}^0_6T \quad = \quad {}^0_1T(\theta_1) \quad {}^1_2T(\theta_2) \quad {}^2_3T(\theta_3) \quad {}^3_4T(\theta_4) \quad {}^4_5T(\theta_5) \quad {}^5_6T(\theta_6)$$

In the inverse kinematics version of the problem, ${}^0_6T$ is known and we can call it ${}^0_6T_D$ (meaning desired), and the θ_i are unknowns. The equation

$${}^0_6T_D = {}^0_6T$$

is really 12 individual equations, one for each element of the first three rows. On inspecting those 12 equations we might find one which can easily be solved for θ_1 or perhaps a pair of equations which could jointly be solved for θ_1. But all of the other unknowns are mixed into complicated equations with no apparent solution. However, when θ_1 is solved, ${}^0_1T(\theta_1)$ becomes a known matrix. We can then write

$${}^0_1T^{-1} \; {}^0_6T_D^{-1} = {}^0_1T(\theta_1)^{-1} \; {}^0_6T \; = \; {}^1_2T(\theta_2) \quad {}^2_3T(\theta_3) \quad {}^3_4T(\theta_4) \quad {}^4_5T(\theta_5) \quad {}^5_6T(\theta_6)$$

which generates a fresh set of 12 equations in which all the elements of the left hand side are knowns. We may now find a new equation or set of equations which we can solve for θ_2. When θ_2 is known, we can write

$${}^1_2T(\theta_2)^{-1} \quad {}^0_1T(\theta_1)^{-1} \quad {}^0_6T = {}^2_3T(\theta_3) \quad {}^3_4T(\theta_4) \quad {}^4_5T(\theta_5) \quad {}^5_6T(\theta_6)$$

Although there are several "might"s in this description, because of the serial nature of the arms, this method works as described more often than one "might" think.

4.4.2 Examples

Example 4.7
Consider a mechanism which corresponds to the z, y, x Euler angles (Section 2.5.2).

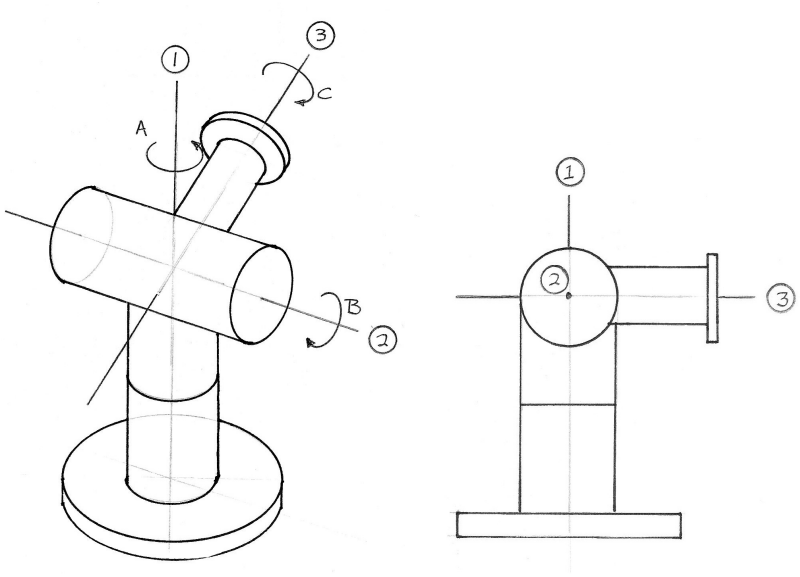

This mechanism has three axes of rotation which intersect at a single point. The axes are arranged so that the first rotation about z, moves the x and y axes for subsequent rotations which corresponds to the definition of Euler angles. The last frame, frame 3, has no offset from the point where the axes intersect, so the homogeneous transform consists only of rotation with no translation. The amounts of rotation about z, y, x are A, B, C. Expanding the 3x3 rotation matrix of Section 2.5.2 into a 4x4 homogeneous transform with zero translation, we get

$$ {}^0_3T(A,B,C) = \begin{bmatrix} cAcB & cAsBsC - sAcC & cAsBcC + sAsC & 0 \\ sAcB & sAsBsC + cAcC & sAsBcC - cAsC & 0 \\ -sB & cBsC & cBcC & 0 \\ 0 & 0 & 0 & 1 \end{bmatrix} $$

The manipulator subspace for this manipulator is

$$ {}^0_3T_D = \begin{bmatrix} \begin{bmatrix} & R & \end{bmatrix} & \begin{bmatrix} 0 \\ 0 \\ 0 \end{bmatrix} \\ \begin{bmatrix} 0 & 0 & 0 \end{bmatrix} & 1 \end{bmatrix} $$

Where R can be any rotation matrix because we can reach nearly any orientation with ZYX Euler angles (see below). The inverse kinematics problem can then be set up to solve

$$ {}^0_3T_D = {}^0_3T(A,B,C) $$

for A, B, C, given ${}^0_3T_D$, Expanding this equation gives

$$ \begin{bmatrix} r_{11} & r_{12} & r_{13} \\ r_{21} & r_{22} & r_{23} \\ r_{31} & r_{32} & r_{33} \end{bmatrix} = \begin{bmatrix} cAcB & cAsBsC - sAcC & cAsBcC + sAsC \\ sAcB & sAsBsC + cAcC & sAsBcC - cAsC \\ -sB & cBsC & cBcC \end{bmatrix} $$

Remember that everything on the left hand side is known as part of the desired EE configuration, and the unknowns are A, B, C.

Example 4.7 cont.
Looking over these 9 equations, we find fairly simple forms in the upper left hand corner:

$$r_{11} = cAcB, \qquad r_{21} = sAcB$$

We can add the squares of these equations together to get

$$r_{11}^2 + r_{21}^2 = cB^2(cA^2 + sA^2)$$

or

$$cB = \pm\sqrt{r_{11}^2 + r_{21}^2}$$

We can use more information from ${}^0_3T_D$ since $r_{31} = -sB$ and use atan2:

$$B = \text{atan2}(-r_{31}, \pm\sqrt{r_{11}^2 + r_{21}^2})$$

if $B \neq \{\pi/2, -\pi/2\}$ then cB is a non-zero constant and we can get

$$A = \begin{cases} \text{atan2}(r_{21}, r_{11}) & cB > 0 \\ \text{atan2}(-r_{21}, -r_{11}) & cB \leq 0 \end{cases}$$

Note that atan2(ay, ax) = atan2(y,x) if $a > 0$ and that $\text{atan2}(y, x) \neq \text{atan2}(-y, -x)$.
Similarly

$$r_{32} = cBsC, \qquad r_{33} = cBcC$$

if $B \neq \{\pi/2, -\pi/2\}$ then cB is a non-zero constant and we can get

$$C = \begin{cases} \text{atan2}(r_{32}, r_{33}) & cB > 0 \\ \text{atan2}(-r_{32}, -r_{33}) & cB \leq 0 \end{cases}$$

Alternatively we can express the multiple solutions slightly differently:

$$C = \begin{cases} \text{atan2}(r_{32}, r_{33}) & cB > 0 \\ \text{atan2}(r_{32}, r_{33}) + \pi & cB \leq 0 \end{cases}$$

Example 4.8
Solve for A, B, C in the wrist of Example 4.7 where:

$$ {}^{0}_{3}T_{D} = \begin{bmatrix} 0.925 & 0.018 & 0.379 \\ 0.163 & 0.883 & -0.441 \\ -0.342 & 0.470 & 0.814 \end{bmatrix} $$

Solution:

$$ B = \text{atan2}\left(0.342, \pm\sqrt{0.856 + 0.027}\right) $$
$$ B = \{20^\circ, 160^\circ\} $$

$$ A = \text{atan2}(0.163, 0.925) = \arctan(0.176) \quad (B = 20^\circ) $$
$$ A = \arctan(0.176) + 180^\circ \quad (B = 160^\circ) $$
$$ A = \{10^\circ, 190^\circ\} $$

$$ C = \text{atan2}(0.470, 0.814) = \arctan(0.577) \quad (B = 20^\circ) $$
$$ C = \arctan(0.577) + 180^\circ \quad (B = 160^\circ) $$
$$ C = \{30^\circ, 210^\circ\} $$

The solutions form a graph which associates the multiple solutions of each individual joint into two solution sets:

$$ [A_a, B_a, C_a], [A_b, B_b, C_b] $$

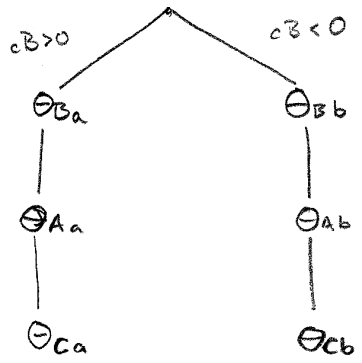

Example 4.9
Inverse Kinematics Example: "Chair Helper" 5-DOF Robot
Problem and solution by Professor Melani Shoemaker.

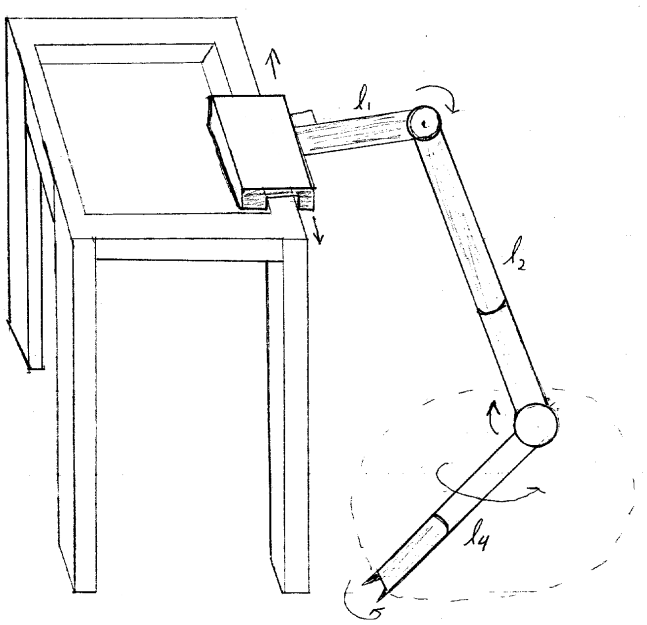

Here is an example of solving the inverse kinematics equations for a 5-DOF robot embedded in 6-DOF space. This is a robot designed to assist a wheelchair user. By application of link frames, derivation of Denavit Hartenberg parameters, and applying them to the link transform matrix,

$$ {}^{N-1}_{N}T = \begin{bmatrix} c\theta_N & -s\theta_N & 0 & a_{N-1} \\ s\theta_N c\alpha_{N-1} & c\theta_N c\alpha_{N-1} & -s\alpha_{N-1} & -s\alpha_{N-1}d_N \\ s\theta_N s\alpha_{N-1} & c\theta_N s\alpha_{N-1} & c\alpha_{N-1} & c\alpha_{N-1}d_N \\ 0 & 0 & 0 & 1 \end{bmatrix} $$

we can get the transform for each link as follows:

$$ {}^{0}_{1}T = \begin{bmatrix} 1 & 0 & 0 & 0 \\ 0 & 1 & 0 & 0 \\ 0 & 0 & 1 & d \\ 0 & 0 & 0 & 1 \end{bmatrix} \qquad {}^{1}_{2}T = \begin{bmatrix} c_2 & -s_2 & 0 & l_1 \\ s_2 & c_2 & 0 & 0 \\ 0 & 0 & 1 & 0 \\ 0 & 0 & 0 & 1 \end{bmatrix} $$

$$ {}^{2}_{3}T = \begin{bmatrix} c_3 & -s_3 & 0 & 0 \\ 0 & 0 & -1 & -l_2 \\ s_3 & c_3 & 0 & 0 \\ 0 & 0 & 0 & 1 \end{bmatrix} \qquad {}^{3}_{4}T = \begin{bmatrix} c_4 & -s_4 & 0 & 0 \\ 0 & 0 & -1 & 0 \\ s_4 & c_4 & 0 & 0 \\ 0 & 0 & 0 & 1 \end{bmatrix} $$

$$ {}^{4}_{5}T = \begin{bmatrix} c_5 & -s_5 & 0 & 0 \\ 0 & 0 & 1 & l_4 \\ -s_5 & -c_5 & 0 & 0 \\ 0 & 0 & 0 & 1 \end{bmatrix} $$

Now we create the forward kinematic equations, by multiplying the link matrices together as:

$$ {}^{0}_{5}T = \quad {}^{0}_{1}T \quad {}^{1}_{2}T \quad {}^{2}_{3}T \quad {}^{3}_{4}T \quad {}^{4}_{5}T $$

Example 4.9 cont.
It turns out that if we start multiplying from ${}^4_5T$ and work our way backwards, we will get highly useful intermediate results. i.e.

$${}^0_5T = \quad {}^0_1T \quad {}^1_2T \quad {}^2_3T \begin{bmatrix} c_4c_5 & -c_4s_5 & -s_4 & -s_4l_4 \\ s_5 & c_5 & 0 & 0 \\ s_4c_5 & -s_4s_5 & c_4 & c_4l_4 \\ 0 & 0 & 0 & 1 \end{bmatrix}$$

The matrix at the right, ${}^3_5T$, will be useful later. Similarly,

$${}^0_5T = \quad {}^0_1T \quad {}^1_2T \begin{bmatrix} c_3c_4c_5 - s_3s_5 & -c_3c_4s_5 - s_3c_5 & -s_4c_3 & -c_3s_4l_4 \\ -s_4c_5 & s_4s_5 & -c_4 & -c_4l_4 - l_2 \\ s_3c_4c_5 + c_3s_5 & -s_3c_4s_5 + c_3c_5 & -s_4s_3 & -s_3s_4l_4 \\ 0 & 0 & 0 & 1 \end{bmatrix}$$

This time the matrix at the right is ${}^2_5T$, and it will also be useful. Continuing this process gives us the complete forward kinematic model:

$${}^0_5T = \begin{bmatrix} c_2c_3c_4c_5 - c_2s_3s_5 + s_2s_4c_5 & -c_2c_3c_4s_5 - c_2s_3c_5 - s_2s_4s_5 & -c_2s_4c_3 + s_2c_4 & -c_2c_3s_4l_4 + s_2c_4l_4 + s_2l_2 + l_1 \\ s_2c_3c_4c_5 - s_2s_3s_5 - c_2s_4c_5 & -s_2c_3c_4s_5 - s_2s_3c_5 + c_2s_4s_5 & -s_2s_4c_3 - c_2c_4 & -s_2c_3s_4l_4 - c_2c_4l_4 - c_2l_2 \\ s_3c_4c_5 + c_3s_5 & -s_3c_4s_5 + c_3c_5 & -s_4s_3 & -s_3s_4l_4 + d \\ 0 & 0 & 0 & 1 \end{bmatrix}$$

We desire the robot to reach the configuration ${}^0_5T_D$, were

$${}^0_5T_D = \begin{bmatrix} r_{11} & r_{12} & r_{13} & P_x \\ r_{21} & r_{22} & r_{23} & P_y \\ r_{31} & r_{32} & r_{33} & P_z \\ 0 & 0 & 0 & 1 \end{bmatrix}$$

Remember, every element of ${}^0_5T_D$ is *known*. We generate equations to solve by equating like terms between ${}^0_5T_D$ and the forward kinematic model. For example, to pick a small one,

$$r_{33} = -s_4s_3$$

So far so good, but how do we attack this mess? Unfortunately, there is no substitute for just going to a quiet room, getting a cup of coffee, and going at it. Here is what Melani did. Let's look in particular at two equations we can write from the above:

$$r_{13} = -c_2s_4c_3 + s_2c_4$$

and

$$P_x = -c_2c_3s_4l_4 + s_2c_4l_4 + s_2l_2 + l_1$$

If we re-write the second one as

$$P_x = (-c_2s_4c_3 + s_2c_4)l_4 + s_2l_2 + l_1$$

we now have the right-hand-side of r_{13} embedded inside the RHS of P_x. Therefore we can substitute to get rid of the unknowns s_2, c_2, s_4, c_4.

$$P_x = r_{13}l_4 + s_2l_2 + l_1$$

This can be solved (because *only* s_2 is unknown) to give

$$s_2 = \frac{P_x - r_{13}l_4 - l_1}{l_2}$$

We can use the exact same logic on the second row of the matrix to get

$$c_2 = \frac{-P_y - r_{23}l_4}{l_2}$$

Now we have the first result:

$$\theta_2 = \text{atan2}(P_x - r_{13}l_4 - l_1, -P_y - r_{23}l_4)$$

(note that we could take out the $\frac{1}{l_2}$ term because it is common to both arguments of atan2 and because it is positive.)

Example 4.9 cont.
What else can we solve? Let's use this same trick on the third row.

$$r_{33} = -s_4 s_3$$

$$P_z = -s_3 s_4 l_4 + d$$

This gives our second result:

$$d = P_z - r_{33} l_4$$

Now it seems like we have run out of such tricks, but this is where our intermediate results come to the rescue. We had

$${}^0_5T = \quad {}^0_1T \quad {}^1_2T \begin{bmatrix} c_3c_4c_5 - s_3s_5 & -c_3c_4s_5 - s_3c_5 & -s_4c_3 & -c_3s_4l_4 \\ -s_4c_5 & s_4s_5 & -c_4 & -c_4l_4 - l_2 \\ s_3c_4c_5 + c_3s_5 & -s_3c_4s_5 + c_3c_5 & -s_4s_3 & -s_3s_4l_4 \\ 0 & 0 & 0 & 1 \end{bmatrix}$$

Since we know d and θ_2, ${}^0_1T$ and ${}^1_2T$ are now known. Thus we can write

$$({}^1_2T)^{-1}({}^0_1T)^{-1} \quad {}^0_5T = \begin{bmatrix} c_3c_4c_5 - s_3s_5 & -c_3c_4s_5 - s_3c_5 & -s_4c_3 & -c_3s_4l_4 \\ -s_4c_5 & s_4s_5 & -c_4 & -c_4l_4 - l_2 \\ s_3c_4c_5 + c_3s_5 & -s_3c_4s_5 + c_3c_5 & -s_4s_3 & -s_3s_4l_4 \\ 0 & 0 & 0 & 1 \end{bmatrix}$$

Let's define:

$$\hat{T} = ({}^1_2T)^{-1}({}^0_1T)^{-1} \quad {}^0_5T_D$$

Though we can't know the values of $\hat{T}$ until d and θ_2 are solved, after that point we can use $\hat{T}$ the same way we used ${}^0_5T_D$. In other words, we can treat $\hat{T}$ as *known*.

$$\hat{T} = \quad {}^2_5T$$

Equating elements we get

$$\hat{T}_{33} = -s_4 s_3$$

$$\hat{T}_{13} = -s_4 c_3$$

If $s_4 \neq 0$, we can treat it like a constant, but since both θ_3 and θ_4 are unknown, we get two possible solutions:

$$\theta_{3,1} = \text{atan2}(\hat{T}_{33}, \hat{T}_{13})$$

and

$$\theta_{3,2} = \text{atan2}(-\hat{T}_{33}, -\hat{T}_{13}) = \theta_{3,1} + \pi$$

Now that we have two solutions for θ_3, we have ${}^2_3T_1$ and ${}^2_3T_2$. We can generate two versions of a third *known* matrix:

$$\tilde{T1} = ({}^2_3T_1)^{-1}({}^1_2T)^{-1}({}^0_1T)^{-1} \quad {}^0_5T_D$$

$$\tilde{T2} = ({}^2_3T_2)^{-1}({}^1_2T)^{-1}({}^0_1T)^{-1} \quad {}^0_5T_D$$

These can be equated to our first intermediate result from the forward kinematics to easily get θ_4 and θ_5:

$$\tilde{T}_{13} = -s_4, \quad \tilde{T}_{33} = c_4$$

$$\tilde{T}_{21} = -s_5, \quad \tilde{T}_{22} = c_5$$

Example 4.9 cont.

but remembering that there are two versions of $\tilde{T}$

$$\theta_{4,1} = \text{atan2}(-\tilde{T1}_{13}, \tilde{T1}_{33})$$

$$\theta_{4,2} = \text{atan2}(-\tilde{T2}_{13}, \tilde{T2}_{33})$$

$$\theta_{5,1} = \text{atan2}(-\tilde{T1}_{21}, \tilde{T1}_{22})$$

$$\theta_{5,2} = \text{atan2}(-\tilde{T2}_{21}, \tilde{T2}_{22})$$

Recap

To summarize, the result of our analysis is a general solution to the inverse kinematics problem *for this robot* that will work for any reachable end effector configuration, ${}^0_5T_D$. Suppose we were now to implement this as a piece of computer code, what would we have to do? Here is a rough outline:

1. Read in the desired end-effector configuration

$${}^0_5T_D = \begin{bmatrix} r_{11} & r_{12} & r_{13} & P_x \\ r_{21} & r_{22} & r_{23} & P_y \\ r_{31} & r_{32} & r_{33} & P_z \\ 0 & 0 & 0 & 1 \end{bmatrix}$$

2. Check that this matrix represents a valid reachable pose for this robot (see below).

3. $$\theta_2 = \text{atan2}(P_x - r_{13}l_4 - l_1, -P_y - r_{23}l_4)$$

4. $$d = P_z + r_{33}l_4$$

5. Using the values of θ_2 and d just computed, compute

$$\hat{T} = ({}^1_2T)^{-1}({}^0_1T)^{-1} \quad {}^0_5T_D$$

6. Verify assumption that $\theta_4 \neq 0$ or π. To do this, we could check that $|\hat{T}_{33}|$ **and** $|\hat{T}_{13}|$ are greater than zero, or we could check $|\hat{T}_{23}| < 1$. If these tests fail, we can only solve for $\theta_3 + \theta_5$.

7. Compute

$$\theta_{3,1} = \text{atan2}(\hat{T}_{33}, \hat{T}_{13})$$
$$\theta_{3,2} = \theta_{3,1} + 3.1415926$$

8. Using the values of θ_2, θ_3, and d just computed, compute

$$\tilde{T1} = ({}^2_3T_1)^{-1}({}^1_2T)^{-1}({}^0_1T)^{-1} \quad {}^0_5T_D$$

$$\tilde{T2} = ({}^2_3T_2)^{-1}({}^1_2T)^{-1}({}^0_1T)^{-1} \quad {}^0_5T_D$$

9. Finally we can compute the joint angles:

$$\theta_{4,1} = \text{atan2}(-\tilde{T1}_{13}, \tilde{T1}_{33})$$

$$\theta_{4,2} = \text{atan2}(-\tilde{T2}_{13}, \tilde{T2}_{33})$$

$$\theta_{5,1} = \text{atan2}(-\tilde{T1}_{21}, \tilde{T1}_{22})$$

$$\theta_{5,2} = \text{atan2}(-\tilde{T2}_{21}, \tilde{T2}_{22})$$

Example 4.9 cont.

Reachability

We have skipped one last detail which makes the problem a bit more tricky. The solution above will only work if ${}^0_5T_D$ represents a valid reachable configuration for our manipulator. Since we have only 5 degrees of freedom, not all orientations are possible at a given position. It is not trivial to generate the ${}^0_5T_D$ matrix but we will leave that topic to another time.

4.5 Geometric Solution

The other major approach to inverse kinematics is to identify and solve for joint angles or displacements by means of plane geometry. Although the manipulator moves through 3D space, often a plane can be identified which always contains one or more mechanism joints and which contains a solvable triangle. Before we see this type of situation, let us assume that we are dealing with manipulators that are confined to the plane.

4.5.1 Planar Examples

Example 4.10

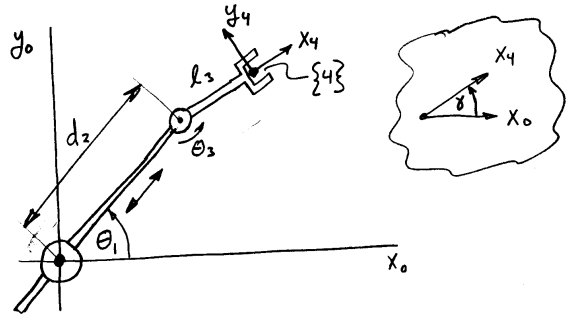

First, assume that joint 3 is locked. For $\theta_3 = 90°$, find θ_1, and d_2, given the end effector coordinates x, y:

$$^0P_4 = \begin{bmatrix} x \\ y \end{bmatrix}$$

How many solutions are there and how do you find them?

Solution:

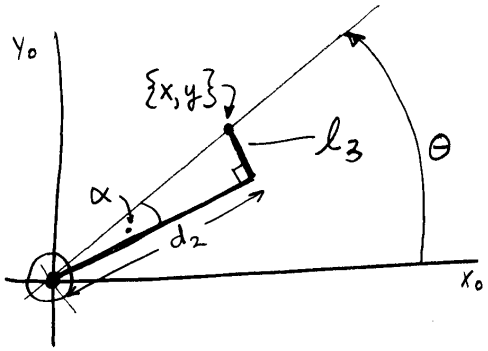

by Pythagorean theorem and a few basic triangle facts:,

$$d_2^2 + l_3^2 = x^2 + y^2 \qquad \beta = \text{atan2}(y, x) \qquad \theta_1 = \beta - \alpha$$

$$d_2 = \pm\sqrt{x^2 + y^2 - l_3^2}$$

$$\alpha = \text{atan2}(l_3, d_2)$$

$$\theta_1 = \text{atan2}(y, x) - \text{atan2}(l_3, d_2)$$

There are two solutions, obtained by taking either positive or negative root of d_2. Choice of θ_1 is automatic.

Example 4.11

Now assume that θ_3 is variable. Given x, y and ${}^0_4R$, or equivalently, the end effector angle, γ, find θ_1, d_2, θ_3. How many solutions are there and how do you find them?

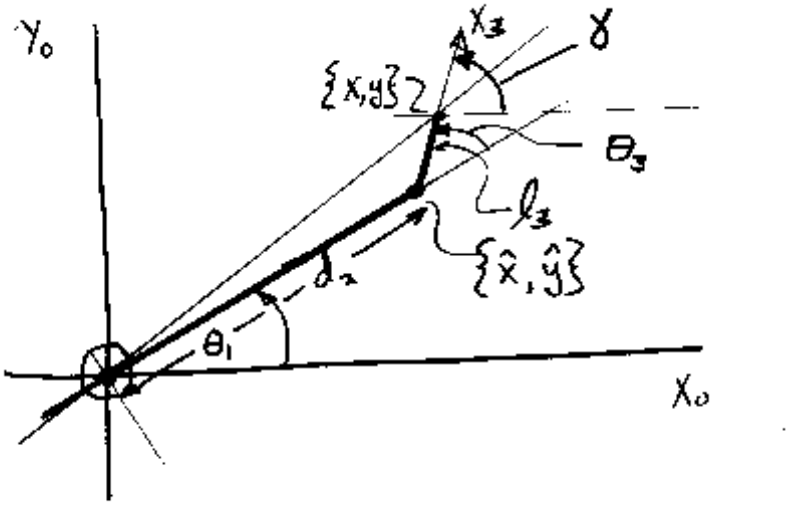

Solution:

The manipulator subspace is the set of T matrices which allow a position in the XY plane, and a rotation angle γ of the end effector in the plane:

$$ManipSS = \begin{bmatrix} c\gamma & -s\gamma & 0 & x \\ s\gamma & c\gamma & 0 & y \\ 0 & 0 & 1 & 0 \\ 0 & 0 & 0 & 1 \end{bmatrix}$$

$${}^0_4R = \begin{bmatrix} c\gamma & -s\gamma & 0 \\ s\gamma & c\gamma & 0 \\ 0 & 0 & 1 \end{bmatrix}$$

$$\gamma = \text{atan2}(r_{21}, r_{11})$$

$$\gamma = \text{direction of } x_3$$

Now let's solve for the position of the elbow, labeled $\hat{x}, \hat{y}$.

$$\hat{x} = x + l_3 \cos(\pi + \gamma)$$

$$\hat{y} = y + l_3 \sin(\pi + \gamma)$$

$$d_2 = \pm\sqrt{\hat{x}^2 + \hat{y}^2}$$

There are two solutions due to the $\pm$ of the square root.

$$\theta_{1a} = \text{atan2}(\hat{y}, \hat{x})$$

or

$$\theta_{1b} = \text{atan2}(\hat{y}, \hat{x}) + \pi$$

$$\theta_{3a} = 90^\circ + \gamma - \theta_1$$

$$\theta_{3b} = 90^\circ - \gamma + \theta_1$$

Example 4.11 cont.
There are two solutions, obtained by taking either positive or negative root of d_2. Add π to θ_1 if $d_2 < 0$. It might be hard to imagine the $d_2 < 0$ case at first, but look at x_1 in the two poses below:

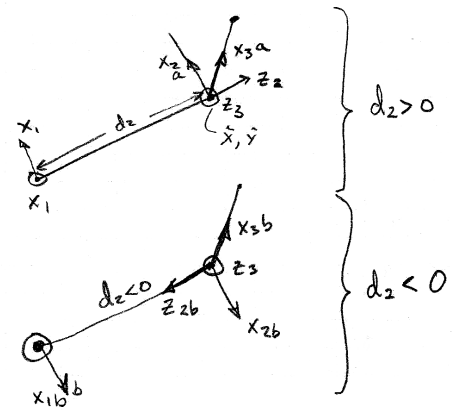

4.5.2 Spatial Example

Now we consider a 3D manipulator in which a plane can be identified (the horizontal plane containing the arm links).

Example 4.12

SCARA robot arm

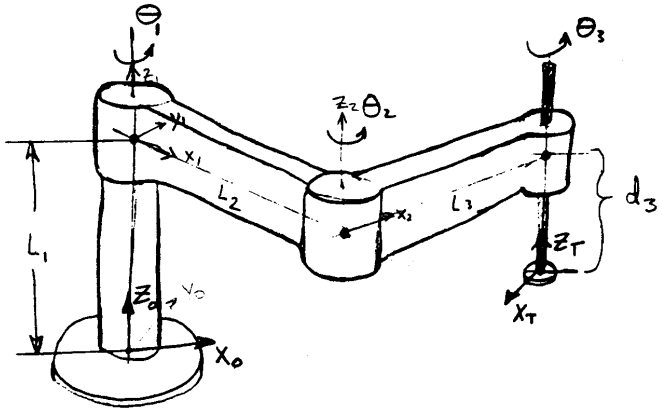

This drawing illustrates a type of 4-DOF arm architecture called the SCARA arm. All three rotary axes are parallel and vertical. The manipulator subspace for this robot is

$$ {}^{O}_{T}T_d = \begin{bmatrix} c\phi & -s\phi & 0 & x_d \\ s\phi & c\phi & 0 & y_d \\ 0 & 0 & 1 & z_d \\ 0 & 0 & 0 & 1 \end{bmatrix} $$

where ϕ is the rotation of the tool frame in the X_0, Y_0 plane. Find the inverse kinematic solutions for this manipulator, i.e. find all solutions for θ_{1-3} and d_3 of

$$ {}^{O}_{T}T\left(\begin{bmatrix} \theta_1 \\ \theta_2 \\ \theta_3 \\ d_3 \end{bmatrix}\right) = {}^{0}_{T}T_d $$

Since forward kinematic equations are not given here, the geometric method is preferred. Make sure you find *all* solutions, and no spurious solutions.

Solution:

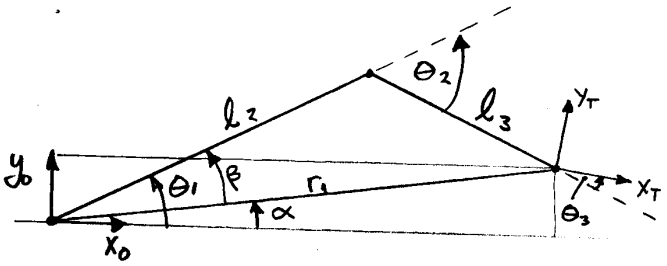

The approach is to solve for θ_1 and θ_3 based on the end point P_0 and then get d_3 and θ_3.

Example 4.12 cont.

$$r_1 = +\sqrt{x^2 + y^2}$$

$$\alpha = \text{atan2}(y_0, x_0)$$

Using law of cosines,

$$r_1^2 = l_2^2 + l_3^2 + 2l_2 l_3 \cos(\theta_2)$$

$$\cos(\theta_2) = \frac{r_1^2 - l_2^2 - l_3^2}{2l_2 l_3} = r_3$$

$$\theta_2 = \pm \cos^{-1}(r_3)$$

$$l_3^2 = l_2^2 + r_1^2 - 2l_2 r_1 \cos\beta$$

$$\cos\beta = \frac{l_2^2 + x_0^2 + y_0^2 - l_3^2}{2l_2 r_1} = r_2$$

$$\beta = \pm \cos^{-1}(r_2)$$

$$\theta_1 = \alpha \pm \beta$$

$$\theta_1 = \text{atan2}(y_0, x_0) \pm \cos^{-1}(r_2)$$

$$\theta_2 = \pm \cos^{-1}(r_3)$$

By inspection:

$$d_3 = L1 - z_d$$

$$\phi = \text{atan2}(t_{d21}, t_{d11})$$

where t_{dij} are the elements of ${}^0_T T_d$. And

$$\theta_3 = \phi - \theta_1 - \theta_2$$

4.6 Summary of Notation

Chapter 5

Differential Kinematics - The Jacobian Matrix

5.1 Problem Statement and Learning Objectives

Problem Statement

Learning Objectives Upon completing this Chapter, the reader should be able to

- compute velocity with different frames of computation and representation and understand the difference between these two frames.
- define the linear and angular velocity of a rigid body.
- compute the velocity and angular velocity of a link, based on the DH parameters and the velocities of the previous link.
- propagate the velocity calculation down the serial link chain to compute linear and angular velocity of an end effector.
- extract a Jacobian Matrix from the velocity propagation calculation.
- state the relationship between joint velocities and end effector velocities using the Jacobian Matrix.
- state the relationship between joint torques and end effector forces using the Jacobian Matrix.

5.2 Velocity

5.2.1 Velocity and Acceleration of a Particle

Velocity is based on a differential measurement or calculation of position, $\Delta X = X(t + \Delta t) - X(t)$. In order for this subtraction to be valid, both $X(t + \Delta t)$ and $X(t)$ must be represented in the same frame which we will call the *computation frame*. If this frame is moving, we might get a very different result from use of a fixed frame. This is not a bad thing however. Depending on our needs, either a moving or fixed frame might be preferable. Another part of the velocity computation is dividing by Δt, but Δt is a scalar, and thus is the same in every frame (leaving out relativistic effects!).

The second key frame is the frame in which we represent the velocity after it is computed, the *representation frame*. Once we have $\frac{\Delta X}{\Delta T}$, we have a free vector, and this may be transformed (by rotation) into any frame we desire. This second frame is called the representation frame.

Velocity of a Vector If ${}^{A}Q$ is a point represented in frame A, then

$$ {}^{A}V_{Q} = \lim_{\Delta t \to 0} \left(\frac{{}^{A}Q(t + \Delta t) - {}^{A}Q(t)}{\Delta t} \right) $$

We have just *computed* the velocity in frame A and it is also *represented* in frame A.

Later we may wish to represent the velocity in another frame e.g.:

$$^B(^AV_Q) = {}^B_AR\,{}^AV_Q$$

If we use the notation:

$$^A(^BV_P)$$

We mean
A is the *representation* frame.
B is the *computation* frame.
P is the point whos velocity we are talking about.

If a velocity is computed and represented in the same frame, we use just one superscript:

$$^A(^AV_P) \rightarrow {}^A\,V_P$$

Example 5.1
To illustrate the difference between *computation* and *representation* of velocity vectors, consider the following example. A car is driving along a road. Its speedometer reads a constant 55 mph. The road is divided into four regions according to the map below.

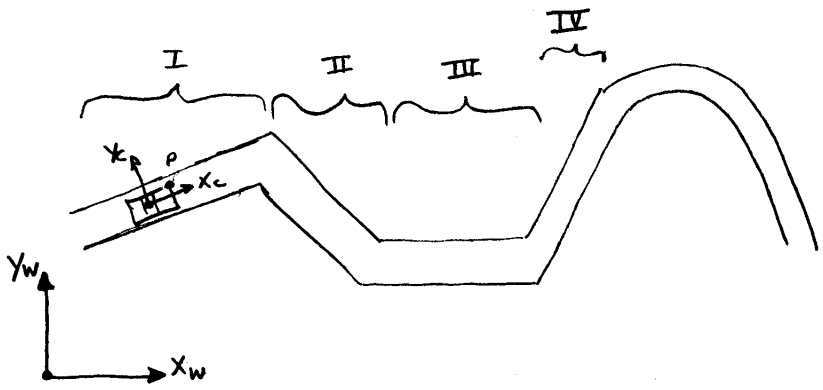

C is a frame fixed to the car. W is a frame fixed to the earth. P is a point on the car.
What are some different velocity vectors for each of the regions I ... IV?

$$^C(^C V_P) = \begin{bmatrix} 0 \\ 0 \\ 0 \end{bmatrix}$$

In this example, the velocity of point, P is computed in the Car frame and represented in the car frame. However since P is a fixed point on the car, it's velocity in the car frame is zero. In fact this is true for all regions of the map. Also, note that

$$^W(^C V_P) = \begin{bmatrix} 0 \\ 0 \\ 0 \end{bmatrix}$$

Why? Because if we rotate this velocity, it's still zero.

$$^C(^W V_P) = \begin{bmatrix} 55mph \\ 0 \\ 0 \end{bmatrix}$$

In this example, the velocity of P is computed in the world frame. This must have a magnitude of 55mph and it must point in the positive X_C direction because we assume the car is going in forward gear! Since the velocity is represented in the car frame, it must be constant and independent of the region.
Supposed we are asked to diagram $^W(^W V_P)$ on the coordinate system $\{X_W, Y_W\}$: What would that look like?

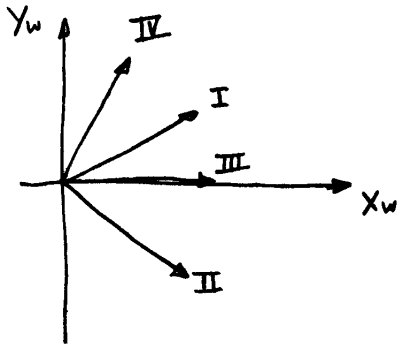

We know $|^W(^W V_P)| = 55mph$ since the speed is a constant 55. Only the direction in frame W changes in each region.

5.2.2 Rigid Bodies and Angular Velocity

Going beyond velocity of single points requires us to consider rigid bodies. Rigid bodies can be thought of as a collection of points, all of which have a fixed location in a frame called an object frame. A rigid body has two types of velocity: linear (translational) velocity which describes its rate and direction of translation, and angular velocity which describes its rotation.

Linear Velocity Linear velocity of a rigid body is represented the same as velocity of a point, having a computation frame and a representation frame. However, nonzero angular velocity of an object will cause each point in the object to have a different linear velocity.

Angular Velocity Angular velocity can be understood through the following properties

- Angular velocity, Ω, is a vector whos direction is the axis of rotation and whos magnitude is the rate of rotation, ω.
- If a point is displaced from the axis of rotation, that point will have a linear velocity component corresponding to the rotation:
$$V = \Omega \otimes r$$
where r is a vector from a point on the axis of rotation to the point.
- The vector cross product $\otimes$ can be defined as
$$A = B \otimes C$$
$$|A| = |B||C| \sin\theta$$
$$A \perp B, A \perp C$$
where θ is the angle between the two vectors by the Right Hand Rule.
- Another way to compute $\otimes$ is using a skew symmetric matrix: If a and b are 3 dimensional vectors,
$$a \otimes b = \begin{bmatrix} 0 & -a_3 & a_2 \\ a_3 & 0 & -a_1 \\ -a_2 & a_1 & 0 \end{bmatrix} \begin{bmatrix} b_1 \\ b_2 \\ b_3 \end{bmatrix}$$
- The angular velocity of a rigid object is the same for all points in that object.

Angular Velocity Generates Linear Velocity In this section we consider the effects of velocity on different parts of an object or robot arising from the second point above.

First, consider a rigid object with a frame, O, attached to it (Figure 5.1).

The origin of frame 0, {O}, has velocity V_O and the object has angular velocity ω_O which are computed in the world frame, W, and represented in *any* frame. What is the velocity of a point, P, on the object?

The answer has two components

- The velocity of the object, V_O.
- Additional velocity due to the rotation of the object: $V = \omega_O \otimes P$

So its total velocity is
$$^*(^W V_P) = V_O + \omega_O \otimes P$$
Where the * is meant to indicate that this equation is true in any frame, so long as all terms are represented in that same frame.

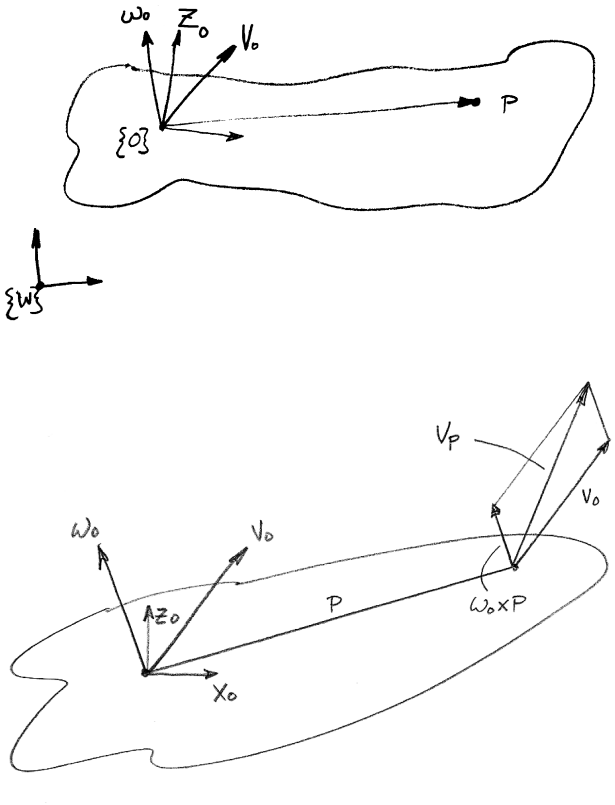

Figure 5.1: Velocity of any point on a rigid object can be computed from it's location in the object frame, using the linear and angular velocity of the body (also represented in the object frame).

5.2.3 Quaternions and Angular Velocity

Quaternion representation of orientation (Section 2.7) can also be differentiated and related to angular velocity. First, we define the notion of the time derivative of a quaternion[1].

Differentiating equation 2.4

$$\frac{dq}{dt} = \frac{1}{2}\dot{\theta}\left[-\sin(\theta/2) + K_x i\cos(\theta/2) + K_y j\cos(\theta/2) + K_z k\cos(\theta/2)\right]$$

then it can be derived that

$$\begin{bmatrix}0\\ \omega_x\\ \omega_y\\ \omega_z\end{bmatrix} = 2\frac{dq}{dt}q^*$$

where q^* is the inverse of q (equation 2.3).

If the angular velocity ω is known, then $\frac{dq}{dt}$ is

$$\frac{dq}{dt} = 1/2\begin{bmatrix}0\\ \omega_x\\ \omega_y\\ \omega_z\end{bmatrix}q$$

.

5.3 The Jacobian Matrix

5.3.1 Velocity Mapping

In the forward kinematics model, we saw that it was possible to relate joint angles, θ, to the configuration of the robot end effector, ${}^0_6T$. In this chapter we will work on the relationship between the joint rates, $\dot{\theta}$, and the velocity of the end effector, $\dot{x}$ with a matrix as follows:

$$\dot{x} = J(\theta)\dot{\theta}$$

Here the velocity $\dot{x}$ describes both linear and rotational components. An expanded version of the previous equation is

$$\begin{bmatrix}\dot{x}\\ \dot{y}\\ \dot{z}\\ \omega_x\\ \omega_y\\ \omega_z\end{bmatrix} = \begin{bmatrix} & J(\theta) & \end{bmatrix}\begin{bmatrix}\dot{\theta_1}\\ \dot{\theta_2}\\ \cdots\\ \dot{\theta_N}\end{bmatrix}$$

ω_i are the components of angular velocity, and $J(\theta)$ is a matrix of size 6xN where N is the number of joints in the robot. We will derive $J(\theta)$ by calculating $\dot{x}$ as a function of $\dot{\theta}$ and factoring out $J(\theta)$. But first, as a simple illustration let us consider a planar example:

[1] http://www.euclideanspace.com/physics/kinematics/angularvelocity/

Example 5.2
Compute the velocity of the end effector of this basic planar robot as a function of its joint velocity $\dot{\theta}$.

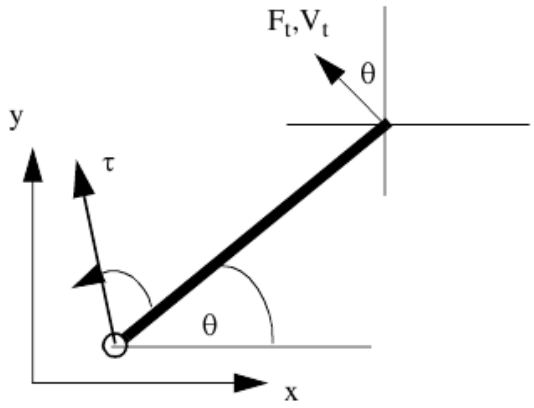

Looking at the figure, we can resolve the velocity of the tip into x and y components as follows:

$$v_x = -r\dot{\theta}\sin(\theta) \qquad v_y = r\dot{\theta}\cos(\theta)$$

This can be expressed as a trivial matrix equation as follows:

$$\begin{bmatrix} v_x \\ v_y \end{bmatrix} = \begin{bmatrix} -r\sin(\theta) \\ r\cos(\theta) \end{bmatrix} \dot{\theta}$$

or

$$J(\theta) = \begin{bmatrix} -r\sin(\theta) \\ r\cos(\theta) \end{bmatrix}$$

This chapter will cover the Jacobian Matrix and how to compute it in detail, but first we want to give the bird's eye view of this powerful matrix. This section aims to show what kinds of problems we can solve once we solve the Jacobian Matrix.

Spaces Consider three spaces relevent to robot arm motion (Figure 5.2).

- Joint Space
  A point in this space is located by the values of the N joint variables of the arm.
- Configuration Space
  A point in this space is located by the X, Y, Z position of the end effector plus three rotation variables which describe its orientation such as roll, pitch, yaw angles.
- Cartesian Task Space
  A point in this space is determined by X, Y, Z. The configuration of a rigid object in Cartesian task space is defined by its 4×4 homogeneous transform.

In Chapters 2 and 3, we've seen the static mappings between Joint Space and Cartesian Task Space, the Forward Kinematic Mapping (Fkin) and the Inverse Kinematic Mapping (Kin^{-1}) (Figure 5.3).

Now we introduce *incremental* mappings between small changes in joint space and small changes in task space. i.e.

$$\Delta X = J(\theta)\Delta\theta$$

$$\dot{x} = J(\theta)\dot{\theta}$$

and

$$\dot{\theta} = J^{-1}(\theta)\dot{x}$$

We can apply these mappings to answer several interesting questions:

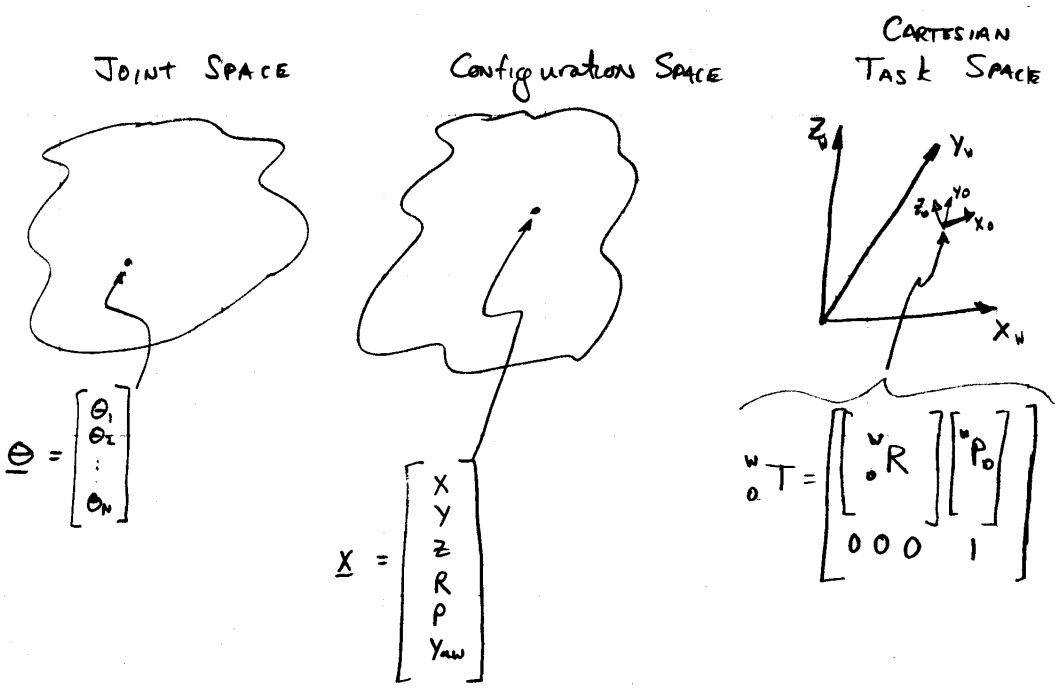

Figure 5.2: Three spaces relevent to robot arm motion: Task space, Joint Space, Configuration Space.

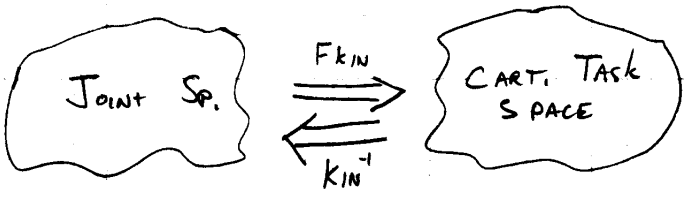

Figure 5.3: Static mappings between Joint space and Cartesian Task Space.

Velocity Mapping **Q:** What velocity and angular velocity will be generated at the tip of the robot if all joints are driven at 0.1 rad/sec?
A:

$$\dot{x} = J(\theta) \begin{bmatrix} 0.1 \\ 0.1 \\ \\ \dots \\ \\ 0.1 \end{bmatrix}$$

note that this solution is a function of θ.

Q: How should we drive the joints so that the end effector tracks a target moving with velocity

$$\dot{x}_t = \begin{bmatrix} 1 \\ 0 \\ 0.5 \\ 0 \\ 0 \\ 0 \end{bmatrix}$$

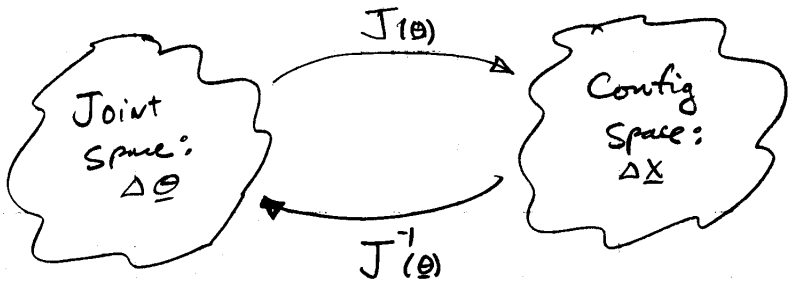

Figure 5.4: Incremental Mapping between spaces

A:

$$\dot{\theta} = J^{-1}(\theta) \begin{bmatrix} 1 \\ 0 \\ 0.5 \\ 0 \\ 0 \\ 0 \end{bmatrix}$$

notes: Does $J(\theta)^{-1}$ exist? What about 'conditioning' of $J(\theta)$?

5.3.2 Force Mapping

Example 5.2 cont.
Referring back to the single-joint arm of this example, we can look at the tip force, and the torque around the joint:

$$\tau = -rF_x \sin(\theta) + rF_y \cos(\theta)$$

This again gives a trivial matrix equation:

$$\tau = \begin{bmatrix} -r\sin(\theta) & r\cos(\theta) \end{bmatrix} \begin{bmatrix} F_x \\ F_y \end{bmatrix}$$

Note that the first term happens to be the transpose of the matrix $J(\theta)$ computed above. As we will show below, this is *not* a coincidence, so we can write

$$\tau = J^T(\theta)F$$

Thus when mapping Forces and Torques between the same spaces:

$$\tau = J(\theta)^T F$$

$$F = J(\theta)^{-T} \tau$$

Notes:

1. $J(\theta)^{-T}$ indicates the inverse of $J(\theta)^T$.
2. Mappings are a function of θ.
3. Does $J(\theta)^{-T}$ exist?

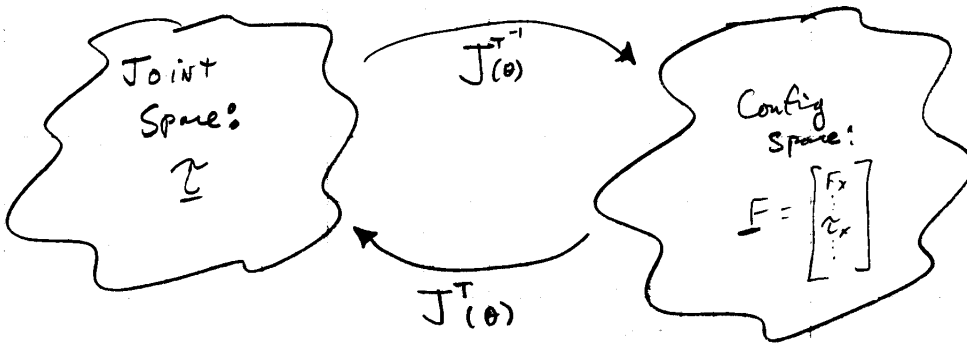

Figure 5.5: Mappings between joint torques and end effector forces.

5.3.3 Virtual Work

It's not obvious that the Jacobian matrix should relate *both* incremental motions and also forces and torques between the joint space and configuration space. The concept of virtual work can be used to derive the force and torque mapping role of the Jacobian Matrix from its incremental motion mapping role.

We consider the mechanism to be purely kinematic. This means that it has no ability to dissipate or store energy:

- no friction (energy loss)
- no inertia (kinetic energy)
- no mass (potential energy due to gravity)
- no compliance (potential energy due to elastic energy of deformation)

These assumptions might seem quite unrealistic. In fact many robot motions involve low enough amounts of energy that the assumptions are quite useful.

Let's review some definitions:

Power $P = \frac{d}{dt}E$ (where E is energy)

Power $P = F \cdot V = F^T V$

Power $P = \tau \cdot \omega = \tau^T \omega$

Work $W = \Delta E = P\Delta t$

Because of the properties above, if we apply some work to part of the mechanism, it must come out of another part instantaneously for energy to be conserved. The locations ("ports") at which we will consider energy flow are the end effector and the joints.

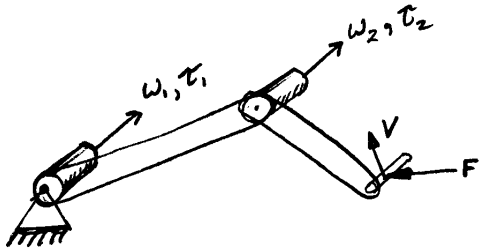

Figure 5.6: Mechanism to illustrate Virtual Work.

Let's consider a planar 2-link mechanism with a handle applied to the end (Figure 5.6). If it helps, think of ideal generators attached to the joints which can extract energy from the joints. If we crank on the handle and compare the force and velocities of the handle with the joint torques and joint angular velocities:

$$F^T V = \tau^T \omega$$

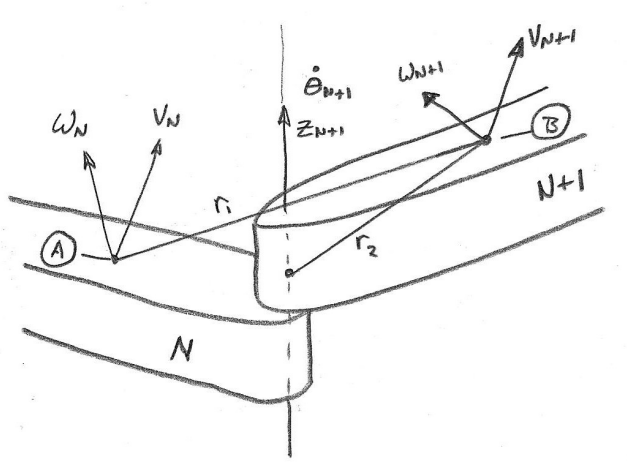

Figure 5.7: Two links of a manipulator connected by a rotary joint.

by the principle of Virtual Work. If we multiply both sides by Δt,

$$F^T \Delta X = \tau^T \Delta \Theta$$

$$\tau^T \Delta \Theta - F^T \Delta X = 0$$

We know that

$$\Delta X = J(\Theta) \Delta \Theta$$

so

$$\left(\tau^T - F^T J\right) \Delta \Theta = 0$$

for finite $\Delta\Theta$:

$$(\tau^T - F^T J) = 0$$

$$\tau^T = F^T J$$

$$\tau = J^T F$$

(because $(AB)^T = B^T A^T$ is a property of the matrix transpose).

5.3.4 Velocity Propagation

Now we investigate robot links arranged in a serial chain. Remember that robot links are rigid bodies, and also that adjacent robot links are rigidly joined or attached to each other *except* for motion about/along the Z_N axis. For now, let's consider only rotary joints.

Figure 5.7 shows two adjacent robot links. For now, an arbitrary point is selected on each link at which we define the linear and angular velocity for that link. r_1 is a vector connecting the the defined points on two adjacent links. r_2 is the unique vector connecting the point on link $N+1$ to the origin of frame $N+1$. Assume that all velocities are computed in the world frame, W, and represented anywhere.

Then, assume they are a single rigid object (i.e. $\dot{\theta}_{N+1} = 0$). In that case, using the result above, we have

$$\omega_{N+1} = \omega_N \qquad V_{N+1} = V_N + \omega_N \times r_1$$

Now, assume that the joint velocity, $\dot{\theta}_{N+1} \neq 0$. This adds a new component to both equations:

$$\omega_{N+1} = \omega_N + Z_{N+1}\dot{\theta}_{N+1} \qquad V_{N+1} = V_N + \omega_N \times r_1 + \dot{\theta}_{N+1} Z_{N+1} \times r_2$$

Finally, we can apply this to robot links and their DH parameters as follows:

1. From our DH analysis, we know ${}^N_{N+1}R$, ${}^N_{N+1}T$.

2. Let point (A) be the origin of frame N, and point (B) be the origin of frame $N+1$
3. In this case, $r_1 = [T_{14}, T_{24}, T_{34}]^T$ (the fourth column of ${}^{N}_{N+1}T$).
4. Because (B) is the origin of frame $N+1$, $r_2 = 0$.

Then, using known rotation matrix ${}^{N+1}_{N}R$ to keep ${}^{N}\omega_N$ represented in its original frame, we get

$$ {}^{N+1}\omega_{N+1} = {}^{N+1}_{N}R \ {}^{N}\omega_N + \begin{bmatrix} 0 \\ 0 \\ \dot{\theta}_{N+1} \end{bmatrix} \tag{5.1} $$

and

$$ {}^{N+1}V_{N+1} = {}^{N+1}_{N}R \left[{}^{N}V_N + {}^{N}\omega_N \otimes {}^{N}P_{N,N+1} \right] \tag{5.2} $$

OK Professor, what have we accomplished? (because all the link linear and angular velocities (${}^{N}V_N$, ${}^{N}\omega_N$) are still unknowns). However, in fact initially *do* know one pair:

$$ {}^{0}\omega_0 = 0 \quad \text{and} \quad {}^{0}V_0 = 0 $$

because the base of the robot is (hopefully) bolted down. We also know the joint velocities, $\dot{\theta}_N$ (from sensors for example), and the rotation matrices ${}^{N+1}_{N}R$, and the link position offsets, ${}^{N}P_{N,N+1}$, from the forward kinematics. Therefore, we can use equations 5.1 and 5.2 to compute each velocity one at a time.

Example 5.3

Derive similar equations for prismatic joints If we identify that joint $N+1$ is prismatic, then we replace the above equations with the following. A prismatic joint does not add *any* rotation, so

$$ {}^{N+1}\omega_{N+1} = {}^{N+1}_{N}R \ {}^{N}\omega_N $$

but it does add a component of linear velocity in the Z_{N+1} direction:

$$ {}^{N+1}V_{N+1} = {}^{N+1}_{N}R \left[{}^{N}V_N + {}^{N}\omega_N \otimes {}^{N}P_{N,N+1} \right] + \begin{bmatrix} 0 \\ 0 \\ \dot{d}_{N+1} \end{bmatrix} $$

Once the linear and angular velocities of the last link (end effector) of the manipulator are computed by this method of "velocity propagation," it is a quick step to get the Jacobian matrix as illustrated by the following example:

Example 5.4
Compute the Jacobian Matrix by the Velocity Propogation method. The manipulator is described by the following Denavit Hartenberg parameters:

i	α_{i-1}	a_{i-1}	d_i	θ_i
1	0	0	0	θ_1
2	$\pi/2$	L_1	0	θ_2
3	0	L_2	0	θ_3
4	0	L_3	0	0

Solution: First we need to generate the link transforms from the DH parameters, ${}^{i-1}_{i}T$ (hopefully we have them around from our forward kinematics step).

$$ {}^{0}_{1}T = \begin{bmatrix} c_1 & -s_1 & 0 & 0 \\ s_1 & c_1 & 0 & 0 \\ 0 & 0 & 1 & 0 \\ 0 & 0 & 0 & 1 \end{bmatrix} $$

$$ {}^{1}_{2}T = \begin{bmatrix} c_2 & -s_2 & 0 & L_1 \\ 0 & 0 & -1 & 0 \\ s_2 & c_2 & 0 & 0 \\ 0 & 0 & 0 & 1 \end{bmatrix} $$

$$ {}^{2}_{3}T = \begin{bmatrix} c_3 & -s_3 & 0 & L_2 \\ s_3 & c_3 & 0 & 0 \\ 0 & 0 & 1 & 0 \\ 0 & 0 & 0 & 1 \end{bmatrix} $$

$$ {}^{3}_{4}T = \begin{bmatrix} 1 & 0 & 0 & L_3 \\ 0 & 1 & 0 & 0 \\ 0 & 0 & 1 & 0 \\ 0 & 0 & 0 & 1 \end{bmatrix} $$

Now we propagate the angular velocities first (since they are needed for the linear step):

$$ {}^{1}\omega_1 = \begin{bmatrix} 0 \\ 0 \\ \dot{\theta}_1 \end{bmatrix} + \begin{bmatrix} 0 \\ 0 \\ 0 \end{bmatrix} $$

$$ {}^{2}\omega_2 = {}^{2}_{1}R\ {}^{1}\omega_1 + \begin{bmatrix} 0 \\ 0 \\ \dot{\theta}_2 \end{bmatrix} $$

$$ = \begin{bmatrix} c_2 & 0 & s_2 \\ -s_2 & 0 & c_2 \\ 0 & -1 & 0 \end{bmatrix} \begin{bmatrix} 0 \\ 0 \\ \dot{\theta}_1 \end{bmatrix} + \begin{bmatrix} 0 \\ 0 \\ \dot{\theta}_2 \end{bmatrix} $$

$$ {}^{2}\omega_2 = \begin{bmatrix} s_2\dot{\theta}_1 \\ c_2\dot{\theta}_1 \\ \dot{\theta}_2 \end{bmatrix} $$

$$ {}^{3}\omega_3 = {}^{3}_{2}R\ {}^{2}\omega_2 + \begin{bmatrix} 0 \\ 0 \\ \dot{\theta}_3 \end{bmatrix} $$

$$ = \begin{bmatrix} c_3 & s_3 & 0 \\ -s_3 & c_3 & 0 \\ 0 & 0 & 1 \end{bmatrix} \begin{bmatrix} s_2\dot{\theta}_1 \\ c_2\dot{\theta}_1 \\ \dot{\theta}_2 \end{bmatrix} + \begin{bmatrix} 0 \\ 0 \\ \theta_3 \end{bmatrix} $$

$$ {}^{3}\omega_3 = \begin{bmatrix} s_2c_3\dot{\theta}_1 + c_2s_3\dot{\theta}_1 \\ c_2c_3\dot{\theta}_1 - s_2s_3\dot{\theta}_2 \\ \theta_2 + \theta_3 \end{bmatrix} = \begin{bmatrix} s_{23}\dot{\theta}_1 \\ c_{23}\dot{\theta}_1 \\ \dot{\theta}_2 + \dot{\theta}_3 \end{bmatrix} $$

$$ {}^{4}\omega_4 = {}^{4}_{3}R\ {}^{3}\omega_3 + \begin{bmatrix} 0 \\ 0 \\ 0 \end{bmatrix} = {}^{3}\omega_3 $$

Now we propagate linear velocity using the previously calculated ${}^{i+1}_{i}T$ and ${}^{i}\omega_i$:

$$ {}^{0}V_0 = \begin{bmatrix} 0 \\ 0 \\ 0 \end{bmatrix} $$

$$ {}^{1}V_1 = {}^{1}_{0}R({}^{0}V_0 + {}^{0}\omega_0 \times {}^{0}P_1) = \begin{bmatrix} 0 \\ 0 \\ 0 \end{bmatrix} $$

Example 5.4 cont.

$$ {}^2V_2 = {}^2_1R({}^1V_1 + {}^1\,\omega_1 \times {}^1P_2) = $$

$$ \begin{bmatrix} c_2 & 0 & s_2 \\ -s_2 & 0 & c_2 \\ 0 & -1 & 0 \end{bmatrix} \left[\begin{bmatrix} 0 \\ 0 \\ \dot{\theta}_1 \end{bmatrix} \times \begin{bmatrix} L_1 \\ 0 \\ 0 \end{bmatrix} \right] $$

Here we can take advantage of the rule we identified in Section 2.11.1 and Section 5.2.2 in which the cross product can be represented as a skew symmetric matrix for faster computation. In each stage of the linear velocity propagation, we will repeat the computation

$$ a \times b $$

where $b = [L_i \quad 0 \quad 0]^T$. For this case,

$$ a \times b = \begin{bmatrix} 0 \\ a_3 L_i \\ -a_2 L_i \end{bmatrix} $$

Applying this we get

$$ {}^2V_2 = \begin{bmatrix} c_2 & 0 & s_2 \\ -s_2 & 0 & c_2 \\ 0 & -1 & 0 \end{bmatrix} \begin{bmatrix} 0 \\ L_1\dot{\theta}_1 \\ 0 \end{bmatrix} = \begin{bmatrix} 0 \\ 0 \\ -L_1\dot{\theta}_1 \end{bmatrix} $$

$$ {}^3V_3 = \begin{bmatrix} c_3 & s_3 & 0 \\ -s_3 & c_3 & 0 \\ 0 & 0 & 1 \end{bmatrix} \left[\begin{bmatrix} 0 \\ 0 \\ -\dot{\theta}_1 L_1 \end{bmatrix} + \begin{bmatrix} s_2\dot{\theta}_1 \\ c_2\dot{\theta}_1 \\ \dot{\theta}_2 \end{bmatrix} \times \begin{bmatrix} L_2 \\ 0 \\ 0 \end{bmatrix} \right] $$

$$ = {}^3_2R \begin{bmatrix} 0 \\ \dot{\theta}_2 L_2 \\ -(c_2 L_2 - L_1)\dot{\theta}_1 \end{bmatrix} $$

$$ {}^3V_3 = \begin{bmatrix} s_3 L_2 \dot{\theta}_2 \\ c_3 L_2 \dot{\theta}_2 \\ -(c_2 L_2 - L_1)\dot{\theta}_1 \end{bmatrix} $$

$$ {}^4V_4 = \begin{bmatrix} 1 & 0 & 0 \\ 0 & 1 & 0 \\ 0 & 0 & 1 \end{bmatrix} \left[{}^3V_3 + \begin{bmatrix} s_{23}\dot{\theta}_1 \\ c_{23}\dot{\theta}_1 \\ \dot{\theta}_2 + \dot{\theta}_3 \end{bmatrix} \times \begin{bmatrix} L_3 \\ 0 \\ 0 \end{bmatrix} \right] $$

$$ {}^4V_4 = \begin{bmatrix} s_3 L_2 \dot{\theta}_2 \\ (c_3 L_2 + L_3)\dot{\theta}_2 + L_3\dot{\theta}_3 \\ -\dot{\theta}_1(L_1 + c_2 L_2 + c_{23} L_3) \end{bmatrix} $$

5.3.5 Jacobian Matrix from velocity expressions.

Now that we have calculated angular and linear velocity of the end effector, we can create the Jacobian matrix by factoring out all of the $\dot{\theta}$ terms:

$$ \begin{bmatrix} {}^N V_N \\ \\ {}^N \omega_N \end{bmatrix}_{6\times 1} = \begin{bmatrix} \quad J \quad \end{bmatrix}_{6\times N} \begin{bmatrix} \dot{\theta}_1 \\ \dot{\theta}_2 \\ \cdots \\ \dot{\theta}_N \end{bmatrix}_{N\times 1} $$

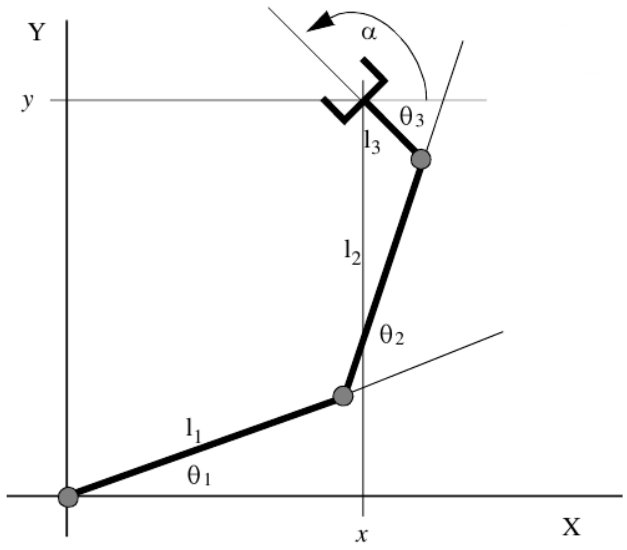

Figure 5.8: 3 Link planar manipulator.

Example 5.4 cont.

$$\begin{bmatrix} {}^4V_4 \\ {}^4\omega_4 \end{bmatrix}_{6\times 1} = \begin{bmatrix} \quad J \quad \end{bmatrix}_{6\times 4} \begin{bmatrix} \dot{\theta}_1 \\ \dot{\theta}_2 \\ \cdots \\ \dot{\theta}_4 = 0 \end{bmatrix}_{4\times 1}$$

$${}^4J = \begin{bmatrix} 0 & s_3L_2 & 0 \\ 0 & c_3L_2 + L_3 & L_3 \\ -(L_1 + C_2L_2 + C_{23}L_3) & 0 & 0 \\ s_{23} & 0 & 0 \\ c_{23} & 0 & 0 \\ 0 & 1 & 1 \end{bmatrix}$$

Note that col 4 of the Jacobian is not defined because $\dot{\theta}_4 = 0$, but L_3 still matters.

5.3.6 Jacobian Matrix by Differentiation

In addition to the method of velocity propagation, the Jacobian matrix can also be obtained by differentiation of the forward kinematic equations. Considering the 3-link planar manipulator of Figure 5.8, define the configuration vector, $x = [x, y, \alpha]^T$. The forward kinematic equations of this arm are:

$$x = l_1c_1 + l_2c_{12} + l_3c_{123} \qquad y = l_1s_1 + l_2s_{12} + l_3s_{123} \qquad \alpha = \theta_1 + \theta_2 + \theta_3$$

Differentiating the first expression gives:

$$\dot{x} = -l_1s_1\dot{\theta}_1 - l_2s_{12}(\dot{\theta}_1 + \dot{\theta}_2) - l_3s_{123}(\dot{\theta}_1 + \dot{\theta}_2 + \dot{\theta}_3)$$

or

$$\dot{x} = -(l_1s_1 + l_2s_{12} + l_3s_{123})\dot{\theta}_1 - (l_2s_{12} + l_3s_{123})\dot{\theta}_2 - (l_3s_{123})\dot{\theta}_3$$

Similarly,

$$\dot{y} = (l_1c_1 + l_2c_{12} + l_3c_{123})\dot{\theta}_1 - (l_2c_{12} + l_3c_{123})\dot{\theta}_2 - (l_3c_{123})\dot{\theta}_3$$

and

$$\dot{\alpha} = \dot{\theta}_1 + \dot{\theta}_2 + \dot{\theta}_3$$

Thus,

$${}^0J\theta = \begin{bmatrix} -l_1 s_1 - l_2 s_{12} - l_3 s_{123} & -l_2 s_{12} - l_3 s_{123} & -l_3 s_{123} \\ l_1 c_1 + l_2 c_{12} + l_3 c_{123} & l_2 c_{12} + l_3 c_{123} & l_3 c_{123} \\ 1 & 1 & 1 \end{bmatrix}$$

Remember that we started with the expression for the end effector configuration in frame 0 so the resulting Jacobian is still in frame 0. We have indicated this with a leading superscript above. In contrast, the Jacobian computed by velocity propagation leaves us with a Jacobian in frame N (we omitted the superscript in the examples above). Both results are valid. In general the Jacobian can be transformed into any desired frame as described in Section 5.5.

Example 5.5

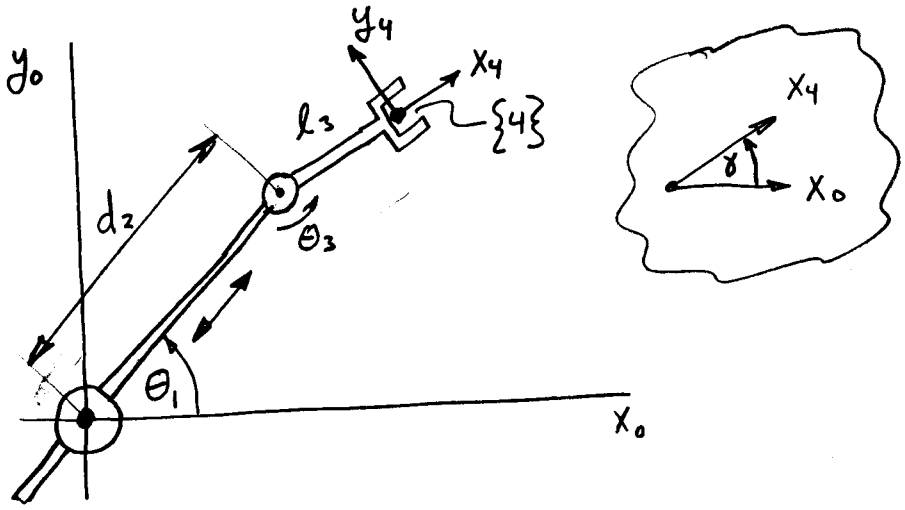

Compute the Jacobian matrix of the arm above where all three joints $\theta_1, \dot{d}_2, \theta_3$ are variables. Consider $\dot{x}, \dot{y}$, and the rate of change of orientation of x_4, $\dot{\gamma}$. The Jacobian matrix should have 3 rows.
Solution:
The forward kinematic equations are:

$$x = d_2 \cos\theta_1 + l_3 \cos(\theta_1 + \theta_3)$$
$$y = d_2 \sin\theta_1 + l_3 \sin(\theta_1 + \theta_3)$$
$$\gamma = \theta_1 + \theta_3$$

Differentiating:

$$\dot{x} = -d_2 \sin\theta_1 \dot{\theta}_1 + \dot{d}_2 \cos\theta_1 - l_3 \sin(\theta_1 + \theta_3)(\dot{\theta}_1 + \dot{\theta}_3)$$
$$\dot{y} = d_2 \cos\theta_1 \dot{\theta}_1 + \dot{d}_2 \sin\theta_1 + l_3 \cos(\theta_1 + \theta_3)(\dot{\theta}_1 + \dot{\theta}_3)$$
$$\dot{\gamma} = \dot{\theta}_1 + \dot{\theta}_2$$

Factoring:

$$J = \begin{bmatrix} -d_2 s_1 - l_3 s_{13} & c_1 & -l_3 s_{13} \\ d_2 c_1 + l_3 c_{13} & s_1 & l_3 c_{13} \\ 1 & 0 & 1 \end{bmatrix}$$

5.4 Inverting the Jacobian Matrix

We saw earlier that we will make frequent use of the Jacobian matrix for relating forces and velocities between the joints and the end effector spaces using the equations

$$\dot{x} = J\dot{\theta} \qquad \tau = J^T F$$

Just as with static kinematics of Chapter 2, these equations are often more useful if inverted. Thus we frequently need a form such as

$$\dot{\theta} = J^{-1}\dot{x}$$

Computation of J^{-1} is not a very time consuming job for today's processors. As we have seen however, the elements of the Jacobian matrix are functions of the joint variables θ so if we use J^{-1} we must compute it frequently as the manipulator moves around. Since the numerical values of J are always changing, we can't make a blanket statement about whether this inverse exists. We often evaluate the ability to invert a matrix using its determinant. In fact, in many practical robotic problems, there are configurations of the joints inside or throughout the workspace where

$$\mathrm{Det}(J) = 0$$

and as a result, any computation, say inside a controller, which relies on a numerical method to find J^{-1} will have problems. The configurations of the joints of a manipulator at which $\mathrm{Det}(J) = 0$ are called *singularities*.

5.4.1 Interpretations of the Jacobian Inverse: Singularities

Here we will look at some implications of basic linear algebra for the Jacobian Inverse. We will make reference to some basic facts about matrices which are given in Appendix B.

Consider the case of a square, 6x6, Jacobian matrix. If $\mathrm{rank}(J(\theta)) < 6$, then there is no solution to

$$\dot{\theta} = J^{-1}(\theta)\dot{x}$$

(see Facts 1 and 2). Also, by Fact 8, if the rank, $r = 5$, there is one non-zero solution to

$$\dot{x} = J(\theta)\dot{\theta} = 0$$

The interpretation of this fact is that there is a direction in joint velocity space for which non-zero joint motion produces no end effector motion. We call any joint configuration, $\theta = Q$ for which

$$\mathrm{rank}(J(Q)) < 6$$

a **singular configuration**.

Furthermore, there are certain directions of end effector motion, $\dot{x}_i$, which are eigenvectors of $J(\theta)$. If J is full rank, we have

$$\dot{x}_i = J(\theta)\dot{\theta} = \lambda_i(\theta)\omega_i(\theta)$$

where λ_i are the eigenvalues of J and ω_i are the eigenvectors of J. If J is full rank, we have

$$\omega_i = J^{-1}(\theta)\dot{x}_i = \lambda_i^{-1}\dot{x}_i$$

(Fact 5). As the manipulator approaches the singular configuration, $\theta \to Q$, there is at least one eigenvalue for which $\lambda_j \to 0$. Thus

$$\omega_j \to \frac{\dot{x}_j}{0} = \infty$$

In words, as the manipulator approaches the singular configuration, motion in the particular direction $\dot{x}_j$

causes joint velocities to approach infinity.

Example 5.6

We will look at the specifics of singularities through an example, the planar 3-link manipulator of Figure 5.8. Let's look at Jacobian in the following configuration:

$$Q = \begin{bmatrix} \pi/4 \\ 0 \\ \pi \end{bmatrix}$$

When the manipulator is posed such that $\theta = Q$, we have

$$s_{12} = s_1 \qquad s_{123} = -s_1, \qquad c_{12} = c_1, \qquad c_{123} = -c_1$$

This gives

$${}^0J(Q) = \begin{bmatrix} (-l_1 - l_2 + l_3)s_1 & (-l_2 + l_3)s_1 & l_3 s_1 \\ (l_1 + l_2 - l_3)c_1 & (l_2 - l_3)c_1 & -l_3 c_1 \\ 1 & 1 & 1 \end{bmatrix}$$

If we denote the rows of J by $\{r_1, r_2, r_3\}$, and recall that for $\theta_1 = \pi/4$, then $s_1 = c_1 = 0.707$, then we note that

$$r_1 = -r_2$$

and therefore $\det[J(Q)] = 0$ (Fact 3). This means that Q is a singular configuration. Note that on closer examination, we can see that θ_1 does not have to be $\pi/4$ for this to happen. This is because, for any θ_1, we still have

$$r1 = r2 \times -\tan(\theta_1)$$

$-\tan(\theta_1)$ is a constant which relates the two rows so that the matrix must be singular. The proper way to describe the singular configuration is thus

$$Q = \begin{bmatrix} \theta_1 \\ 0 \\ \pi \end{bmatrix}$$

for any θ_1.

Example 5.7
Find any singular configurations of the manipulator of Example 5.5 For each singular configuration:
1) Draw it and indicate which direction of motion cannot be achieved.
2) State whether it is an interior singularity or workspace boundary singularity.
Use analysis of the Jacobian to derive the result or confirm your graphical analysis.
Solution:
For $\theta_3 = 0$, $s_{13} = s_1$, $c_{13} = c_1$.

$$J = \begin{bmatrix} -(d_2 + l_3)s_1 & c_1 & -l_3 s_1 \\ (d_2 + l_3)c_1 & s_1 & l_3 c_1 \\ 1 & 0 & 1 \end{bmatrix}$$

This is only singular when $d_2 = 0$, making two collumns equal.

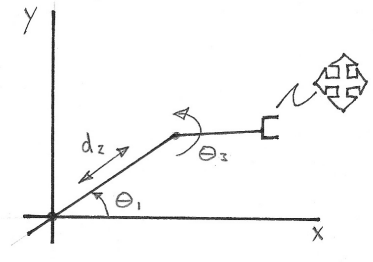

Non singular pose: end point can move in all directions.

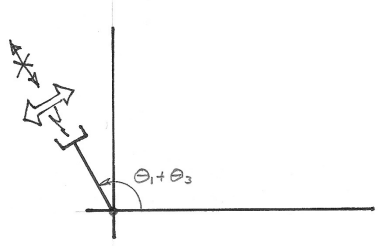

Singular pose where $d_2 = 0$. Direction of blocked motion shown by thin arrow (crossed out). Thick arrow shows direction in which motion is still possible.

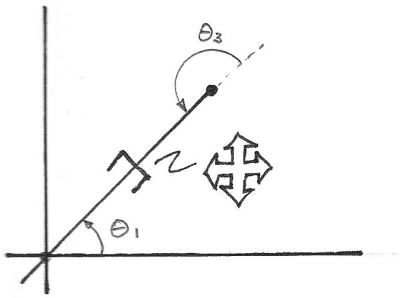

Pose where $\theta_3 = \pi$. Even though this "looks" like a singular pose, in fact it is not since manipulator can still move in two directions.
Note that there are no joint limits, infinite workspace, no workspace boundary singularities.

5.4.2 Force and torque at a kinematic singularity

Since $\tau = J^T F$, at a singular point, Q, we can expect non-zero forces F_j such that

$$J^T(Q)F_j = 0$$

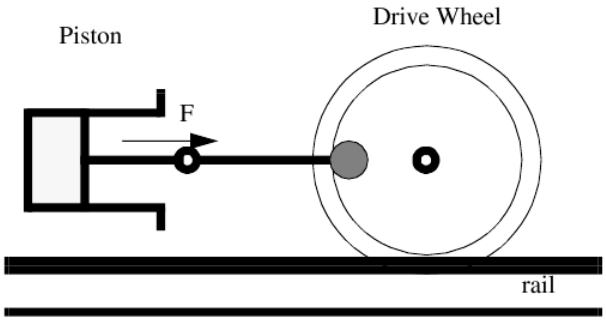

Figure 5.9: A piston from a steam locomotive in the "Top-Dead-Center" position.

In words, there will be some force vector or vectors (F_j) which can be applied to the end effector, which generate no torques at the joints. So, in a singular configuration, the mechanism can "lock up" with respect to tip forces or torques in certain directions becuase these directions allow no torque to develop at the joints. For example, suppose Q is defined as in Example 6 and

$$F_1 = \begin{bmatrix} -F\cos\theta_1 \\ -F\sin\theta_1 \\ 0 \end{bmatrix}$$

Note that this corresponds to a force applied to the tip in the direction opposite to the outstretched arm, and that no external torque is applied to the tip. Now, writing $J^T(Q)$ in a simplified form:

$$\tau = J^T(Q)F_1 = \begin{bmatrix} as_1 & -ac_1 & 1 \\ bs_1 & -bc_1 & 1 \\ cs_1 & -cc_1 & 1 \end{bmatrix} = \begin{bmatrix} -Fc_1 \\ -Fs_1 \\ 0 \end{bmatrix}$$

where $a = -l_1 - l_2 + l_3$, $b = -l_2 + l_3$, $c = l_3$. And

$$\tau = \begin{bmatrix} -aFs_1c_1 + aFs_1c_1 + 0 \\ -bFs_1c_1 + bFs_1c_1 + 0 \\ 0 \end{bmatrix} = \begin{bmatrix} 0 \\ 0 \\ 0 \end{bmatrix}$$

The end effector force is finite, but the torque on all joints is zero. This situation is an old and famous one in mechanical engineering. For example, in an old railroad steam engine, "top dead center" refers to the state depicted in Figure 5.9. The piston force, F, cannot generate any torque around the drive wheel axis because the linkage is in a singular configuration as shown.

5.4.3 Velocity at a kinematic singularity

Note that although in a singular configuration (i.e. certain "poses" or values of $[\theta_1, \theta_2, \ldots, \theta_i]^T$) $\dot{\theta} = J^{-1}(Q)\dot{x}$ has no solution in general, if we assume that J looses rank by only one (i.e. $r - N = 1$), then there are $N-1$ eigenvectors in the task velocity space, $\dot{x}_j$, for which solutions *do* exist. However, there will be multiple solutions. For example, if

$$\dot{x}_1 = \begin{bmatrix} -Vs_1 \\ Vc_1 \\ 0 \end{bmatrix}$$

Assume the manipulator is posed as in Figure 5.10. The velocity vector we have just described is also plotted in Figure 5.10.

We can see (by looking at the lever arms between joints and the end effector) that the valid solutions for the resulting joint velocities will be

$$\underline{\dot{\theta}}_1 = \begin{bmatrix} \frac{V}{(l_1+l_2-l_3)} \\ 0 \\ 0 \end{bmatrix}$$

$$\underline{\dot{\theta}}_2 = \begin{bmatrix} 0 \\ \frac{V}{(l_2-l_3)} \\ 0 \end{bmatrix}$$

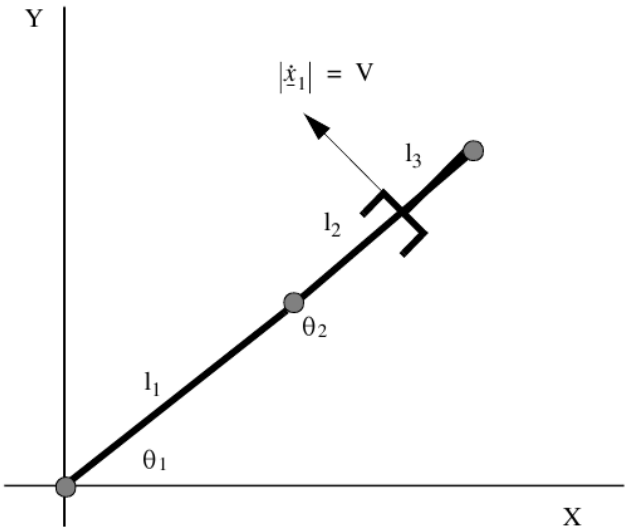

Figure 5.10: A singular configuration of a 3 link manipulator.

$$\dot{\underline{\theta}}_3 = \begin{bmatrix} 0 \\ 0 \\ \frac{V}{(-l_3)} \end{bmatrix}$$

where the underlined variable, $\dot{\underline{\theta}}_i$ is a vector of the individual joint velocities. The end effector velocity is also satisified by linear combinations of these solutions such as

$$\dot{\underline{\theta}}_n = a_1\dot{\underline{\theta}}_1 + a_2\dot{\underline{\theta}}_2 + a_3\dot{\underline{\theta}}_3$$

where $a_1 + a_2 + a_3 = 1$. This can be verified by multiplying any of the solutions by $J(Q)$ to obtain $\dot{x}_1$.

However, if any component of the tip velocity in the direction corresponding to the zero eigenvalue of J is non-zero, then at least one joint rate will go to infinity.

5.4.4 Kinematic Conditioning

So far we have looked at kinematic singularities from the point of view of specific joint values which cause the determinant to be zero. For example, in Example 6, when

$$\theta = Q = \begin{bmatrix} \theta_1 \\ 0 \\ \pi \end{bmatrix}$$

The manipulator was singular. In practical cases and computational implementations however, we have to be concerned about situations where the manipulator is *almost* singular. Suppose

$$\theta = \begin{bmatrix} \theta_1 \\ 0.01 \\ 3.15 \end{bmatrix}$$

Technically this is not singular. However J^{-1} may be difficult to compute. A measure of this difficulty is the *condition number* of the Jacobian, designated $\kappa(J)$. The condition number is

$$\kappa(J) = \frac{\sigma_{max}(J)}{\sigma_{min}(J)}$$

where σ_{max} is the maximum singular value J. When the Jacobian matrix looses rank, at least one singular value becomes zero. As we approach the singualrity, the condition number becomes very large.

As a practical matter, when using J^{-1} in a computation, it is not the exact singular configurations which must be avoided, but rather the regions around and including the singular configurations where the condition number of J exceeds a threshold.

5.5 Transformation of Jacobian between Representation Frames

Recall that in both the velocity propagation and the differentiation methods, we computed a velocity first and then factored out $\dot{\theta}$ to create the Jacobian matrix. Like any velocity, the one we base our Jacobian on could be represented in any frame and could be transformed by rotation between frames. Factoring each of these representations of end effector velocity will thus give us a different Jacobian matrix. The Jacobian matrix can thus be transformed among different frames by rotation as follows:

$$ {}^{A}J(\theta) = \begin{bmatrix} \begin{bmatrix} & {}^{A}_{B}R & \end{bmatrix} & 0 \\ 0 & \begin{bmatrix} & {}^{A}_{B}R & \end{bmatrix} \end{bmatrix} {}^{B}J(\theta) $$

The special 6×6 matrix contains two identical submatrices which are ${}^{A}_{B}R$. These transform the linear and rotational components of the end-effector configuration space velocity separately but identically. Importantly, since the above 6×6 matrix contains two orthonormal sub-matrices, the eigenvalues of J are unchanged by this transformation. Thus singularities and condition number are not changed by rotation of the Jacobian into different frames.

5.6 Summary of Notation

Chapter 6

Manipulator Dynamics

This chapter studies the relationship of manipulator motion to the forces and torques applied to the joints of the manipulator. Forces (especially pertinent to prismatic joints) and torques (rotary joints) are conceptually very similar because they are often thought of "causes" of motion. However, their mathematics tend to be rather different. Since many manipulators are a mix of prismatic and rotary joints, we have to treat lots of special cases. A notation which partially simplifies this solution is a set of generalized joint coordinates q. For example, if the third joint of a six axis manipulator is prismatic, we would have:

$$q = \begin{bmatrix} q_1 \\ q_2 \\ q_3 \\ q_4 \\ q_5 \\ q_6 \end{bmatrix} = \begin{bmatrix} \theta_1 \\ \theta_2 \\ d_3 \\ \theta_4 \\ \theta_5 \\ \theta_6 \end{bmatrix}$$

and

$$\dot{q} = \begin{bmatrix} \dot{q}_1 \\ \dot{q}_2 \\ \dot{q}_3 \\ \dot{q}_4 \\ \dot{q}_5 \\ \dot{q}_6 \end{bmatrix} = \begin{bmatrix} \dot{\theta}_1 \\ \dot{\theta}_2 \\ \dot{d}_3 \\ \dot{\theta}_4 \\ \dot{\theta}_5 \\ \dot{\theta}_6 \end{bmatrix}$$

etc.

6.1 Problem Statement and Learning Objectives

Problem Statement

Learning Objectives Upon completing this Chapter, the reader should be able to

-

6.2 Basic Gravity Compensation

In this section we will solve a relatively simple dynamics problem, but one of great practical importance: we will develop some equations to compute the torques in each robot joint due to gravity.

First, let's consider a simplified situation in which a rigid shaft in an arbitrary direction supports a point mass at a distance (Figure 6.1). Suppose a point mass, having mass, m, and located at point P, is rigidly connected to the shaft but offset at some distance from the shaft and subject to the force of gravity, mg.

Assume a frame, $\{1\}$, exists whose origin is on the shaft, and in which Z_1 is pointing along the shaft. The moment generated about the origin of frame 1 is

$$^1\tau = P \otimes F = m(^1P \otimes^1 g)$$

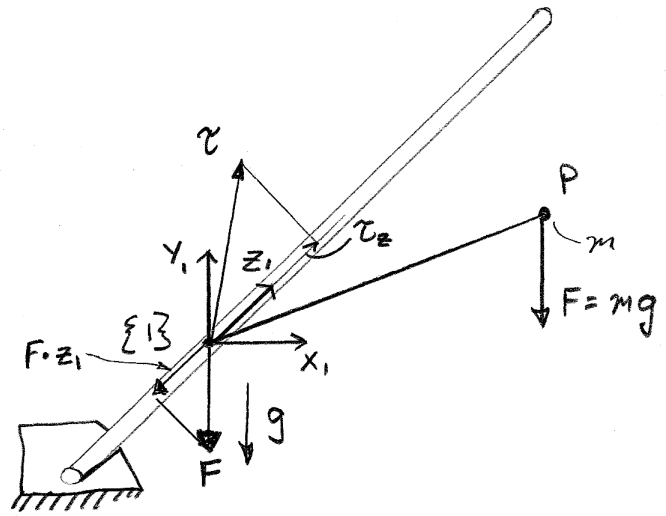

Figure 6.1: A shaft with an off-axis mass generating a torque and a force on the shaft.

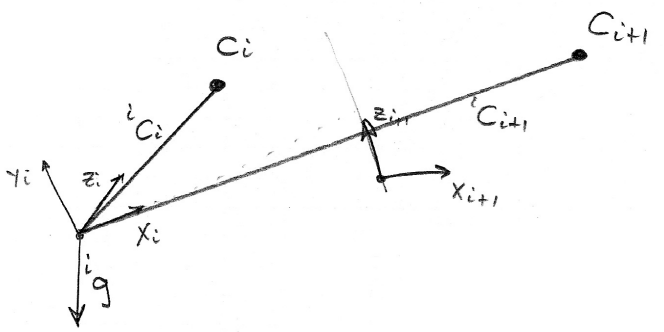

Figure 6.2: Two robot link frames (i, $i+1$) with centers of mass (C_i) and the gravity vector (g) shown for computation of gravity torques.

$$ {}^1\tau = \begin{bmatrix} 0 & -Pz & P_y \\ P_z & 0 & -P_x \\ -P_y & P_x & 0 \end{bmatrix} \begin{bmatrix} g_x \\ g_y \\ g_z \end{bmatrix} = \begin{bmatrix} P_y g_z - P_z g_y \\ P_z g_x - P_x g_z \\ P_x g_y - P_y g_x \end{bmatrix} $$

When we apply this to robot links, frame {1} will be the link frame and Z_1 will be the axis. Thus the torque we are interested in is the z component of τ

$$ \begin{bmatrix} 0 \\ 0 \\ P_x g_y - P_y g_x \end{bmatrix} $$

Now consider the force, $F = mg$ pointing "down". Besides the torque, the force, F, can also be represented in frame {1}, and it has a projection onto the Z_1 axis:

$$ F_z = F \cdot Z_1 $$

Applying this to a robot, we assume that the robot is not moving and that the joints are in some pose, θ.

Each link has mass, m_i located at its center of mass: C_i (Figure 6.2). In link i, we wish to compute the z component of torque due to the gravitational force on each center of mass which is more distal to the joint (has a greater subscript, i). The moment on frame i due to the mass in frame j is therefore

$$ \tau_{ij} = C_j \otimes m_j g = m_j (C_j \otimes g) $$

where we assume that all quantities are represented in the same frame. For joint i, the natural frame is frame $\{i\}$:

$$
\begin{aligned}
{}^i\tau &= \sum_{j=i,n} m_j({}^iC_j \otimes {}^ig) \\
&= \left[\sum_{j=i,n} m_j {}^iC_j\right] \otimes {}^ig
\end{aligned}
$$

The quantity

$$C_{mi} = \sum_{j=i,n} m_j C_j$$

is called the *first moment of mass* which is the center of mass times the total mass for the entire part of the manipulator distal to joint i and it can be expressed in any frame in general.

The torque in the i'th joint, τ_i is therefore:

$$\tau_i = \hat{z} \cdot {}^i\tau = [0 \quad 0 \quad 1]\, {}^i\tau = \begin{bmatrix} 0 \\ 0 \\ {}^i\tau_Z \end{bmatrix}$$

for rotary joints.

For prismatic joints, we have the analogous equation

$$F_{ij} = \sum_{j=i,n} m_j {}^ig$$

and the joint force is just the z component of F_{ij}.

$$F_{Zi} = \hat{z} \cdot F_{ij} = \begin{bmatrix} 0 \\ 0 \\ F_{ijZ} \end{bmatrix}$$

Example 6.1
For the manipulator shown below, each Z_i is shown in red and each center of mass is shown as a blue dot labeled with the total mass of each link, m_i. The gravity vector is shown (drawn next to frame 0) to indicate its direction.

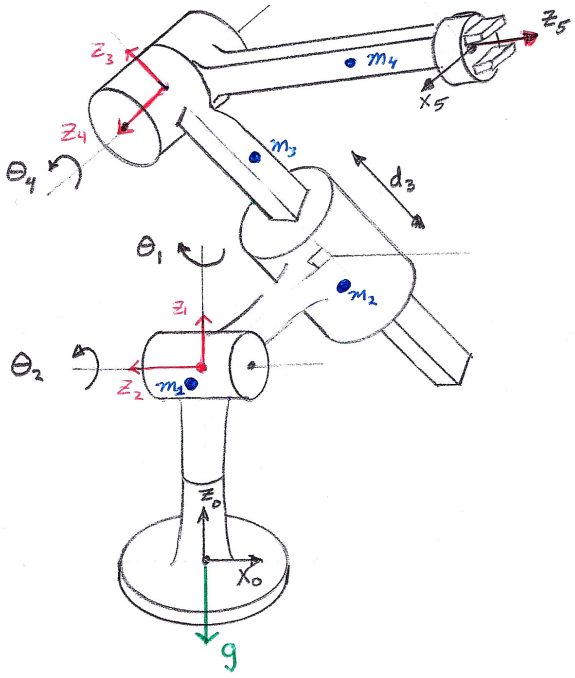

Part I

Draw a vector on the diagram to illustrate each center of mass in the link's own frame: ${}^iC_i$:
Draw the gravity force on each link.

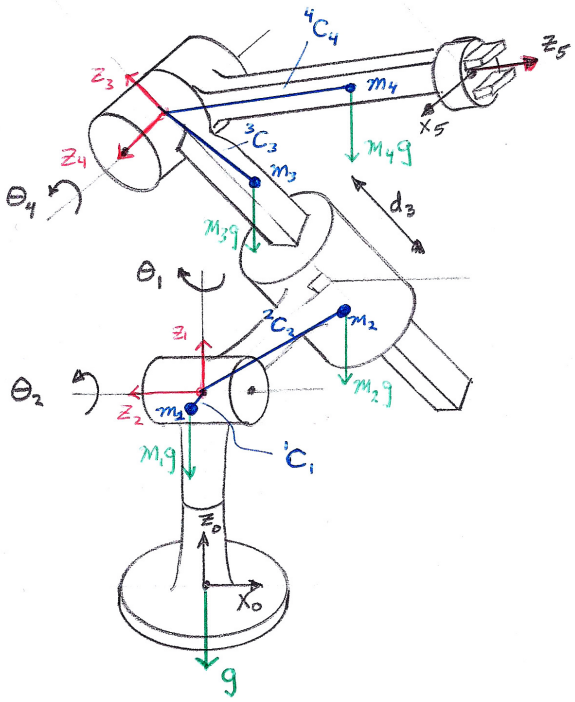

Example 6.1 cont.

Part II

Which masses contribute to torques on joint 2?
Draw a vector in place to illustrate each center of mass (that contributes to τ_2) in Frame 2: ${}^2C_j$:

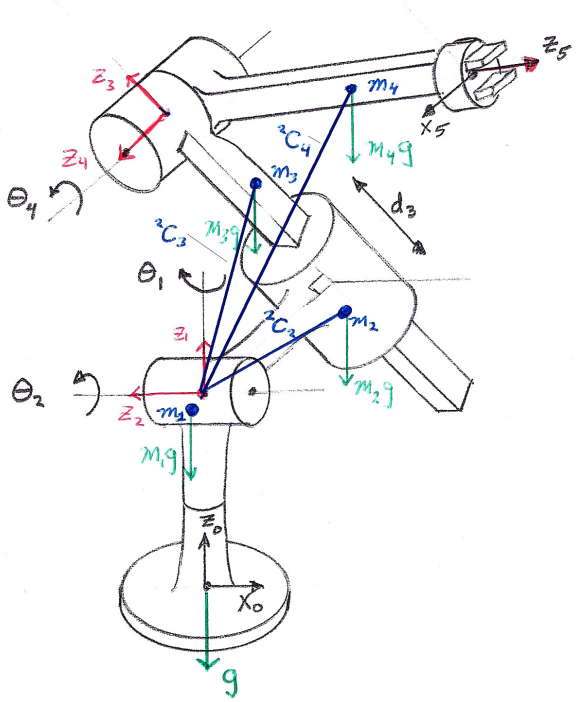

Example 6.2
Derive the gravity torques for a three-link manipulator. Joint 1 is rotary, Joint 2 is prismatic, joint 3 is rotary. Assume that the robot is mounted on a level factory floor. We know little about this manipulator, but we have obtained values for m_j and ${}^jC_j$ and the ${}^N_{N+1}T$ matrices of forward kinematics (which depend on the robot pose of course).

Joint 1 Transform the centers of mass, ${}^jC_j$s into frame {1}:

$$ {}^1C_3 = {}^1_2T\ {}^2_3T\ {}^3C_3 $$

$$ {}^1C_2 = {}^1_2T\ {}^2C_2 $$

$$ {}^1C_1 = {}^1C_1 $$

also because of the standard level floor mount:

$$ {}^0g = [0 \quad 0 \quad -9.8]^T $$

now compute the acceleration of gravity in the current frame:

$$ {}^1g = \begin{bmatrix} {}^0_1R^{-1} \end{bmatrix}\ {}^0g $$

Then we are ready:

$$ {}^1\tau = \left(m_1{}^1C_1 + m_2{}^1C_2 + m_3{}^1C_3\right) \otimes {}^1g $$

Then the joint torque is

$$ \tau_1 = [0 \quad 0 \quad 1]\ {}^1\tau $$

Joint 2

$$ {}^2g = {}^1_2R^{-1}\ {}^0_1R^{-1}\ {}^0g $$

The gravity force vector arising from supporting the links distal to joint 2 is

$$ {}^2F = (m_2 + m_3)\ {}^2g $$

and the force on the prismatic joint is

$$ F_{Z2} = [0 \quad 0 \quad 1]\ {}^2F $$

Joint 3 Joint three has torque only generated by its own weight.

$$ {}^3g = {}^2_3R^{-1}\ {}^1_2R^{-1}\ {}^0_1R^{-1}\ {}^0g $$

$$ {}^3\tau = m_3{}^3C_3 \otimes {}^3g $$

$$ \tau_3 = [0 \quad 0 \quad 1]\ {}^3\tau $$

6.3 Acceleration

6.3.1 Acceleration of a Particle

A particle (point mass) moving in space is subject to acceleration when forces are applied to it according to

$$ F = mA $$

where A is a vector of the acceleration in three dimensions:

$$ A = \ddot{x} = [\ddot{X}, \ddot{Y}, \ddot{Z}]^T $$

The particle may be subject to resistance due to viscous or damping forces such as friction or springs. In this case these resistance forces, combined with mA sum up to the applied force, F:

$$F = mA + B\dot{x} + Kx$$

6.3.2 Acceleration of a Rigid Body

A rigid body can be thought of as a collection of point masses which move together. For linear motion, acceleration of a rigid body, measured at its center of mass, can be treated the same as that of a point mass.

6.4 Equation of Motion of Rigid Bodies

6.4.1 Newton Equation

Newtons equation is the fundamental equation of motion for linearly translating rigid bodies:

$$\sum F = 0$$

For example, a rigid body subject to a external force, F, having mass, m, and damping and elastic coefficients, B, K respectivly, would

$$0 = -F + mA + B\dot{x} + Kx$$

6.4.2 Euler Equations

For rotation, each of the particles comprising a rigid body undergoes different motion. The force acting on each particle is in general different. However the analogous concept of Moment or torque has been developed to predict rotational motion. Moment, M, is an combination of force, F, acting through a lever arm $\vec{r}$.

$$M = F \otimes \vec{r}$$

Where $\otimes$ stands for the vector cross product. For a rotating body, Euler's equation of motion is

$$\sum M = 0$$

This analysis procedes similarly to linear motion, however the concept of mass must be generalized to an "Inertia Tensor", I (which will be explained in more detail below). For example, a rigid body subject to a external moment, M, having inertia tensor, I, and rotational damping and elastic coefficients, B, K respectivly, would

$$0 = -M + AI + B\dot{\theta} + K\theta$$

where

$$A = \ddot{\theta} = [\ddot{\theta_X}, \ddot{\theta_Y}, \ddot{\theta_Z}]^T$$

6.5 Inertia Tensor and Transformation of the Inertia Tensor

6.6 Derivation of the Inverse Dynamic Equations

Fundamental to dynamic analysis of a manipulator is an answer to the question

> If a manipulator moves through the trajctory $\theta(t)$, what are the torques in each of its joints?

Goal:

$$\tau = M(\theta)\ddot{(\theta)} + C(\theta, \dot{\theta}) + g(\theta)$$

6.7 Recursive Newton-Euler Formulation

In this section, we will formulate the following problem:

> Given the motion of a manipulator, specified in terms of the motion of it's joints, $q(t), \dot{q}(t), \ddot{q}(t)$, compute the torques in each joint, $\tau(t)$.

6.7.1 Propagation of Acceleration

From the previous chapter, we had

$$ {}^{N+1}\omega_{N+1} = \quad {}^{N+1}_{N}R \quad {}^{N}\omega_N + \begin{bmatrix} 0 \\ 0 \\ \dot{\theta}_{N+1} \end{bmatrix} $$

and

$$ {}^{N+1}V_{N+1} = \quad {}^{N+1}_{N}R \left[{}^{N}V_N + {}^{N}\omega_N \otimes \quad {}^{N}P_{N,N+1} \right] $$

for rotary joints, and

$$ {}^{N+1}\omega_{N+1} = \quad {}^{N+1}_{N}R \quad {}^{N}\omega_N $$

$$ {}^{N+1}V_{N+1} = \quad {}^{N+1}_{N}R \left[{}^{N}V_N + {}^{N}\omega_N \otimes {}^{N}P_{N,N+1} \right] + \begin{bmatrix} 0 \\ 0 \\ \dot{d}_{N+1} \end{bmatrix} $$

for prismatic.

If we combine them, but assume that only one of the pair $\{\dot{\theta}, \dot{d}\}$ is non-zero for any one joint, then

$$ {}^{N+1}\omega_{N+1} = \quad {}^{N+1}_{N}R \quad {}^{N}\omega_N + \begin{bmatrix} 0 \\ 0 \\ \dot{\theta}_{N+1} \end{bmatrix} $$

$$ {}^{N+1}V_{N+1} = \quad {}^{N+1}_{N}R \left[{}^{N}V_N + {}^{N}\omega_N \otimes {}^{N}P_{N,N+1} \right] + \begin{bmatrix} 0 \\ 0 \\ \dot{d}_{N+1} \end{bmatrix} $$

is one set of equations we can use for both types of joint. For dynamics we need acceleration (Newton's equation) and angular acceleration (Euler's equation) so we need to differentiate these expressions. There are terms in these equations of the form

$$ RV $$

where V is a vector and R is a rotation matrix between the links. Unfortunately, R is changing with time since links can be rotating with respect to each other (${}^{i}\omega_{i+1} \neq 0$). When we take the derviative of this term, we need to apply the product rule and obtain

$$ \frac{d}{dt} R(t) $$

In Appendix B.4, we derive that if we have the term

$$ f(t) = R(t)V(t) $$

its derivative is

$$ \frac{d}{dt} R(t)V(t) = R(t)\dot{V}(t) + \omega \otimes R(t)V(t) $$

where ω is the angular velocity vector which represents the orientation change, and $\otimes$ designates the vector cross product. Thus, to differentiate the angular velocity propagation expression, we have

$$ \frac{d}{dt} {}^{N+1}\omega_{N+1} = {}^{N+1}\dot{\omega}_{N+1} = {}^{N+1}_{i}R \; {}^{i}\dot{\omega}_i + \dot{R}^{i}\omega_i + \begin{bmatrix} 0 \\ 0 \\ \ddot{\theta}_{N+1} \end{bmatrix} $$

$$ = {}^{N+1}_{N}R \quad {}^{N}\dot{\omega}_N + {}^{N+1}\omega_N \otimes {}^{N+1}_{N}R \, {}^{N}\omega_N + \begin{bmatrix} 0 \\ 0 \\ \ddot{\theta}_{N+1} \end{bmatrix} $$

or

$$ {}^{N+1}\dot{\omega}_{N+1} = {}^{N+1}_{N}R \left[{}^{N}\dot{\omega}_N + {}^{N}\omega_N \otimes \begin{bmatrix} 0 \\ 0 \\ \dot{\theta}_{N+1} \end{bmatrix} \right] + \begin{bmatrix} 0 \\ 0 \\ \ddot{\theta}_{N+1} \end{bmatrix} \tag{6.1} $$

After we have computed all the ${}^{N}\omega_N$, we can do the linear acceleration. We obtain the method by differentiating

$$ {}^{N+1}V_{N+1} = \quad {}^{N+1}_{N}R \left[{}^{N}V_N + {}^{N}\omega_N \otimes {}^{N}P_{N,N+1} \right] + \begin{bmatrix} 0 \\ 0 \\ \dot{d}_{N+1} \end{bmatrix} $$

To perform this derivative, we will use the $\dot{R}$ result above, and also we will need a term of the form

$$\frac{d}{dt}\ {}^{N}P_{N,N+1}$$

To get this derivative we need to understand particular properties of ${}^{N}P_{N,N+1}$ which is the offset between Frame N and frame $N+1$. Let's look at how ${}^{N}P_{N,N+1}$ changes during a brief time interval Δt. First, since link N is a rigid body, and its angular velocity is ${}^{N}\omega_N$, we have a term which is a cross product of the two. Second, if the link is prismatic, there is a change in the origin of Frame $N+1$ due to the sliding motion along Z_{N+1}, ΔZ_{N+1}. The sum of these terms is:

$$\frac{d}{dt}\ {}^{N}P_{N,N+1} = \ {}^{N}\omega_N \otimes \ {}^{N}P_{N,N+1} + \ {}^{N}_{N+1}R \begin{bmatrix} 0 \\ 0 \\ \dot{d}_{N+1} \end{bmatrix}$$

This situation is illustrated below

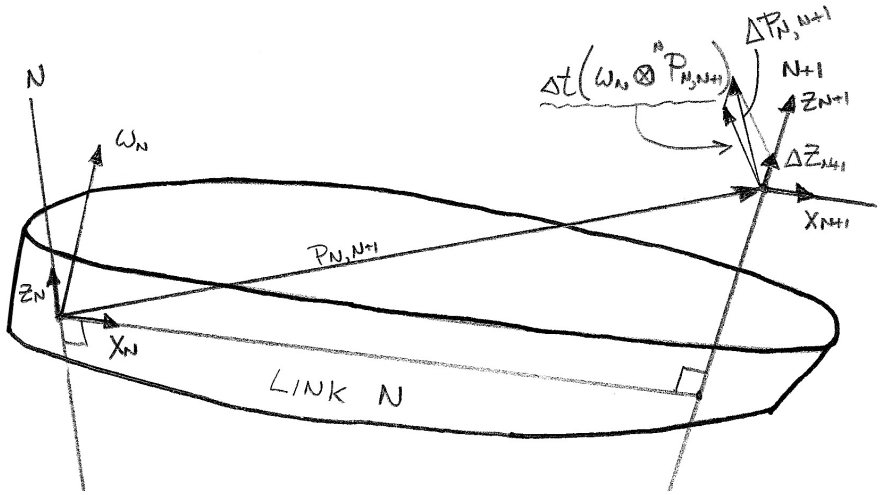

[[More derivation steps here ...]]

$${}^{N+1}\dot{V}_{N+1} = {}^{N+1}_{N}R \left[{}^{N}\omega_N \otimes \ {}^{N}P_{N+1} + \ {}^{N}\omega_N \otimes \ {}^{N}\omega_N \otimes \ {}^{N}P_{N+1} + \ {}^{N}\dot{V}_{N+1} \right] + 2\,{}^{N+1}\omega_{N+1} \otimes \begin{bmatrix} 0 \\ 0 \\ \dot{d}_{N+1} \end{bmatrix} + \begin{bmatrix} 0 \\ 0 \\ \ddot{d}_{N+1} \end{bmatrix} \tag{6.2}$$

For rotary joints, the $\dot{d}, \ddot{d}$ terms are zero.

Acceleration of the link mass center

To get Newtonian reaction forces on each link, we need to derive the acceleration of the center of mass of each link. We designate the Center of Mass of link N in frame N as

$${}^{N}P_{CN}$$

Then the velocity of the center of mass is (see Section 5.2.2) can be expressed by

$$V_{CN} = V_N + \ \omega_N \otimes P_{CN}$$

(in any frame)

Differentiating this in frame N,

[[More derivation steps]]

$${}^{N}\dot{V}_{CN} = {}^{N}\dot{V}_N + \ {}^{N}\dot{\omega}_N \ \otimes \ {}^{N}P_{CN} + \ {}^{N}\omega_N \otimes \ {}^{N}\omega_N \otimes \ {}^{N}P_{CN}$$

6.7.2 Propagation of Forces and Moments

Step 1: First we start with link i at rest:

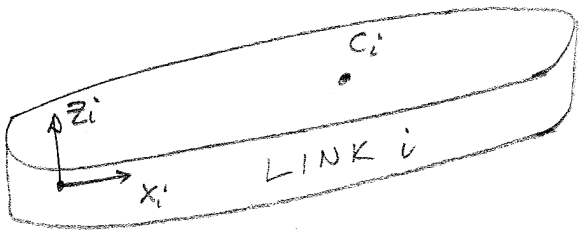

Step 2: Now let

f_i = force on link i by link $i-1$
n_i = moment on link i by link $i-1$

Step 3: Add effects from link $i-1$:

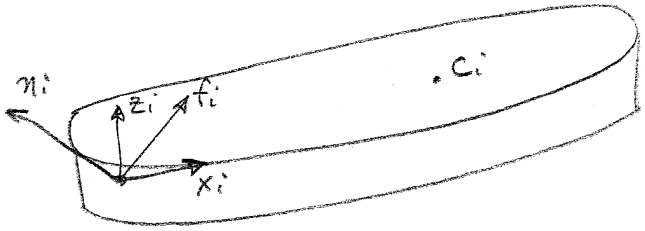

Step 4: Add in the effects from the next link, $i+1$:

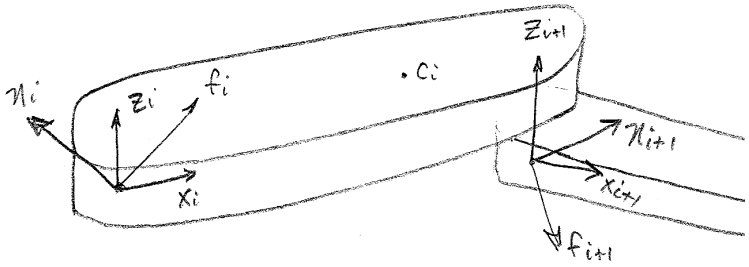

Step 5: Balance forces and torques for static equilibrium in any frame

$$f_i + f_{i+1} = 0$$

Torque, unlike force, must be computed and balanced in a specific frame:

$$n_i + n_{i+1} + P_{i,i+1} \otimes f_{i+1}$$

We will also need this balance in the center of mass (COM) frame, which is an arbitrary point, C_i on link i:

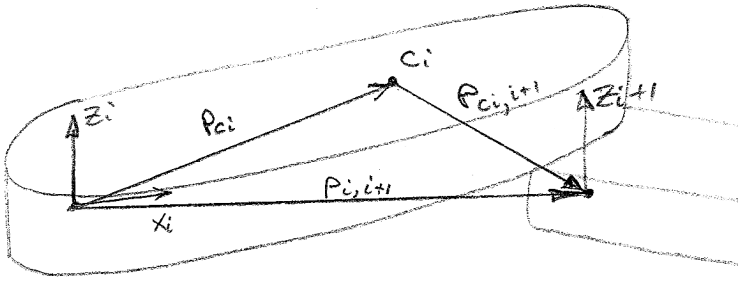

$$n_i + n_{i+1} + (P_{Ci}) \otimes f_i + (P_{ci,i+1}) \otimes f_{i+1}$$

where $P_{ci,i+1} = P_{i,i+1} - P_{Ci}$.

Step 6: Now we add in dynamic terms due to motion:

$$F_i = m_i \dot{V}_i \qquad N_i = {}^C I \dot{\omega}_i + \omega_i \otimes {}^C I \omega_i$$

getting

$$f_i + f_{i+1} = F_i \tag{6.3}$$

$$n_i + n_{i+1} + P_{Ci} \otimes f_i + (P_{i,i+1} - P_{Ci}) \otimes f_{i+1} = N_i \tag{6.4}$$

Step 7: Rewriting the torque balance:

$$n_i + n_{i+1} + P_{Ci} \otimes f_i + (P_{i,i+1}) \otimes f_{i+1} - (P_{Ci}) \otimes f_{i+1} = N_i$$

$$n_i + n_{i+1} + P_{Ci} \otimes F_i + (P_{i,i+1}) \otimes f_{i+1} = N_i \tag{6.5}$$

where we have used

$$P_{Ci} \otimes f_i - (P_{Ci}) \otimes f_{i+1} = P_{Ci} \otimes (f_{i+1} + f_i) = P_{Ci} \otimes F_i$$

Step 8: Now assume frame i quantites are all known in frame i. For example, ${}^{i+1}f_{i+1}$ is known. Then we re-write the Force/Torque balance

$${}^i f_i - {}^i_{i+1}R \, {}^{i+1}f_{i+1} = {}^i F_i$$

or

$${}^i f_i = {}^i F_i + {}^i_{i+1}R \, {}^{i+1}f_{i+1} \tag{6.6}$$

and similarly

$${}^i n_i = {}^i_{i+1}R \, {}^{i+1}n_{i+1} + {}^i P_{Ci} \otimes {}^i F_i + ({}^i P_{i,i+1}) \otimes \left({}^i_{i+1}R \, {}^{i+1}f_{i+1}\right) + {}^i N_i \tag{6.7}$$

Step 9: Now, using Newton's and Euler's equations to get ${}^i F_i$ and ${}^i N_i$ for the last link and propagate downward.

6.8 Lagrangian Formulation

6.9 Cartesian Transformation

6.10 Friction and Gravity Effects

6.11 Dynamic Simulation

6.11.1 Inverse Dynamics

Computational Loads in Real Time Control

6.12 Direct Dynamics

Simulations

6.13 Identification of Manipulator Dynamics

6.14 Summary of Notation

Chapter 7

Trajectory Generation

7.1 Problem Statement and Learning Objectives

Problem Statement If a manipulator is asked to move from one pose to another, it must do so smoothly and with speed and acceleration which is under the control of the programmer. This chapter describes techniques for generating smooth trajectories between two positions of the robot manipulator. Mathematically this problem can be thought of as that of finding a function of time which meets specified boundary conditions and other constraints.

Learning Objectives After completing this chapter, the student will be able to

- Design or program linear trajectories with parabolic start and stop periods.
- Design or program trajectories based on cubic polynomials.
- Design or program trajectories which are constrained to move through via points.
- Design trajectories for the joints of a robot arm which result in straight trajectories in Cartesian space.

7.2 Trajectory Generation

Much of control theory focuses on the response of the system to a step input (Figure 7.1). There are good historical and contemporary reasons for this focus, but it is often inappropriate for motion control systems including robotics. Although no physical system can accurately follow the instantaneous position change of a step input, when viewed through the lens of control systems theory, the object is to design a controller which achieves desireable characteristics in the error. For example, the designer may adjust controller parameters to get fast response with overshoot or slow response without overshoot.

In both cases however, there is a large error between input and output (Figure 7.2). In this chapter we will avoid the problem of tracking a step input by changing to a smoother input. Such an input will demand lower velocities and accelerations and thus generate smaller tracking errors. Overshoot can be particularly bad when a robot operates in a crowded environment.

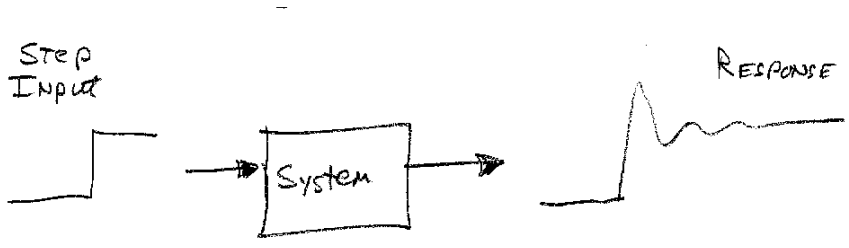

Figure 7.1: Most control analysis and design focuses on step inputs.

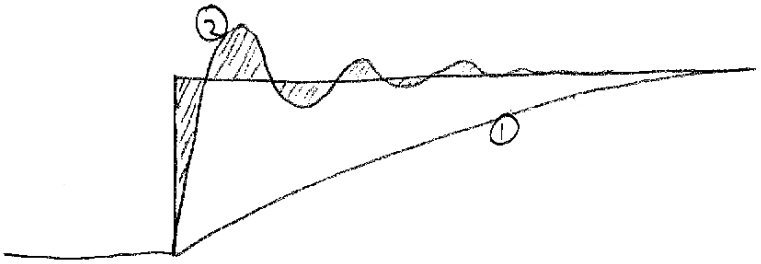

Figure 7.2: There is usually a significant error between the output of a well designed control system and a step input.

7.3 Joint Space Trajectory Generation

Suppose one joint of a robot arm needs to go from

$$\theta_A \rightarrow \theta_B$$

in an amount of time t_f. The problem of trajectory generation boils down to specifying a time function $\theta(t)$ such that

$$\theta(0) = \theta_A \quad \text{and} \quad \theta(t_f) = \theta_B$$

In addition, we will initially assume the manipulator should be at rest before and after the move giving

$$\dot{\theta}(0) = \dot{\theta}(t_f) = 0$$

The shortest distance between two points is a straight line. This naive approach to generating a trajectory gives us

$$\theta(t) = \theta_A + t \times \frac{\theta_B - \theta_A}{t_f}$$

However, because we have assumed the velocity at $t = 0^-$ and $t_f^+ = 0$, our acceleration must be infinite at the start and end of the trajectory. No robot can accelerate that fast and so we will have significant tracking error. Before we start looking at some candidate functions then, we should think about what we want in the function $f(t)$. We will consider a trajectory a "good" one if it satisifies two criteria: "Smoothness" and "Attainability".

We will consider the function smooth if $\theta(t)$ and $\dot{\theta}(t)$ are continuous.

We will consider the function attainable if $|\ddot{\theta}(t)| \leq \ddot{\theta}_{MAX}$.

There are many possible functions which could meet these criteria. We will consider two in depth,

1. A polynomial
2. A linear function with parabolic start and end regions to limit maximum acceleration.

7.3.1 3rd Order Polynomial

A simple trajectory to start with is the 3rd order polynomial (Figure 7.3). We need a function of the form

$$\theta(t) = a_0 + a_1 t + a_2 t^2 + a_3 t^3$$

with the following boundary conditions

$$\theta(0) = \theta_A \qquad \dot{\theta}(0) = 0$$

$$\theta(t_f) = \theta_B \qquad \dot{\theta}(t_f) = 0$$

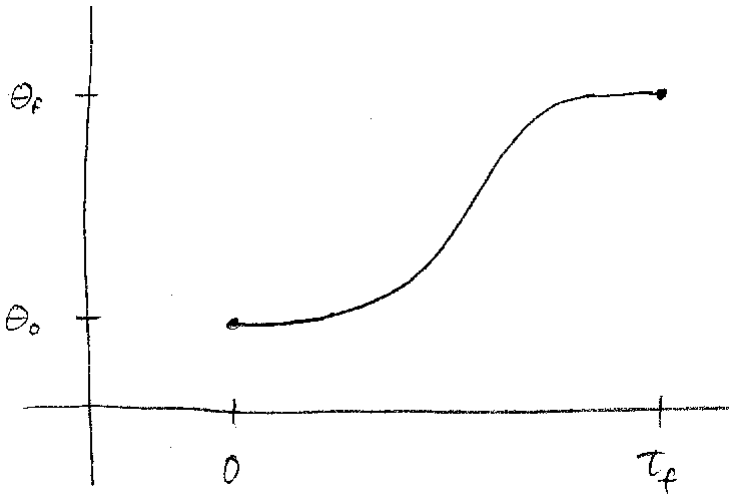

Figure 7.3: With the right coefficients, a third order polynomial can make a smooth trajectory between two values in a finite time.

There are four unknowns ($a_0 \rightarrow a_3$) and the four equations above. By differentiating and applying the boundary conditions we can obtain

$$a_0 = \theta_A \qquad a_1 = 0$$
$$a_2 = \frac{3(\theta_B - \theta_A)}{t_f^2} \qquad a_3 = \frac{-2(\theta_B - \theta_A)}{t_f^3}$$

Note that the derivatives are easy to compute analytically:

$$\dot{\theta}(t) = 2a_2 t + 3a_3 t^2 \qquad \ddot{\theta}(t) = 2a_2 + 6a_3 t$$

The resulting trajectory and its derivatives looks like Figure 7.4.
We can also easily get:

$$\ddot{\theta}_{MAX} = \ddot{\theta}(0) = 2a_2 = \frac{6(\theta_B - \theta_A)}{t_f^2}$$

$$\dot{\theta}_{MAX} = \dot{\theta}(t_f/2) = \frac{3}{2}\frac{(\theta_B - \theta_A)}{t_f}$$

This function meets our requirements for smoothness and attainability if

$$\ddot{\theta}_{MAX} \geq 2a_2$$

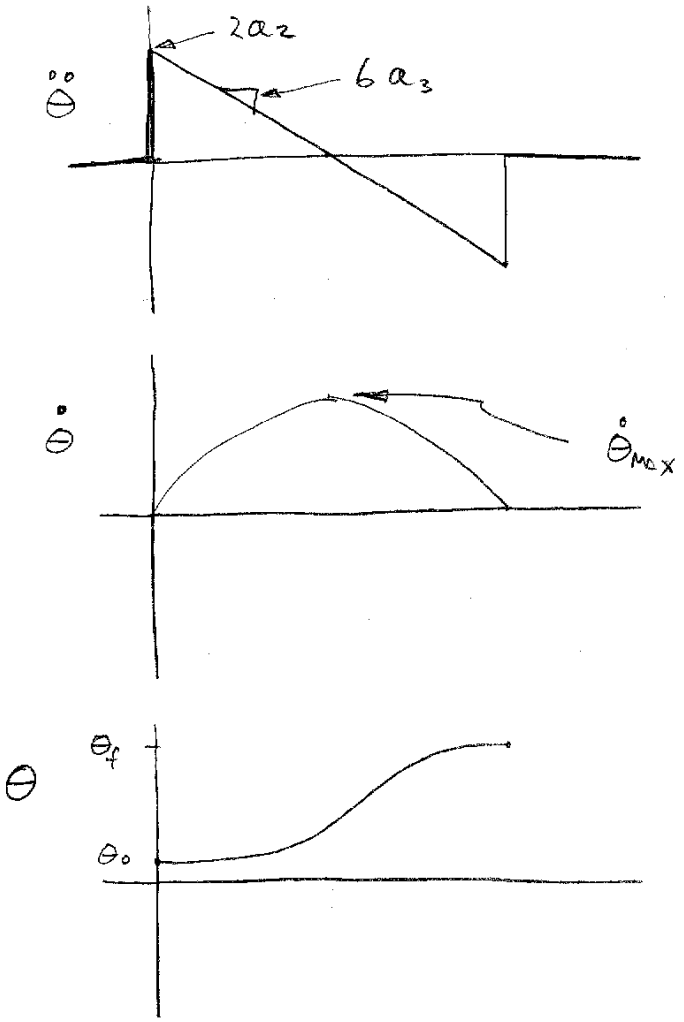

Figure 7.4: Position (θ), velocity ($\dot{\theta}$), and acceleration($\ddot{\theta}$)

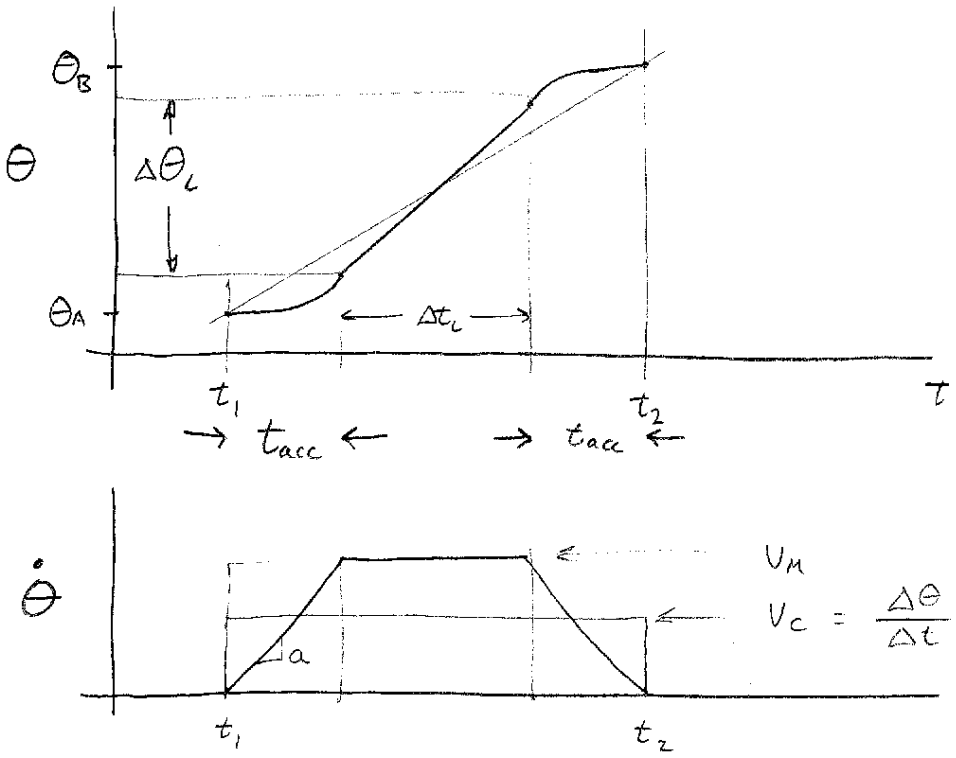

Figure 7.5: A smooth three-segment trajectory can be formed by a parabola, a straight line, and another parabola. This trajectory is defined by the time interval and the limits on velocity and acceleration.

Example 7.1
Design a 3rd order polynomial trajectory with $\theta_A = 40°$, $\theta_B = 120°$, $t_f = 2.4$sec. Also derive the velocity and acceleration of the trajectory:
ANS:

$$a_0 = 40°$$

$$a_2 = \frac{240°}{2.4^2} = 41.67$$

$$a_3 = \frac{-2 \times 80°}{13.824} = -11.57$$

$$\theta(t) = (40 + 41.67t^2 - 11.57t^3)°$$

by differentiation:

$$\dot{\theta}(t) = 83.34t - 34.71t^2$$

$$\ddot{\theta}(t) = 83.34 - 69.42t$$

7.3.2 Linear with Parabolic Blends

To understand this trajectory, it is easiest to look first at the velocity curve of Figure 7.5.

Using this trajectory type, the velocity increases linearly for a time interval t_{acc}, then continues at a constant velocity, V_M, and then decreases linearly to zero for t_{acc} seconds prior to the end of the trajectory.

The key constraint is that the area under the velocity curve must be equal to the displacement, $\theta_B - \theta_A = \Delta\theta$. The area of the velocity curve is $V_M(t_2 - t_1 - t_{acc})$. Thus:

$$V_M(t_2 - t_1 - t_{acc}) = \Delta\theta$$

$$V_M = \frac{\Delta\theta}{t_2 - t_1 - t_{acc}}$$

We can further obtain the acceleration of the velocity ramp, a

$$a = \frac{V_M}{t_{acc}} = \frac{\Delta\theta}{t_{acc}(t_2 - t_1 - t_{acc})}$$

Implementation of this trajectory in software is a bit more complex than the polynomial. We must divide the trajectory time into three phases: acceleration, cruising, and deacceleration.

Example 7.2
Write pseudo code to generate a linear trajectory with parabolic blends. Divide your code into two functions, one which plans the trajectory and returns the constants V_M, a etc. and a second one which is called every 0.001 seconds and computes $\theta(t)$. Make sure that acceleration is not greater than a predefined `A_MAX`.
ANS:

```
\\ generate constants
lin_parab_init(float delta_theta, float delta_t)
 {
 t_acc = 0.25 * delta_t; // arbitrary, other ways could be better
 VM = delta_theta/(delta_t - t_acc);
 a = VM / tacc;
 if(abs(a) > A_MAX) { error("Acceleration too high"); }
 }

\\run time call
lin_parab_run(float t, float t_0, float theta_A, float delta_t,
                                  float t_acc, float a, float VM)
 {
 dt = t-t_0;
 if(dt < t_acc) { // acceleration phase
   return(0.5 * a * (t-t_0)^2 + theta_A);
   }
 else if (dt > t_acc && dt < delta_t-t_acc) { // cruise
   return(0.5 * t_acc*VM + VM*(t-t_0-t_acc) + theta_A);
   }
 else if (dt > delta_t - t_acc) {  // decelleration
   return((theta_A+delta_theta)- 0.5*a*(t-delta_t)^2);
   if(t == delta_t)  stop;
   }
 }
```

7.3.3 Via Points

We may need to specifiy an intermediate point between a start and a goal. For example, in Figure 7.6, starting at the point A, we must go to the point V before B in order to avoid the obstacle.

If we translate the three points, A, V, B, to joint configuration, and we consider just one joint, we need a trajectory something like one of the two trajectories shown in Figure 7.7. In the first option (left) the joint value corresponding to the Via point θ_V is outside the range between θ_A and θ_B. In the second, (right) $\theta_A < \theta_V < \theta_B$.

In the example at left, we need to go through zero velocity at point V but in the case at right it would break up the motion to require zero velocity at the via point. We should specify some non zero velocity

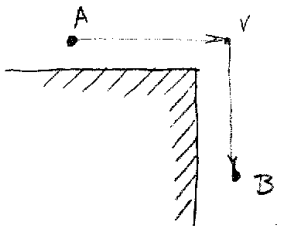

Figure 7.6: An intermediate (via) point must be established to avoid the corner-shaped obstacle.

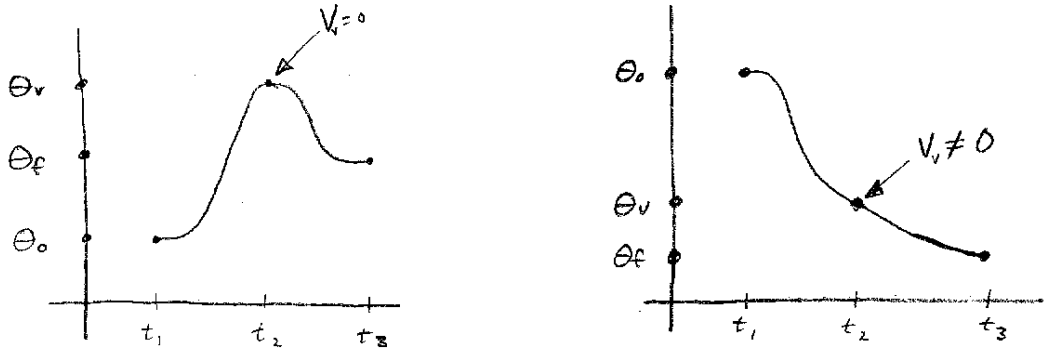

Figure 7.7: Two possible smooth trajectories combining trajectory AV and trajectory VB. (need to correct subscripts in graphics.

at the via point for smoother motion. We could allow the user to specify this velocity. Alternatively, to automatically generate it, we can use some heurisitics such as

1. if the difference in θ changes sign, $V_V = 0$.
2. if not, average the slopes:

$$V_V = 1/2 \left(\frac{\Delta\theta_1}{\Delta_{t1}} + \frac{\Delta\theta_2}{\Delta_{t2}} \right)$$

Once we have derived a value for the velocity in the via point, V_V, we can compute the new trajectory as follows:

First, redo the derivation of Section 7.3.1 but alter the boundary conditions:

$$\dot{\theta}_1(t_2) = \dot{\theta}_2(t_2)$$

Where the left hand side is the final velocity of the first sub-trajectory, and the right hand side is the initial velocity of the second sub-trajectory.

Alternatively, we can require that the acceleration, $\ddot{\theta}(t)$ is continuous at $t = t_2$. Consider two example trajectories shown in Figure 7.8:

Let's introduce intermediate time variables so that we can keep each polynomial simple:

$$t' = t - t_1 \qquad t'' = t - t_2$$

Then the two segments have the equations:

$$\theta_1(t) = a_{10} + a_{11}t' + a_{12}t'^2 + a_{13}t'^3$$

$$\theta_2(t) = a_{20} + a_{21}t'' + a_{22}t''^2 + a_{23}t''^3$$

There are thus 8 unknowns and we need eight equations to solve them:

1. $\theta_0 = a_{10}$

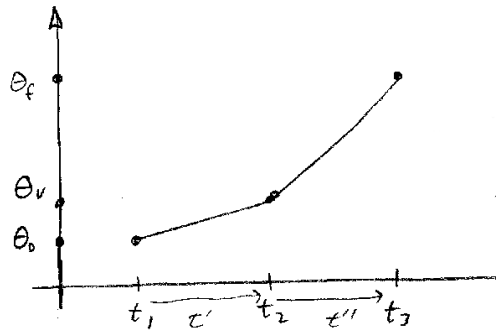

Figure 7.8: Two trajectories which join at a Via point (θ_V). Note that at this point we DO NOT have a smooth combined trajectory.

2. $\theta_f = a_{20} + a_{21}(t_{f2}) + a_{22}t_{f2}^2 + a_{23}t_{f2}^3$
3. $\theta_V = a_{20}$
4. $\theta_V = a_{10} + a_{11}t_2 + a_{12}t_2^2 + a_{13}t_2^3$
5. $\dot{\theta}_1(t_1) = 0$
6. $\dot{\theta}_2(t_3) = 0 = a_{21} + 2a_{22}t_{f2} + 3a_{23}t_{f2}^2$
7. continuous velocity:
$$\dot{\theta}_1(t_2) = \dot{\theta}_2 t_2 \rightarrow a_{11} + 2a_{12}t_2' + 3a_{13}(t_2')^2 = a_{21}$$
8. continuous acceleration:
$$\ddot{\theta}_1(t_2) = \ddot{\theta}_2 t_2 \rightarrow 2a_{12} + 6a_{13}t_2' = 2a_{22}$$

where $t_{f2} = t_3 - t_2$. This can be solved readily and coded into a subroutine.
Such a trajectory might look like Figure 7.9.

The methods above could generate the trajectory for a single joint, $\theta_i(t)$. To move a robot arm from one pose to another, we work out the joint angles for the starting and ending poses (using inverse kinematics) and then plan a trajectory for each joint from its value in pose A to its value in pose B where each joint uses the same t_f. This produces nicely synchronized and smooth motion.

7.4 Cartesian Straight Line Motion

7.4.1 Position

Sometimes it is not enough to plan the trajectory in the manipulator's joint space. While the joint space trajectory may be smooth and attainable, we do not know where it goes between the start and end points in Cartesian space. In the welding task shown below, we need to make sure that the end effector motion goes in a straight line at a constant speed (Figure 7.10).

First, consider only the Cartesian end effector position and neglect orientation. If we have 3×1 start position P_A and end position P_B, we can generate a straight line path by linear interpolation. Letting the time variable, t be referenced to the start of the trajectory,

$$P(t) = P_A + \frac{t}{t_f}(P_B - P_A)$$

Then, at each sample of time, we can compute the joint positions with inverse kinematics. Note that for now we have neglected the starting and stopping accelerations.

Now, we know where the end effector is at each point along the Cartesian trajectory. This is very important when obstacles might be present or when the trajectory is important to the task itself such as welding. Two important issues however which must be considered with this method are choosing correctly

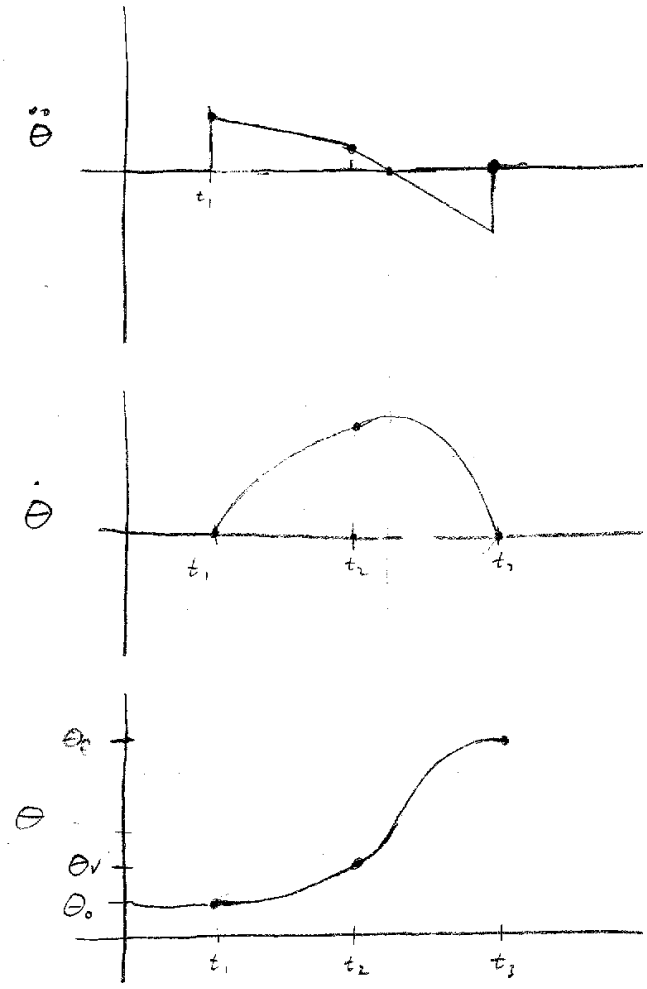

Figure 7.9: Two trajectories through a via point which are constrained to have continuous acceleration through the via point.

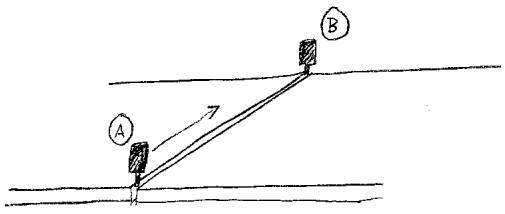

Figure 7.10: Cartesian straight line trajectory example: move the robot end effector so as to make a weld along a straight line joining two metal plates.

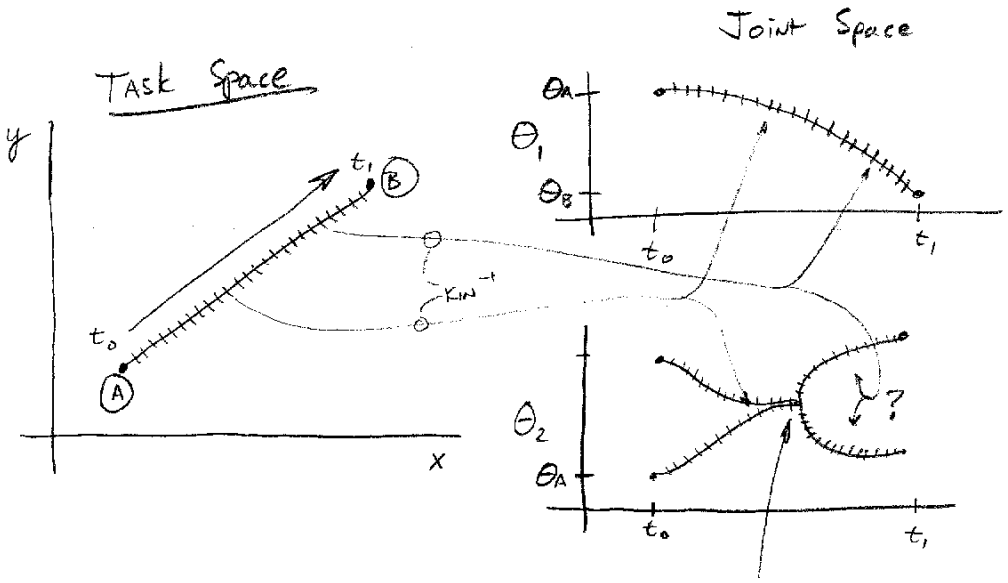

Figure 7.11: An apparently simple trajectory in task space (left) can map to multiple and complex trajectories in joint space throught the inverse kinematics computation.

between multiple solutions of the inverse kinematics, and dealing with trajectories which go through singular point (Figure 7.11).

On the left, a straight line trajectory is shown in the Cartesian end effector space of the robot. The path is divided into sample points corresponding the linear interpolation function at several points in time. On the right are the corresponding inverse kinematics solutions for two joints of the robot. For θ_1 (top) the inverse kinematics equations produce a single solution at each point for an unambiguous path. However for θ_2, the inverse kinematic equations produce two solutions. Furthermore, at a singular point (see Chapter 5), the two solutions merge into one and afterwards diverge into two separate solutions again. When controlling an actual robot, it is important that the algorithms consistently pick solutions which are close to each other in the joint space and make an intelligent choice of solutions when coming out of the singularity. If control algorithms rely on the Jacobinan matrix inverse, they must be robust to the numerical problems which arise both at and in the neighborhood of the singularity.

Not all paths will go through singular points, but trajectory generation algorithms which rely on inverse kinematics must be prepared to encounter them.

7.4.2 Orientation

What if the start and end points have different orientations of the end effector? How do we interpolate orientation? A naive approach might be to interpolate the orientation matrices from R_A to R_B. However it is easily shown that the interpolated matrices produced are not valid rotation matrices. The answer is to convert the rotation matrices to one of the parameterized forms such as equivalent angle-axis form. First, derive a rotation matrix which maps from the initial to final orientation. Using the transform graph in Figure 7.12, we can solve for ${}^A_B R$ as

$$ {}^A_B R = {}^0_A R^{-1} {}^0_B R $$

where ${}^0_A R$ is the orientation at the initial point A etc. Using Chapter 2, we can convert ${}^A_B R$ to a fixed axis, K, and a rotation angle around that axis, θ_{AB}. Now we can keep K fixed, and use one of the preceding trajectory generation methods for the angle $\theta_{AB}(t)$:

$$ \theta_{AB}(t) = (S(t))\,\theta_{AB} $$

where, for the case of a third order trajectory,

$$ 0 < S(t) < 1.0 \qquad 0 < t < t_f \qquad S(t) = a_1 t + a_2 t^2 + a_3 t^3 $$

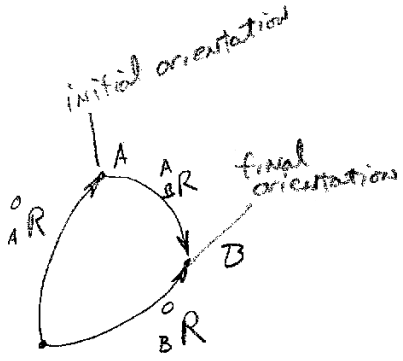

Figure 7.12: To design a trajectory in orientation, we must find a way to interpolate ${}^A_B R$ but interpolation between two rotation matrices is not valid (see text).

the first term, a_0 is zero because ${}^A_B R$ was defined relative to position A. Then, the current rotation change is reconstructed from K and $\theta_{AB}(t)$ and combined with ${}^0_A R$ to get the current rotation matrix

$$ {}^A_B R = {}^0_A R \, {}^A_B R(t) $$

A similar method can be used with quaternions.

7.4.3 Parameterized Cartesian Trajectories

In the previous treatment of linear interpolated trajectories through cartesian space, we have ignored the inifinite acceleration at the start. Full consideration of this problem requires consideration of dynamics in future chapters, but we can at least address the concern by doing the linear interpolation with a parameter, $0 \leq p \leq 1$, and generating a smooth time function for p. Considering position, we can convert our interpolation function to p by

$$ P(t) = P_A + p(t)(P_B - P_A) $$

where, for example,

$$ p(t) = a_0 + a_1 t + a_2 t^2 + a_3 t^3 $$

We solve for a_0 to a_3 as in Section 7.3.1 where

$$ p(0) = 0 \qquad p(t_f) = 1 $$

$$ \dot{p}(0) = \dot{p}(t_f) = 0 $$

giving

$$ a_0 = 0 \qquad a_1 = 0 \qquad a_2 = \frac{3}{t_f^2} \qquad a_3 = \frac{-2}{t_f^3} $$

While this gives us a smoother straight line trajectory, we do not know which trajectories are attainable. Also, a task like welding may require constant velocity over the entire path. To properly perform the weld then we should use the linear-parabolic function instead of the polynomial for $p(t)$ and extend the length of the trajectory to allow space for the manipulator to accelerate and decelerate before and after the weld line.

7.5 Summary of Notation

Chapter 8

Motion Planning

8.1 Problem Statement and Learning Objectives

Problem Statement Motion planning is the process of finding a collision free path between two configurations of a manipulator, considering the presence of obstacles in the workspace.

Interestingly, this type of motion planning is usually very easy and natural for humans. One exception is the case of moving a large bulky object such as a piano through small hallways and doors into a desired room. This "piano mover's problem" is similar to the motion planning problem we have posed above. However if the object (piano) were being manipulated by a (large) serial robot arm, we would also have to consider all potential collisions between the arm and the environment, in addition to the collisions between the piano and the environment.

Learning Objectives Upon completing this Chapter, the reader should be able to

- Explain the major problems in motion planning
- Identify which ones are most computationally time consuming in typical manipulation applications.
- Explain the Configuration Space.
- Describe some sampling based motion planning methods.

8.2 Path Planning

From the standpoint of robot manipulators, the basic problem of motion planning is to find a path between two configurations of the manipulator (possibly including an object held in the end effector) such that it does not collide with any parts of the environment. This is a function which humans do so naturally that it might take a moment of reflection to realize why it is a computationally hard problem and why it is still an active area of research.

First let's consider an extremely simple version of the problem, an obstacle free workspace. In this case, our path from point A to point B would most likely be a straight line, interpolated in the configuration space (as in Chapter 7). The next problem to take on is to add some obstacles inside the manipulator workspace.

We must first obtain a representation of the obstacles. In industrial environments, these are commonly fixtures, racks, conveyors or equipment which are of known dimensions and in fixed locations. In less structured environments, the obstacles must be sensed, for example by 3D vision systems or laser range finders.

In either case, we still have the difficult problem of searching for a path of the manipulator through any gaps which exist between the obstacles.

8.3 Configuration Space

We start by making a clever simplification of the problem originally made by Thomas Lozano Perez. First, we imagine a world containing a robot arm and a set of static obstacles. The robot's configuration is represented by a N-dimensional vector such as its joint variables. *Configuration space* is the space of all possible points representing the robot's joint variables, the same space we have referred to as joint space up until now. The

Figure 8.1: How to move the piano up the stairs without touching the walls?

robot thus becomes a point, and the obstacles become blobs representing all arm configurations in which any part of the arm collides with an obstacle in the end effector space. The motion planning task now becomes the apparently simpler one of moving a point from location A, to location B between the obstacle blobs.

8.3.1 Collision Detection

The first problem is to determine whether or not a manipulator in a given pose collides (overlaps in space) with obstacles in the workspace. This problem is important because we must find routes through the configuration space in which no collisions occur. Collision detection algorithms are also central to the related problem of haptic rendering, in which collisions must be tracked between a user's hand or an object in the user's hand, and a a virtual environment so that force feedback can be computed.

Note that for practical cases we care about all possible collisions between the arm and the obstacles, not simply those involving the end effector.

** Review of CD algorithms and speedups **

There are many applications for algorithms which can detect if two bodies described by geometrical models are colliding or not. First, we simplify a few aspects of the problem by making some assumptions:

- We have a good method for modeling objects such as polygons, implicit surfaces etc.
- We model a world containing a number. N_s, of static objects, and N_m moving objects. The static objects model the world around the manipulator, and the moving objects are the links of the manipulator and any object it might be holding.
- We assume that the world model, the moving object model, and its position and orientation are modeled exactly. Although this is unrealistic in most practical applications, we can get around this limitation by artificially growing the objects by an amount equal to the uncertainty in the measurements.
- We assume a function exists: `check(`A`,`B`)` which returns a one if objects A and B intersect.
- We assume that collisions between the static objects are not interesting.

The `check()` function is not trivial to implement except for basic geometric shapes such as spheres and rectangular solids. Depending on how detailed the object models are, this function can be computationally expensive.

Our task is thus to check all the moving objects against all the static objects and against each other. This would require running the `check()` function $N_m(N_s + (N_m - 1)/2)$ times. For situations where the environment is realistically modeled, this can be computationally prohibitive. A number of algorithms speed this up by simplifying the search for colliding objects.

One basic speedup uses *axis-aligned bounding boxes* (aabb's, Figure 8.2). A bounding box is a rectangular solid which just encloses an object model. "Axis aligned" means that the boxes are aligned with the x, y, z axes of the Cartesian space.

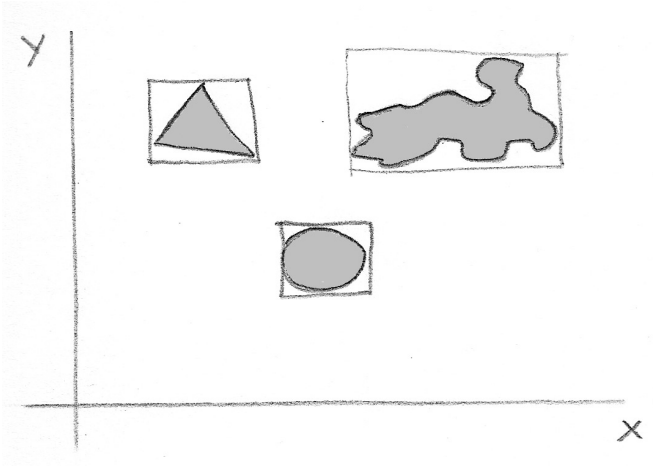

Figure 8.2: Three 2D objects shown with their axis-aligned-bounding-boxes (aabb's).

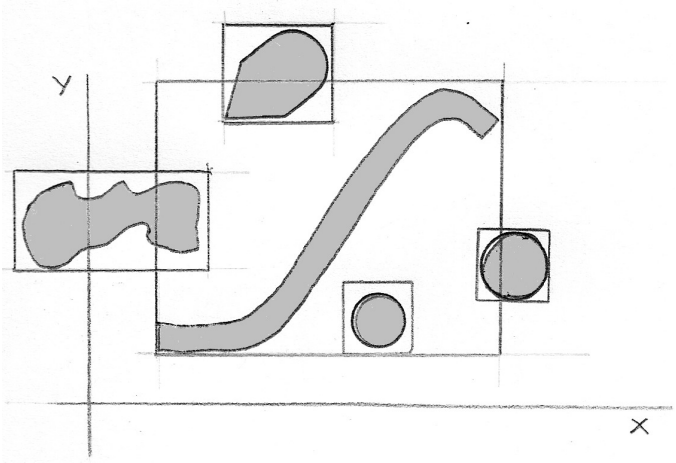

Figure 8.3: axis-alinged bounding boxes can generate excessive checking when the object is elongated and diagonal.

Once aabb's are defined for each obstacle, they can be kept in a list. The lists can be sorted in the x, y, z directions and then rapidly checked for overlaps. If two bounding boxes overlap in all three axes, then the objects inside must be checked for collisions. One problem with aabb's is that they must be recomputed for moving objects, especially as their orientation changes. A second problem is that they can be unnecessarily large, for example, with a diagonal object, generating too many checking steps (Figure 8.3)

An improvement on aabbs are *oriented bounding boxes* (obb's). In this method, an algorithm computes the smallest rectangular solid of any orientation which can enclose a given object. Although the algorithm to check obbs for collisions is a bit more involved than checking aabb's, it is still faster than checking general objects. Finally, bounding boxes can be arranged hierarchically in a tree so that the number of bounding box checks can be further reduced.

Finally, another class of speedups can be developed by exploiting what is known as temporal and spatial coherency. In realistic applications, a robot can change its position only a small amount between control samples. These algorithms exploit this fact by checking for collisions only in an immediate neighborhood of the current position. When properly implemented this can substantially reduce the computation.

In configuration space, the collision detection task becomes very simple. At each point in the configuration space, the robot is either colliding with an obstacle or it is not. Each blocking obstacle in the Cartesian space, defines a blob of points in the configuration space. The set of all such points, due to all obstacles, is called the forbidden region. The complement of that space is the free region. At any configuration space point we can ask "Does the manipulator point occupy any of the blobs in configuration space?"

8.3.2 Obstacles in Configuration Space

However, the simplification of configuration space generates a new and difficult problem: how to find the c-space blob corresponding to each obstacle in the end effector space. This is another computationally intensive problem which must be solved prior to motion planning. Assuming the c-space blobs have been found, we can verify that both the starting and ending configurations are reachable without collisions. Then the motion planner must find a continuous path through the free region from start point to the goal point.

A naive approach to the motion planning problem boils down to the following steps:

1. Obtain a geometric model of the entire workspace including all obstacles.
2. Obtain a collision detection algorithm which can return a single bit for any point, P, in configuration space. If the configuration, P, is one in which any part of the robot arm collides with one or more obstacles, return 1. If there is no collision, return 0.
3. Use the collision detection algorithm to obtain a description of the free space.
4. Plan a path through the free space to the goal point.

However, in a realistic problem with multiple obstacles of arbitrary shape, computing the forbidden region (or its complement the free space) is prohibitively difficult. Thus many realistic motion planning problems must be solved without generating the complete c-space! For now however we will study a simple planar 2D example so that the free space of the configuration space can be computed.

8.3.3 Computing the C-space

It is very challenging to compute a representation of the C-space both in terms of the amount of computation required, and the difficulty of the algorithms. Most algorithms which compute explicit representation of the obstacles rely on models such as polygonal models or traingular meshes. Although algorithms exist which can compute a c-space boudary representing the collisions of one polygonal solid with another, their complexity grows very rapidly with the c-space and the number and complexity of obstacles so that they are prohibitive for many realistic cases.

8.3.4 2-D computational example

In this section we will illustrate some of these issues with a very simple implementation for a two dimensional example. It will be obvious that the algorhithms presented here are rudimentary. However they are given to illustrate the types of computations which must be scaled up for use with actual manipulators in 3D.

We consider the two-link planar manipulator of Example 4.2 (page 63). This manipulator had the following parameters:

$$l_1 = 4, \qquad l_2 = 1.5, \qquad 0 \leq \theta_1 \leq 180^\circ \qquad -90^\circ \leq \theta_2 \leq 180^\circ$$

We will add a set of obstacles consisting of rectangles and circles (Figure 8.4). How can we map these obstacles from the workspace to the joint space? It is very easy to check whether or not a point is inside a circle or a rectangle. However, we must check for collisions with any point in the arm. To approximately check this, we will generate a series of points along the arm with a Scilab function `pointcloud(N,t1,t2)` where `N` is the number of points to distribute along the arm, and `t1,t2` are the values for θ_1, and θ_2. A representation of the arm model used by `pointcloud(10,45,30)` is given in Figure 8.5. The algorithm takes care to make sure that in addition to N evenly spaced points, the elbow and the end point are also labeled.

Our second scilab function accepts a series of points generated by `pointcloud()`, and checks them against a rectangle. It returns a 1 if any point is inside the rectangle. This function is called `checkrect(v,r)` where `v` is the set of points generated by `pointcloud` and `r` is a vector containing the boundaries of the rectangle, *[xmin,xmax,ymin,ymax]*. For the first rectangular obstacle (upper right of Figure 8.4),

```
R = [ 1, 2, 3, 6 ]
```

Finally, we make a script `confmap.sci` which loops through joint space. Each value of θ_1, θ_2 generates a pose of the manipulator. At each pose, the points distributed along the manipulator are checked against the obstacles, and the joint angles are recorded if any of them collide with an obstacle.

Running `confmap.sci` with rectangle 1, gives the configuration space obstacle shown in Figure 8.6, upper left. Our second rectangle (upper left) can be similarly checked (`R2=[-5,-1,4,5]`) to generate the c-space obstacle of Figure 8.6, upper right. Our circlular obstacle can be checked with a similar function

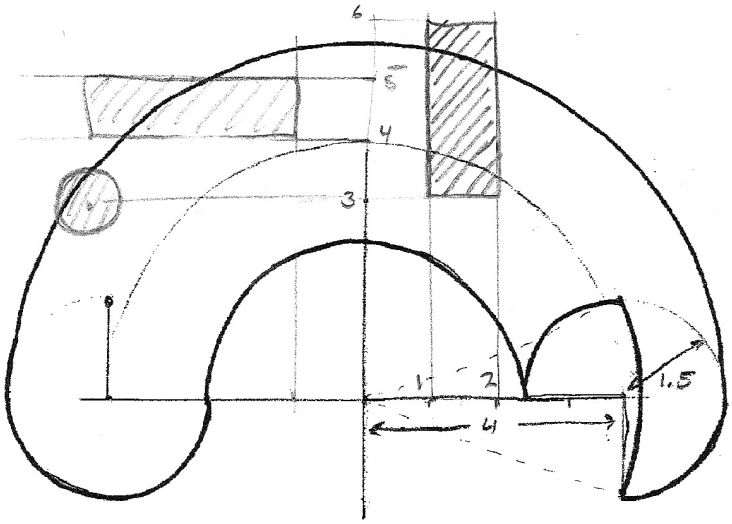

Figure 8.4: Workspace from Example 4.2 with the addition of two rectangular and one circular obstacles.

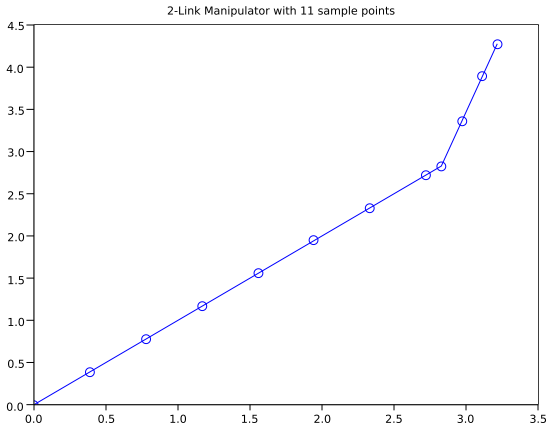

Figure 8.5: Basic 2-link manipulator with 11 points distributed along its length.

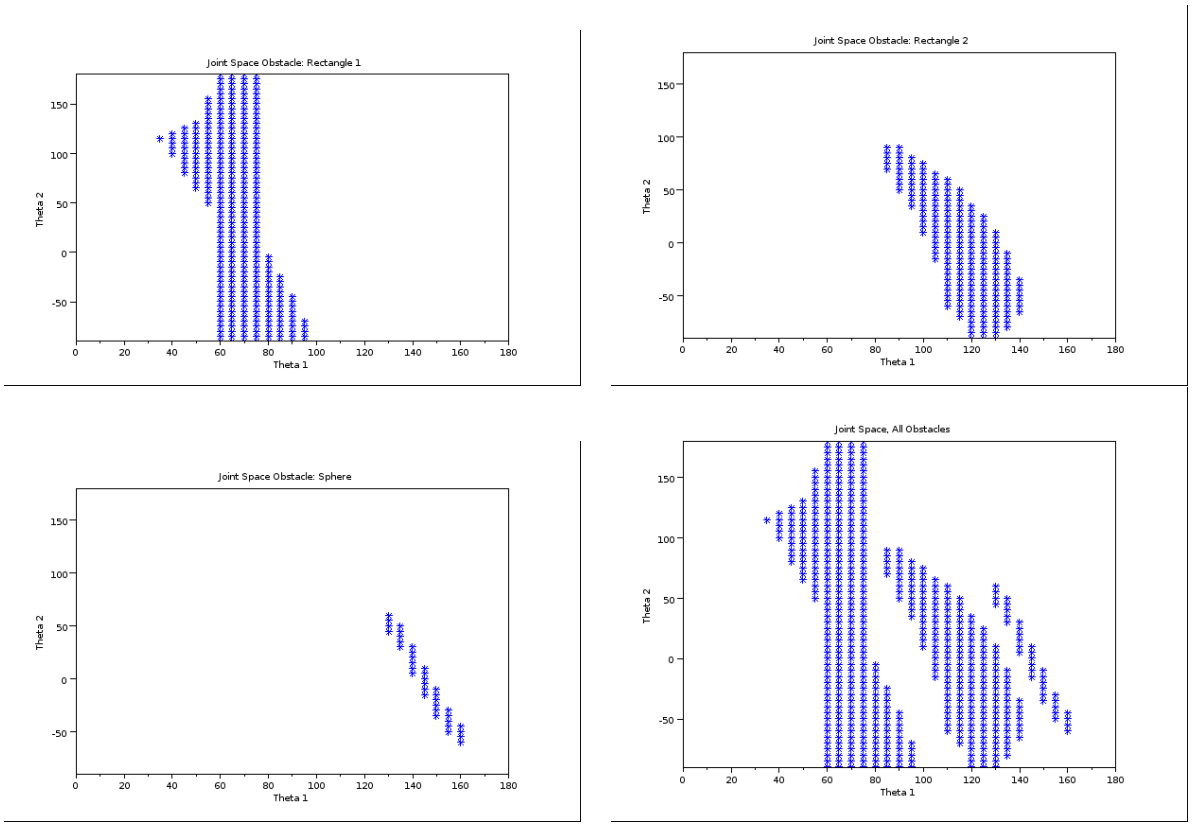

Figure 8.6: Computational results of 2-link planar arm configuration space with up to three obstacles as shown in Figure 8.4. Configuration space is plotted only within the joint limits.

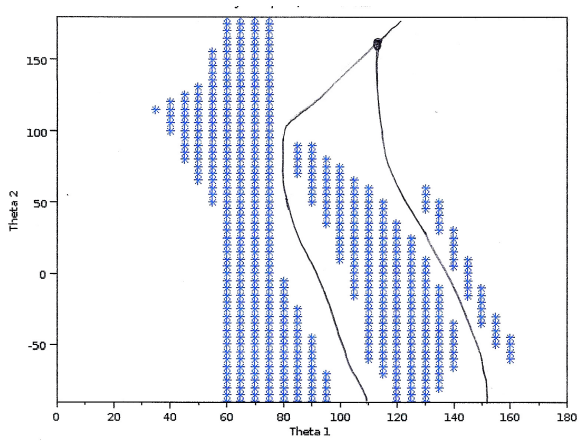

Figure 8.7: Voronoi diagram for the obstacles of Figure 8.4.

`checksph(v,S)` where `S = [center_X, center_Y, radius]`. For `S = [-4.2, 3, 0.333]`, we get the configuration space obstacle shown in Figure 8.6, lower left. Finally, we can consider all obstacles simultaneously and get the set of obstacles shown in Figure 8.6, lower right.

We can see from Figure 8.6, lower right, that there can be no path from the free region approximately defined by $\theta_1 < 50°$ and the other region approximately defined by $\theta_1 > 80°$ which does not violate the R1-obstacle or the joint limits. However this fact is not obvious from looking at the workspace and the obstacles (Figure 8.4). Rectangle 1 blocks all motion between these two regions because the elbow (always 4 units from the origin) cannot avoid passing through it.

8.4 Static Planning for Obstacle Avoidance

In this section, we assume that the forbidden region of the configuration space is known. Even so, it is still not trivial to find a pathway through the obstacles. We need a method to represent the possible pathways

8.4.1 Voronoi Diagrams and Graph Search

An important tool for understanding the free region is the Voronoi diagram. To construct the Voronoi diagram, we identify all points in the free region which are equidistant between two obtacles. In 2D space, these points lie along a line. Such lines merge at points which are equidistant from three or more obstacles which we call nodes. Once the Voronoi diagram is computed, we have a graph which identifies potential collision free pathways between regions of the c-space. The Vornoi diagram for the 2D example we have been studying is shown in Figure 8.7.

With a Voronoi diagram in place, the path planning algorithm can be expressed as

1. Find the nearest point on the Voronoi diagram from the start point, and the nearest node to that point.
2. Find the nearest point on the Voronoi diagram from the end point, and the nearest node to that point.
3. Abstract the Voronoi diagram into a graph.
4. Search the graph for the shortest (by some measure) pathway between the start and end nodes.
5. Create a series of joint space trajectories, following the selected segments on the Voronoi diagram between start and end points.

Search

The Voronoi graph has some important properties. First, (unlike transform graphs of Chapter 2) it is an undirected graph because there is no inherent direction between the nodes of the Voronoi diagram. Second, we can compute the length of each edge on the Voronoi graph and use this length as a "weight" on each edge. Thus our graph is a undirected, weighted graph.

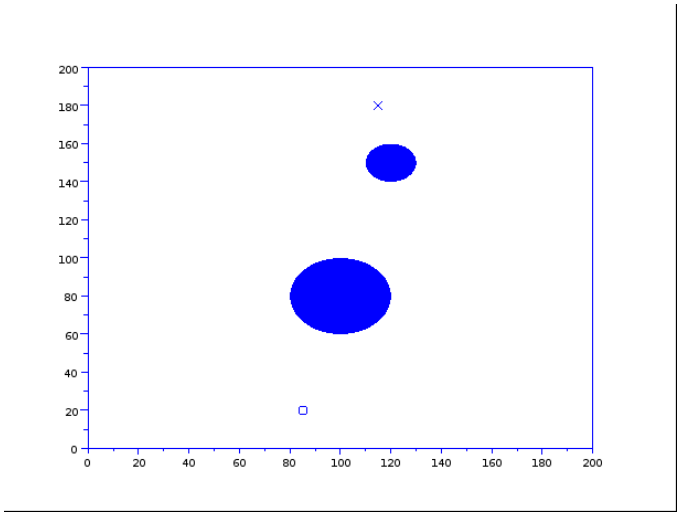

Figure 8.8: 2D configuration space with a start point ('X') a goal point ('O'), and two basic obstacles.

Once a graph has been constructed based on the Voronoi diagram, a route must be found by searching through the graph. There are many published algorithms for searching undirected weighted graphs for the "best" route from one node to another known as "graph search" or "pathfinding" algorithms and many of these have been around since the one developed by famous computer scientist Edsger Dijkstra in the 1950's. Most of the research on search algorithms since then is aimed at maximizing the speed or performance of the search as the size of the graph increases.

Among the attributes of a search algorithm that we care about are

- Whether or not it finds the optimum path or just a correct path.
- Whether or not it is guaranteed to find a path if such a path exists.
- If heuristics are used to speed up the search, do the heuristics result in sub-optimal paths being returned?
- The way its computation cost scales with the problem size ("Big-O" notation).

The Voronoi diagram approach converts the planning problem to a graph search problem.

Voronoi Based Methods	
Advantages	Disadvantages
Can use robust graph search algorithms.	Requires full knownledge of c-space
Deterministic	

8.4.2 Potential Fields

If the entire configuration space and forbidden region are known, another approach to planning a path has been developed using an analogy to the motion of particles in energetic fields such as electric fields, the "Potential Field Method". In this approach, we try to simulate a physical situation where a particle has its maximum energy at the start point, and its minimum energy at the end point. Obstacles are represented as regions of very high energy and a "potential field" function on the c-space is created by generating a function combining these two energies. A virtual particle is placed at the start point and at each time step, the algorithm computes a local gradient of the potential function and the particle is moved by an increment in the direction of steepest descent.

Consider the 2D configuration space shown in Figure 8.8. Assume we have identified a start point ('X'), a goal point ('O'), and that there are two obstacles. These two obstacles are rather unusual in that they become perfect circles in configuration space! To construct the potential function, we need two properties. First, the function must have a minimum at the goal point. An example of such a function is a basic parabola:

$$p_g = \left((x - g_x)^2 + (y - g_y)^2\right) m$$

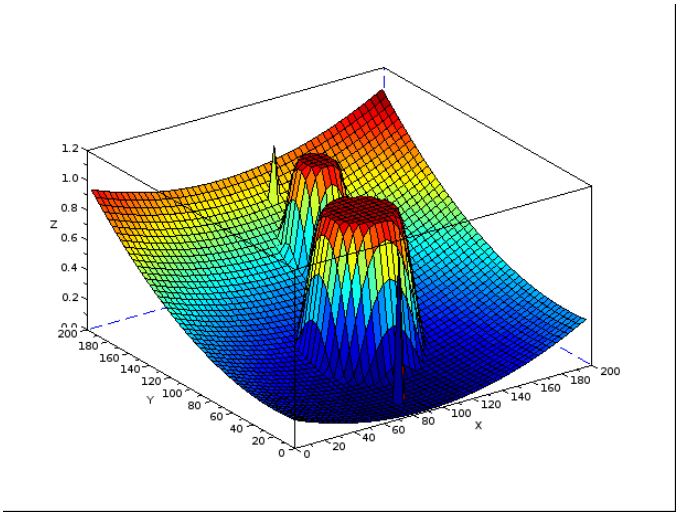

Figure 8.9: 3D plot of the potential function on the 2D configuration space. Start and end poitns are indicated by spikes.

where m is a scaling factor to set the height of the parabola. Second, the potential function must have high values inside the obstacles. Ideally, this high "potential" smoothly descends within the neighborhood of the obstacle. For circular obstacles, such a function is

$$p_o = \begin{cases} 1.0 & r < R \\ 1.0 - 3\frac{r^2}{d^2} - 2\frac{r^3}{d^3} & r \geq R \end{cases}$$

where r is the distance of the current x, y point from the center of the obstacle, R is the radius of the obstacle, and d is the size of the neighborhood of the obstacle. We can combine these functions using the $max()$ operator. For a space in which there is just one obstacle:

$$p(x, y) = max(p_g, p_o)$$

A 3D plot of such a function for the situation shown in Figure 8.8 is given in Figure 8.9.

Once the potential function is constructed, we can use a numerical method to estimate the local gradient of the potential function and to move in the negative gradient direction. We can terminate this process when (if!) we find ourselves in a small neighborhood of the goal point. A very simple algorithm which approximates this is the following pseudocode:

```
i = si;  j = sj;    //  initialize i and j to start point indices
while((i-gi)^2+(j-gj^2) > 2)   // distance to goal
   {
   find smallest value of P(i,j) in all neighboring squares
   i = imin ; j = jmin;
   }
```

This algorithm was run on the situation of Figure 8.8. The resulting pathway is superimposed on a contour plot of the same potential function as Figure 8.9 in Figure 8.10.

The Potential Function approach has converted the planning problem to a gradient descent numerical optimization problem.

Potential Function Method	
Advantages	Disadvantages
Conceptually clear.	Can stick on local minima
Well known gradient descent algorithms,	Requires full C-space to be computed

8.4.3 Sampling Based Methods

The examples of the previous sections rely on at least one major assumption. They assume that the entire configuration space can be computed and represented within reasonable computing resources. However, there

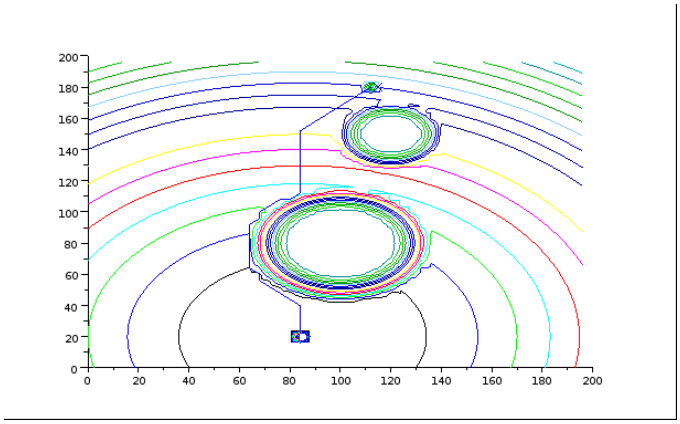

Figure 8.10: A trajectory from start to goal generated by basic gradient descent algorithm.

are many aspects of computing and representing the entire configuration space which are very difficult. The configuration space of a useful manipulator is at least six dimensional. The collision detection process is computationally intensive for a large number of complex-shaped obstacles, and for manipulator links which are realistically modeled. Finally, how do we get the model of the environment in the first place? In many applications at today's frontier, such as service robots in the home, the environment model must be obtained by sensors such as 3D cameras and laser range-finders. This technology itself requires extensive computation. If the environment is changing in any way, or the robot arm is on a mobile base, then the entire C-space must be regenerated in real time. Many of these factors apply to practical cases in which the computational complexity of generating the configuration space is intractable.

A class of algorithms called *sampling based methods*, avoids the need to generate the entire configuration space. These algorithms still assume that the environment is known so that collision detection between arm and environmental obstacles can still be performed, but they do not require that the entire configuration space be computed explicitly.

The sampling strategy of motion planning works as follows:

1. Select a set of sample points throughout the C-space.
2. Compute collision detection to determine which of these points are in free space.
3. Search for paths between the sample points which are clear of obstacles. This will require checking all points in the path between free points.
4. The free space points and the free paths between them create a undirected weighted graph which can be searched as in Section 8.4.1.

A sampling based motion planning strategy in which the sample points are selected randomly by a pseudo-random number generator has been called the *Probabilistic Road Map* method (cites?). Random sampling is not ideal however because it can leave large holes in the space which are unexplored. An alternative is a type of deterministic sequence called a *quasi-random number* sequence based on a type of sequence called the Van der Corput sequence. In one dimension, this sequence is easily obtained by 1) converting the integers to binary numbers, 2) reversing the order of their bits so that the highest order bit becomes the lowest order bit, 3) converting back to an integer. The Van der Corput sequence, and its multi-dimensional variants, have many properties of random sequences, but can guarantee a certain maximum size of the largest gap between points (Figure 8.11).

Sampling Based Methods	
Advantages	Disadvantages
Does not require full c-space	
Can use robust graph search algoritms.	

8.5 Dynamic Constraints

Dubowsky work.

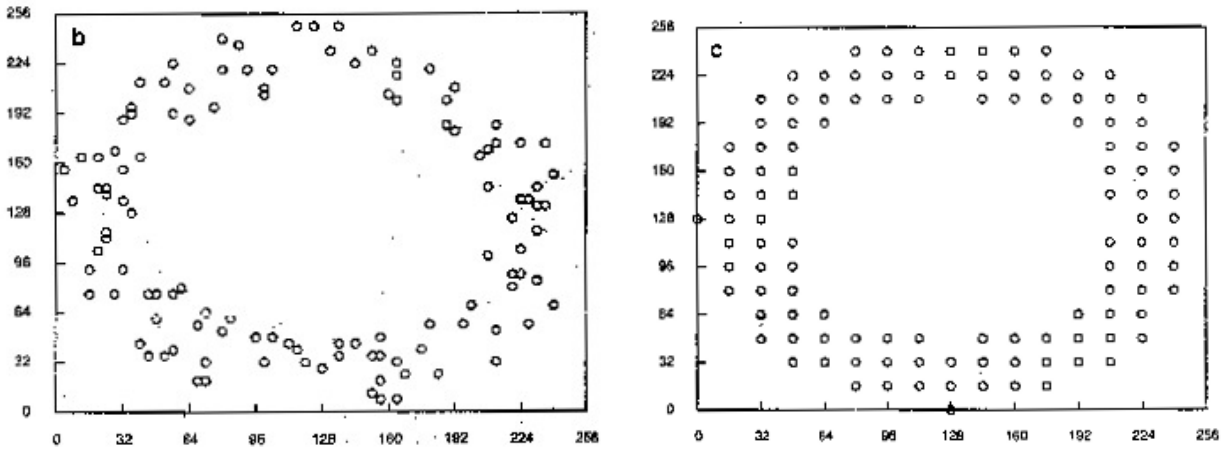

Figure 8.11: Scans of a donut shaped object performed by a pseudo random number generator (left) and a quasi-random scanning method based on the Van der Corpus Sequence. Images from B. Hannaford, "Resolution-First Scanning of Multi-Dimensional Spaces," CVGIP: Graphical Models and Image Processing, vol. 55, pp. 359-369, September 1993.

8.6 Planning With Moving Obstacles ??

(Fiorini ??)

8.7 Summary of Notation

Chapter 9

Mechatronics and Design of Manipulators

9.1 Problem Statement and Learning Objectives

Problem Statement This chapter considers some aspects of design of serial link mechanisms for manipulation.

Learning Objectives Upon completing this Chapter, the reader should be able to

-

9.2 Sensors

9.2.1 Force Sensors

Load Cell A **"Load Cell"** is a structure which supports the load and deflects a known amount in response to applied forces and torques. The deflections are measured to characterize the applied forces and torques.

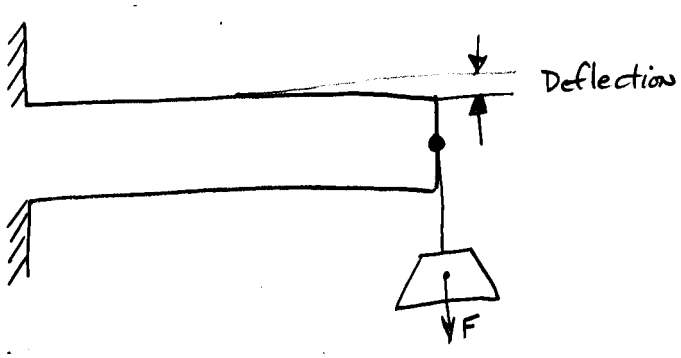

Figure 9.1: Cantilever Beam. When load F is applied to the end of the beam, the beam deflects a known amount.

Example: Cantilever Beam

Stress and Strain

Stress

- Stress (σ): Force per unit area in one dimension.

$$\sigma = \frac{F}{A}$$

  Units: Pascals = $\frac{N}{M^2}$, psi.

- Stress can be refered to as "Compressive" (tending to compress the material)and "Tensile" (tending to elongate it).

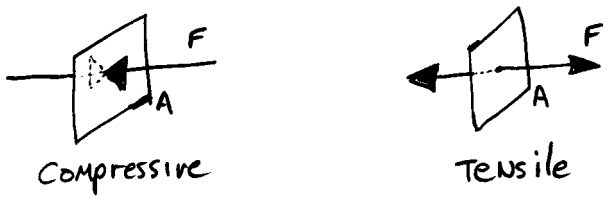

Figure 9.2: Illustrations of Compressive and Tensile stress through a patch of area A.

- Shear stress refers to forces *in* the plane. Shear stress can cause material to tear.

Figure 9.3: Shear stress. Shear stress is due to forces in the plane.

- 3-Dimensions: Full analysis of stress in 3-dimensions is complex an requires notion of *Stress Tensor* — a 3×3 matrix giving the complete state of stress at a given point in the material.

Strain

- Strain, (ϵ), is relative deformation.
- 1 Dimension: Elongation Ratio

$$\epsilon = \frac{\Delta L}{L}$$

- if $\frac{\Delta L}{L} = 10^{-5}$ we say "10 micro-strain".
- Strains of typical metal structures are very small (i.e. micro-strain).
- Strains in biological tissues can be much larger ($\epsilon \approx 1$).
- Advanced: Several Types of Strain

Hooke's Law (Elastic Deformation)

$$\sigma = \mathrm{E}\epsilon$$

where E is Young's Modulus.

- Biological materials rarely obey Hooke's Law.
- Metals obey Hooke's Law very well for stresses below the *elastic limit.* If stress is greater, material permanently deforms.

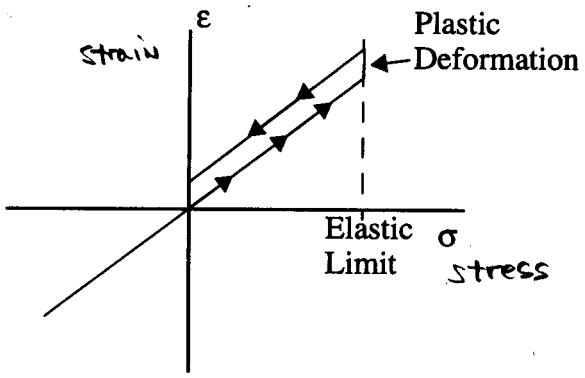

Figure 9.4: Hookean behavior with Elastic Limit. If stress increases beyond Elastic Limit, material is permanently deformed.

Cantilever Beam In this section we will analyze the basic cantalever beam (Figure 9.5) so that we can make it into a force sensor. Once we calculate the strain on the surface as a function of applied force, we can use a strain gauge to measure applied force.

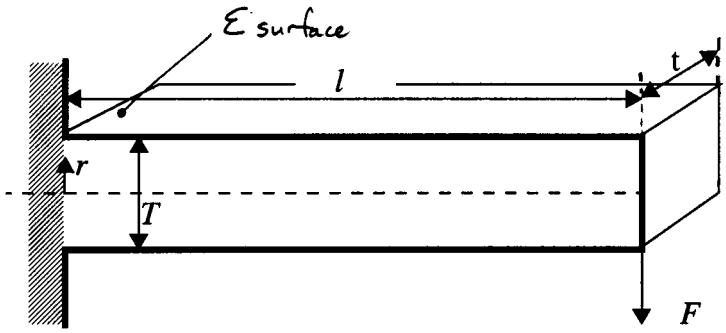

Figure 9.5: Rectangular cantilever beam is a simple load cell structure for basic analysis.

We want to derive $\epsilon_{surface}$ as a function of the applied load, the dimensions of the beam, and the beam material's stiffness (Young's modulus). First, we assume that the beam is at static equilibrium around the centerline along the wall. The moment developed by the beam as it meets the wall is composed of forces produced by the elastic behavior of patches of the surface where the beam meets the wall. Because of the way we apply force in Figure 9.5, we can analyze these inifinitesimal patches as strips in the width direction (Figure 9.6).

We equate the moment developed in the structure around the center line with the moment applied by the external load. As $\Delta r \to 0$, we integrate up the height of the beam and equate that moment to $F \times l$.

$$F \times l = \int_{-\frac{T}{2}}^{\frac{T}{2}} r\sigma(r)tdr$$

where r, t, F, l are defined in the figure, and $\sigma(r)$ is the internal stress where the beam joins the wall. Let us assume that $\sigma(r)$ varies linearly through the beam so that

$$\sigma(r) = \alpha r$$

where α is some positive constant.

Then we have

$$Fl = \alpha t \int_{-\frac{T}{2}}^{\frac{T}{2}} r^2 dr = \frac{\alpha t T^3}{12}$$

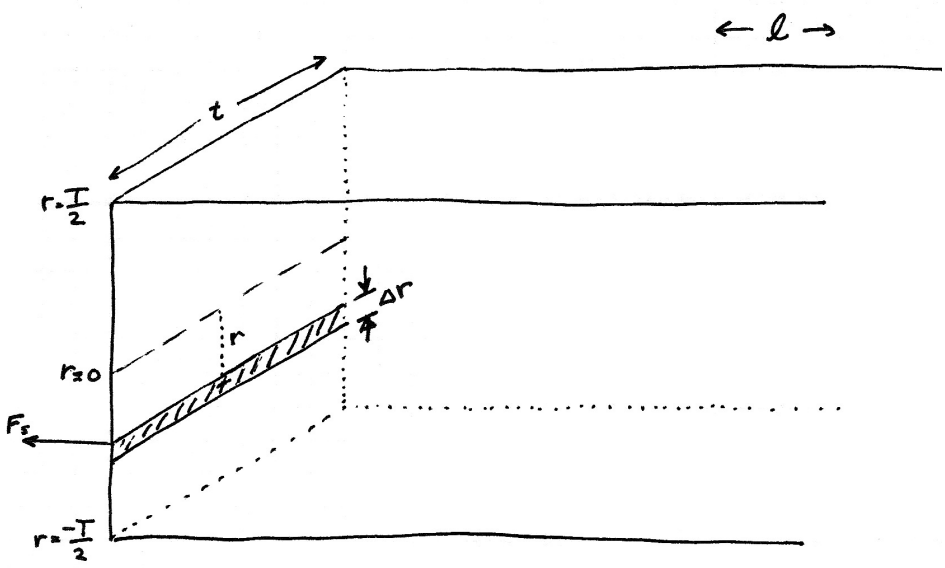

Figure 9.6: Detail of the rectangular cantilever beam showing strips of constant stress. We integrate the moment due to each strip to get the total moment at equilibrium.

Solving for α,

$$\alpha = \frac{12l}{tT^3}F$$

$$\sigma(r) = \frac{12lr}{tT^3}F$$

Finally, we can evaluate $\sigma(r)$ at the surface and use Young's modulus to convert stress to strain:

$$\sigma(\frac{T}{2}) = \frac{12l\frac{T}{2}}{tT^3}F$$

$$= \frac{6l}{tT^2}F$$

$$\epsilon_{surface} = \frac{6l}{\mathrm{E}tT^2}F$$

Strain Gages (see `http://www.measurementsgroup.com/guide/index.htm`)

A strain gage is a device which transduces strain on a surface. There are two types in common use, resistive metal foil, and semiconductor. Both transduce strain by taking advantage of the variation of electrical resistance with strain.

Metal Foil Strain Gages Metal foil gages are bonded to the surface and their resistance changes in proportion to the surface strain.

In simplified form,

$$R = R_0(1 + \epsilon g)$$

where $g = \frac{\Delta R}{R_0 \epsilon}$ is called the "gage factor". For metal foil gages, $g \approx 3$.

Semiconductor strain gages These are small chips of silicon with a single region of doping to create a resistor. The chip is bonded to the load cell and its resistance varies with strain. With a semiconductor strain gage, the designer can expect signficantly higher gage factor of around $g \approx 150$.

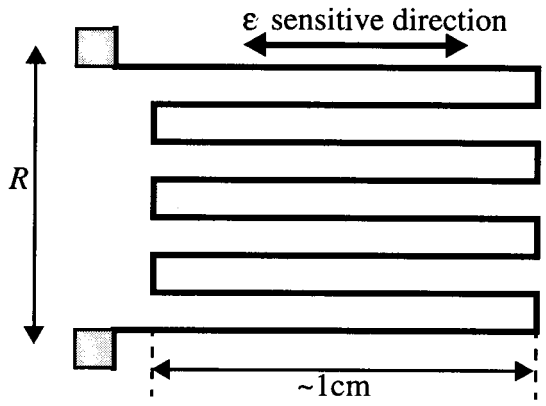

Figure 9.7: Diagram of a metal foil strain gage. Conductor in the shape shown is attached to surface. As surface deforms, conductive pattern changes length which changes resistance between contact pads (left).

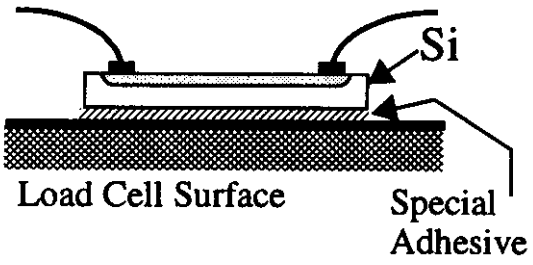

Figure 9.8: Diagram of a semiconductor strain gage.

Properties of Strain Gages

1. Very linear. 1% is achievable due to Hooke's law. Elastic limit must be avoided with a safety margin.
2. Wide dynamic range. Example: Force/Torque sensor designed by JPL for Space Shuttle RMS robot arm design range: 1N to 4×10^5N. 112db.
3. Temperature Sensitivity. Both types are highly sensitive to temperature.
4. Interface between gage and structure requires care due to different coefficients of thermal expansion between gage and structure.
5. Practicalities. Foil gages are robust and cheap. Semiconductor gages are delicate and expensive. Foil gages are fixed with an adhesive which usually requires curing in an oven. Semiconductor gages require an elaborate process for attachment which must be done by a specialist.

Temperature Sensitivity Careful thermal analysis is important for accurate force sensing with strain gages. Two effects account for the temperature sensitivity of metal foil strain gages:

- Thermal Coefficient of Resistance of gage material.
- Difference in thermal coefficient of expansion of gage and load cell structure.

The first causes resistance to change only as a function of temperature and not of strain. The second causes strains in the gage as a function of temperature only.

The temperature dependence of the gage resistance can be described by:

$$r = \frac{\frac{\Delta R}{R_0}}{\Delta T} = \beta_g + g\left(\frac{1+K_t}{1+\nu_0 K_t}\right)(\alpha_s - \alpha_g)$$

Where

β_g = thermal coefficient of resistance of the gage material.

K_t = transverse sensitivity of the gage: the gage factor for strains orthogonal to the sensitive direction (extremely small for most gages and will be neglected).

ν_0 = Poisson's ratio (typically 0.3)

α_s, α_g = coefficients of thermal expansion of substrate and gage respectively.

The first step to reduce temperature sensitivity is to make sure the thermal expansion coefficients of the gage (α_g) and substrate (α_s) are as close as possible.

We can then relate resistance to strain and temperature through

$$R = R_0(1+g\epsilon)(1+r\Delta T)$$

The second step to compensating for the remaining temperature sensitivity is to make a differential measurement of two gages which have the same temperature but opposite strains. In the case of a cantilever beam, if we assume that the beam is at a uniform temperature, this can be arranged by putting gages on either side of the beam. By symmetry, $\epsilon_1 = -\epsilon_2$.

Dual Gage beam By symmetry, $\epsilon_1 = -\epsilon_2$.

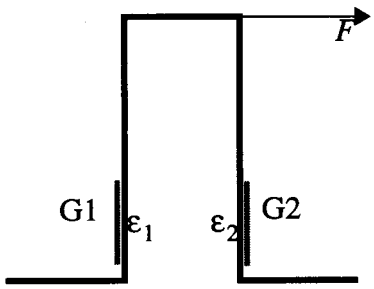

Figure 9.9: Cantilever beam load cell with gages on either side. Strains ϵ_1 and ϵ_2 will be equal and opposite. If temperature is same on both sides of beam, we can correct for temperature sensitivity.

Wheatstone Bridge Subtraction of the two strain signals is usually accomplished right in the load cell itself using a Whetstone Bridge Circuit.

A very nice javascript animation illustrating this principle is available at `http://www.rdpe.com/us/hiw-sglc.htm`. Be sure to drag the beam tip with your mouse!

Analysis of the bridge circuit yields:

$$\frac{\Delta V}{V_{ex}} = \frac{R_4}{R_3+R_4} - \frac{R_2}{R_1+R_2} = \frac{R_4R_1 - R_2R_3}{(R_1+R_2)(R_3+R_4)}$$

In this example, we place the two strain gages into the bottom legs of the bridge, (R_2, R_4). The other two legs of the bridge are non-strain-sensitive resistors (but still temperature sensitive).

We define $\hat{R} = R_0(1+r\Delta T)$.

$$R_1, R_3 = \hat{R}$$

$$R_2 = \hat{R} + (1+r\Delta T)gR_0\epsilon_1$$

$$R_4 = \hat{R} + (1+r\Delta T)gR_0\epsilon_2$$

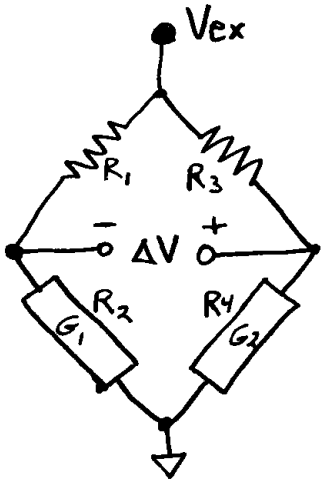

Figure 9.10: Whetstone Bridge circuit used to subtract resistance changes of the two strain gages.

From the load cell design, we have $\epsilon_2 = -\epsilon_1$.
Computing the output voltage we get:

$$\frac{\Delta V}{V_{ex}} = \frac{\hat{R}(1 + r\Delta T)2gR_0\epsilon_2}{4\hat{R}^2 - (1 + r\Delta T)^2 g^2 R_0^2 \epsilon_1^2}$$

Expanding $\hat{R}$ and canceling terms:

$$\frac{\Delta V}{V_{ex}} = \frac{2g\epsilon_2}{4 - g^2\epsilon_1^2}$$

Ignoring the high order terms:

$$\frac{\Delta V}{V_{ex}} = \frac{g\epsilon_2}{2}$$

Temperature variation is eliminated! Non-linear term contributes insignificant errors because ϵ is very small.

Multi-Axis Sensing In robotics and surgery it is rarely of interest to measure a single force. In general we want to measure the 6 components of force and torque,

F_X
F_Y
F_Z
τ_X
τ_Y
τ_Z

We want to characterize these force/torque components at some interface between two objects. Examples of these interfaces: robot wrist — robot hand, surgical tool handle — surgical tool body, etc. So that the sensor does not distort the forces and torques present, it should be as rigid as possible. Therefore the two objects connected by the sensor should normally be rigidly connected.

Design of load cells for this measurement takes substantial effort and is beyond the scope of this course. However it is useful to consider two example designs.

"Maltese Cross" Sensor

Variations of this design have been produced in a number of laboratories and are available commercially (Fig. 9.11). In this design, the spokes of a wheel are instrumented with gages and calibrated to measure forces and torques applied to the hub relative to the rim.

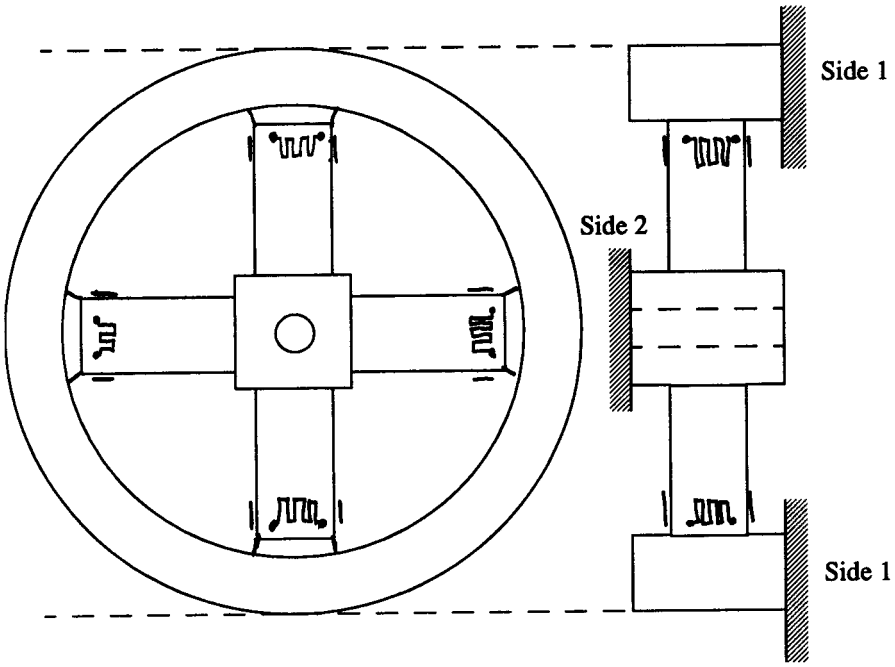

Figure 9.11: "Maltese Cross" force-torque sensor. Forces and torques applied to the surface labeled 'side 1' cause strains in the spokes which are picked up by 8 attached gages.

Four gages are applied to each beam for a total of 8 differential measurements.
A 6x8 calibration matrix C is computed to relate the strain measurements to forces/torques

$$\begin{bmatrix} F_x \\ F_Y \\ F_Z \\ \tau_X \\ \tau_Y \\ \tau_Z \end{bmatrix} = \begin{bmatrix} \qquad C \qquad \end{bmatrix}_{6\times 8} \begin{bmatrix} \epsilon \end{bmatrix}_{8\times 1}$$

In practice, manufacturing tolerances are not adequate to compute C from the load cell design with sufficient accuracy so it must be obtained from measurements of strain outputs as a function of applied forces and torques for each device using regression analysis.

Parallel-Plate Structure

(See T. Yoshikawa and T. Miyazaki, "A six-axis force sensor with three dimensional cross shape structure," Proc. Intl. Conference on Robotics and Automation, pp. 249-254, 1989.)

An alternative to the bending beam load cell is the parallel plate structure (also known as a flexure). In this case, two thin beams are arranged in parallel (Figure 9.12).

Analysis At the point of maximum strain concentration, labeled ϵ_{max}, the strain is

$$\epsilon_{max} = \frac{3lF}{\mathrm{E}tT^2}$$

where t is the width of the parallel plate structure, and E is Young's Modulus for the material.

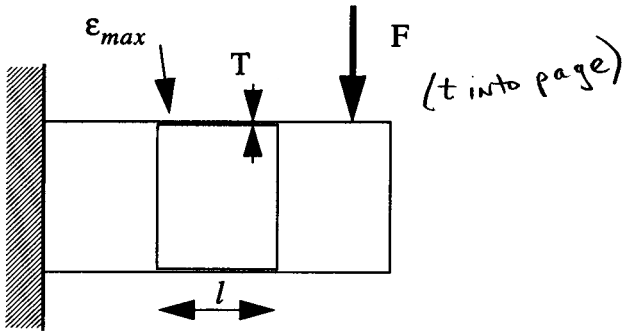

Figure 9.12: Parallel plate flexure load cell for a single axis.

Overload Protection We saw that above a certain critical strain, the "elastic limit," a material will permanently (plastically) deform. This has two important consequences. First, if the material deforms plastically, the zero reading of the load cell will have to be recalibrated. Second, the load cell will be damaged and will eventually break or suffer reduced life.

In most realistic force sensing applications, it is difficult or impossible to predict the maximum forces likely to be experienced by the sensor. This is because collisions between the sensor and the environment often occur, either deliberately or as a result of errors. The transient forces which occur in these collisions (especially with hard objects) are hard to control and may exceed the design force limit for the sensing beam.

To prevent damage from these types of events, overload protection is sometimes designed into force/torque sensors. An overload protection device must allow safe deflection of the load cell in all active directions without disturbance forces, but must provide greatly increased stiffness and strength for deflections above the safe operating point (which may be a factor of two or more *below* the elastic limit.)

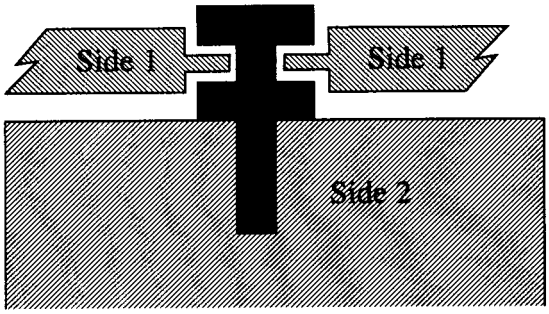

Figure 9.13: Overload protection scheme for a force/torque sensor. a high-strength structural element connects the two sides when deflection exceeds the size of its gap to protect the sensing structure from excessive strain.

In the example illustrated in Figure 9.13, a pin of strong material (i.e. steel in an aluminum load cell design) is affixed between the two sides of the load cell so that there is a calibrated gap between the two sides. When the strain reaches the maximum safe operating point, the two sides touch and the stiffness of the overall loadcell is greatly increased. Once the two sides come into contact through the pin, the amount of force required to reach the elastic limit is greatly increased. Any further deflection is thus reduced or eliminated.

9.3 Actuators

9.3.1 DC Motors

Introduction

This is a quick overview of DC motors as applied to robot manipulators and haptic devices. Although DC motors are a very mature technology, the companies which produce them are mainly focused on a non-robotics market. Many commercial applications are aimed at high velocities and moderate torques. Robots often require low velocities and high torques.

The most common way to match available motors to robot needs is to use gears. A gearbox with ratio n will reduce motor velocity by n^{-1} and increase torque by n. Unfortunately, some undesirable properties, such as the effective inertia of the motor and any friction present in the motor are increased by n^2. For high performance robotics, including force controlled robots, teleoperators, and haptic interfaces, these negative effects of gears are significant and so n must be minimized or made equal to 1.

When $n = 1$ in a robotic application, the motor "sees" a load characterized by velocities near zero and "high" torques. When torques are adequate for the application motors tend to get hot. The designer can select among different motors, but there is a trade-off which cannot be avoided between heat capacity and the mass of the motor. Furthermore, large currents can be required which in turn require large power supplies and thick wires. Many of the standard techniques for selecting motors (such as those discussed in motor catalogs) can be too conservative and result in too much weight for your robot.

This section explores how to optimize the selection of a motor for robotic requirements and how to better understand the thermal behavior of motors.

Basic Theory

DC motors are one of the most common actuators for robotics. Althought there are many important electric motor technologies for robot manipulators, here we consider the most basic, brushed DC motors.

Two basic laws describe the operation of DC motor in terms of the pair of electrical input variables, V and I, and mechanical output variables, torque, τ and angular velocity, ω.

$$\tau = K_m \times I \tag{9.1}$$

$$V = IR + K_m\omega + L\dot{I} \tag{9.2}$$

where R is the resistance of the armature windings, K_m is the motor constant[1] and L is the motor inductance. We will consider constant currents (i.e. $\dot{I} = 0$) and ignore the motor inductance.

To illustrate the use of these equations, let us pose some problems:

Stall Torque

A Maxon RE-25/118752 DC motor[2] has a motor constant, K_m of .0234 Nm/A, Coil resistance, R of 2.32 Ω, and winding inductance, I, of 0.24 mH. In a haptic application, assume $\omega = 0$ (this is referred to as "stall"). Assume $\frac{dI}{dt} = 0$. Find the current and voltage required to generate a torque of 0.05 Nm.

Solution: Using Equation (9.1),

$$0.05Nm = 0.0234Nm/A \times I$$

$$I = \frac{0.05}{0.0234} = 2.14A$$

Using Equation 9.2 for $\omega = 0$, we have

$$V = IR$$

In other words, for $\omega = 0$, the motor acts like a resistor.

$$V = 2.14A \times 2.32\Omega + K_M \times 0 + L \times 0$$

$$V = 4.96V$$

[1] Note that when MKS units are used there is only one such constant. When other unit systems are used, two different constants must be used in the two laws.

[2] `http://www.maxonmotorusa.com`

Figure 9.14: Maxon brushed DC Motor with gearhead and optical encoder (http://www.maxonmotorusa.com).

Free Running / Viscous Load

Using the same motor as in problem 9.3.1 find the speed the motor will run with no load ($\tau = 0$) when 5V is applied. What will be the current and power dissipation? Assume $\frac{dI}{dt} = 0$ and that there is no friction in the motor.

Solution: Using Equation (9.2),

$$5.0V = I \times 2.32\Omega + 0.0234Vsec \times \omega$$

Using Equation (9.1)

$$I = 0(!)$$

Solving:

$$\omega = 213.7rad/sec = 2041rpm$$

One way to think about this is that the term $K_m \times \omega$ is a voltage (called "back EMF") generated internally by the motor which opposes the applied voltage. At no-load, this voltage exactly cancels the applied voltage and the current is zero.

Since the current is zero, the power is also zero! This is not a perpetual motion machine, because we have assumed there is no friction. Electrical Power in = mechanical power out:

$$V \times I = \tau \times \omega = 0$$

Now, let us consider frictional load to the motor. The load will be viscous friction with coefficient $B = 1.2 \times 10^{-4} nMsec/rad$. Physically, this load could be due to 1) the motor's internal bearing friction and air friction, 2) the friction of the transmission mechanism such as gears, belt drives, cable drives, or 3) the external load (such as a hole being drilled, drink being blended, etc). Find ω, the current, and the power dissipation when the viscous load is applied.

Solution: The viscous friction load forms another equation which much be solved simultaneously with the motor equations:

$$\tau = B \times \omega$$

Bringing in Equations (9.2) and (9.1),

$$5.0V = I \times 2.32\Omega + .0234 \times \omega$$

$$\tau = 0.0234 \times I$$
$$\tau = 1.2 \times 10^{-4} \times \omega$$
$$I = \frac{1.2 \times 10^{-4}}{.0234}\omega \quad = 5.128 \times 10^{-3}\omega$$
$$5.0 = (5.128 \times 10^{-3} + .0234)\omega$$
$$\omega = 175.2 rad/sec = 1674 rpm, \quad I = 0.898A$$
$$P = 5.0V \times 0.898A = 4.49 Watts$$

We can also solve this graphically:

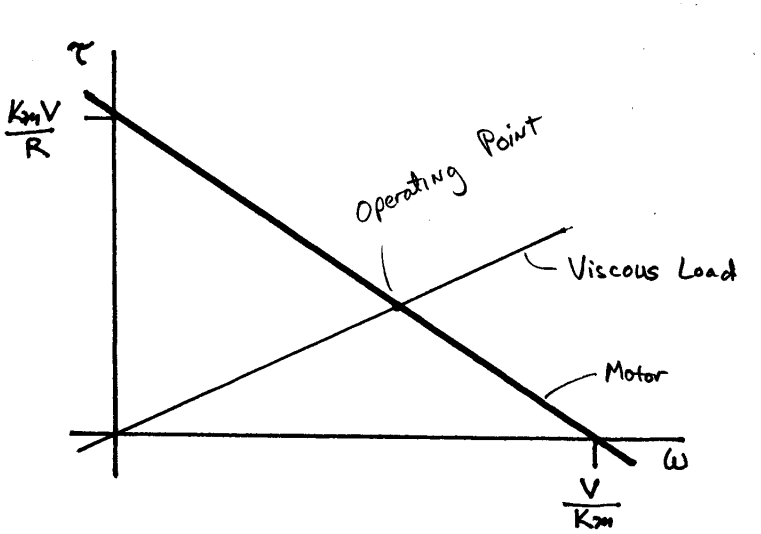

Power Supply / Winding Selection

A DC motor is rated at 150 Watts continuous power (this means that the elecrical power cannot exceed 150 Watts in the steady state or the coils will burn out). The manufacturer has a variety of 150 Watt motors available, each with various values of stall torque (τ when $\omega = 0$), coil resistance, motor constant, etc, which are listed in a table. The manufacturer obtains all these different motors by winding the coils with different diameter wire. For small wire, the number of turns which fit into the space is greater (greater K_m), but the resistance becomes higher. We want to use a 30Volt power supply. **Problem:** Find the value of R which will give us 150 Watt power dissipation at 30V when $\omega = 0$. This way we can get the most stall current and therefore the most stall torque. Find the current I_{max} and torque τ_{max} at 30V.

Solution: We want our 30V power supply to give the maximum permissable power in this case so:

$$P = \frac{E^2}{R}$$
$$150 = \frac{900}{R}$$
$$R = 6\Omega$$

Now we look through the catalog table for the motor who's coil resistance is closest to 6Ω. In this case, the stall current is

$$I = \frac{30}{6} = 5A$$

The torque constant for this motor (made up 150W/ 6Ω motor) is 0.1Nm/A.

$$\tau_{max} = 0.1 \times 5A = 0.5Nm$$

Maximizing Power through duty cycle

In advanced applications like haptic interfaces, using the motor's continuous power output can be too conservative. This is because in haptics the maximum torque output is rarely needed 100% of the time. If we need higher stall torque, we might have to go up to a motor with a higher wattage rating. The problem is these can be very heavy and bulky. In many haptics applications, this high power capacity is wasted 90% of the time. If we can guarantee that the peak torque output (i.e. peak current) will be present for less than 100% of the time, we can calculate a higher corresponding electrical power. If this power were applied to the motor continuously, it would burn out, but transiently it will cool off between peaks. As a rule of thumb, if we can guarantee an *average* torque value is no more than 10% of the peak, then we can drive the motor at a peak power level 10× its continuous rating. The percentage of time that peak current is applied is called the "duty cycle" of the application.

So if the motor (and its resistance) is fixed, we need to use a higher voltage power supply to get a greater power:

$$\frac{V^2}{R} = 150 \times 10$$

$$R = 6\Omega$$

$$V = 95V$$

$$I_{max} = \frac{95V}{6\Omega} = 15.8A$$

$$\tau_{max} = 0.1 \times 15.8A = 1.58Nm$$

To summarize, by ASSUMING that the duty cycle is 10% or less, we can increase the supply voltage from 30V to 95V and get a peak torque which is 3.16 times higher. Since I_{max} increased from 5A to 15.8A, our power supply's peak output goes from $30V \times 5A = 150W$ to $95V \times 15.8A = 1500W$. So we tripled peak force output but our power supply cost (proportional to Watts) went up by a factor of 10!

We must be very careful when using this strategy because if we are wrong about the average duty cycle, we can burn an expensive motor.

The same duty cycle trick can be used to reduce the power supply size and cost. Capacitors can be used to provide the peak current output required for haptic peaks. Then the power supply rating can be reduced back to match the motor's steady state rating.

Thermal Analysis

In many applications, the ultimate limitation on DC motor performance is dissipation of heat coming from resistive losses in the motor coils. When the temperature gets too high (typically above 180°F) the insulation on the coil wires melts or burns and the coil shorts out. The block diagram illustrates the heat generation process from the input of electrical current, to heat generation in the motor winding (always equal to I^2R), to convective heat transfer out of the motor coils and into the environment.

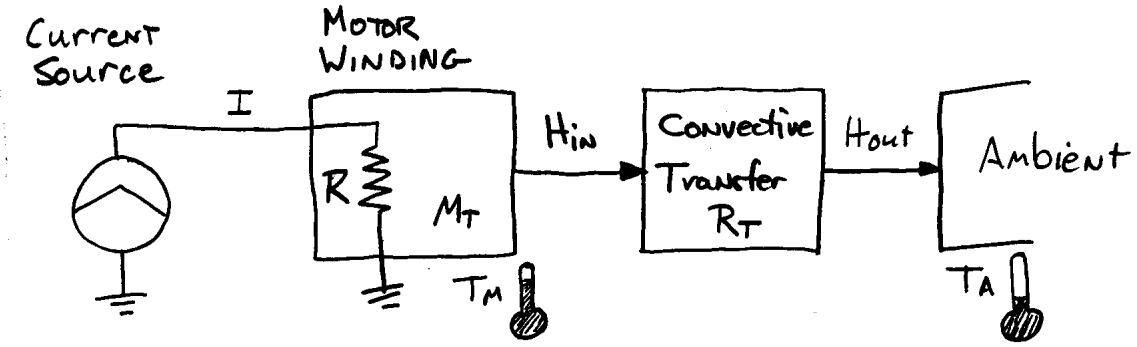

Let us analyze this system:

In robotics we are most likely starting with some algorithm (usually a control law) which would like to command a certain torque to the motor. For a given motor, we need a current

$$I = \frac{\tau}{K_m}$$

Heat produced in the coils is always I^2R regardless of τ and ω.

$$H_{in} = P = I^2R$$

We can derive the steady state temperature as a function of H_{in}:

$$T_{in} = PR_T$$

where R_T is the thermal resistance of the motor (often listed in the catalog units: $^\circ/Watt$).

Heat flows through a thermal resistance in a manner analogous to current flowing through an electrical resistance. Temperature plays the role of voltage. Thus

$$H_{out} = \frac{T_M - T_A}{R_T}$$

where T_M is the motor internal temperature, T_A is the ambient temperature.

In addition to thermal resistance, objects have a "thermal mass" which determines how much thermal energy they can store, and also how fast temperature builds up when there is a net flow of heat into the object:

$$T_M = \frac{1}{M_T}\int_0^t (H_{in} - H_{out})dt + T_A$$

where M_T is the thermal mass, and we assume $T_M = T_A$ at $t = 0$.

Substituting:

$$T_M = \frac{1}{M_T}\int_0^t (P - \frac{T_M - T_A}{R_T})dt + T_A$$

Let $T = T_M - T_A$

$$T = \frac{1}{M_T}\int_0^t (P - \frac{T}{R_T})dt$$

Let $\hat{T} = PR_T = I^2RR_T$. This is the equilibrium temperature if the current were held constant.

$$T = \frac{1}{R_T M_T}\int_0^t (\hat{T} - T)dt$$

Taking the LaPlace Transform:

$$T(s) = \frac{1}{sR_T M_T}(\hat{T}(s) - T(s))$$

$$\frac{T(s)}{\hat{T}(s)} = \frac{1}{(1 + sR_T M_T)}$$

Or equivalently:

$$\frac{T(s)}{I^2(s)} = \frac{RR_T}{(1 + sR_T M_T)}$$

This transfer function describes a thermal system whos input is current squared (proportional to power) and whos output is motor temperature. This system is first order and the time constant is $R_T R_M$. Thus our model of motor winding temperature becomes:

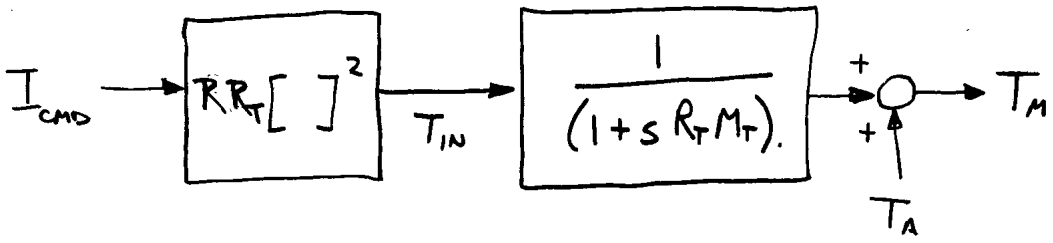

Future Material:

[Use of this model to estimate motor winding temperature on-line. Use of winding temperature sensor to adapt model parameters.]

[Real time control of motor current based on measured or estimated winding temperature.]

[Brushed vs. Brushless Motors]

Chapter 10

Manipulability

10.1 Problem Statement and Learning Objectives

Enter Problem Statement and Objectives here.

10.2 Kinematic Manipulability

10.2.1 Decomposition of Jacobian Matrix

Review of geometric interpretation of matrix multiplication
Mapping circles to elipses
SVD (refer to apdx)
Manipulability Elipsoid

10.2.2 Generalized Jacobian - Peudoinverse

(Do we need this for Manip? How about move to next chapter?)

10.2.3 Manpulability Measures and Indices

10.2.4 Examples

10.3 Dynamic Manipulability

10.3.1 Dynamic Manipulability Elipsoid

10.3.2 Examples

10.4 Design of Manipulators for Workspaces

10.4.1 Performance Indices over a Path

10.4.2 Performance Indices over a Workspace

10.4.3 Optimization

10.5 Summary of Notation

Chapter 11

Kinematic Redundancy

11.1 Problem Statement and Learning Objectives

11.2 The Pseudoinverse

The basic problem is solving the velocity equation

$$\dot{x} = J\dot{\theta} \tag{11.1}$$

when the diminsions of $\dot{x}$ and $\dot{\theta}$ are not the same. Let us call the dimensionality of the task space n and the number of joints, m. The Jacobian matrix, J, has dimensions $n \times m$ and we cannot invert a non-square matrix. Let's consider three cases:

1. $m > n$ (# joints > # task freedoms)
   $\dot{\theta}$ is "bigger" than $\dot{x}$. There are thus many possible solutions (many joint velocities for the same end-effector velocity).

2. $m = n$

   If $\text{rank}(J) = m = n$, $\dot{\theta} = J^{-1}\dot{x}$.

3. $m < n$
   $\dot{\theta}$ is "smaller" than $\dot{x}$. There is no solution. However, we might be interested in a joint velocity vector which is closest to a solution.

Moore-Penrose Pseudo-Inverse Let's look at how to invert a non-square matrix by first looking at some properties of a square inverse:

If we choose a square matrix A, which is full rank, and compute its inverse: $X = A^{-1}$, then we have

$$XA = I \tag{11.2}$$

There are also four similar properties (Penrose conditions) which are true:

$$AXA = A \tag{11.3}$$

$$XAX = X \tag{11.4}$$

$$(AX)^T = AX \tag{11.5}$$

$$(XA)^T = XA \tag{11.6}$$

When A is non-square, we cannot satisfy 11.2, but various schemes can give us a matrix which satisfies one or more of 11.3 — 11.6.

The matrix A^+, called the Moore-Penrose inverse or also the *pseudoinverse*, satisfies 11.3 — 11.6. In addition, it satisfies two more properties:

$$(A^+)^+ = A \tag{11.7}$$

$$(A^T)^+ = (A^+)^T \tag{11.8}$$

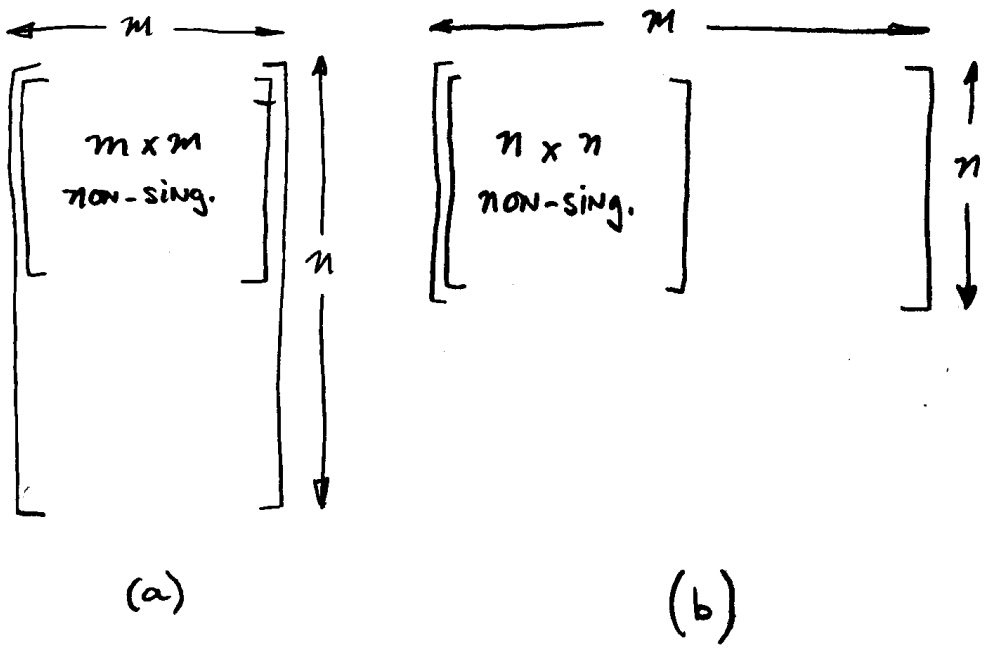

Computation of A^+ The definition of A^+ depends on the structure of $A \epsilon \mathcal{R}^{n \times m}$ as follows:

1. if rank$(A) = m$
   $A^+ = A^T(AA^T)^{-1}$
   (see illustration (a)).
2. if rank$(A) = n$
   $A^+ = (AA^T)^{-1}A^T$
   (see illustration (b)).
3. otherwise, if the SVD of A is

   $$A = U\Sigma V^T$$

   and rank$(A) = r$, then

   $$A^+ = V\Sigma^+ U^T$$

   where

$$\Sigma^+ = \left[\begin{array}{cccc|c} \sigma_1^{-1} & 0 & 0 & 0 & 0 \\ 0 & \sigma_2^{-1} & 0 & 0 & 0 \\ 0 & 0 & \dots & 0 & 0 \\ 0 & 0 & 0 & \sigma_r^{-1} & 0 \\ \hline 0 & 0 & 0 & 0 & 0 \end{array}\right]$$

Solving Equations Let's apply this to solve equations. We will start with

$$y = As \tag{11.9}$$

where $y \epsilon \mathcal{R}^n$ and $s \epsilon \mathcal{R}^m$. Let's consider the case, $m > n$. It turns out, the pseudo inverse allows us to write:

$$s = A^+ y + (I - A^+ A)z \tag{11.10}$$

where z is an arbitrary vector which selects among multiple solutions. One possible value for z is 0 which gives.

$$s_0 = A^+ y$$

It turns out s_0 has the smallest Euclidian norm of any solution. This is true because the two terms:

$$A^+ y \quad \text{and} \quad (I - A^+ A)z$$

are orthogonal to each other.

Exercise: Recall that for any orthogonal vectors q, v, $q^T v = 0$. Use this to show the terms above are orthogonal.

11.3 Accomplishing Additional Tasks (Task Decomposition)

Solving inverse velocity problem I: Additional Task Now we can return to the problem

$$\dot{x} = J\dot{\theta}$$

for the kinematically redundant manipulator. Using eqn. 11.10, we have

$$\dot{\theta} = J^+ \dot{x} + (I - J^+ J)\dot{z} \tag{11.11}$$

where $\dot{z}$ is an arbitrary vector to select among solutions.

The columns of $(I - J^+ J)$ define the *null space* of J, i.e. a subspace of the joint space in which joint motion causes zero end effector velocity.

Definition: The null space of a matrix A, is the set of all non-zero x such that

$$Ax = 0$$

Let's apply this to eqn 11.11:

Let $\hat{\dot{\theta}} = (I - J^+ J)\dot{z}$. Then

$$\begin{aligned} \hat{\dot{x}} &= J\hat{\dot{\theta}} \\ &= J(I - J^+ J)\dot{z} \\ &= (J - JJ^+ J)\dot{z} \\ &= 0 \end{aligned}$$

by the first Penrose condition (eqn. 11.3). So the arbitrary vector $\dot{z}$ causes joint motion, but causes no end effector motion. We call this type of motion,

"Self Motion"

"Null-space motion"

The matrix $(I - J^+ J)$ projects $\dot{z}$ into the null-space of the manipulator. The dimensionality of the null-space is

$$\text{rank}(I - J^+ J)$$

which is $m - n$ or the number of joints, minus the number of task DOF.

Example: 7 DOF Robotics Research Arm We will use a specific example to illustrate how the vector $\dot{z}$ can be used to satisfy an additional task.

$m = 7$, $n = 6$

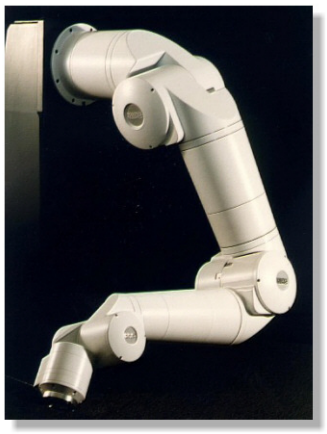

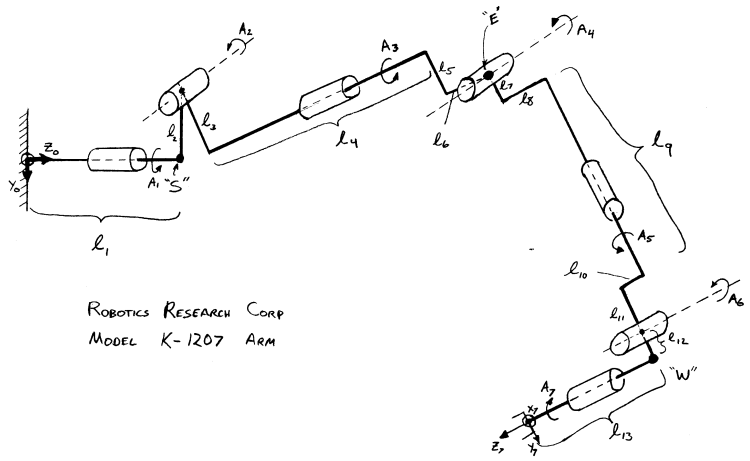

The Robotics Research Arm is a 7-DoF arm (figure). It has one DOF left over after the 6 DOF end effector positioning task is satisfied. The joint offsets $(l_2, l_3, l_5, l_8, 1_{10}, l_{12})$ make the kinematic equations for this arm very complex.

We will assume that the inverse kinematics of the arm have been solved, but we note that the same issue exists with regular inverse kinematics as with the Jacobian inversion. There are more unknown joint variables than equations.

When this arm performs self-motion, it's elbow rotates in a circle around an imaginary line connecting the shoulder and wrist. This is especially easy to see if we draw a simplified version of this manipulator as follows:

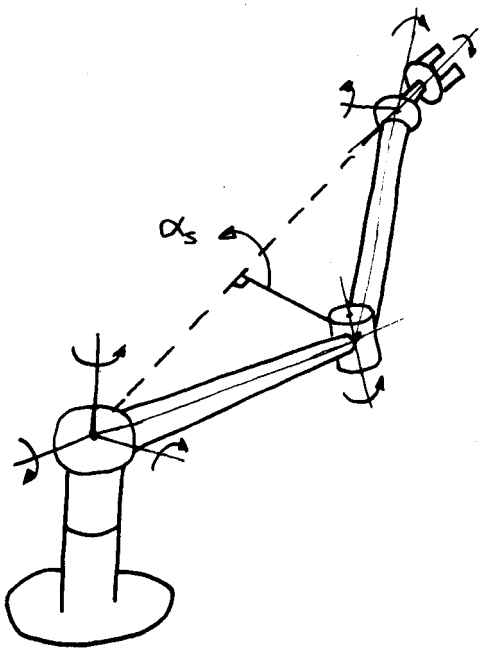

Now these offsets have been removed and we can more easily imagine the elbow being able to swing around in a circle without moving the end effector's position or orientation. We will add one more "DOF" to the *task* by specifing the angle of a ray between this imaginary line and the elbow. We will call this angle α_s.

Without solving for this angle, we will assume that there is some function which specifies

$$\alpha_s = f(\theta)$$

We also assume that this can be differentiated:

$$\dot{\alpha_s} = J_s(\theta)\dot{\theta}$$

where J_s is an $m \times 1$ vector:

$$J_s = \left[\begin{array}{cccc} \frac{\partial \alpha_s}{\partial \theta_1}, & \frac{\partial \alpha_s}{\partial \theta_2}, & \cdots & \frac{\partial \alpha_s}{\partial \theta_m} \end{array} \right]$$

Now we can specify an additional task,

$$\dot{\alpha_s} = \dot{\alpha}_d$$

in addition to the usual

$$\dot{x} = \dot{x}_d$$

Now we can make use of the additional DOF to make use of the extra flexibility of this arm.

First, we recall the solution for the redundant arm (eqn 11.11).

$$\dot{\theta} = J^+ \dot{x} + (I - J^+ J)\dot{z}$$

The basic strategy will be to assume that tasks can be satisfied by some $\dot{z}$ and then solve eqn 11.11 for $\dot{z}$. let

$$\dot{x} = \dot{x}_d, \dot{\alpha_s} = \dot{\alpha}_d$$
$$\dot{\alpha}_d = J_s(J^+ \dot{x}_d + (I - J^+ J)\dot{z})$$
$$\dot{\alpha}_d = J_s J^+ \dot{x}_d + J_s(I - J^+ J)\dot{z}$$

$$\dot{\alpha}_d - J_s J^+ \dot{x}_d = J_s(I - J^+ J)\dot{z}$$

Now let

$$\tilde{J}_s = J_s(I - J^+ J)$$

Using eqn 11.10,

$$\dot{z} = \tilde{J}_s^+(\dot{\alpha}_d - J_s J^+ \dot{x}_d) + (I - \tilde{J}_s^+ \tilde{J}_s)\dot{y}$$

Let's look at what we have. Now, assuming that we have chosen an end-effector task, $\dot{x}$, and an elbow-angle task $\dot{\alpha}_s$, then we now have a way to get $\dot{z}$.

$$(I - \tilde{J}_s^+ \tilde{J}_s)$$

describes the null-space of $\tilde{J}_s$ and the size of this null space tells us how many DOF are left *after* the elbow-angle task is complete. If our subtask (i.e. $\dot{\alpha_s} = \dot{\alpha}_d$) uses up all the remaining freedoms in the arm (which it does in this case), then rank$((I - \tilde{J}_s^+ \tilde{J}_s)) = 0$.

Now we can plug $\dot{z}$ back into the original solution (eqn. 11.11) to get

$$\dot{\theta}_d = J^+ \dot{x}_d + (I - J^+ J)\tilde{J}_s^+(\dot{\alpha}_d - J_s J^+ \dot{x}_d)$$

Yoshikawa (cf page 247 & eqn 7.9) shows that

$$(I - J^+ J)\tilde{J}_s^+ = \tilde{J}_s^+$$

so a simpler form of the solution is:

$$\dot{\theta}_d = J^+ \dot{x}_d + \tilde{J}_s^+(\dot{\alpha}_d - J_s J^+ \dot{x}_d)$$

For the RRC arm, we have introduced an additional task ($\dot{\alpha_s} = \dot{\alpha}_d$) and used up all the mechanism's freedom. Sometimes this may not be clear. In general, we can evaluate

$$(I - \tilde{J}_s^+ \tilde{J}_s)$$

If it is not equal to zero, the manipulator has additional capability to do another task.

11.3.1 Rank M-1

11.3.2 More Redundancy

11.4 Optimization using Redundant Degrees of Freedom

Solving inverse velocity problem II: Optimization of Pose

Introduction As an alternative to using an explicit additional task, we might want to use the kinematic redundancy to optimize some performance measure such as manipulability. Let's call the performance measure:

$$p = V(\theta)$$

Define $\dot{z}_d$ as

$$\dot{z}_d = K_p \bigtriangledown p = K_p \left[\begin{array}{cccc} \frac{\partial p}{\partial \theta_1}, & \frac{\partial p}{\partial \theta_2}, & \cdots & \frac{\partial p}{\partial \theta_m} \end{array} \right]^T$$

Now we are performing a sort-of mechanical gradient ascent and we can see the two approaches are the same. This gives us

$$\dot{\theta}_d = J^+ \dot{x} + (I - J^+ J) K_p \bigtriangledown p \tag{11.12}$$

Improvement of Performance Let's try to show that with $\dot{z}$ defined as above, the null space motion will not not decrease p[1].

$$\frac{dp}{dt} = \frac{\partial p}{\partial \theta_1}\frac{\partial \theta_1}{\partial t} + \frac{\partial p}{\partial \theta_2}\frac{\partial \theta_2}{\partial t} + \cdots + \frac{\partial p}{\partial \theta_m}\frac{\partial \theta_m}{\partial t} \tag{11.13}$$

$$= \left[\begin{array}{cccc} \frac{\partial p}{\partial \theta_1}, & \frac{\partial p}{\partial \theta_2}, & \cdots & \frac{\partial p}{\partial \theta_m} \end{array} \right] \left[\begin{array}{c} \frac{\partial \theta_1}{\partial t} \\ \frac{\partial \theta_2}{\partial t} \\ \cdots \\ \frac{\partial \theta_m}{\partial t} \end{array} \right] \tag{11.14}$$

$$= \bigtriangledown p^T \dot{\theta}$$

Using eqns 11.12 and 11.13,

$$\frac{dp}{dt} = (\bigtriangledown p)^T (J^+ \dot{x} + (I - J^+ J) K_P \bigtriangledown p)$$

$$\dot{p} = (\bigtriangledown p)^T J^+ \dot{x} + (\bigtriangledown p)^T (I - J^+ J) K_P \bigtriangledown p \tag{11.15}$$

The two terms in eqn 11.15 represent the main task of end effector motion and the subsidiary task of kinematic optimization respectively. The first term may *reduce or increase* p because it is not related to the gradient of p. The second term always moves the arm in a way that does not decrease p. Note that these two terms may "fight" each other.

Examples of performance functions

1. Manipulability — Drive the null space motion in such a was that manipulability (of the end effector) is maximized.

2. Distance from singular points. Use a performance measure such as kinematic conditioning index (ratio of smallest to largest singular value) as performance measure.

3. Distance from joint limits. This one is really important for real-world implementations. Define a performance function, P_{JL_n}, which is zero at joint limits and maximized in between.

[1] See *Characterization of Optimal Solutions in Kinematic Resolutions of Redundancy*, by J. Park, W.K. Chung, Y. Youm, IEEE Trans. Robotics and Automation, v 12., no 3, pp. 471-478, June 1996.

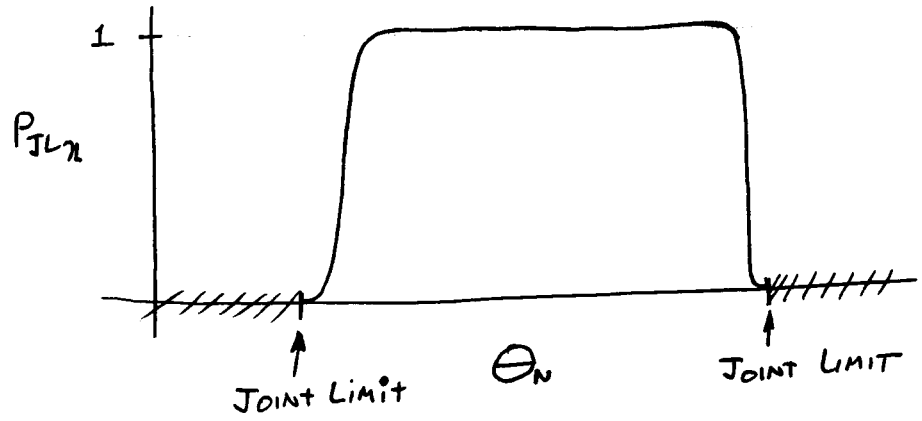

Example:

4. Height of elbow off the ground (Z_{elbow}, the Z component of elbow position.)

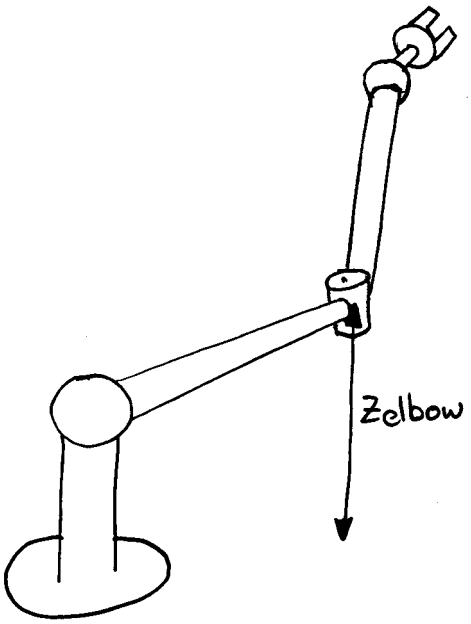

5. "Potential function energy" — a virtual energy attached to the inverse of distance between the robot and environmental obstacles.

11.5 Applications

Obstacle Avoidance
Avoiding Singularities

11.6 Joint Velocity - Computational Method

11.7 Hyperredundant Manipulators

Brief look at snake robots.

11.8 Summary of Notation

Chapter 12

Teleoperation

12.1 Problem Statement and Learning Objectives

Kinematics of Teleoperation Systems

12.2 Introduction

This chapter will introduce analytical models of teleoperation systems with multiple degrees of freedom.

12.3 Four Approaches

1. Joint Rate Control
2. Resolved Rate Control
3. Master-Slave Control
4. Generalized Master-Slave Control

12.3.1 Joint Rate Control

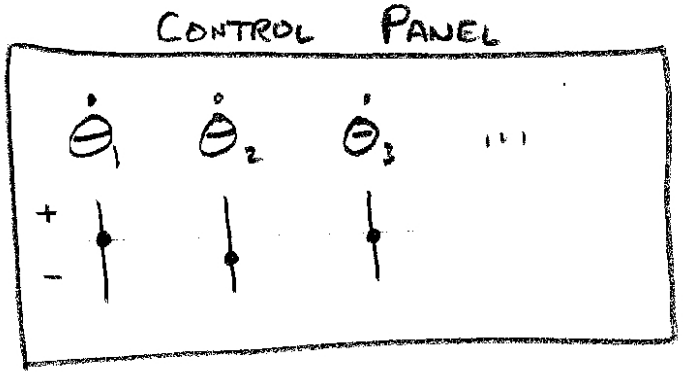

A basic control panel with knobs to control the rate of each joint.
Examples: Hydraulic construction Equipment
Must have spring return to zero!

Advantage

Cheap!

Disadvantage

Human must do inverse kinematics in their heads.

12.3.2 Resolved Rate Control

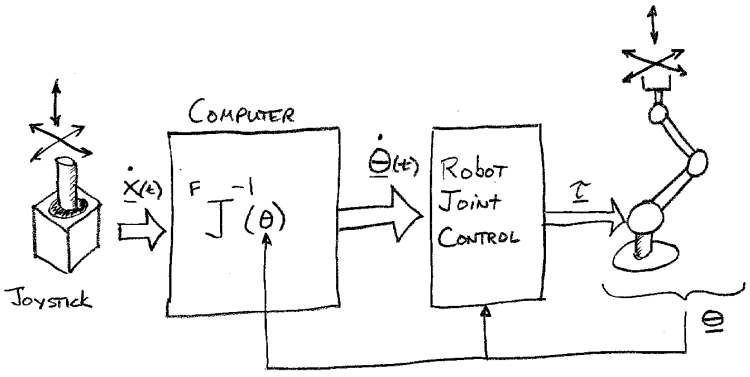

Advantages

- Modest computational requirements
- Can be adapted to task (i.e. change of reference frame or reference point).

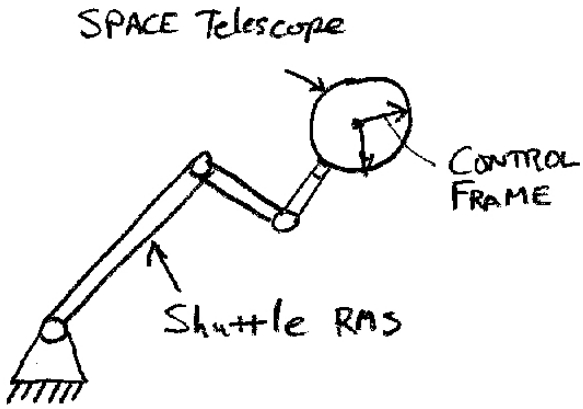

Example of the Hubble space telescope manipulated by space shuttle robot arm (RMS). The reference frame for resolved rate control can be programmed to the center of mass of the telescope or any convenient point.

Disadvantages

- Cognitive Load

- Operator must differentiate desired trajectory.
- Rate control of orientation is difficult

- Need to watch out for singualrities in Jacobian Matrices.
  System may demand infinite joint rates from slave robot.

12.3.3 Master Slave Control

This situation describes teleoperators where the master and slave devices are kinematically the same.

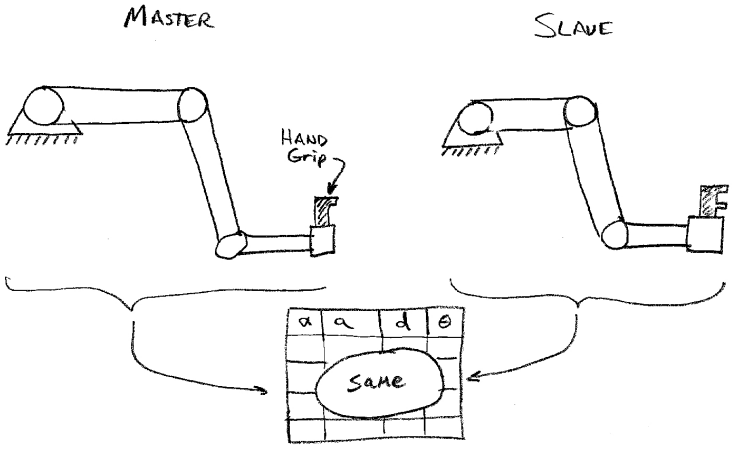

Controller must make sure that

$$\theta_s = \theta_m \tag{12.1}$$

Since the kinematic parameters (i.e. Denavit Hartenberg Parameters) are the same, this implies

$${}^0_6T_s = {}^0_6T_m \tag{12.2}$$

Also, if

$$\tau_m = \tau_s$$

then

$$F_m = F_s \tag{12.3}$$

One such controller is

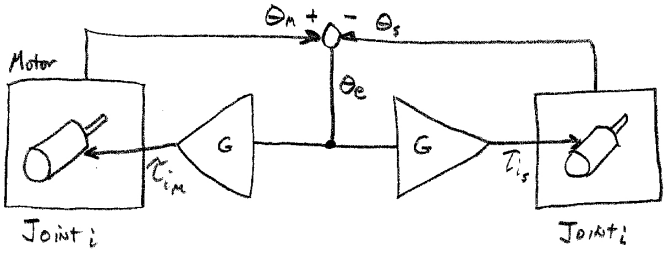

Advantages

- Simple Architecture (e.g. six separate analog controllers in 1950's).
- Good operator interface (1:1 motion and force feedback)

Disadvantages

- Master and Slave must be same design.
- Master and Slave must be in same configuration
- Can't index or scale the motion.

12.3.4 Indexing and Scaling

Definitions

Indexing: Provision of an arbitrary offsett between master and slave configurations.

Scaling: Ability to multiply position commands by an arbitrary constant.

Problems with Scaling and Indexing

Consider a Master/slave system which is moved by Δx_i at the master resulting in slave motion Δx_0.

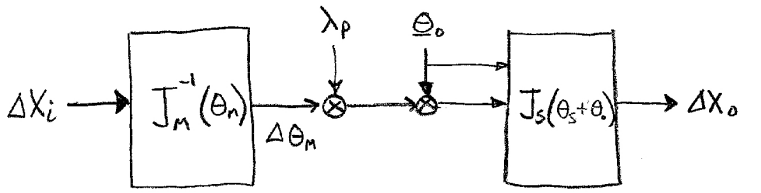

if $\lambda_p = 1$ and $\theta_0 = 0$, then

$$\theta_m = \theta_s, J_m(\theta_m) = J_s(\theta_s) \tag{12.4}$$

and

$$\Delta x_0 = J_s(\theta_s) J_m^{-1}(\theta_m) \Delta x_i$$

$$\Delta x_0 = \Delta x_i$$

Consider indexing:
if $\theta_0 \neq 0$

$$\theta_s = \theta_m + \theta_0$$

$$J_s(\theta_m + \theta_0) J_m^{-1}(\theta_m) \neq I$$

Consider scaling:
if $\lambda_p \neq 1$

$$\theta + s = \lambda_p \theta_m$$

$$J_s(\lambda_p \theta_m) J_m^{-1}(\theta_m) \neq \lambda_p I$$

12.3.5 Generalized Master Slave Control

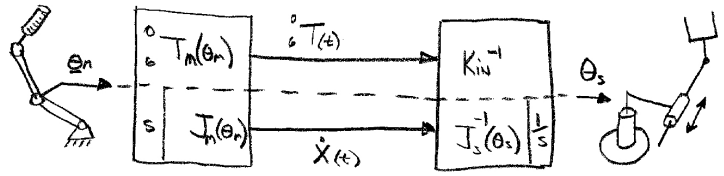

Master and Slave mechanisms kinematically different.
Communication options:
1) send 4x4 matrices indicating end effector frame (absolute coordinates)
2) send cartesian increment commands.

Indexing (using 4x4 Frames)

1) No indexing:

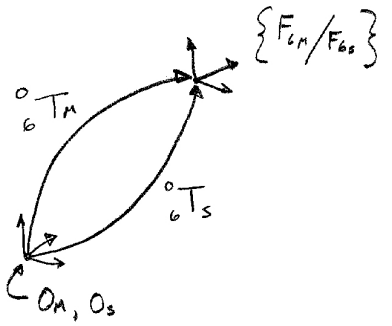

The master and slave frames are superimposed on the same points(!) There is actually of course an offset between the frames but mathematically we ignore it to lock their motions together.

2) With an index offset:

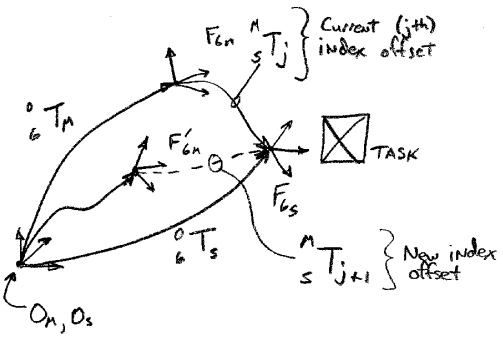

Operator first works with index offset j, and then creates a new offset ${}^m_sT_{j+1}$ by pressing a button and moving the master to a new location (with the slave frozen). Analyzing the diagram,

$$ {}^m_sT_{j+1} = \left({}^6_0T'_m\right)^{-1} {}^6_0T_s \tag{12.5} $$

The system then discards ${}^m_sT_j$ and continues on with ${}^m_sT_{j+1}$

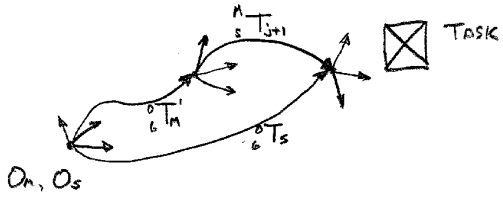

Procedure for Change of Index Offset

1) Normal Teleoperation:

$$ {}^0_6T_s = {}^0_6\,T_m(t)\,{}^M_sT_j \tag{12.6} $$

2) Operator presses and holds index button:

$$ \text{Slave position locked} \qquad {}^0_6T_s = constant \tag{12.7} $$

3) Operator moves to new position, ${}^0_6T'_m$:

$$ {}^M_sT_{j+1} = \left({}^0_6T'_m\right)^{-1} {}^0_6T_s \tag{12.8} $$

4) Resume Manipulation:

$$ {}^0_6T_s = {}^0_6\,T_m(t)\,{}^M_sT_{j+1} \tag{12.9} $$

Indexing (using incremental cartesian commands)

Easier!

$$ \Delta X_s = \Delta X_m = X_m(t) - X_m(t - \Delta t) \tag{12.10} $$

to index:

1. Set $\Delta X_s = 0$
2. Move master device to new position.
3. resume teleoperation using equation 12.10

Scaling (using 4x4 Frames)

We might apply the following method to scale the command to the slave:

$$ {}^0_6T_s = \lambda_p I \left({}^0_6T_m\,{}^m_sT_j\right) \tag{12.11} $$

this is **not** OK. (Why?)

However we could break inside the T matrix and use

$$ {}^0_6T_s = \begin{bmatrix} & [R] & & \lambda_p \begin{bmatrix} P_x \\ P_y \\ P_z \end{bmatrix} \\ [0 & 0 & 0] & 1 \end{bmatrix} \tag{12.12} $$

because orientation is not scaled by λ_p.

Scaling (using incremental cartesian commands)

$$ \Delta x_s = \lambda_p \Delta x_m \tag{12.13} $$

Simple!

Rate Control Option for Generalized Master Slave

Resolved rate control is an option which can be software selected in a generalized master slave system.

$$ \Delta x_s = \alpha_i (x_m - x_0) \tag{12.14} $$

where x_0 is a zero reference position such as the middle of the master device motion range.

Slave moves with a velocity proportional to master deflection

Need hardware or software spring return.

12.4 Position Teloperation Kinematics: Summary

Modes:

- Joint Rate Control
- Resolved Rate Control
- Master Slave Control
- Generalized Master Slave Control

	Indexing	Scaling	Kinesthesia	Ease
Joint Rate	Y	Y	N	Low
Resolved Rate	Y	Y	N	
Master Slave	N	N	Y	
Generalized Master Slave	Y	Y	Y	High

12.5 Applications

12.6 Summary of Notation

Chapter 13

Bilateral Control

Kinesthetic Interaction with Teleoperation Systems

13.1 Introduction

It was recognized in the earliest efforts to implement teleoperation systems that feedback of contact forces or constraints was very valuable for task performance. Such a system becomes quite different from a traditional control system. In traditional control systems, the input command (desired output) is a static value which is not influenced by any physical variable present at the output. In a telemanipulation system with force feedback, the output state affects the input and vice-versa. We refer to systems with this property as bi-lateral systems. Although bi-lateral systems can be modeled with traditional block diagram or signal-flow-graph techinques, more insight is obtained with methods drawn from the theory of electrical and other networks which share this bi-lateral property. In this chapter, we develop this understanding by introducing some concepts in the simplified context of a single degree of freedom bi-lateral system consisting of combined electrical, computational, communication, and mechanical components.

13.2 Modeling Combined Systems

Definitions:

- **Lumped Parameter Elements.** Physical entities who's energy (storage elements) or power (dissipative elements) is defined by a scalar.

  Examples: mass: $E = \frac{1}{2}mv^2$ resistor: $P = i^2R$

  Counter Example: Vibrating string, drum head.

- **Network.** A system described by lumped parameter elements connected in series and parallel. Each element consists of one constitutive relation.

  Example: An electric circuit consisting of R, L, C in arbitrary connections.

  Counter Examples: cloud, flame, ocean wave.

- **Port.** A location where energy can move into or out of a network. An effort $\mathcal{E}_i$ and flow, $\mathcal{F}_i$ are defined for each port.

  Examples: Electric wall socket. Contact point between human and haptic interface. Hydraulic coupling.

  Counter Examples: Ethernet jack. table supporting a mass.

13.2.1 Effort and Flow

Key insights can be obtained by focusing on energy movement within and between systems.

If energy is E, the time derivative of energy is power,

$$P = \frac{dE}{dt} \tag{13.1}$$

Since total energy must be conserved, power must be caused by energy moving between systems or system elements. For mechanical and electrical systems,

$$P = f \times \dot{x} \qquad P = i \times v \tag{13.2}$$

We generalize the two variables which form power as Effort ($\mathcal{E}$) and Flow ($\mathcal{F}$) respectively. Thus

$$P = \mathcal{E} \times \mathcal{F} \tag{13.3}$$

13.2.2 Impedance and Admittance

Effort and flow variables are linked together by the behavior of systems at their ports. Two ways to represent this relationship are impedance,

$$Z = \frac{\mathcal{E}(s)}{\mathcal{F}(s)} \tag{13.4}$$

and the admittance

$$A = \frac{\mathcal{E}(s)}{\mathcal{F}(s)} = 1/Z \tag{13.5}$$

13.2.3 Effort and Flow Summary

To summarize,

"Effort", $\mathcal{E}$	$\frac{dE}{dt}$	Force	Voltage
"Flow" , $\mathcal{F}$	$\frac{d}{dt}$ State	Velocity ($\frac{dx}{dt}$)	Current ($\frac{dq}{dt}$)

where C is capacitance, E is energy (or Work) and q is charge. "State" refers to a state variable such as position, x, and charge, q.

13.3 Constitutive Relations

A constitutive relation is a function which relates effort to either flow, the integral of flow, or its derivative.

In the study of linear systems, we assume the constitutive relations are linear functions, but this is not required in general.

The six basic linear constitutive relations are given in Figs 13.1 and 13.2.

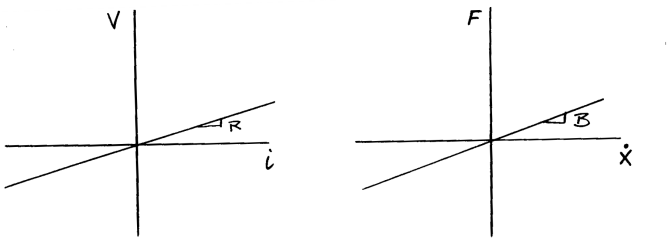

Figure 13.1: Constitutive relations for the linear dissipative elements resistance, R, and damping, B.

13.3.1 Analogies

The similarity of the electrical and mechanical constitutive relations, as well as the definition of effort and flow, generate the following analogies between electrical and mechanical systems. Additional columns can be added for hydraulic systems, thermal systems, etc.

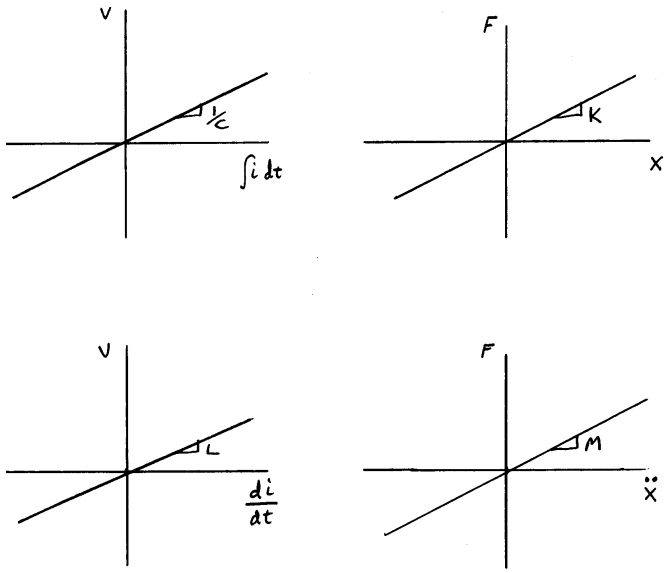

Figure 13.2: Constitutive relations for the linear energy storage elements, capacitance, C, stiffness, K, inductance, L, and mass, M.

Voltage	Force
Current	Velocity
Charge	Position
Inductance	Mass
Capacitance	Stiffness
Resistance	Damping

In some books on dynamics and control, another analogy is given in which the table above starts off

Voltage	Velocity
Current	Force

A valid system of analysis can also be constructed based on these analogies, but the following disadvantages obtain

- The notions of effort and flow cannot be abstracted to aid expansion of the analysis to other domains such as thermodynamics.
- Physical intuition which arises from the definition of voltage as "Electromotive Force" is lost.

An advantage of this analysis is that it can be easier to map directly between a mechanical diagram and electrical circuit.

13.4 Energy Ports

One definition of a system is simply region of space which is isolated to some degree from the environment and which contains energy storage and dissipative elements. At some points along the boundary between the system and environment we can identify locations at which energy may move into and out of the system. We call these locations ports. Such a general notion of system with a port having effort and flow variables and signs is shown in Figure 13.3

13.5 One-port networks

A system which has a single port is called a one-port system or simply a one-port (Figure 13.4).

For example, a mechanical impedance is a one-port network where

$$\mathcal{E} = F \qquad \text{and} \qquad \mathcal{F} = \frac{dx}{dt} = \dot{x} \tag{13.6}$$

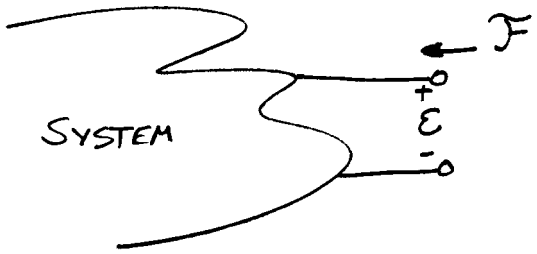

Figure 13.3: A port is a location where energy can be exchanged between a system and its environment described by the variables effort, $\mathcal{E}$, and flow, $\mathcal{F}$.

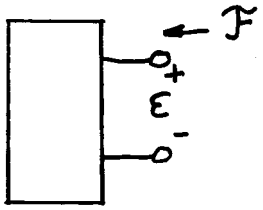

Figure 13.4: A one port network has a single location at which effort and flow define positive or negative power going into the network. We define the signs of effort and flow so that power is positive flowing into the port.

13.5.1 One Port Examples

Example of mechanical one-port (Figure 13.5).
Example of electrical one-port (Figure 13.6).

13.5.2 Vectors, Scalars, and Sign Conventions

In mechanical systems, the effort and flow variables are often vector quantities. In this chapter however, we simplify the system to consider scalar variables such as force and velocity in a single direction. However just as vectors must be expressed with respect to a coordinate system, scalar effort and flow variables must be expressed with respect to a one-dimensional coordinate system which is also thought of as a sign convention. Graphically we represent these one-dimensional coordinate systems or sign conventions with an arrow, just as with a single component of a 3 dimensional coordinate system. In electrical network systems, the analogy to coordinate systems for current (flow) is an arrow which indicates the direction of positive current. Voltage in networks is defined by subtracting the potential at two discrete points or terminals (and their location in space does not matter). However we must indicate which terminal will be considered positive.

It will be very important to keep track of power flowing into and out of networks so we must be careful with signs. Signs for efforts and flows can be thought of as a simple version of a coordinate system. Although there are multiple correct ways to do this, we will stick with the following convention:

1) Choose the sign of flow so that it is positive going *into* the port.
2) The effort of interest at the port is that being exerted *on* the port, not the effort exerted *by* the port on the environment. 3) Choose the sign of effort so that

$$\mathcal{E} \times \mathcal{F} > 0 \tag{13.7}$$

when energy flows *into* the port. This means that effort has the same sign as flow.

The electrical and mechanical network examples (Figures 13.5 and 13.6) have sign conventions applied according to the rules above.

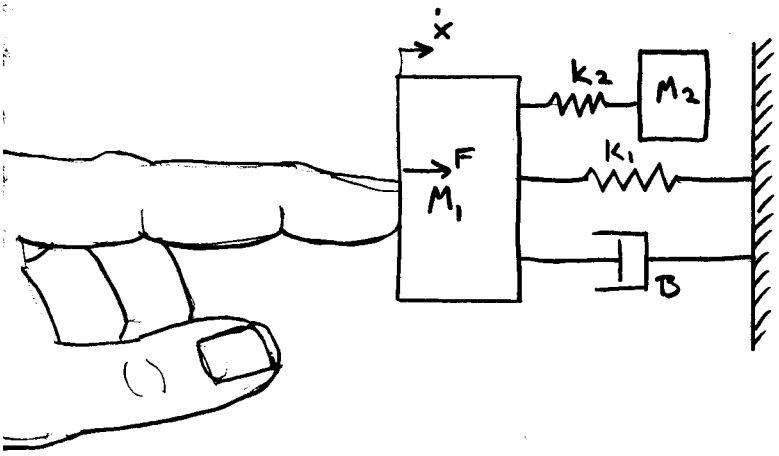

Figure 13.5: Example of a mechanical one-port network being touched by a fingertip.

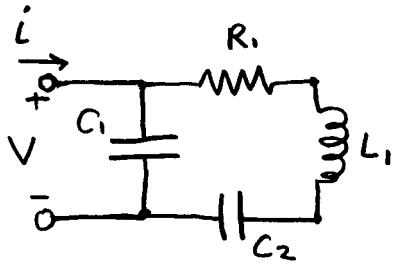

Figure 13.6: Example of an electrical one-port network.

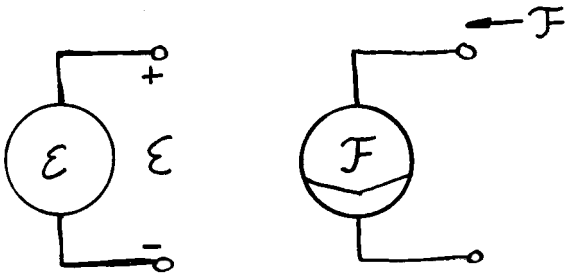

Figure 13.7: Effort and flow sources are one-ports which hold one variable constant.

13.5.3 Sources

Two additional one-port elements are effort and flow *sources*. An effort source is an element for which

$$\mathcal{E} = c \tag{13.8}$$

where c is a constant. And a flow source gives

$$\mathcal{F} = c \tag{13.9}$$

We can also have *dependent sources* which are defined above but where $c = \alpha x$ where x is another network variable.

13.5.4 Connected 1-Ports

When two systems are connected to each other, their ports are in contact and share the effort and flow variables. For example, consider a human operator touching a haptic interface (Figure 13.8).

13.6 Two-port networks

Now we consider systems which have two ports. We can see the need for this if we break up the haptic interface of Figure 13.8 to indicate the haptic device hardware, the haptic device controller, and the virtual reality model as separate components (Figure 13.9). Two-ports have separate effort and flow variables, defined for each port, and a separate coordinate system (sign convention) for each port (Figure 13.10)

13.6.1 Electrical Network Example:

In the electrical 2-port of Figure 13.11, i_1 and i_2 are the currents flowing *into* the ports at the *positive* terminals. When voltage and current are defined this way positive power means power flowing *into* the network port.

13.6.2 Other Notations

Bond Graphs (Paynter, 1961)

When two ports are connected as in Figure 13.8, we can say they are wired in series, but also that they are wired in parallel. However if three ports are connected together, we need to consider how they are connected. Series connection means that all the ports have the same flow value and parallel means they share the same effort but have different flows. Bond Graphs are an abstraction of networks into energy bonds between lumped parameter elements. A "bond" is a general way of connecting multiple ports together. Elements are connected at bonds which correspond to Kirchoffs/Newtons laws.

"1 Junction" a bond in which $\sum_i \mathcal{E}_i = 0$ and $\mathcal{F}_i = \mathcal{F}_j$. For example an electrical series loop or a mass.

"0 Junction" a bond in which $\sum_i \mathcal{F}_i = 0$ and $\mathcal{E}_i = \mathcal{E}_j$. For example an electrical node (parallel connection) or mechanical elements which share the same force.

An example of an electrical network and its associated Bond Graph is given in Figure 13.13.

Port Hamiltonian Systems (Stramigioli, 2000's)

Same idea as bond graphs.

13.6.3 2-Port Network Models

First, make a key assumption: Linearity. In this case, all two port networks can be modeled by

$$A \begin{bmatrix} \mathcal{F}_1 \\ \mathcal{F}_2 \end{bmatrix} + B \begin{bmatrix} \mathcal{E}_1 \\ \mathcal{E}_2 \end{bmatrix} = 0 \tag{13.10}$$

Where A and B are 2×2 matrices.

There are two more useful forms of this equation however known as "projections" of eqn (13.10).

$$\begin{bmatrix} \mathcal{E}_1 \\ \mathcal{E}_2 \end{bmatrix} = Z \begin{bmatrix} \mathcal{F}_1 \\ \mathcal{F}_2 \end{bmatrix} \tag{13.11}$$

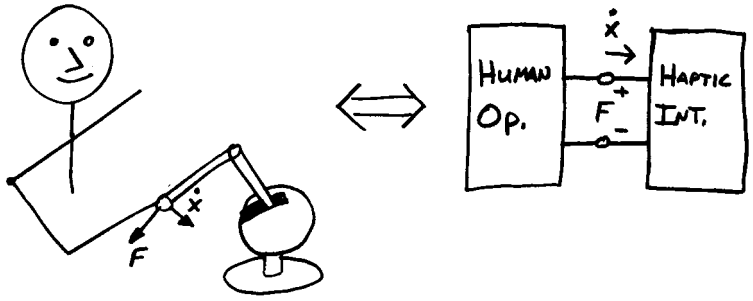

Figure 13.8: Human operator holding a haptic interface can be represented as two connected one-ports. In this case, the effort and flow variables are the force and velocity respectively.

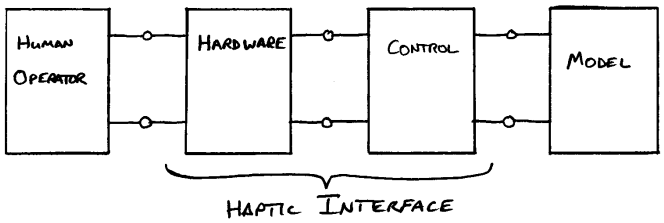

Figure 13.9: Expanded network diagram of human interacting with haptic interface showing haptic device hardware and haptic device controller as separate two-ports.

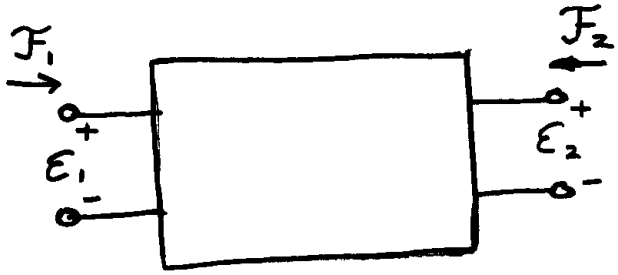

Figure 13.10: A two port network with effort and flow defined separately at each port.

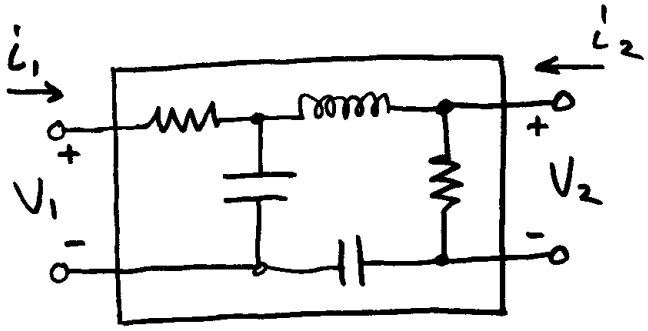

Figure 13.11: Example of two-port electrical network.

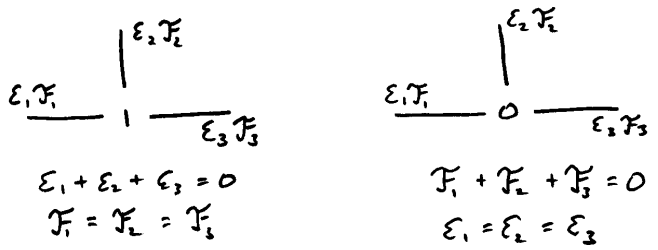

Figure 13.12: Bond graphs (Figure 13.12) illustrate ways energy can flow within networks.

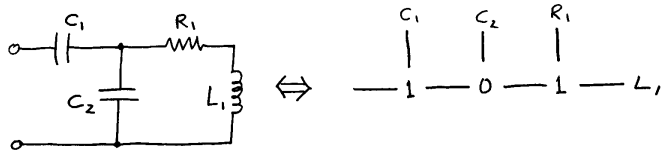

Figure 13.13: Example of an electrical 1-port and its equivalent bond graph.

where Z is a 2×2 "Impedance Matrix".

and

$$\begin{bmatrix} \mathcal{E}_1 \\ \mathcal{F}_2 \end{bmatrix} = H \begin{bmatrix} \mathcal{F}_1 \\ \mathcal{E}_2 \end{bmatrix} \tag{13.12}$$

where H is a 2×2 "Hybrid Matrix".

13.6.4 Finding Elements of Z

First expand eqn(13.11) to get

$$\begin{aligned} \mathcal{E}_1 &= z_{11}\mathcal{F}_1 + z_{12}\mathcal{F}_2 \\ \mathcal{E}_2 &= z_{21}\mathcal{F}_1 + z_{22}\mathcal{F}_2 \end{aligned} \tag{13.13}$$

Now set some boundary conditions on the network: $\mathcal{F}_1 = 0$ or $\mathcal{F}_2 = 0$. This allows us to solve for each element of Z:

$$Z = \begin{bmatrix} z_{11} = \left.\frac{\mathcal{E}_1}{\mathcal{F}_1}\right|_{\mathcal{F}_2=0} & z_{12} = \left.\frac{\mathcal{E}_1}{\mathcal{F}_2}\right|_{\mathcal{F}_1=0} \\ z_{21} = \left.\frac{\mathcal{E}_2}{\mathcal{F}_1}\right|_{\mathcal{F}_2=0} & z_{22} = \left.\frac{\mathcal{E}_2}{\mathcal{F}_2}\right|_{\mathcal{F}_1=0} \end{bmatrix} \tag{13.14}$$

Note: The boundary conditions ($\mathcal{F}_1 = 0$ or $\mathcal{F}_2 = 0$) which allow us to solve for the elements of Z are not only mathematically useful, they define simple physical experiments which can be peformed on the 2-port network:

		Mechanical	Electrical
Flow:	$\mathcal{F} = 0$	motion blocked	open circuit
Effort:	$\mathcal{E} = 0$	free motion	short circuit

13.6.5 Finding Elements of H

Exercise: Find the elements of H (eqn(13.12)

First expand eqn(13.12) to get

$$\begin{aligned} \mathcal{E}_1 &= h_{11}\mathcal{F}_1 + h_{12}\mathcal{E}_2 \\ \mathcal{F}_2 &= h_{21}\mathcal{F}_1 + h_{22}\mathcal{E}_2 \end{aligned} \tag{13.15}$$

Now set some boundary conditions on the network: $\mathcal{F}_1 = 0$ or $\mathcal{F}_2 = 0$. This allows us to solve for each element of H:

$$H = \begin{bmatrix} h_{11} = \frac{\mathcal{E}_1}{\mathcal{F}_1}\Big|_{\mathcal{E}_2=0} & h_{12} = \frac{\mathcal{E}_1}{\mathcal{E}_2}\Big|_{\mathcal{F}_1=0} \\ h_{21} = \frac{\mathcal{F}_2}{\mathcal{F}_1}\Big|_{\mathcal{E}_2=0} & h_{22} = \frac{\mathcal{F}_2}{\mathcal{E}_2}\Big|_{\mathcal{F}_1=0} \end{bmatrix} \tag{13.16}$$

So far we have treated the Z and H matrix elements h_{ij} and z_{ij} as scalar real numbers. If we are able to model the system with differential equations however, we can use LaPlace transforms and the matrix elements become functions of complex frequency, s. However for simplicity we will usually omit the (s).

13.7 Models of Teleoperation

13.7.1 Interpretation of the H Parameters

Recall that we have the analogies:

Velocity ↔ Current
Force ↔ Voltage

With Impedance Control from robotic manipulation, we study the control of mechanical impedance at the contact point between robot and environment: a port. Both the robot and the environment are one-ports which are conected.

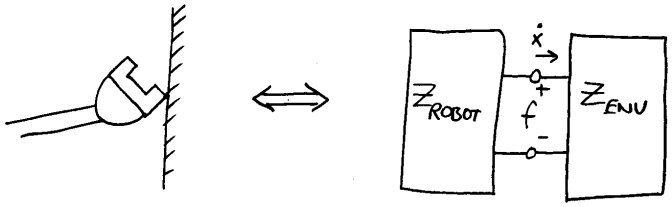

Figure 13.14: Contact between a robot manipulator and environment (Left) is a port at which mechanical energy can flow back and forth between the robot and environment. It is represented as two one-ports connected together (Right).

For a bilateral teleoperation system (Figure 13.15) we have two contact points and therefore use a two-port model.

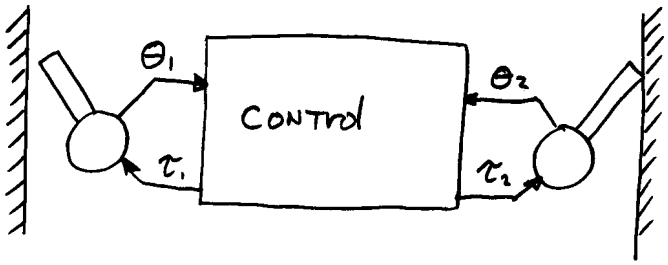

Figure 13.15: Simple bi-lateral teleoperation system has two ports: the master and slave robots (here shown as a completely symmetrical system) contact two separate environments. The human operator is usually shown in place of the left side environment.

We then use the H parameters (i.e. the elements of H) to study the system. Let's express the definition of the h_{ij} elements in terms of the mechanical effort and flow variables:

$$h_{11} = \frac{f_1}{\dot{x}_1}\Big|_{f_2=0} \tag{13.17}$$

$$h_{12} = \left.\frac{f_1}{f_2}\right|_{\dot{x}_1=0} \tag{13.18}$$

$$h_{21} = \left.\frac{\dot{x}_2}{\dot{x}_1}\right|_{f_2=0} \tag{13.19}$$

$$h_{22} = \left.\frac{\dot{x}_2}{f_2}\right|_{\dot{x}_1=0} \tag{13.20}$$

Note that h_{11} (eqn (13.17)) is an effort over a flow and thus it is an impedance. Furthermore, we observe:

- h_{11} involves only variables at the input port.
- Because of the applicable boundary condition, $f_2 = 0$, h_{11} can only be measured or computed when the output port is in free motion.
- $h_{11} = z_{11}$

With these considerations, h_{11} represents the input impedance (i.e. resistance felt by the human operator) when the slave is not touching anything.

Similarly, h_{12} is a ratio of the two forces at the ports. We observe:

- h_{12} is dimensionless.
- h_{12} represents a gain or transfer function from slave force to master force.
- h_{12} characterizes the nature of force feedback to the operator.
- The boundary condition for h_{12} requires that it be measured or computed with the master device locked so that it cannot move.

Extending this reasoning to the other H parameters, we have

h_{11}	Input Impedance with Free Slave Motion.
h_{12}	Force Feedback Gain with Locked Master, λ_f.
h_{21}	Forward Velocity Gain with Free Slave Motion, λ_p.
h_{11}	Input impedance with Free Slave Motion.

Where we have also defined λ_p and λ_f to conveniently denote the position/velocity and force scales respectively.

13.7.2 Equivalent Circuits

The mathematical form of the H and Z matrices suggest that there is an equivalent circuit model which can represent any two port network. This is analogous to Thevenin and Norton forms of the one-port network.

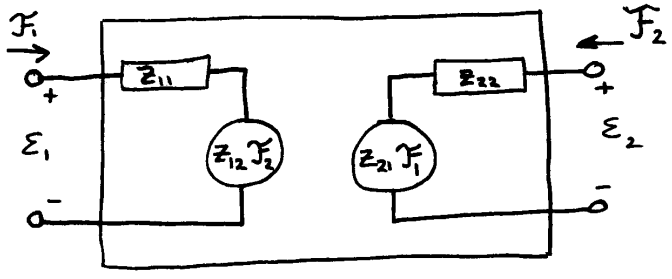

Figure 13.16: Equivalent circuit two-port based on the impedance matrix, Z.

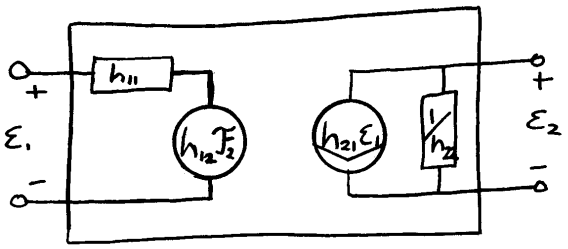

Figure 13.17: Equivalent circuit two-port based on the hybrid parameters.

The impedance matrix creates an equivalent circuit with a Thevenin style network at each port (Figure 13.16). The effort souces are controlled based on the flow variable in the other port.

The hybrid matrix representation lends itself more naturally to a different equivalent circuit with the same circuitry on port 1, but a Norton form on port 2 (Figure 13.17).

Remember that both H and Z forms can represent any network, and transformations exist which can translate between the forms (see a book on network theory).

13.8 Kinesthesia

> "The sensation of **movement** or **stress** in muscles, tendons, and joints."
> Random House Dictionary.

Two components: "Movement" and "Stress".

Clearly this channel is used in natural manipulation. How can kinesthesia be supported in telemanipulation?

Approaches:

- Send force from master to slave and force from slave to master.
- Send position from master to slave, force from slave to master ("force feedback").
- Send position in both directions.

Which is best? What is our analytical approach?

How do we analyze a control system where each end is both an input and output?

13.9 Ideal Bilateral teleoperator: Massless Stick

First let's put these ideas to work on bilateral kinesthetic systems. First consider a massless stick with which a human is pushing on the environment in the axial direction (Figure 13.18).

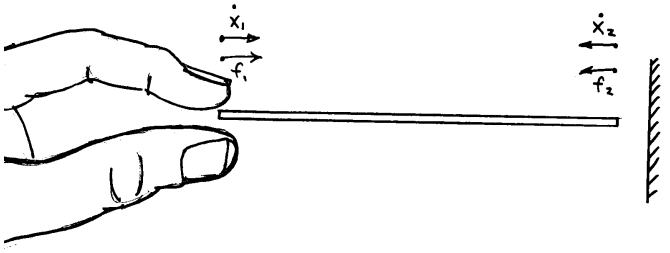

Figure 13.18: Massless stick held by operator at one end and touching an environment at the other can be analyzed as a two port system.

Clearly the ports are the two ends of the stick. Following Section 13.5.2, we assign signs to the effort and flow variables as follows:

1. Positive direction for velocity is into the ends of the stick, i.e. to the right on the left end and to the left on the right end.

2. When power flows into the stick, force must be in the same direction as the velocity, so force has the same sign.

Note:
Designation of "Master" and "Slave" ends is completely arbitrary.
With a massless stick, we have a direct kinesthetic correspondance between hand force/velocity and environment force/velocity.

13.9.1 Hybrid Matrix of Massless Stick

With the correct sign conventions, and using intuition about massless sticks, we write

$$\dot{x_1} = -\dot{x_2} \qquad \text{and} \qquad f_1 = f_2 \tag{13.21}$$

(**Note:** f_1 and f_2 must represent forces exerted on the stick. In a single global coordinate system they would be normally in opposite directions. However with the two coordinate systems we have chosen for the two ends of the stick, compressive forces on the stick would have the same sign.)
Now let's derive the H parameters using equations (13.17 — 13.20):

$$h_{11} = \left.\frac{f_1}{\dot{x}_1}\right|_{f_2=0} = 0 \tag{13.22}$$

$$h_{12} = \left.\frac{f_1}{f_2}\right|_{\dot{x}_1=0} = 1 \tag{13.23}$$

$$h_{21} = \left.\frac{\dot{x}_2}{\dot{x}_1}\right|_{f_2=0} = -1 \tag{13.24}$$

$$h_{22} = \left.\frac{\dot{x}_2}{f_2}\right|_{\dot{x}_1=0} 0 \tag{13.25}$$

or

$$H_{ideal} = \begin{bmatrix} 0 & 1 \\ -1 & 0 \end{bmatrix} \tag{13.26}$$

Note that applying similar analysis to the Z matrix give us

$$Z_{ideal} = \begin{bmatrix} \infty & \infty \end{bmatrix} \tag{13.27}$$

The different two port models do not always exist.

13.10 Position error-based Master-Slave Teleoperation

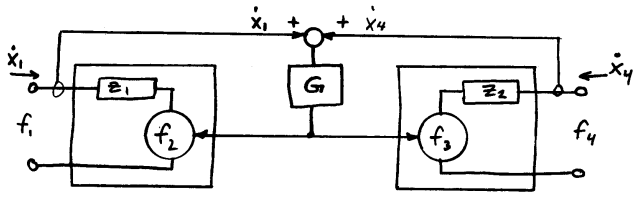

Figure 13.19: Classical master-slave bi-lateral teleoperation control system. Master and slave devices are represented as Thevenin equivalent circuits. Mechanical impedances represent viscous and inertial properties of the devices such as motor inertia.

We now consider the original bilateral control method (going back to Ray Goertz) in which position error between master and slave is used to generate a force feedback signal (Figure 13.19). Here we have a diagram showing the master and slave units as Thevenin equivalent one-ports. These are reasonable models of electric motor driven motion axes. The source in each one-port is a dependent effort source such that

$$f_2 = f_3 = (\dot{x}_1 + \dot{x}_2)G \tag{13.28}$$

$$\begin{bmatrix} f_1 \\ \dot{x}_4 \end{bmatrix} = H_{cs} \begin{bmatrix} dotx_1 \\ f_4 \end{bmatrix} \tag{13.29}$$

You can show:

$$H_{cs} = \begin{bmatrix} Z_3 + G\left[1 - \frac{G}{Z_3+G}\right] & \frac{G}{Z_3+G} \\ \frac{-G}{Z_3+G} & \frac{1}{Z_3+G} \end{bmatrix} \tag{13.30}$$

Example solution:

$$h_{12} = \left.\frac{f_1}{f_4}\right|_{\dot{x}_1=0} \tag{13.31}$$

when $\dot{x}_1 = 0$, $f_1 = f_2 = \dot{x}_4 G$. then we have

$$\dot{x}_2 = \frac{f_4 - f_3}{Z_3} = \frac{1}{Z_3} f_4 - \dot{x}_2 \frac{G}{Z_3} \tag{13.32}$$

Now, if we are given the task to design G in order to achieve ideal behavior (equation 13.26) we can try to make $|G|$ as large as possible over some frequency range, but ideal teleoperation will never be achieved because

$$h_{11} \to Z_3 \qquad \text{as} \quad |G| \to \infty \tag{13.33}$$

13.11 Forward Flow Master Slave Teleoperation

(future material)

13.12 Lever Bilateral teleoperator: Artist's Paintbrush

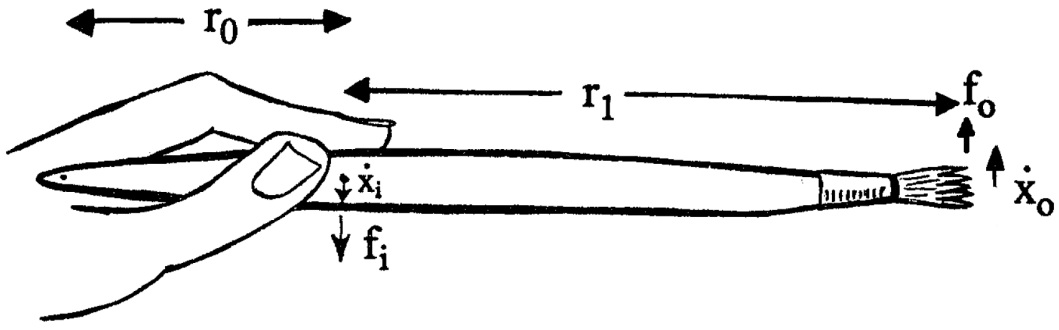

Figure 13.20: An artist's paintbrush will serve as an example of how two-port modeling can be used to study tool use.)

Consider a long artist's paint brush (Figure 13.20). The following section will analyze such a tool with two-port network theory to gain some informal insight into how a brush might be used by the painter for different effects. This time we assume the stick has some mass, expressed in terms of a linear density, ρ which describes the mass per unit of length.

13.12.1 H Matrix of Paintbrush

We leave it as an exercise to the reader to derive the following hybrid matrix for the brush.

$$H_{ideal} = \begin{bmatrix} \frac{\rho(r_0+r_1)^2 s}{2} & \frac{r_0+r_1}{r_0} \\ -\left(\frac{r_0+r_1}{r_0}\right) & \frac{r_1 s}{k} \end{bmatrix} \tag{13.34}$$

Where ρ is the linear density of the brush ($\frac{\partial m}{\partial x}$), k is the spring constant for bending the brush, and s is the LaPlace transform variable.

Here's how the h parameters describe physical phenomena in the brush.

$$H_{ideal} = \begin{bmatrix} \text{Brush inertial behavior.} & \text{Mechanical Advantage} \\ \text{Mechanical Advantage} & \text{Spring} - \text{like Bending} \end{bmatrix} \tag{13.35}$$

As for any system based on a lever/fulcrum,

$$\lambda_f = h_{12} = \frac{r_0 + r_1}{r_0} \qquad \lambda_p = -h_{21} = -\frac{r_0 + r_1}{r_0} \tag{13.36}$$

We can also show that when using the paintbrush, the impedance "seen" by the paint, in other words the combined effects of the artist impedance and brush impedance, Z_{AB}, is

$$Z_{AB} = Z_A \left(\frac{r_0}{r_0 + r_1}\right)^2 \tag{13.37}$$

By varying his/her grip on the brush, the artist changes r_0 and r_1 keeping their total constant.

Let's consider extreme cases,

1) $r_0 \to 0$

In this case $Z_{AB} \to 0$. Recall that when impedance is 0, we have an ideal force (effort) source.

2) $r_1 \to 0$

In this case $Z_{AB} \to Z_A$. Recall that when impedance is ∞, we have an ideal velocity/position (flow) source. Although the artist cannot achieve infite impedance, Z_A may be the highest impedance that the artist can achieve.

13.13 Scaled Bi-Lateral Teleoperation

For many applications, we might want to scale force and position up or down from a comfortable range for the human operator to some other domain ideal for a task. For example in a micro surgery system we might want to scale down the operator's motion and scale up force feedback to the operator so that tiny delicate tissues are easier to feel.

Already a huge range of scale factors (10^{10}) have been implemented in teleoperation (Figure 13.21)

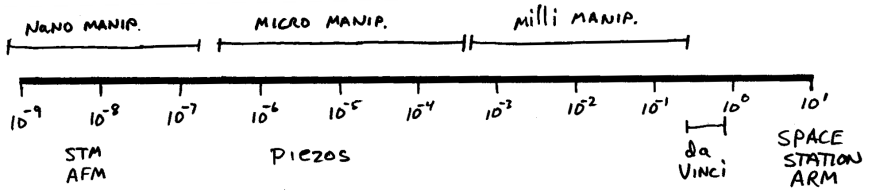

Figure 13.21: A huge range of scale factors has been used in teleoperation systems that have been developed.

13.13.1 Scaled Mechanical Impedance

Consider $\lambda_p \neq 1$ and $\lambda_f \neq 1$. If the slave robot is in contact with a mechanical impedance Z_E, what is the impedance experienced or felt by the human operator? We denote this impedance Z_{felt} and illustrate where it is measured and defined in Figure 13.22.

$$Z_{felt} = \frac{f_1}{\dot{x}_1} \tag{13.38}$$

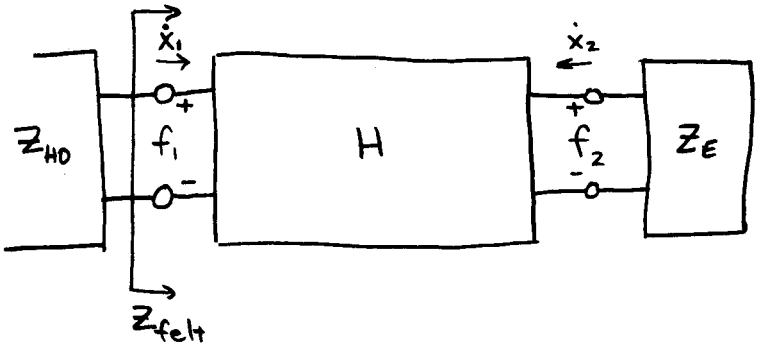

Figure 13.22: Two-port model of scaled teleoperation illustrating the impedance, Z_{felt}, experienced by the operator when contact with an environment is mediated by a scaled teleoperator.

Expanding equation (13.29), and solving for f_2, we have

$$f_1 = h_{11}\dot{x}_1 + h_{12}(-\dot{x}_2 Z_E) \tag{13.39}$$

and

$$\dot{x_2} = h_{21}\dot{x}_1 + h_{22}(-\dot{x}_2 Z_E) \tag{13.40}$$

Solving for $\dot{x}_1$,

$$\dot{x}_1 = h_{21}\frac{\dot{x}_1}{1 + Z_E h_{22}} \tag{13.41}$$

and

$$f_1 = h_{11}\dot{x}_1 - \frac{h_{12}h_{21}}{1 + Z_E h_{22}} Z_E \dot{x}_1 \tag{13.42}$$

With these two components, we get:

$$Z_{felt} = h_{11} - \left[\frac{h_{12}h_{21}}{1 + Z_E h_{22}}\right] Z_E \tag{13.43}$$

or equivalently

$$Z_{felt} = h_{11} + \left[\frac{\lambda_p \lambda_f}{1 + Z_E h_{22}}\right] Z_E \tag{13.44}$$

If the master and slave mechanisms are perfect or idealized (that is they have no losses due to friction or compliance), then ideally $h_{11} = 0$ and $Z_E h_{22} = 0$. Giving

$$\boxed{Z_{felt} = \lambda_p \lambda_f Z_E} \tag{13.45}$$

13.13.2 Power Gain from Master to Slave

It can be shown[1] that for the system of Figure 13.22,

$$P_1 = -P_4\left(-\frac{h_{21}}{h_{12}} + \frac{2h_{11}h_{22}}{h_{21}^2}\right) + f_2^2 h_{22}\left(\frac{h_{21}}{h_{12}} + \frac{h_{11}h_{22}}{h_{21}^2}\right) + \dot{x}_2^2\frac{h_{11}}{h_{21}^2} \tag{13.46}$$

where P_1 is the power going into port 1 and P_4 is the power going into port 2. Let us assume an ideal scaled teleoperator having hybrid matrix

$$H = \begin{bmatrix} 0 & \lambda_f \\ -\lambda_p & 0 \end{bmatrix} \tag{13.47}$$

Then we have

$$P_1 = -P_4\frac{\lambda_p}{\lambda_f} \tag{13.48}$$

Thus, power at the human operator side is scaled relative to the environment side by $\frac{\lambda_p}{\lambda_f}$.

[1] B. Hannaford, 'Kinesthetic Feedback Techniques in Teleoperated Systems,' In "Advances in Control and Dynamic Systems", pp. 1-32, C. Leondes, Ed., Academic Press, San Diego, 1991.

13.14 Stability

13.14.1 Basic Linear Control Theory

13.14.2 Passivity

13.14.3 Time Delay

13.15 Lawrence Four-Channel Architecture

13.15.1 Scaled Teleoperation Conclusions

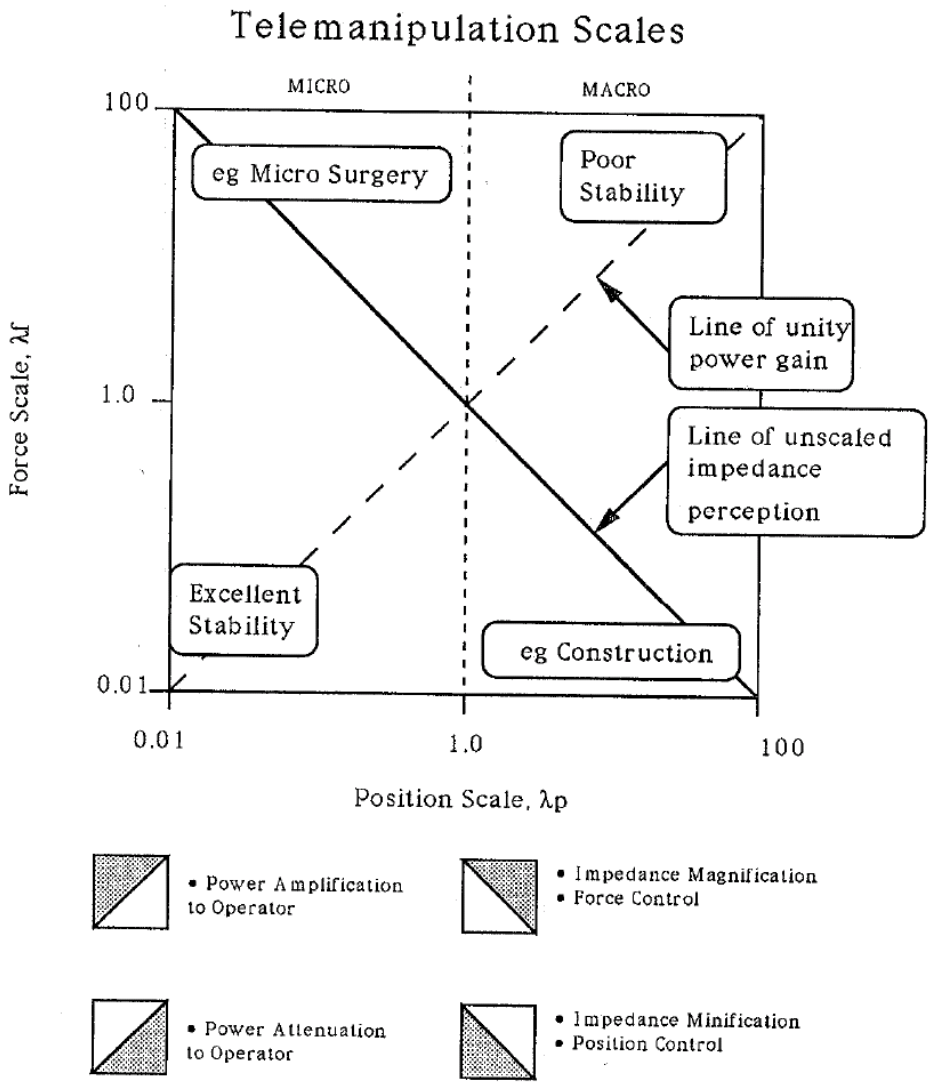

Figure 13.23: Properties of bi-lateral teleoperators depending on position and forces scales: λ_p and λ_f.

We have the following observations sumarized in Figure 13.23.

- For all levers, $\lambda_p = \lambda_f$.
- If $\lambda_p \lambda_f > 1$, environment impedance is magnified to the operator.
- If $\lambda_p \lambda_f < 1$, environment impedance is reduced to the operator.

- If $\frac{\lambda_p}{\lambda_f} > 1$ power is amplified from the environment to operator and attenuated from operator to environment.
- If $\frac{\lambda_p}{\lambda_f} < 1$ power is attenuated from the environment to operator and amplified from operator to environment.

Appendix A

Mathematical Fundamentals

Affine Transformation An Affine Transformation is one of the form

$$y = Ax + b$$

Where x,y,b are N vectors, and A is an $N \times N$ matrix. Such transformations perserve straight lines and include an offset (b) so that they can represent displacement as well as other types of linear transformations.

A.1 Trigonometric Identities and Formulas

$$\sin^2(x) + \cos^2(x) = 1$$

$$\sin(\pi/2 - x) = \cos(x) \qquad \cos(\pi/2 - x) = \sin(x)$$

$$sin(-x) = -sin(x) \qquad \cos(-x) = cos(x)$$

$$\sin(x + y) = \sin(x)\cos(y) + \cos(x)\sin(y) \qquad \cos(x + y) = \cos(x)\cos(y) - \sin(x)\sin(y)$$

"Law of Cosines"

$$c^2 = a^2 + b^2 - 2ab\cos(\gamma)$$

A.2 Euler Angle Sets

A.3 The Atan2 Function

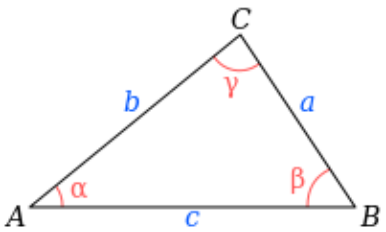

Figure A.1: Source: wikipedia

Appendix B

Linear Algebra Basics

Source: "Introduction to Matrices and Determinants," F. Max Stein, 1967.

Assume A is a square matrix.

Facts:

1. A^{-1} exists if and only if
$$\det[A] \neq 0$$
if $\det[A] = 0$, we say that A is a *singular* matrix and that its inverse does not exist.

2. The *rank* of A is the size of the largest square sub-matrix, S, for which
$$\det[S] \neq 0$$

3. If two rows or columns of A are equal, or related by a constant, then $\det[A] = 0$.

4. Any singular matrix has at least one eigenvalue equal to zero.

5. If A is non-singular, and λ is an eigenvalue of A corresponding to the eigenvector, x, then
$$A^{-1}x = \lambda^{-1}x$$

6. If A is square, then A and A^T have the same eigenvalues. I.e.
$$Ax_i = \lambda_i x_i \qquad A^T y_i = \lambda_i y_i$$

7. If the nxn matrix A is of full rank (i.e. $r = n$) then the only solution to $Ax = 0$ is the trivial one, $x = 0$.

8. If $r < n$, then there are $n - r$ linearly independent (i.e. orthogonal) solutions
$$x_j \qquad 1 < j < n - r$$
for which $x_j \neq 0$ and $Ax_j = 0$.

B.1 Matrix Multiplication

Conceptual Definition:

A *matrix* is a mapping of a vector from one space to another which preserves straight lines. The matrix thus represents a linear transformation.

Algebraic Definition:
If A is a 3x3 matrix and B is a 3x1 vector,

$$AB = \begin{bmatrix} a_{11} & a_{12} & a_{13} \\ a_{21} & a_{22} & a_{23} \\ a_{31} & a_{32} & a_{33} \end{bmatrix} \times \begin{bmatrix} b_1 \\ b_2 \\ b_3 \end{bmatrix} = \begin{bmatrix} a_{11}b_1 + a_{12}b_2 + a_{13}b_3 \\ a_{21}b_1 + a_{22}b_3 + a_{23}b_3 \\ a_{31}b_1 + a_{32}b_3 + a_{33}b_3 \end{bmatrix}$$

The rule is to multiply **row by column** and add component wise. This can also be written:

$$AB_i = \sum_{j=1}^{N} a_{ij}b_j$$

For matrix - matrix multiplication, this becomes

$$AC_{ij} = \sum_{m=1}^{N} a_{im}c_{mj}$$

where C is a 3x3 matrix with components c_{ij}.
(Did you know that Albert Einstein invented the idea of dropping the $\sum$ and the subscripts to simpilify the notation of matrix multiplication?) Putting it another way,
if

$$A = \begin{bmatrix} a^T \\ \alpha^T \\ \aleph^T \end{bmatrix}, \text{and} \qquad B = [b \quad \beta \quad \lambda],$$

then

$$AB = \begin{bmatrix} a \cdot b & a \cdot \beta & a \cdot \lambda \\ \alpha \cdot b & \alpha \cdot \beta & \alpha \cdot \lambda \\ \aleph \cdot b & \aleph \cdot \beta & \aleph \cdot \lambda \end{bmatrix}$$

where $\cdot$ is the vector dot product.

B.2 Matrix Inverse

B.2.1

The inverse of a matrix A, A^{-1} is most clearly defined by $AA^{-1} = I$.

We can find A^{-1} by

$$A^{-1} = \frac{adjA}{detA} = \begin{bmatrix} \frac{a_{11}}{|A|} & \frac{a_{12}}{|A|} & \frac{a_{13}}{|A|} \\ \vdots & \vdots & \vdots \\ \cdots & & \frac{a_{ij}}{|A|} \end{bmatrix}$$

$adjA$ is a matrix of *cofactors* A_{ij} of A where

$$A_{ij} = (-1)^{n(j)} Det(A\text{-}(i,j))$$

where $A\text{-}(i,j)$ is the matrix A when row i and col j are removed and

$$|A| = Det(A) = \sum_{\{j\}} (-1)^{n(j)} a_{1j_1} a_{2j_2} a_{3j_3} \dots a_{nj_n}$$

where $\{j\}$ is the set of all permutations of the integers $i \dots n$, and $n(j)$ is the number of interchanges of the order of these permutations.

B.2.2

For the case of a 2x2 matrix we have

$$\begin{bmatrix} a_{11} & a_{12} \\ a_{21} & a_{22} \end{bmatrix}^{-1} = \frac{1}{a_{11}a_{22} - a_{21}a12} \begin{bmatrix} a_{22} & -a_{12} \\ -a_{21} & a_{11} \end{bmatrix}$$

(This detail is included simply for completeness of the review. For more information see your favorite Linear Algebra textbook.)

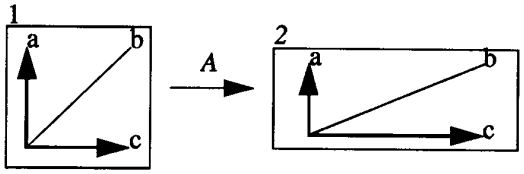

Figure B.1: Matrix multiplication can be used to represent linear transformations such as the stretching of a rubber sheet.

B.3 Interpretations of Matrix Vector Multiplication

The following are helpful ways to think about the meaning or application of matrix-vector multiplication. We will use a notation in which leading superscripts denote coordinate systems in which quantities are represented. For example the point x may be represented by different coordinates in two different coordinate systems 1 and 2. We denote these representations of x as ${}^1x, {}^2x$.

1. Stretched Sheet

   The matrix transformation ${}^2b = A^1b$ can be visualized as the transformation of point ${}^1b$ on a rubber sheet which is deformed to give a new point ${}^2b$. Suppose a rubber sheet has three points a, b, c printed on it and is streched as shown in Figure B.1:

   In this example, the stretching of the sheet can be described by the matrix A. Looking at the figure we note that the vector b is longer after the stretch and points in a slightly different direction. We also note that although a and c have had their lengths changed, they still point in the same direction. We can express this mathematically as

   $$^2a = \lambda_1 a = A^1a$$

   and

   $$^2c = \lambda_2 c = A^1c$$

   where λ_1 and λ_2 are scalar constants. In other words, for this particular example, for certain vectors (a, c), the linear transformation A is eqivalent to multiplication by a constant, but not for general vectors such as b. We call the scalars λ_1 and λ_2 the *eigenvalues* of A, and we call the vectors a and c the *eigenvectors* of A.

2. Rotation

   We will cover this in considerable detail in Chapter XXXXXXX.

3. Magnification

   Many aspects of optics including image magnification and some distortions such as keystoning can be represented by matrix vector multiplication.

4. Perspective Transformation

   The mapping of 3D space to 2D such as is done in perspective drawings and camera imaging can be represented by matrices.

B.4 Derivative of a Rotation Matrix

In computing accelerations for dynamics we sometimes need the time derivative of a rotation matrix. Consider a point rotated by angular velocity vector ω. The rotation represented by ω can also be represented by a time-varying rotation matrix, $R(t)$. Let's remember that every rotation matrix relates two frames. In this case, a fixed frame, F, and the time-varying frame which we will call frame R, so that $R(t)$ could be written ${}^F_R R(t)$. For now, assume that the angular velocity vector ω is known in $R(t)$ (somewhat unrealistic because $R(t)$ is constantly changing).

Using the classical definition of derivative:

$$\frac{d}{dt}R(t) = \lim_{\Delta t \to 0} \frac{R(t+\Delta t)P - R(t)}{\Delta t}$$

$$= \lim_{\Delta t \to 0} \frac{R(t+\Delta t) - R(t)}{\Delta t}$$

What is the difference between the two rotation matrices in the numerator? The illustration below shows the two rotations, the vector ω, and one of the three components of the difference: $\Delta t(\omega \times X)$.

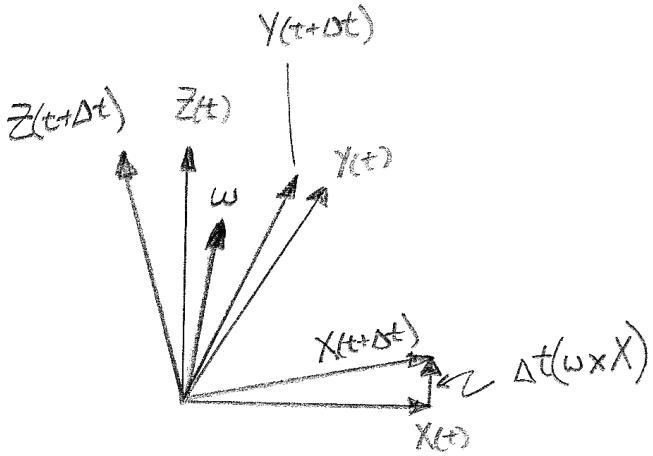

Since each column of R represents a unit vector of the frame, the difference of each column is the change introduced by the rotation ω:

$$\frac{d}{dt}R(t) = \lim_{\Delta t \to 0} \frac{\begin{bmatrix}\Delta t\,[\omega \times X] & \Delta t\,[\omega \times Y] & \Delta t\,[\omega \times Z]\end{bmatrix}}{\Delta t}$$

$$= \lim_{\Delta t \to 0} \frac{\Delta t \begin{bmatrix}\omega \times \begin{bmatrix}1\\0\\0\end{bmatrix} & \omega \times \begin{bmatrix}0\\1\\0\end{bmatrix} & \omega \times \begin{bmatrix}0\\0\\1\end{bmatrix}\end{bmatrix}}{\Delta t}$$

$$= \omega \times \begin{bmatrix}1 & 0 & 0\\0 & 1 & 0\\0 & 0 & 1\end{bmatrix}$$

$$\frac{d}{dt}R(t) = \dot{R} = \begin{bmatrix}0 & -\omega_Z & \omega_Y\\ \omega_Z & 0 & -\omega_X\\ -\omega_Y & \omega_X & 0\end{bmatrix}$$

What we have found now is that we can express the time derivative of a rotation matrix as a skew-symmetrix matrix as a function of the components of the angular velocity vector ω. There is only one problem: in this expansion, we assumed that the vector ω was known in the time varying frame, R. Instead we want an expression with the known angular velocity: ${}^F\omega$.

Let's apply our result to mapping a point to a time varying rotated frame:

$$\dot{R}P = \begin{bmatrix}0 & -\omega_Z & \omega_Y\\ \omega_Z & 0 & -\omega_X\\ -\omega_Y & \omega_X & 0\end{bmatrix} P$$

$$\dot{R}P =^{R} \omega \times P$$

where we applied the matrix interpretation of the cross product.

To fix the problem that ${}^{R}\omega$ is not known, we note that if we rotate ω from F to R we can express ${}^{R}\omega$ in terms of the known ${}^{F}\omega$:

$$\dot{R}P = {}^{R}_{F}R\,{}^{F}\omega \times P$$

by application of a cross-product property:

$$\dot{R}P = {}^{F}\omega \times {}^{F}_{R}R\,P$$

Thus when it appears in a matrix-vector or (by extension) matrix-matrix multiplication, we can write the derivative of the rotation matrix R as

$$\dot{R} = \omega \times R \qquad \text{or} \qquad \begin{bmatrix} 0 & -\omega_Z & \omega_Y \\ \omega_Z & 0 & -\omega_X \\ -\omega_Y & \omega_X & 0 \end{bmatrix} R$$

B.5 Inspiration

The engineer generalizes the 1,2, or 3 dimensional problem of the physicist into k dimensions."

Gabriel Kron, "Tensor Analysis of Networks," 1938.

Appendix C

Comparison of Rotation Representations

In Chapter 2 we covered several methods to represent the rotation of rigid objects and end effectors. It is natural to ask which of these is "best" to use in writing analysis and writing software to control robot manipulators. We have covered the following representations:

- 3-parameter systems: roll-pitch-yaw, ZYX Euler angles, etc.
- Equivalent angle-axis
- Quaternions
- Rotation Matrices

In choosing a "best" representation, we must define a set of criteria.

- Compatibility with dynamics, sensor processing, and control equations
- Numerical roundoff and normalization issues.
- Numerical singularities
- Memory Usage
- Computational efficiency

Compatibility This and other books have reviewed several widely used computations for forward and inverse kinematics, Jacobian matrices, dynamics, joint-space and cartesian space trajectory planning, and many others. Most of these algorithms stick to one or two of the representations we have reviewed. Robust, well known algorithms for each computation are not widely available for each representation. Thus we must evaluate the choice of representation according to how well it can be used in the various computations needed to control and operate a robot manipulator.

Numerical Issues Each method has strengths and weaknesses when they are implemented in computer software.

Computational and Memory Efficiency In considering all of these factors, we must also consider Moore's Law which reduces the cost of computational resources by about two orders of magnitude each time a new robotics textbook comes out. Moore's well known Law states that the available computation per unit cost increases by a factor of 2 every 1.5 years. Specifically, since the 1980's (30 years as of this writing) if C_{1982} is the amount of computing power avialable in 1982,

$$C_{2012} = 2^{(30/1.5)} C_{1982} = 1048576 C_{1982}$$

In other words, computer power today is 1 Million times greater than in the 1980's! Since the kinematic complexity of robot manipulators grows much more slowly than Moore's Law, at the time of this writing

computational efficiency and memory usage differences between the methods are essentially insignificant for computational implementation of the kinematic and dynamic models of practical manipulators.

We are thus left with only the first three criteria, Compatibility with dynamics, sensor processing, and control equations. Numerical roundoff and normalization issues, and Singularities.

C.1 Comparison of Rotation Representations

In this section we will evaluate each rotation representation in the context of each of the criteria described above.

C.1.1 Compatibility with Inverse Kinematics, dynamics, sensor processing, and control equations

Dynamics Dynamic equations are commonly computed by either the recursive Newton Euler method, or the Lagrange method. When derived using the Lagrange method, rotational velocities are used to compute kinetic and potential energy. In most references, these computations are done with respect to the manipulator joint variables (θ_i, d_j, most commonly refered to as q_k) and so do not require a choice of reprsentation for link angular velocity or acceleration. Thus the following systems will be assessed for the Newton-Euler method.

- 3-parameter systems: roll-pitch-yaw, ZYX Euler angles, etc.

  When orientation is expressed in one of the three-parameter systems, rate of change in orientation is most often expressed as as angular velocity, and angular acceleration vectors defined as:

  $$\omega = [\omega_x, \omega_y, \omega_z] \qquad \dot{\omega} = \frac{d}{dt}\omega = [\dot{\omega}_x, \dot{\omega}_y, \dot{\omega}_z]$$

  When dynamics are computed using the Recursive Newton-Euler method, $\omega, \dot{\omega}$ are commonly used. But singularities are a potential problem.

- Equivalent angle-axis

  The dynamic equations are rarely expressed in Equvalent angle-axis form.

- Quaternions

  Quaternions have historically been used in rigid body dynamics. Euler's equation for rotational motion can be written in quaternion form[1] as

  $$\ddot{q}(t) = \dot{q}q^*\dot{q} + \frac{1}{2}q\left[I^{-1}(\tau(t, q, \dot{q}) - 4(q^*\dot{q}) \times (I(q * \dot{q})))\right]$$

  where I is the rigid body intertia tensor, and $\tau(t, q, \dot{q})$ is the sum of external, elastic, and viscous torques on the rigid body. This equation can be integrated twice to get the quaternion, $q(t)$, specifying the orientation of the rigid body with time.

- Rotation Matrices

  Rotation matrices by themselves are used in dynamic equations for coordinate transformations, but are not used to represent angular velocities or accelerations.

C.2 Roundoff and Normalization

Computers represent floating point numbers with finite precision. In some computations, entities like rotation matrices and quaternions are successively multiplied over and over. In such cases, roundoff errors can accumulate. One difficulty with such accumulation of error is that unit quaternions and rotation matrices can loose properties such as normalization or orthonormality.

Numerical procedures exist to correct these errors called normalization or re-normalization procedures. They can be performed every so often as a precaution against loss of normality constraints. Renormalization does not guarantee lack of error however. Although the cost of renormalization varies considerably, we shall also consider it insignificant for computations covered in this book.

Numerical issues can arise in multiple different ways. For specificity, we consider here the process of frequently updating an orientation reference by an increment of orientation.

[1] "Rigid Body Dynamics using Euler's equations, Runge-Kutta and quaternions," Indrek Mandre, 2008.

- 3-parameter systems: roll-pitch-yaw, ZYX Euler angles, etc.

  Three parameter representations can be updated by addition if about an unchanging axis which causes few numerical issues. If the axis of rotation is changing, this representation becomes difficult to update.

- Equivalent angle-axis

  With respect to numerical issues, equivalent angle-axis can be thought of as a version of quaternions (below).

- Quaternions

  Quaternions are updated by multiplication (Equation (2.6)) and are subject to cumulative roundoff errors which can lead to loss of normalization. A quaternion can be re-normalized similarly to a vector: If $q = [w, x, y, z]$, the normalized version, $\hat{q}$ is

$$\hat{q} = \frac{q}{\sqrt{w^2 + x^2 + y^2 + z^2}}$$

- Rotation Matrices

  Rotation matrices gradually loose their orthonormality due to build up of roundff errors which accumulate from multiple computations. As a result, a matrix which should represent the product of hundreds or thousands of rotations may, due to accumulated roundoff errors, represent a dilation in addition to rotation. Renormalization of a rotation matrix is more involved than for a vector because the columns and rows must be orthogonalized as well as re-set to unit magitude.

  The cure for this is to periodically apply a renormalization algorithm to the matrix $\tilde{R}$ which is in need of renormalization. In one such method, use singular value decomposition to convert $\tilde{R}$ into three components:

$$U\Sigma V^* = \text{SVD}(\tilde{R})$$

  Then the renormalized matrix $\hat{R}$ is

$$\hat{R} = U \begin{bmatrix} 1 & 0 & 0 \\ 0 & 1 & 0 \\ 0 & 0 & 1 \end{bmatrix} V^*$$

  Although SVD computation is $O(n^4)$, $3^4 = 81$ computations must be considered a reasonable number with current and future available computing power.

C.3 Singularities

We consider here the difference between algorithmic singularities and mechanical singularies. A robot has a mechanical singularity whenever it occupies a joint configuration which causes its Jacobian matrix to loose rank. This corresponds to a physical "lock-up" of the mechanism and a loss of at least one direction of motion freedom. On the other hand, the equations which convert a rotation matrix to, for example, roll-pitch-yaw angles, have a singularity whenever xxxxx(cite to chapter 2)xxxxx. This is independent of the actual mechanism state and depends on the chosen coordinate system — an algorithmic singularity.

- 3-parameter systems: roll-pitch-yaw, ZYX Euler angles, etc.

  As we saw in Chapter 2, each 3-parameter system has a specific orientation containing an algorithmic singularity. Algorithms which use a 3-parameter approach must be careful to check for this singularity or find guarantees that the computations stay away from the singularty in the chosen coordinate system and application.

- Equivalent angle-axis

  Equivalent angle-axis is defined for any finite rotation, but can be considered singular when the rotation is zero, corresponding to the case where

$${}^A_B R = \begin{bmatrix} 1 & 0 & 0 \\ 0 & 1 & 0 \\ 0 & 0 & 1 \end{bmatrix}$$

  This singularity may be relatively benign in many applications because 1) it is independent of the chosen coordinate system and 2) it corresponds to a null rotation.

- Quaternions

  Quaternions have the same singularity situation as Equivalent angle-axis

- Rotation Matrices

  Rotation matrices have no singularities. They are well defined (have determinant = 1) for any orienation in any coordinate system.

Bibliography

[1] The following books have been invaluable in preparation of these notes.

[2] B. Siciliano and O. Khatib, editors. *Springer Handbook of Robotics*. Springer, Berlin, Heidelberg, 2008.

[3] Richard P Paul. *Robot manipulators: mathematics, programming, and control: the computer control of robot manipulators*. the MIT Press, 1981.

[4] Haruhiko Asada and Jean-Jacques E Slotine. *Robot analysis and control*. J. Wiley New York, NY, 1986.

[5] Yoshihiko Nakamura. *Advanced robotics: redundancy and optimization*. Addison-Wesley Longman Publishing Co., Inc., 1990.

[6] Tsuneo Yoshikawa. *Foundations of robotics: analysis and control*. The MIT Press, 1990.

[7] J. Craig. *Introduction to Robotics: Mechanics and Control*. Addison Wesley, 1986.

[8] Reza N Jazar. *Theory of applied robotics: kinematics, dynamics, and control*. Springerverlag Us, 2007.